Final Report: Scale-up of Algal Biofuel Production Using Waste Nutrients

California Polytechnic State University
San Luis Obispo, California

Advanced Algae Systems Program
Bioenergy Technologies Office
U.S. Department of Energy

September 2018

Final Report
Scale-Up of Algal Biofuel Production Using Waste Nutrients

WBS: 9.5.1.5, Award Number: DE-EE0006317

Prepared by

Ruth Spierling[1,2], Braden Crowe[1,2], Neal Adler[2], Kyle Poole[2], Matt Hutton[1,2], Michael Huesemann[3], Todd Lane[4], Kunal Poorey[4], Dan Anderson[3], John Benemann[2], and Tryg Lundquist[1,2]

Recipient:
[1]**California Polytechnic State University**
1 Grand Avenue
San Luis Obispo, CA 93407

Principal Investigator:
Tryg Lundquist, Ph.D., P.E.
Civil and Environmental Engineering Department
(805) 756-7275 | TLundqui@CalPoly.edu

Consortium Partner Leads:
[2] MicroBio Engineering Inc.: John Benemann

[3]Pacific Northwest National Laboratory: Doug Elliot, Dan Anderson and Michael Huesemann

[4]Sandia National Laboratory, Livermore, Calif.: Todd Lane

For
Advanced Algae Systems Program
Bioenergy Technologies Office
U.S. Department of Energy
Washington D. C.

Project Officer: Daniel Fishman
Golden, Colorado

September 30,2018

Acknowledgment: This material is based upon work supported by the Department of Energy's Office of Energy Efficiency and Renewable Energy under the Bioenergy Technologies Office, Award Number EE0006317.

Contents

Table of Tables

Table of Figures

Table of Equations

Acknowledgments

We thank Daniel Fishman, Project Officer, and Evan Mueller, Project Monitor, for their guidance during this project.

The participation in this project by the staff of MicroBio Engineering Inc., as part of their cost share contribution, is gratefully acknowledged, the guidance and advice provided by Dr. John Benemann, CEO, and the work by engineers Ian Woertz, Neal Adler, and Kyle Poole and Matt Hutton, which was essential to the accomplishment of this project. The pilot-pond system used in this research was provided and designed by MicroBio Engineering Inc. We are also grateful for their support in the operation of these pond systems, and the performance of the hydraulic study as well as the technoeconomic and lifecycle assessment services provided in the final analysis.

We are grateful to our other project partners including Michael Husemann, Andrew Schmidt, and Dan Anderson at Pacific Northwest National lab and Todd Lane and Kunal Poorey at Sandia National Lab who each completed major project tasks. We appreciate the cooperation of the Delhi County Water District in providing the main field site. Thank you to the Delhi operators, specifically Doug Paulson who provided invaluable help throughout the project.

Thank you to the Cal Poly Sponsored Projects Office and Grants Development Office staff for their hard work and support in the management of the project.

The authors are thankful for the opportunity to help train and guide the hundreds of undergraduate students, student employees, senior project students, and foreign exchange students who participated in this project over the years via the Cal Poly Water-Energy Sustainability Training program. In addition, the following three graduate students from the Civil and Environmental Engineering Department poured their full effort into the laboratory and field experiments, thousands of water and biomass analyses, and the preparation of their master's theses, which focused on the tasks of this project: Yakov Suvorov, Chris Pittner, and Lauren Parker

Executive Summary

Renewable fuels can be more environmentally friendly than conventional fuels and can be produced locally, supporting energy independence. Liquid renewable fuels are of special interest due to their high energy density. Algae are a promising prospective feedstock for low carbon intensity liquid biofuels, due to their high productivity and potential for high lipid or carbohydrate content. Their ability to grow on wastewater and waste nutrients and on non-arable land are cost and sustainability advantages. The organic matter content of wastewater promotes mixotrophic and/or heterotrophic growth of both algae and bacteria, boosting biomass productivity further. However, economic and technologic challenges persist that prevent the scale-up of algal biofuels to commercial relevance. These challenges include algal harvesting, drying, dewatering, and the conversion of algal biomass to usable fuels (Hannon et al 2010, Dunlap and Shaw 2009, Pienkos et al. 2009). The US Department of Energy (DOE) Bioenergy Technologies Office (BETO) supports research to overcome these challenges and outlines the research and development goals for algal biofuels in their Multi-Year Program Plan (MYPP). The long-term goals of the MYPP for algal biofuels research are briefly as follows: develop the domestic ability to produce algal biofuels at a scale of 5 billion gallons per year (BGY) by 2030 and demonstrate technologies that produce biofuel intermediates from algae at a cost of $3/gallon of gasoline equivalent (GGE) by 2022 (BETO MYPP 2016). This research reported herein was funded to investigate methods of meeting an intermediate milestone of 2,500 gallons of biofuel intermediate per acre per year for a non-integrated process by improving algal productivity, harvesting efficiency, and conversion to biofuel intermediates. Use of wastewater and wastewater nutrients was a key distinguishing characteristic of this project.

In pursuit of 2,500 gallons of biofuel intermediate (BFI) per acre per year, California Polytechnic State University, San Luis Obispo (Cal Poly) sought to develop the capability to produce biofuel intermediates from microalgae grown on municipal wastewater at a 20-acre algae-based wastewater treatment facility in Delhi, California (37.43° N), which includes 7 acres of raceway ponds. Coupling algal biofuel production with wastewater treatment capitalizes on the abundant waste nutrients and carbon present in wastewater and reduces use of clean water in algal biorefinery systems (Figure 1). In this research, the performance of the full-scale wastewater treatment plant was characterized by measuring productivity, wastewater treatment performance, hydraulic characteristics, and energy consumption. Nine 1,000-L pilot raceways with CO_2 addition were used in experiments to maximize productivity. Low-cost, energy-efficient algae bioflocculation and settling were monitored. Population genetics were monitored in an attempt to correlate taxa with superior productivity and/or settling. Algae-bacterial biomass was converted to biofuel intermediates via bench-scale hydrothermal liquefaction (HTL), and the resulting fuel quality was characterized. To develop rapid strain screening capabilities, a climate simulating photobioreactor ("LEAPS") was developed and validated against outdoor raceways. A techno-economic analysis (TEA) and a lifecycle assessment (LCA) were performed to model process economics and sustainability.

The major outcomes of this research included demonstration of 33 g/m^2-day annual average algal-bacterial productivity in pilot raceways, and a biofuel intermediate yield of 0.35 g intermediate/g algae biomass via HTL, for a yield of 4,100 gallons BFI per acre per year, assuming a 90% harvest efficiency and ignoring other minor losses. This exceeded the project goal of 2,500 gallons of BFI per acre per year and nearly met the 2030 program goal, highlighting the promise of integrating wastewater treatment and biofuels production.

The biocrude BFI produced by the process in Figure 1 is refined to diesel and naphtha fuels as shown in Figure 120. These fuels are normalized to the energy content of gasoline (gallons gasoline equivalent, GGE, for comparison to other fuels). Results from the TEA of the this complete "well-to-wheel" process demonstrated that, at a 400-ha scale, a minimum fuel selling price (MFSP) of $12.55/GGE, which could be decreased 57% to $7.14/GGE when including revenue from coupling the biofuel production with the co-products of wastewater treatment services and low carbon fuel credits from California and Federal

programs. Due mainly to the high capital costs of thickener centrifuges and hydrothermal processing equipment, the fuel cost is sensitive to scale, with significantly lower costs expected for larger farms.

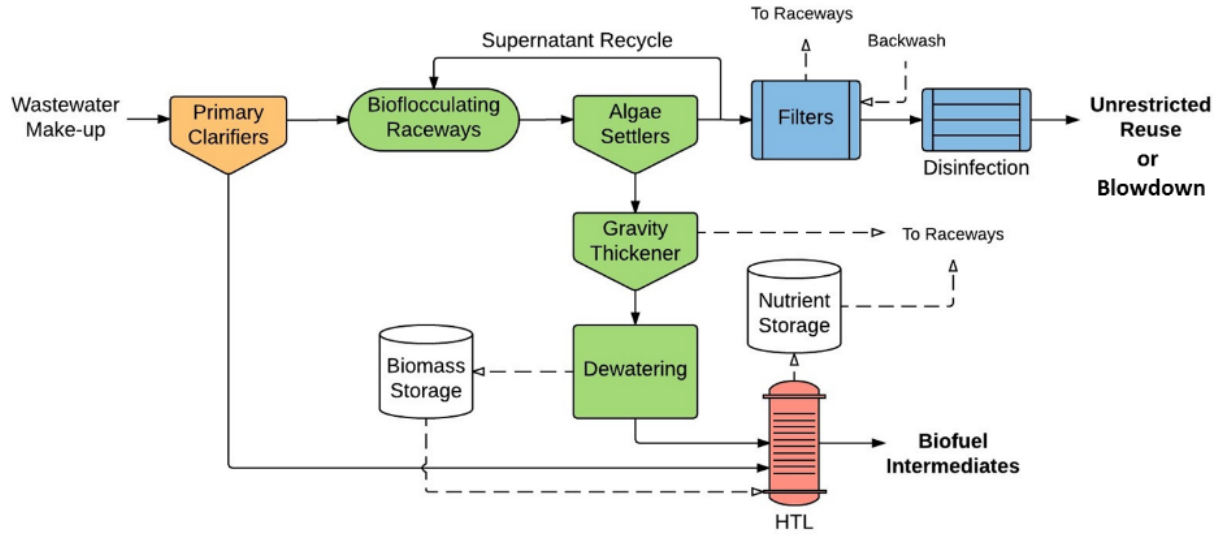

Figure 1: Integrated wastewater treatment and biofuel production facility with nutrient and water recycling. For once-through systems, the effluent would be treated to the unrestricted reuse level. If instead water is intensively recycled within the system, the effluent would be saline blowdown. Biofuel intermediates are refined to biofuels by additional processes discussed in the TEA/LCA section.

Areas for future work to reduce cost further include improvement of biomass productivity and HTL yield, and reducing the cost of CO_2 capture from flue gas. The results of the LCA showed that the renewable biodiesel product would have greenhouse gas (GHG) emissions of 45.7 g $CO_{2\text{-eq}}$/MJ of fuel, substantially lower than the conventional ultra-low sulfur diesel at 102.82 g $CO_{2\text{-eq}}$/MJ (ARB 2014). In addition, the studied process resulted in a net energy ratio of 3.1, meaning over 3 times more energy is produced than is consumed. These results suggest that this renewable diesel pathway has the potential to reduce net carbon emissions in the transportation sector if it were widely used.

In this research project, significant advances were made in improving raceway algal productivity and fuel production from algae biomass, while also improving process economics. These outcomes brought the algal biofuel technology closer to being a sustainable and marketable process. The remainder of this executive summary is organized into the following six primary project tasks: (1) to optimize biomass productivity for a selected strain at Delhi, (2) to maximize algal productivity and harvesting efficiency in Delhi pilot ponds, (3) a full-scale raceway hydraulic characterization, (4) biomass processing to biofuel intermediates, and (5) scale-up engineering analysis, modeling, and planning.

TASK 1: Optimize biomass productivity for a selected strain at Delhi.

Pacific Northwest National Laboratory (P.I. Michael Huesemann), in collaboration with Cal Poly and MicroBio Engineering Inc.

Introduction, background, state of research

For economic feasibility and sustainability, algae biofuels production requires algal strains with high annual biomass productivities, greater than 25 g/m^2-day in outdoor culture systems (Davis et al., 2016). A major challenge is the identification and selection of strains that have the potential to achieve such high annual biomass productivities in outdoor ponds. To date, many candidate strains which exhibited robust growth in laboratory trials failed to meet productivity targets in outdoor pond settings. Outdoor testing is slow and costly, but simulations speed testing. Two types of simulation were used in this project: indoor climate-simulated culturing and biomass growth modeling.

The PNNL biomass growth model (Huesemann et al., 2016) predicts outdoor pond performance based on strain-specific model parameters, which are determined in laboratory cultures. Sunlight intensity and culture water temperature are the inputs for each strain. These data, in time series termed "scripts" (ML1.0, 1.1) are derived from the PNNL Biomass Assessment Tool (BAT) (Wigmosta et al. 2011). As light intensity and temperature are the main determinants of biomass productivity in outdoor ponds, under nutrient (N, P, CO_2, trace elements) replete conditions, with representative mixing and similar water chemistry, small-scale indoor reactors should, in principle, be able to simulate large-scale outdoor raceways (Huesemann et al., 2016). This requires that light and temperature regimes can be accurately replicated between indoor and pond cultures.

Experimental goals and methods

A major objective of this task was the development and testing of a new photobioreactor design, the Laboratory Environmental Algae Pond Simulator (LEAPS). The specific objectives were to (a) design and build the LEAPS (ML 1.4), (b) evaluate its ability to accurately replicate incident light and culture temperature conditions observed in outdoor ponds (ML 1.5), (c) validate its performance by comparing biomass productivity of *Chlorella sorokiniana* and *Nannochloropsis salina* grown in outdoor ponds and in the LEAPS, using similar light, temperature, and culture conditions (ML 1.6), and (d) apply the validated LEAPS to evaluate the growth and productivity of several additional strains (*Scenedesmus obliquus* and S*tichococcus minor*) under climate-simulated conditions. The results of this study have been published (Huesemann et al. 2017c).

One limitation of the current biomass growth model was that the strains, such as *Chlorella sorokiniana* DOE 1412, were only parameterized for one constant pH (pH 7). Therefore, one objective of this task (ML 1.2, 1.3) was to determine the effect of other pH values (6 to 9) on the maximum specific growth rate of this strain, pH being a critical model input parameter.

Milestones tasks and subtasks and purpose

Purpose: Develop laboratory and computer modeling methods capable of rapidly identifying high-productivity strains and optimal culture methods specific to locations. The Delhi location and *Chlorella sorokiniana* (DOE 1412) will be used in the current project.

+ ML1.0 Climate Model Output: Generate a year of daily sunlight and temperature scripts for the Delhi site. Three seasonal scripts (summer, fall/spring, and winter) will be defined (April 30, 2014).

+ ML1.1 Growth Model Output: Use the PNNL Biomass Growth Model (BGM) to predict the productivity of DOE 1412 at Delhi using the ML1.0 seasonal scripts (May 30, 2014).

+ ML1.2 pH Experiment for Growth Model Improvement: Report the maximum specific growth rate of DOE 1412 as a function of pH (6-9) (September 30, 2014).

+ ML1.3 Growth Model Improvement incorporating pH: Extend the BGM for DOE 1412 to account for pH effects based on ML1.2 results and generate new Delhi productivity predictions (December 31, 2014).

+ ML1.4 Develop Climate-Simulating Photobioreactors (csPBRs): Design and build, using off-the-shelf components, a benchtop photobioreactor system that accurately simulates the growth performance of outdoor pond cultures under fluctuating light intensity and water temperature (December 31, 2014). (Note: the csPBRs are now designated as 'Laboratory Environmental Algae Pond Simulator' or LEAPS).

+ ML.1.5 Initial Validation of csPBRs: Evaluate these climate-simulation photobioreactors (csPBRs or LEAPS) using DOE 1412 by comparing csPBR productivity data (to be collected under the current milestone using previously collected Arizona scripts) with previously collected DOE 1412 data from outdoor ponds in Arizona (March 31, 2015).

> **S1.5 Additional csPBR Experiments**: Use the ML1.4 validated csPBRs to predict the productivity of DOE 1412 at Delhi using the ML1.0 seasonal scripts or actual weather data from the Delhi site. Batch cultivation on defined media will be used. Two rounds of successful csPBR operation will be completed (June 30, 2015 and September 20, 2015).

+ ML1.6 Validation of Growth Model & csPBRs with Delhi Pond Data: Compare Biomass Growth Model predictions to pilot pond and csPBR productivity measurements. The BGM input will be actual weather data from the period of pilot measurements (ML2.3). DOE 1412 will be piloted on defined media at Delhi in batch mode. pH will be kept within a narrow band to make use of the pH-modified BGM of ML1.2 (December 21, 2015).

Results and Conclusion

The developed LEAPS PBR is a fully functioning pond simulator that can out-perform currently commercially available small-scale pond simulators and photobioreactors (PBRs) in terms of reliability and accuracy in reproducing outdoor climate patterns and predicting outdoor growth rates. LEAPS predicted biomass productivities within 10% of values measured in outdoor ponds using climate data from two geographically distinct locations (Figure 2). Currently the LEAPS is capable of simulating pond temperatures between 10 and 31°C and can deliver up to 2675 µmol/m^2/s within 5% of set-point values. To our knowledge, this is the only bench-scale pond simulator that can replicate growth in outdoor algae ponds located in a wide range of climatic zones, geographical locations, and with various depths (up to 35 cm). LEAPS is small enough to for six simultaneous cultures on a normal bench but still large enough to allow AFDW measurements without excessive culture sacrifice. LEAPS was found to enable high-throughput testing of candidate strains for a more cost-effective screening approach.

In conclusion, the LEAPS was demonstrated to be a reliable photobioreactor system for quantifying the biomass productivity of microalgae under climate-simulated conditions. Key benefits of using the LEAPS photobioreactors, rather than outdoor ponds, for strain evaluation are the following: First, using light and temperature scripts can be generated by PNNL's Biomass Assessment Tool for any geographic location where meteorological data are available (Wigmosta et al. 2011). Strains can be tested for any climate or season of choice at any time, thereby allowing for much faster throughput. Second, testing in LEAPS is less capital and labor intensive than outdoor ponds. Third, it is easy to test different operational strategies for optimizing seasonal or annual biomass productivities, such as varying culture depth, changing dilution rates, or evaluating harvesting strategies. Finally, strains can be objectively compared to each other by using the same seasonal light and temperature scripts, something that is very difficult to do in outdoor ponds due to the vagaries of weather. Since development the LEAPS reactors have been widely used for algal biofuels research including in several DOE funded research efforts including the RAFT, AOP,

DISCOVR, and Incubator projects. A current disadvantage is the lack of continuous media flow through LEAPS. Operation is batch or by manual semi-continuous dilution.

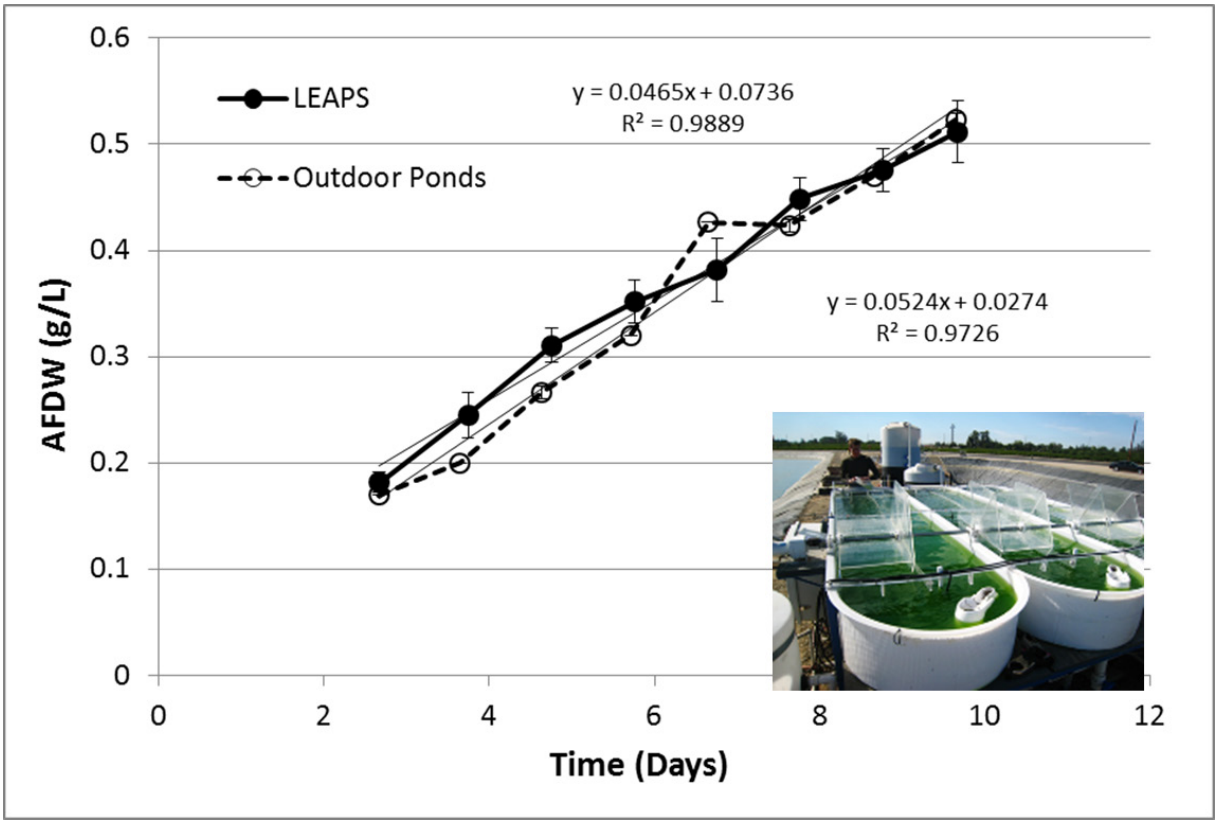

Figure 2: Volumetric productivity of *Chlorella sorokiniana* (DOE 1412) outdoors in Delhi and in the LEAPS reactors demonstrating the ability of LEAPS to reproduce outdoor raceway productivity.

Task 2: Maximize algal productivity and harvesting efficiency in Delhi pilot ponds.

Cal Poly and Todd Lane Lab, in consultation with MicroBio, PNNL, and Delhi County Water District.

Introduction, background, state of research

Algae-based wastewater treatment systems are prevalent, with over 5,000 pond-based municipal wastewater treatment plants in use in the US (EPA 2002). Many, if not most, of these pond-based systems are not optimized for algae biomass production and use deep facultative ponds (0.6-6 m deep) without CO_2 addition. Typically, these systems are highly effective at removing suspended solids and biochemical oxygen demand (BOD) from wastewater at a relatively low energy input and low cost compared with conventional mechanical treatment systems but have poor and variable nitrogen removal performance.

Raceway ponds (aka high-rate ponds) are an alternative to facultative and similar oxidation ponds and have the potential for better nutrient removal (Craggs et al 2012, Park et al. 2011, Lundquist et al. 2010, Garcia et al. 2000, Oswald et al. 1957). Coupling wastewater treatment with biomass production allows for the recycling and use of the water, carbon, and nutrients in the wastewater and substantially lowers the cost of biofuels production (see Task 5). Another benefit of optimized algae-based wastewater treatment is the potential for bioflocculation of the biomass into aggregated particles that settle by gravity without the aid of chemicals or energy intensive harvesting processes such as membrane filters or centrifuges.

In this task, we investigated algal cultivation and harvesting practices to maximize the outdoor biomass/biofuel productivity for wastewater grown polycultures to >2,500 gallons BFI /acre-year. Research was performed in the inland community of Delhi, California at a 0.6 MGD full-scale wastewater treatment facility. The full-scale system consisted of two raceway ponds (3.2 and 3.4 acres) operated in series and was characterized to determine baseline productivity under the existing operational conditions. Nine 1,000-L pilot-scale raceways ponds were used to explore operational conditions including dilution rate and CO_2 addition that optimized biomass productivity and waste treatment. The growth rate of *Chlorella sorokiniana* (DOE 1412) in the 1,000-L ponds was used to validate the Biomass Growth Model (BGM) and climate simulating reactors (LEAPS) developed by PNNL in Task 1. Finally, the samples were analyzed genetically to evaluate whether any consortia and/or strains were associated superior or inferior periods of treatment, setting and/or productivity.

Experimental goals and methods

The major experimental goals of this task were to characterize the existing full-scale non-optimized algae-based wastewater treatment plant under two operational schemes and to optimize biomass productivity in nine 1,000-L pilot ponds to inform operational changes at the full-scale wastewater treatment plant that would result in higher productivity. Additionally, the prokaryotic and eukaryotic communities in the 10,000-L pilot ponds at the San Luis Obispo, Calif. field station were studied to optimize the cultivation and harvesting of algae biomass from algal wastewater treatment systems.

Delhi, California, (population 11,000) operates a 0.6 MGD (2.4 ML/day) wastewater treatment plant on a 48.3-acre property. The treatment plant is located at latitude 37.4 N on Highway 99 and serves 7,500 residents and 2,300 residential and commercial connections. The full-scale treatment plant consists of a rotary auger screen followed by two deep facultative ponds in parallel and two shallow raceway ponds in series. Biomass from the final raceway pond is harvested using coagulants and settled in algae settling ponds. The supernatant from the settling ponds then travels to a baffled maturation pond followed by discharge to percolation basins to recharge the ground water. The harvested biomass is solar dried on three sand beds and one concrete pad. During this research, the wastewater treatment plant was also operated under a high loading condition where only one facultative and one high rate pond were used. The productivity results from this period of high wastewater loading were compared to productivity under the typical lower loading conditions of the previous year.

The pilot-scale system consisted of nine 3.5-m^2 ponds (30-cm depth, 1,000 L) with automated CO_2-pH and influent control, settling units and drying beds. The ponds were operated in triplicate and called the North (N1, N2, N3), Middle (M1, M2, M3) and South (S1, S2, S3) ponds. Influent to the ponds was semi-continuous to maintain a hydraulic residence time (HRT) of 1.8-6 days, depending on experimental needs, and came from two sources: a pilot-scale primary clarifier and from a constant head tank that received water pumped from the north facultative pond (Equation 1). All productivity was reported as the gross productivity of the pond effluent, that is, without the influent suspended solids concentrations subtracted. The gross productivity represents the total amount of biomass in the pond effluent available for biofuel production.

Equation 1: Hydraulic residence time

Hydraulic residence time (t) = Volume (L) / Flow rate (L/t)

Milestones tasks and subtasks and purpose

Purpose: Maximize algal productivity and harvesting efficiency in the Delhi pilot ponds. Develop cultivation and harvesting practices to maximize outdoor biomass/biofuel intermediate productivity for polyculture and DOE 1412 (targeting >2,500 gallons/acre-year).

+ML 2.0 Characterize Existing Full-Scale System: Estimate baseline biomass productivity and settleability for the existing full-scale plant under two different process flow configurations. Evaluate current full-scale wastewater treatment plant practices and productivity and settleability. Suggest improvements based on pilot work (January 31, 2015).

This milestone was completed in Q1 of CY15.

+ML 2.1 Design and Install Pilot plant: Design and install tank raceway ponds (August 31, 2014).

+ML2.2 Shakedown Pilot Plant: Install controllers and demonstrate trouble-free operation of the pilot scale systems for algae growth and bioflocculation studies, settling tanks, pond water temperature monitors, pH controllers, and influent flow rate controllers (November 30, 2014).

S2.2 Pilot versus full scale. Compare the pilot ponds to the full-scale ponds.

Milestone 2.1 and 2.2 were completed in Q1 of CY15.

+ML 2.3 Compare Strains: Compare biomass productivity of (1) a wastewater polyculture and (2) DOE 1412 grown on defined media. The DOE1412 data will also be used for ML 1.6 model and csPBR validation Generate pilot plant performance data to evaluate the Biomass Growth Model and the climate simulating photobioreactors of Task 1(April 30, 2015).

S2.3 Compare strains continued.

This milestone was completed in Q3 of CY15.

+ML 2.4 Dilution Study: Determine the effect of wastewater dilution rate on biomass productivity, treatment performance, nutrient assimilation, settling efficiency, and dewaterability with native polyculture (September 30, 2015).

This milestone was completed in Q3 of CY15.

+ML 2.7 Organism ID: Identify genetically strains or consortia, along with identification of other dominant organisms in the cultures, such as zooplankton. Look for relationships between dominant organisms and culture performance (August 30, 2015).

This milestone was completed in Q1 of CY16. Results of this task are reported in Task 1.

Results and Conclusion

The annual average productivity in the un-optimized full-scale system was 20 g/m^2-day (ML2.1) (Figure 3). This productivity was increased in the pilot scale system (ML 2.1, ML2.2 and S2.2) by reducing the residence time from 3.7-5.2 days in the full-scale system to two-days in the pilot system and controlling the pH in the pilot-scale system with CO_2 addition to a pH of 7.4-7.9. These changes increased the productivity 40% over the full-scale system to 33 g/m^2-day (Figure 4). In the pilot-scale system, along with CO_2 addition, higher organic loadings were found to result in the highest productivities; therefore, short hydraulic residence times (2 days) and dilution with primary clarified wastewater were found to increase productivity compared to hydraulic residence times greater than 2 days and dilution with facultative pond water (ML 2.4), as would be expected due to heterotrophic and/or mixotrophic growth on wastewater dissolved organic matter.

These results were preliminarily confirmed with the full-scale system when it was operated under a higher organic load and shorter residence from 4/07/14 - 6/30/14. For this experiment, one facultative pond and raceway pond were bypassed, and the productivity increased to 18.97 ±8.1 g/m^2-day (mean ±standard deviation of the measurements over time) from 15.8 ±5.3 g/m^2-day for the same date range in 2015 under normal operating conditions. A longer duration experiment in the full-scale system would confirm these trends.

Additionally, the short residence times and high organic loads in the pilot ponds encouraged bioflocculation and reduced by half the required coagulant dose that would be needed to meet permitted discharge requirements (Figure 5). Reducing the coagulant dose has several benefits including reduced addition of ash and salts to the final biomass product which may improve the fuel yield and final fuel product when hydrothermal liquefaction is used (Task 4), and reduced process costs (Task 5). The positive effect of short hydraulic residence times, CO_2 addition, and high organic loading on productivity and biomass settling is confirmed in the literature (Park et al. 2011, Valigore et al. 2012, Park et al. 2010).

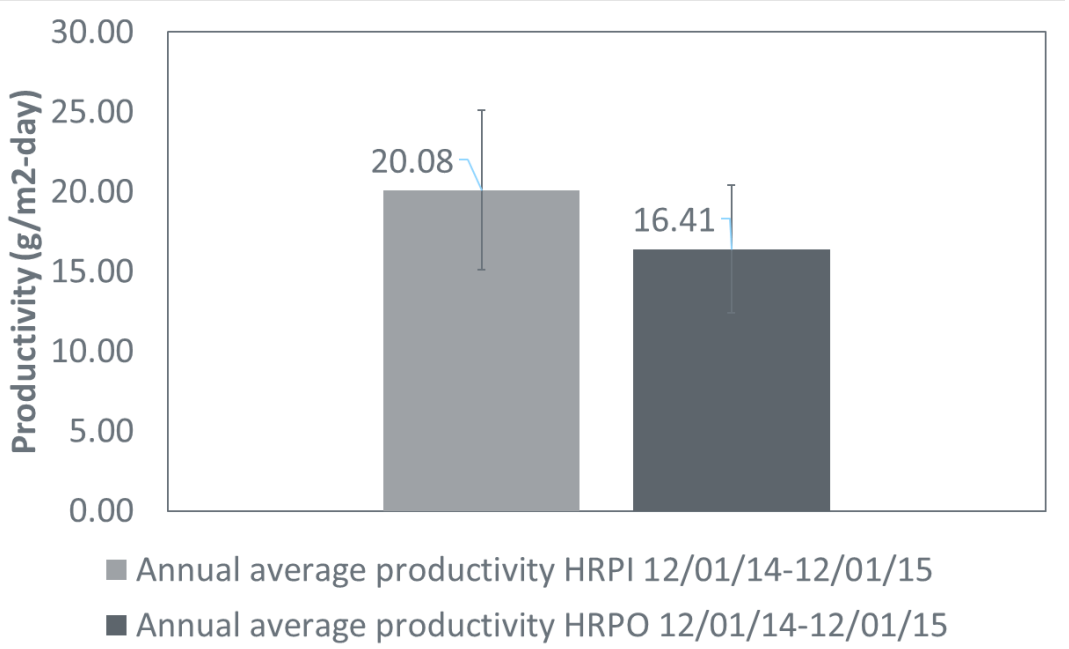

Figure 3: Gross productivity of the full-scale Delhi wastewater treatment plant.

For the organism identification, at the San Luis Obispo raceways, genera found in raceways fed either primary influent or reclaimed water included *Scenedesmus*, *Desmodesmus*, *Pediastrum*, *Tetraedron*, *Chlorella*, *Oocystis*, *Closterium*, *Chlorococcum*, *Tetradesmus, Oocystis*, *Pediastrum*, and *Scotiellopsis*, with minor but consistent levels of reads from golden algae and diatoms (ML 2.7). Read counts of suspected algal predators and pathogens were regularly detected, including rotifers, chytrids, and ciliates. Replicate ponds frequently maintained different genera composition despite having similar productivity. For example, in two replicate ponds, *Scenedesmus* gave the highest percentage of read counts in Pond 1, with *Chlorella*, *Desmodesmus*, and *Tetradesmus* as the primary secondary components. Pond 2 favored *Tetradesmus* and *Chlorella*, with the remaining genera constituting minor components (generally fewer than 5,000 reads). Given the morphological similarity of *Tetradesmus*, *Desmodesmus*, and *Scenedesmus*, the subtle difference in species composition was not noticed during microscopy which demonstrates the importance of genetic analysis.

Cannonical correspondance analysis (CCA) revealed few correlations between pond productivity and genera read count. Deleterious organisms reported as pond crash agents or responsible for reductions in productivity, such as Cryptomycota infections of *Scenedesmus* cultures (Letcher 2013), predation of *Chlorella* by the flagellate *Poteriochromonas* sp. (May 2017), or grazing by zooplankton (2017 Montemezzani), were found in most samples, although were not found correlated with changes in biomass productivity. Only the ciliate *Hemiophyrs procera* was found to be negatively correlated (-0.5

CCA factor) with productivity, while the ciliate *Loxophyllum* was weakly positively correlated (0.2 CCA). Additionally, it was unanticipated that *Botrycoccos sp*., an organism with generally low reported biomass productivity in outdoor raceway pond settings (Benemann 2013), was the most strongly positively correlated (CCA 0.5) with biomass productivity.

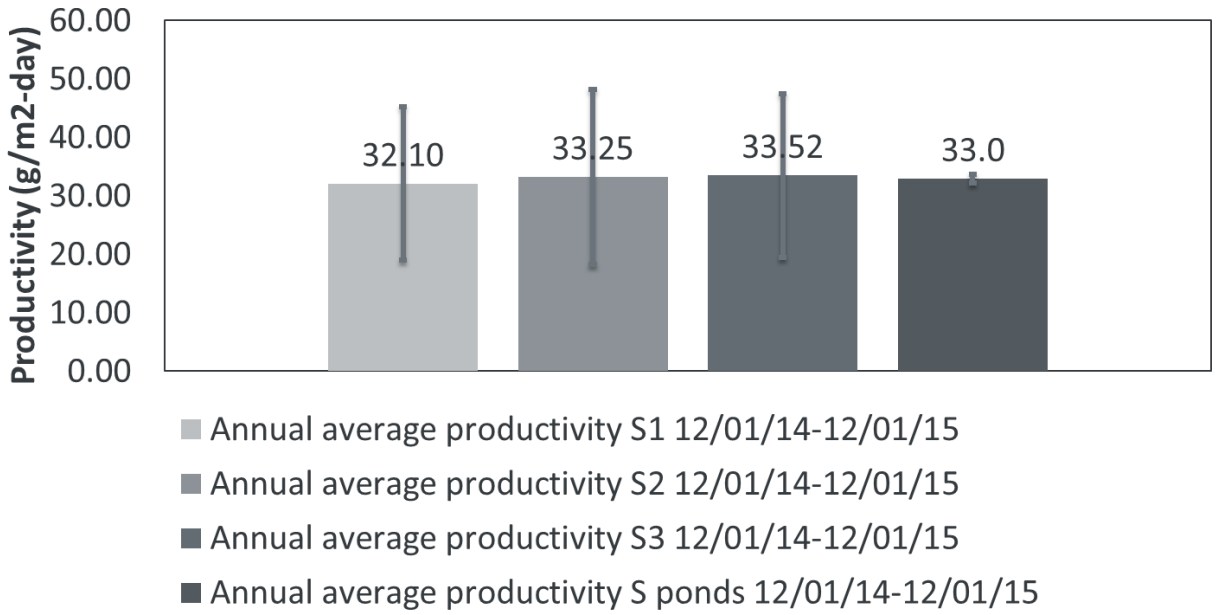

Figure 4: Annual average productivity in the ponds with the 2-day hydraulic residence time diluted with primary clarified wastewater. Ponds were run in triplicate and the variability between the replicate ponds was low even though the seasonal variation in productivity was high. Error bars on S1, S2, and S3 columns indicate the standard deviation for each over time, while the bar on the S average column is the standard deviation of the triplicate raceways.

In contrast to weak statistical interactions between the microbiome and productivity, the genetic community appears to have a more significant influence on settling efficiency. Settling was positively correlated with predatory organisms, including *Rhizophydium* and the ciliate *Hemiophyrs procera*, which have been shown to induce defensive responses in primary producers, ranging from an increase in the number of cells per colony and spine generation (*Pediastrum*, *Desmodesmus*) to colony clumping (*Micractinium*), resulting in a more readily settleable culture (Montemezzani 2017). Curiously, another ciliate, *Loxophyllam*, had the strongest negative correlation with settling efficiency (CCA -1.1), suggesting diverse roles within the microbiome. Small, round, and nuetrally bouyant, *Chlorella* is generally difficult to settle. Despite a significant relative read count of *Chlorella*, Pond 2 achieved over 90% settling efficiency by the end of the sampling period. Looking for insights into the settleability, Lee (2013) found that while axenic *Chlorella* cultures remained colloidal, settling performance improved in xenic cultures, and identified *Sphingomonas* a primary component of the within the bacterial community. Similarly, *Sphingomonas* showed one of the strongest positive correlations to setting efficiency here. Of the negatively correlated bacteria, *Algoriphagus* sp. (Bowman 2003) potentially discourages floc formation, with filamentous bacteria notorious in activated sludge systems for disrupting settling performance.

Interesting overall trends emerge from the CCA. Of strains with moderate negative correlations to settling (~0.5 CCA), most are weakly positively correlated with biomass productivity (~0.2 CCA). By

comparison, only one strain (*Hemiophyrs procera*) hows the opposite influence with any confidence; it is positively correlated with settling performance, but negatively influences biomass productivity. Only two members of the 18s community *Botryococcus* sp. (UTEX 2629) and *Rhizophydium* sp. JEL317 were positively correlated to both productivity and settling. Few genera exist with positive correlations to both productivity and settling efficiency. Most genera positvely correlated to biomass productivity appear detrimental to settling efficiency, and conversely those that are positvely correlated to settling efficiency are detrimental to biomass productivity. Longer term studies, such as those conducted with settling activate sludge cultures, are likely needed to to confirm trends and further identify useful genera.

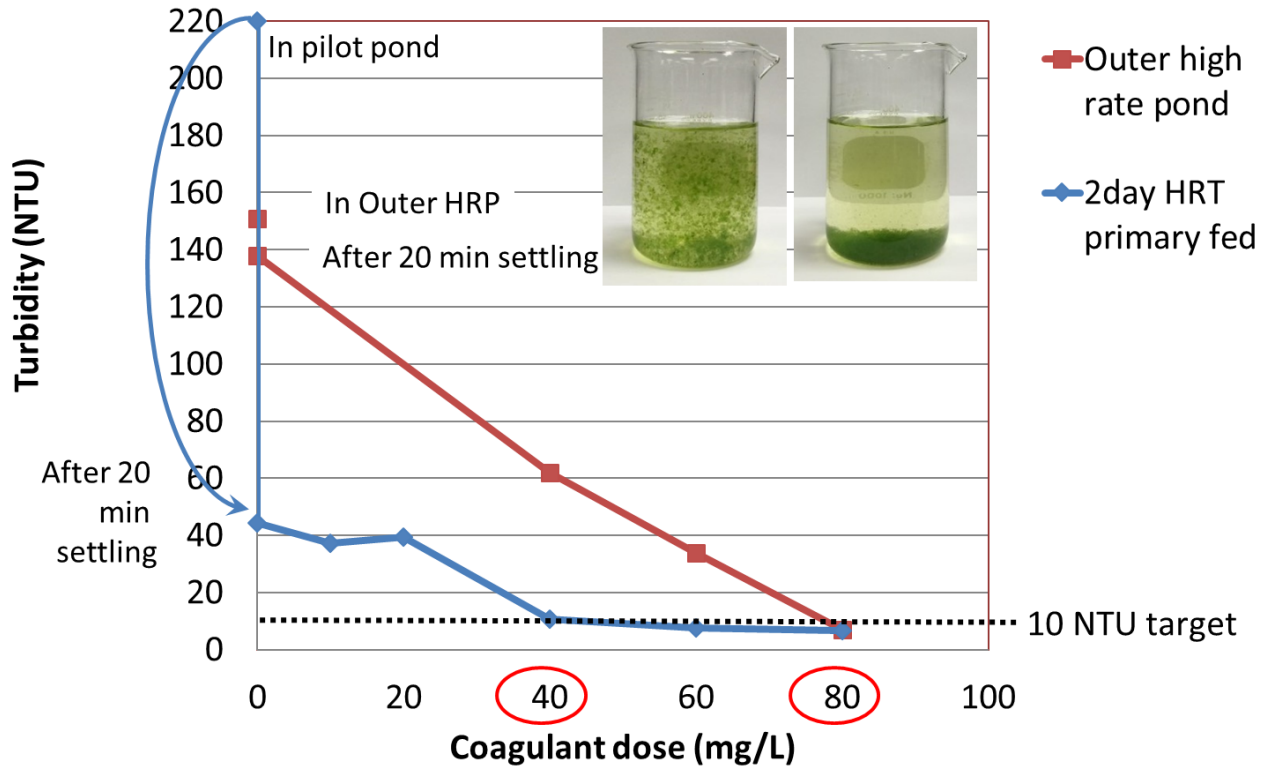

Figure 5: Bioflocculation reduces the coagulant dose required to meet permitted discharge requirements by half, improving process economics. Initial drop in turbidity indicates the settling efficiency without any coagulants after 20 minutes. Then several coagulant doses were tested on the jar test apparatus.

TASK 3. Full-scale raceway hydraulic characterization

(Cal Poly and MicroBio Engineering, in consultation with the Delhi County Water District)

Introduction, background, and state of research

In this task, the hydraulic characteristics of 1.3- and 1.4-hectare algae raceway ponds were measured at Delhi County Water District Wastewater Treatment Plant. A relationship was identified between channel velocity and power use in these raceways. Subtasks included planning the hydraulic study, calculating the roughness coefficient of the raceway channel for use in hydraulic modeling, and conducting a mixing study to determine the mean hydraulic residence time and extent of axial dispersion.

Experimental goals and methods

Direct measurements at the Delhi raceways included channel water velocity, head loss around the channel, axial dispersion determined via a dye tracer study, and electricity consumption by the paddle wheel motors. The water velocity and head loss measurements were used in Manning's equation for open channel flow to estimate hydraulic power. The measured hydraulic power was compared to the measured electrical power use. The ratio of hydraulic and electrical power yielded an efficiency factor for the paddle wheel station.

The Delhi facility has two adjacent raceways, termed Inner and Outer, which are laid out in a large loop. The raceway depths are adjusted seasonally from 60-cm in summer to 90-cm in winter. The hydraulic studies were conducted twice, once in winter and once in summer, to investigate the effect of depth on the hydraulics.

Milestones tasks and subtasks/ purpose

Purpose: Preliminary operation and hydraulic characterization of the full-scale raceways.

S3.0 Plan Hydraulic Study: Develop the detailed methods for hydraulic characterization of the Delhi raceways (April 30, 2015).

S3.1 Determine Friction Factor: Measure velocity and water surface elevation profile to determine hydraulic friction factors (July 31, 2015).

S3.2 Mixing Study: Characterize mixing and flow short-circuiting with dye tracer studies (November 30, 2015).

+ ML3.3 Mixing Power Determination: Develop velocity versus energy consumption relationship for 3-acre raceways (December 31, 2015).

Results and Conclusions

The summary of results from flow velocimetry, power consumption, and head loss observations are tabulated, along with the raceway dimensions used in calculations.

Table 1: Summary Table: Measured and calculated hydraulic characteristics of the inner and outer raceways at the Delhi County Water District wastewater treatment plant at 60- and 90-cm depths.

	Water Depth:	60 cm	60 cm	90 cm	90 cm
	Raceway Name:	Inner	Outer	Inner	Outer
Measured Values	Units				
Channel Velocity	m/s	0.12	0.13	0.11	0.11
Head Loss	m	0.021	0.021	0.013	0.016
Channel Flow Rate	m^3/s	0.81	0.91	1.20	1.17
Calculated Values					
Hydraulic Power	kW	0.17	0.19	0.15	0.18
Electrical Power Demand	kW	1.6	1.6	1.1	1.2
Wire-to-water efficiency	%	10%	12%	14%	15%
Area Normalized Power	kW/ha	1.21	1.11	0.80	0.79
Manning's Roughness Coefficient	-	0.024	0.022	0.027	0.028

The calculated roughness coefficient for the asphalt-lined raceway channels ranged from 0.022 to 0.028, which is like “cemented rubble masonry” in standard tables of Manning’s equation roughness coefficients. This is much rougher than the 0.010-0.015 value listed for “smooth clay” or “plastic-lined” channels, which would be the expected values in new raceway ponds. The Delhi raceways were last cleaned over a decade ago, and the high roughness was likely due to accumulation of settled sludge and road gravel fallen from the surrounding berms. The calculated roughness is also influenced by the head loss coefficient assumed for the channel bends.

The Peclet number and dispersion coefficient, which are dimensionless group parameters that describe dispersion characteristics, were 340 and 0.43, respectively, which indicates that these raceway channels have strong plug flow characteristics and axial dispersion of the influent water occurs only slowly.

The mixing energy observed was less than what current models (Lundquist et al. 2010, Davis et al. 2016; Neenan 1986; Hreiz et al. 2014) assume. This is due in large part to the Delhi facility operating their raceways at a slower velocity and at 2- or 3-times greater depth. The paddle wheel mixing power observed ranged from 1.21 to 0.79 kW/ha at 0.13 – 0.11 m/s channel velocity and at a range of channel depths from 0.62 to 0.97 m. This indicates that full scale paddle-wheel mixed non-flocculating algae raceways can operate at a significantly lower channel velocity and power consumption than assumed in techno-economic models (Lundquist et al. 2010, Davis et al. 2016; Neenan 1986; Hreiz et al. 2014).

Maintaining channel velocity of as little as 0.11 m/s has been enough for operating the nominally 1.3- and 1.4-ha raceways at the Delhi County Water District Wastewater Treatment Plant of non-settling algae in paddle wheel mixed raceway ponds. For algae cultures grown in raceways that can settle on their own, 0.20 to 0.25 m/s is still recommended to reduce biomass accumulation in ponds, but no more than 0.25 m/s should be considered to keep raceway mixing operating costs to less than 5% of annual costs.

Power demand in the Delhi raceways was determined to be higher with shallower depth and indicate that the power demand of 30-cm depth raceways used for optimal biofuel production will be higher than values measured in present study.

The raceways at Delhi have strong plug flow characteristics and axial dispersion of the influent water occurs slowly, which suggests the units effectively limit short circuiting of partially treated wastewater to the outfall of the system. For algae producers growing algae on fertilizers, this is a reason to bleed in fertilizer gradually versus rapidly.

While the calculated wire-to-water efficiencies are low (10-15%), the Area Normalized Power is the key factor in evaluating different mixing methods. Other mixing methods, like a transfer pump, may have a higher efficiency but the entire channel flow must be constricted through pipes to achieve this higher velocity, sharply increasing the friction losses of the system and in turn increasing overall Area Normalized Power demand.

TASK 4. Biomass processing to biofuel intermediates

(Pacific Northwest National Laboratory, Doug Elliott team and Cal Poly, in consultation with MicroBio Engineering)

Introduction, background, state of research

In this task, wastewater grown microalgae biomass was converted into biofuel intermediates through hydrothermal liquefaction (HTL). Hydrothermal liquefaction is a high temperature, high pressure process that converts organic carbon from biomass into "biocrude." Biocrude is like crude oil in that it can be refined into various fuel fractions through distillation and is an attractive fuel conversion process because all fractions of the intercellular organic carbon are mostly converted to fuel. This contrasts with other fuel conversion processes in which specific biochemical components such as lipids or carbohydrates alone are converted to biodiesel and ethanol.

Experimental goals and methods

The major goals of this task were to demonstrate and optimize the conversion of wastewater grown microalgal feedstock into a biofuel intermediate suitable for further upgrading and to characterize the air emissions from HTL to provide information as needed to air regulators. Additionally, the task included hydrotreating and distillation tests to characterize the biofuel intermediate for downstream upgrading requirements and report mass balances and fuel yield. For all samples, process performance was characterized by mass (C, N, P, S, H, and O). Due to differences in genera and harvesting conditions, both Delhi and San Luis Obispo algae were tested as HTL feedstock.

Wastewater grown microalgal biomass was produced, harvested and thickened at Cal Poly research sites in San Luis Obispo and Delhi and used as a feedstock for HTL. HTL process performance was evaluated based on biocrude yield (g_{oil}/g_{algae}) and composition (% carbon yield), and mass balances were performed. The biocrude was then upgraded via hydrotreating to confirm the liquid fuel value of the process and to obtain a comparison with conventional petroleum-based liquid fuels. Air emissions from the HTL process were also measured for the purpose of refining capital and operating cost projections in case of a requirement for air emission control equipment. The nutrients and carbon retained in the solid and aqueous waste fraction were recycled in regrowth studies under a separate award (DE-EE0005994) and the results of these experiments were reported in the May 2017 final report on that project (Figure 6).

HTL was performed on several algae biomass feedstocks in a total of five samples:

1. Biomass from the nine 33-m^2 pilot-scale wastewater treatment raceway ponds at the San Luis Obispo Water Resource Recovery Facility, (two samples).
2. Biomass from the full-scale (1.4-ha) outer raceway pond at the municipal wastewater treatment system at Delhi, California, (two samples).
3. Biomass from the nine 3.3-m^2 pilot-scale wastewater treatment raceway ponds at the Delhi wastewater treatment plant (one sample).

In all cases, biomass was harvested, thickened by local project staff and prepared for shipping to Pacific Northwest National Laboratory (PNNL) in Richland, Washington. At PNNL, the samples were homogenized in a high shear mixer, diluted to approximately 20% solids, and characterized to determine HTL feed composition. HTL was performed in a bench-scale unit. The HTL process accepts homogenous algae "slurry" and applies heat and pressure, resulting in a three-phase effluent with oleaginous, aqueous, and solid fractions.

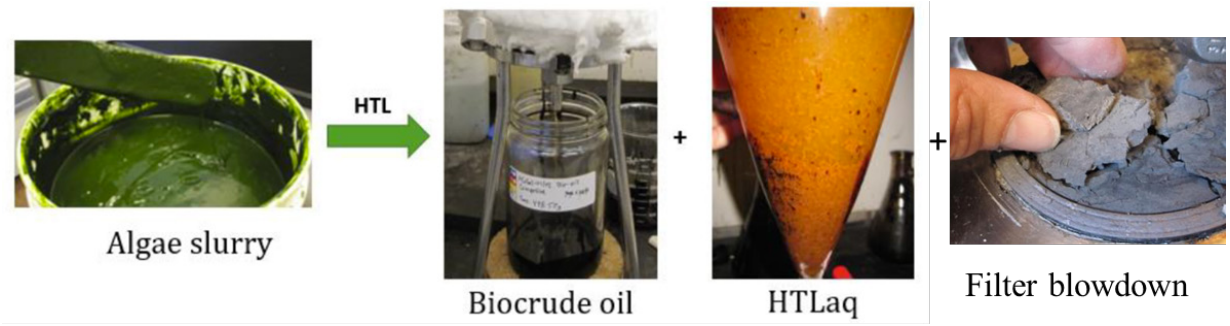

Figure 6: The products of HTL include the biocrude oil, which can be distilled into various fuel fractions similar to crude oil, the aqueous fraction (HTLaq) where much of the nitrogen is retained, and the filter blowdown where the multivalent minerals such as phosphates are retained.

Milestones tasks and subtasks and purpose

The Task 4 work plan was broken down into three milestones and one subtask.

ML4.1 HTL Run 1: Deliver first biomass samples to PNNL for hydrothermal liquefaction (HTL) and biofuel intermediate analyses (April 30, 2014).

The milestone was completed in Q2 of CY14 when the first Sample 1 materials were delivered form Cal Poly to Pacific Northwest National Laboratory for testing.

S4.1: Evaluate the effect of thickening on HTL yield (June 30, 2014).

This subtask was completed in April of 2014 when the first sample was sent to PNNL

ML4.2 Hydrotreating: Conduct hydrotreating and distillation tests. Characterize the biofuel intermediate for downstream upgrading requirements. Report mass balances and fuel yield (September 30, 2014).

This milestone was completed in Q4 of CY14. It comprised the hydrotreating analyses undertaken on Sample 1.

ML4.3 HTL Runs 2-5: During Year 2, conduct at least four HTL runs on wastewater-derived biomass, while characterizing air emissions on at least one run (December 31, 2015).

This milestone was completed in Q4 of CY15 and when the last of Samples 2 through 5 were treated and analyzed by the Pacific Northwest National Laboratory/Cal Poly team.

Results and Conclusion

The major outcomes of this research were as follows:

1. The yield of biocrude was sensitive to the solids content of the feed. It was determined that 20% solids slurry was the maximum, over which reactor clogging was likely.
2. The yield of the biocrude was sensitive to the ash content of the feed. Lower ash content resulted in less filter clogging and higher oil yields. Algal harvesting systems that use coagulants will likely have a higher ash content and lower biocrude yield. Similarly, systems that utilize solar dewatering and drying of the biomass to 20% solids should be protected from blowing sand and dust.
3. The normalized mass yield of oil ranged from roughly 17% to 36% and the normalized mass yield of carbon in the oil ranged from about 33% to 55%. The highest yield was achieved with algae harvested by bioflocculation from the San Luis Obispo pilot plant. This sample also had the lowest ash and the highest normalized carbon yield in the oil of 55%, and lower oxygen, moisture and nitrogen in the bio-oil. The lowest yield was from biomass that was well below 20% solids.
4. The produced oil was within 50% of the boiling point range of diesel, 30% that of gasoline. The mass fraction of diesel in the simulated distillation was ~52%.
5. The gaseous emissions from HTL were primarily CO_2 (93%), with the remaining 7% consisting of small fractions of hydrogen, nitrogen, methane, ethylene, carbon monoxide, hydrogen sulfide, isobutene and n-butane. These results are encouraging but likely require validation at scale to determine air pollution control requirements.
6. Re-growth of algae on the HTL wastewater is likely minimally inhibited compared to the control (BG-11 medium) at concentrations needed to satisfy algae nitrogen requirements at full-scale (400x).

For the purposes of modeling the process and projecting cost and environmental performance of the integrated biofuel production scheme, the biocrude yield used was 0.35 g_{oil}/g_{algae} and a 55% carbon yield in crude bio-oil.

Task 5. Scale-up engineering analysis, modeling, and planning

MicroBio Engineering and Cal Poly, in consultation with Delhi County Water District, PNNL, and SNL

Introduction, background, state of research

Task 5 evaluated the scale-up potential of a full-scale biofuels facility. The goal of this research was to project the costs and carbon intensity of the proposed algal biofuel: renewable diesel blendstock produced by refining HTL biocrude from algal biomass. This was accomplished by process modeling, cost estimation, and environmental life cycle assessment.

Experimental goals and methods

For the scale-up engineering analysis, modeling, and planning, sites were assessed for scale-up of the proposed algal biofuels production facility (Figure 7). Data were gathered to establish a process engineering model, which calculates mass and energy balances. The results of the process modeling were used to conduct techno-economic analysis (TEA) and a life cycle assessment (LCA) of the proposed facility, which gave the outputs of minimum fuel selling price (MFSP) and GHG emissions associated with the algae-derived diesel blendstock.

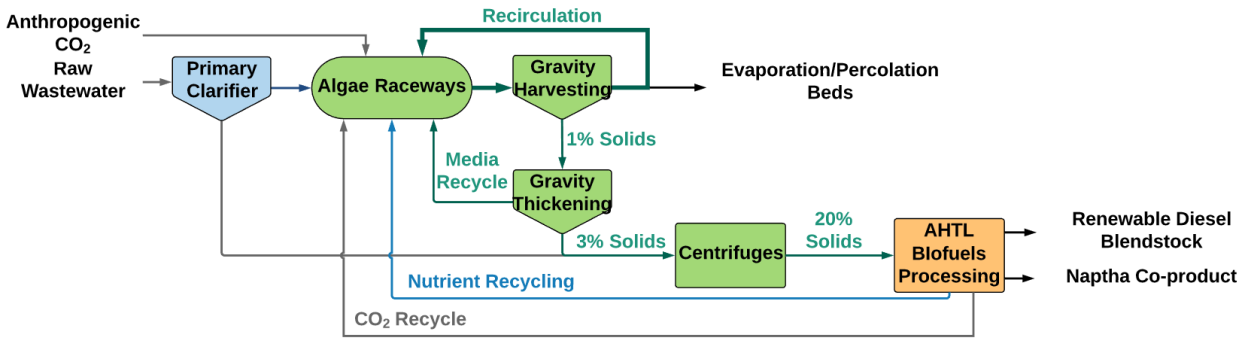

Figure 7: Process flow diagram used for process modeling and assessment of future scale-up facilities. "AHTL Biofuels Processing" refers to hydrothermal processing of biomass followed by hydrotreating of the resulting biocrude followed by distillation to diesel and naphtha (Figure 120).

An iterative approach was used to determine what technologies should be used for unit processes (specifically, harvesting and drying) to reduce the minimum fuel selling price (MFSP) and GHG emissions of the hydrothermal liquefaction (HTL) derived diesel blendstock.

Milestones tasks and subtasks/ purpose

Purpose: Develop refined engineering models of the process developed and evaluate its projected costs and net greenhouse gas emissions. Prepare the Phase 2 scale-up preliminary engineering plan, evaluate additional sites for Phase 2 and full-scale facility implementations (Fresno, Hilmar, and other promising sites), and a Stage Gate review of these issues.

S5.0 Gather Design Information: At conferences, meetings, and interviews, gather and disseminate information relevant to the design of the Phase 2 scale-up of the biofuel-wastewater process (February 28, 2016).

S5.1 Assess Scale-Up Sites: Identify and assess locations for the Phase 2 scale-up and additional full-scale implementations of wastewater-based algae biofuels (e.g., Hilmar, Fresno) (February 28, 2016).

S5.2 Process Engineering Model: Create a process engineering model for the Delhi Phase 2 design (January 30, 2016).

+ **ML5.3 Harvesting and Dewatering Study:** Prepare an engineering study on algae harvesting, dewatering, and drying to the level required by HTL (June 30, 2015).

S5.4 Facility Improvements Study: Prepare an engineering study on any facility improvements needed to meet Regional Water Quality Control Board discharge standards while simultaneously producing biomass sufficient to produce the equivalent of 2500 gallons per acre per year of biofuel intermediate. Gather information on permissions needed from water regulators to conduct Phase 2 (February 28, 2016).

S5.5 Air Permitting Study: Prepare an engineering report on air permitting and HTL flue gas clean-up technology expected to be needed (October 31, 2015).

+ **ML.5.6 Economics and Lifecycle Study:** Prepare facility economic and LCA analyses for the algae wastewater treatment/biofuels process for conditions in California's Central Valley (February 28, 2016).

Results and Conclusions

Five different MFSPs are reported below to show how different revenue streams impact the MFSP (Figure 8). Combining all revenue streams results in a MFSP of $7.14/GGE (gallons gasoline equivalent). However, low carbon fuel credit revenue from federal and state carbon trading markets (California Low Carbon Fuel Standard [LCFS] and US EPA Renewable Fuel Standard [RFS]) is highly variable. In our model, we determined that a reduction of $2.18/GGE was the most reasonable estimate.

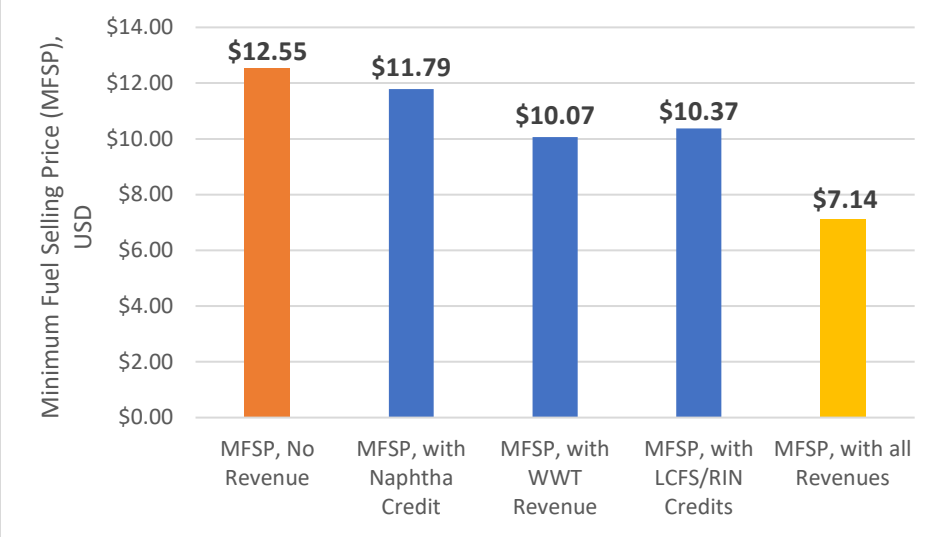

Figure 8: Five MFSP values are reported. The first bar represents the total annualized cost of the production facility allocated to the diesel blendstock product. Bars 2 – 4 represent the MFSP with individual revenue streams (naphtha coproduct, wastewater treatment revenue, and low carbon fuel credits. The last bar represents the MFSP with all revenues combined.

LCA results indicate a GHG emission of 45.7 g CO_2e/MJ. This is a substantial reduction in GHG emissions compared with conventional fuel products (CARBOB Gasoline; 99.78 g CO_2e/MJ). The well-to-tank energy requirement was calculated to be 325,000 J/MJ of fuel.

Diesel blendstock produced by refining HTL biocrude from algae feedstock has a low carbon intensity (45.7 g CO_2e/MJ) compared to conventional petroleum-based fuels (99.78 g CO_2e/MJ for CARBOB gasoline). However, the MFSP of the algal diesel blendstock is too expensive to compete with conventional fuels even with revenue from carbon trading markets. The combined results of the LCA and TEA show that although algal diesel produced from an HTL process can reduce greenhouse gas emissions, more research is required to reduce MFSP to the BETO goal of $3/GGE.

Broader Impacts

The impact of this funding extends well beyond the research findings and successful execution of tasks and milestones. From hosting visiting international scholars (funded by their respective institutions), to mentoring Cal Poly masters degree and senior project students and creating a campus wide interdisciplinary research program for undergraduate and graduate training, those involved have not only contributed to the project but also take with them the lessons learned and knowledge gained to a diverse array of research settings and career paths in the water-energy nexus. The following are lists of international student participants and dissemination products.

International Research Scholars Hosted
2016

Alessandro Solimeno, Ph.D. Student, Environmental Engineering and Microbiology Research Group, Universitat Politècnica de Catalunya, Barcelona, Spain.

Antonie Jardin, M.S. student, Centre d'Etudes Superieures Industrielles (CESI), School of Engineering, Saint-Nazaire, France.

Alexandre Bourgiugnon, M.S. student, Institut national superieur, School of Agricultural Science, Dijon, France.

2015

Thomas Chene, M.S. student, Centre d'Etudes Superieures Industrielles (CESI), School of Engineering, Angouleme, France.

Gustavo Henrique Oliveira, B.S student, Brazil Scientific Mobility Program.

California Polytechnic State University M.S. Theses Describing This Research

Pittner C. 2018. Increasing Algal Productivity and Treatment Potential in Raceways Fed Clarified Municipal Wastewater. Thesis. California Polytechnic State University.

In Preparation:

Parker L. 2018. Study on the effect of sampling frequency on measured productivity. Seasonal night aeration to increase nitrification in algae-based wastewater treatment in the winter.

Suvorov Y. 2018. Evaluation of High-Rate Algae Municipal Wastewater Treatment Ponds for Production of Biofuel Intermediates, in Delhi, California.

NSF Research Experiences for Undergraduates (REU) Students Involved

Marissa Liccese, Environmental Engineering
2014 California Polytechnic State University, San Luis Obispo
"Lipid Extraction and Anaerobic Digestion for Recycle of Algal Biomass"

Felix Pinto, Chemical Engineering
2014 University of Oklahoma
"Nutrient Limitation in Waste Water Algal Cultures"

Noelle Patterson, Biological Systems Engineering
2014 University of California, Davis
"Exploring Methods of Algae Bioflocculation in High Rate Ponds"

Lili Gevorkian, Biological Sciences
2015 California Polytechnic State University, San Luis Obispo
"Anaerobic Digestion of Hydrothermal Liquefaction Liquid "

Kimberly Pugel, Environmental Engineering
2015 California Polytechnic State University, San Luis Obispo
"Effects of Water and Nutrient Recycling and Coagulant Addition on Anaerobic Digestion of Algae Biomass"

Involvement of Cal Poly Undergraduates

Over the course of this project Cal Poly undergraduate students contributed significantly to this project

through the class called the Water-Energy Sustainability Training Team (WESTT). This class was created by Dr. Lundquist as an interdisciplinary research program to provide students hands-on exposure to research. Students from all grade levels and from all majors on the Cal Poly campus participate in the program bringing diverse views, experience, and ideas to the program. Through this program, students participate in hands-on research, learn safe lab practices and quality control and quality assurance, participate in a large task/goal-driven organization with complicated scheduling, have a foretaste of graduate school, learn the importance of precision, analyze data of their own making, and contribute to innovative solutions in the water-energy environmental space. Nearly 250 undergraduate students were directly involved in preforming analytical tests and analyzing data for this project.

Selected Publications and Presentations

Papers

Huesemann, M., A. Chavis, S. Edmundson, D. Rye and M. Wigmosta, "Climate-Simulated Pond Culturing of *Chlorella sorokiniana* DOE 1412: Quantifying the Maximum Achievable Annual Biomass Productivity in the United States", *Journal of Applied Phycology*, to be submitted.

A. Solimento, L. Parker, T. Lundquist, J. Garcia, Integral microalgae-bacteria model (BIO-ALGAE): application to wastewater high rate algal ponds, Bioresource. Technol. (2017).

Michael Huesemann, Patrick Williams, Scott Edmundson, Peter Chen, Robert Kruk, Valerie Cullinan, Braden Crowe, Tryg Lundquist. The Laboratory Environmental Algae Pond Simulator (LEAPS) Photobioreactor: Validation Using Outdoor Pond Cultures of *Chlorella sorokiniana and Nannochloropsis salina, Algal Research*, submitted.

Gevorkian et al. "Recycling carbon and nutrients in an algae biocrude production system using hydrothermal liquefaction," in preparation

K. Poorey, T. Lane. Relating community genomics to productivity and harvesting of algal-bacterial biomass for biofuel production. In preparation.

L. Parker, R. Spierling. Effect of Sampling Frequency on Microalgae Productivity Estimates. In preparation

Presentations

S. Blackwell, R. Spierling, M. Hutton, T. Lundquist, K. Poorey, and T. Lane. (2016). Dynamics in Algal Productivity and Bioflocculation in Wastewater fed Raceway Ponds. Presentation. Algae Biomass Summit, October 26, 2016, Phoenix, AZ. Conference Presentation.

R. Spierling, L. Parker, C. Pittner, C. Quigley, J. Haserot, N. Hess, B. Crowe, N. Adler, and T. Lundquist. (2016). Enhanced nitrogen conversion and removal in algae-based wastewater treatment systems. Algae Biomass Summit, October 26, 2016, Phoenix, AZ. Conference Presentation.

M. Hutton, S. Blackwell, E. Zardouzian, R. Spierling, T. Lundquist. (2016). Long term study of low-cost harvesting by bioflocculation. Algae Biomass Summit, October 26, 2016, Phoenix, AZ. Conference Presentation.

T. Lundquist, B. Crowe, L. Gevorkian, R. Spierling, C. Pittner, L. Parker, N. Adler, M. Hutton, J. Benemann, A, Schmidt, D. Elliot. (2016). From wastewater to fuel distillates: cultivation and processing of microalgae grown during sewage treatment. Algae Biomass Summit, October 26, 2016, Phoenix, AZ. Conference Presentation.

T. Lundquist, R. Spierling, N. Adler, B. Crowe, M. Hutton, A. Schmidt, D. Elliot. (2016). Integrated algae cultivation- hydrothermal liquefaction pilot studies using wastewater media. Presentation. Algae Biomass, Biofuels and Bioproducts Conference June 18-21 San Diego CA.

J. Benemann, T. Lundquist. (2016). Multi-trophic algal municipal wastewater treatment. Presentation. Algae Biomass, Biofuels and Bioproducts Conference June 18-21 San Diego CA.

R. Spierling, T. Lundquist, B. Crowe, L. Gevorkian. (2016). Water, nutrient and carbon recycling in the biorefinery system. Presentation. Algae Biomass, Biofuels and Bioproducts Conference June 18-21 San Diego CA.

T. Lundquist, C. Pittner, Y. Suvorov, T. Chene, L. Medina, T. Steffen, B. Crowe, N. Adler, R. Spierling. (2015). Towards scale-up of biofuel production and wastewater treatment using microalgae. Presentation. Algae Biomass Summit. October 1 Washington DC.

Posters

L. Parker, Y. Survov, C. Pittner, S. Blackwell, N. Adler, R. Spierling, T. Lundquist. (2016). Effect of Sampling Frequency on Microalgae Productivity Estimates. Algae Biomass Summit, October 26, 2016, Phoenix, AZ. Poster Presentation.

L. Gevorkian, R. Spierling, and T. Lundquist. (2015). Anaerobic co-digestion of hydrothermal liquefaction process water with wastewater solids. 9th Annual Algae Biomass Summit; September 29th – October 2nd; Washington, D.C. Poster Presentation.

Y. Suvorov, C. Pittner, N. Adler, R. Spierling, T. Lundquist. (2015). Optimization of Algae Biomass Productivity and Harvesting at Existing High-Rate Pond Municipal Wastewater Treatment Plant. Algae Biomass, Biofuels and Bioproducts Conference Jun 7-10, San Diego CA. Poster presentation.

Detailed Task Reports

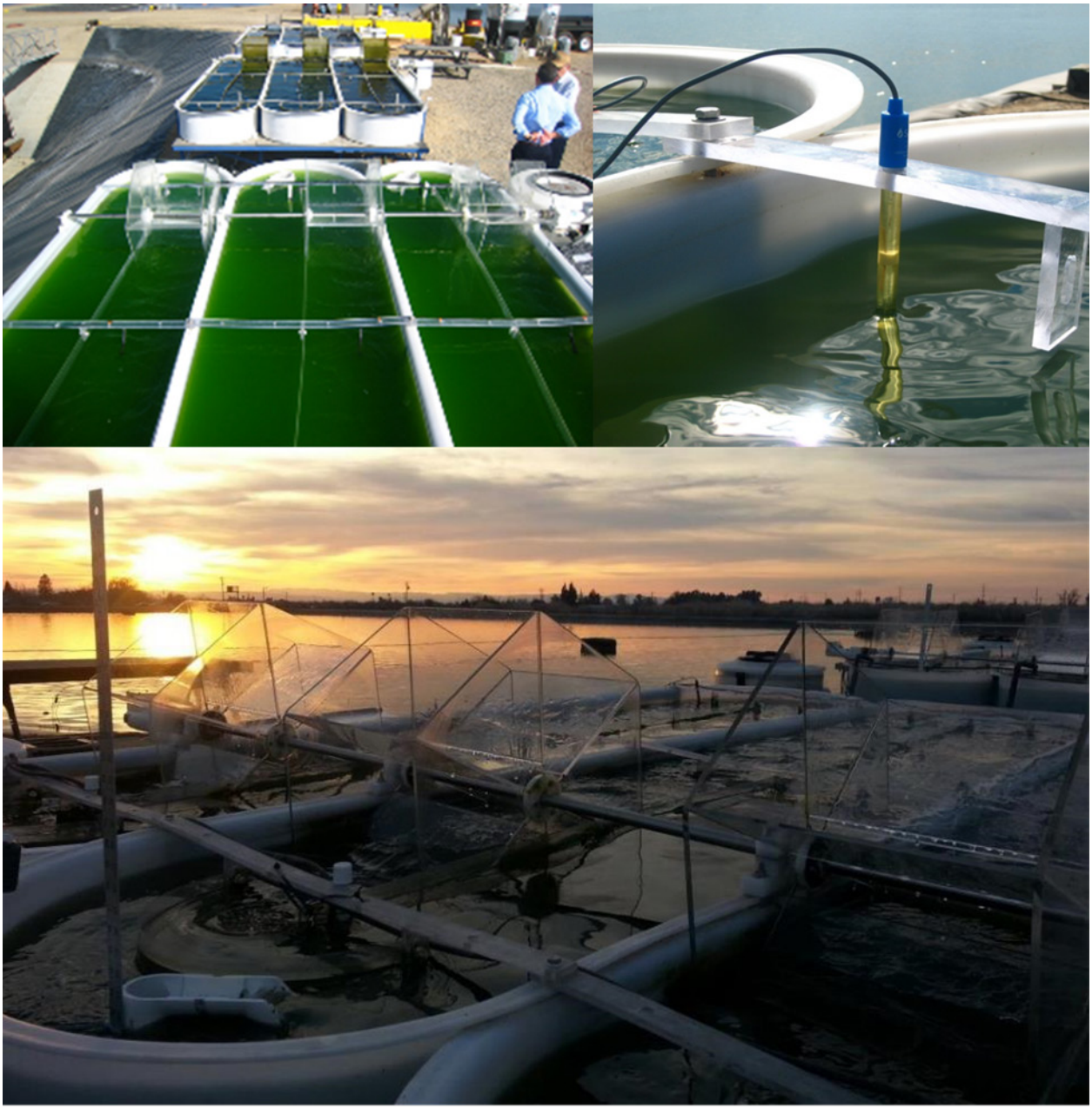

Task 1: Optimize biomass productivity for a selected strain at Delhi.

Pacific Northwest National Laboratory (P.I. Michael Huesemann), in collaboration with Cal Poly and MicroBio Engineering Inc.

Introduction, Background, and State of Research

The use of microalgae to produce carbon-neutral drop-in biodiesel and jet-biofuel has attracted increasing interest. An economically feasible biofuels production process requires that strains be found that exhibit high annual biomass productivities (greater than 25 g/m^2-day) in outdoor culture systems (Davis 2016). Significant efforts have been undertaken in a variety of research organizations to find microalgae strains, through prospecting or genetic engineering, suitable for large-scale, economic biofuel production in low-cost open ponds. This turns out to be a challenge: strains that grow well in laboratory cultures under specific conditions (temperature, light intensities), are not guaranteed to perform satisfactorily in outdoor pond cultures, subject to daily and seasonal water temperature and insolation variations, and short-term light fluctuations.

Two possible solutions to address this problem, both used in this project, are biomass growth modeling and climate-simulated culturing.

The PNNL biomass growth model (Huesemann et al., 2016) has been used to predict outdoor pond performance using a limited number of strain-specific model input parameters measured in laboratory cultures in conjunction with measured or predicted pond temperature and insolation. using The PNNL Biomass Assessment Tool (BAT) (Wigmosta et al. 2011) can be used to provide for specific locations and dates, sunlight intensity and pond water temperature data (or time series, termed "scripts", ML1.0, 1.1). One limitation of the current biomass growth model is that the strains, such as *Chlorella sorokiniana* DOE 1412, were only parameterized for one constant pH (7). Therefore, one objective of this task (ML 1.2, 1.3) was to determine the effect of pH (6-9) on the maximum specific growth rate of this strain, the critical model input parameter to the model.

To reduce the risks associated with initial outdoor pond cultivation trials, accurate laboratory-scale outdoor pond simulators are needed to rapidly screen microalgae strains for high biomass productivity and co-product yields, using simulated sunlight intensity and water temperature scripts, as generated by the Biomass Assessment Tool (Wigmosta et al., 2011) for any geographic location where adequate meteorological data are available.

Light intensity and temperature are the main determinants of biomass productivity in outdoor ponds, assuming nutrient (N, P, CO_2, trace elements) replete conditions and adequate mixing (Huesemann et al., 2016). Therefore, small-scale indoor photobioreactors should, at least in principle, be able to simulate large-scale outdoor raceways if the light and temperature regimes can be adequately replicated. A recent evaluation of the performance of two pond simulators, the PNNL indoor LED-lighted climate-simulation raceways, and the Phenometrics photobioreactors, ePBR^{TM} (Lucker et al., 2014), found that biomass productivity by *C. sorokiniana* DOE 1412 was slightly higher (8-13%) in the PNNL climate-simulation ponds but significantly lower (44%) in the ePBRs, compared to actual outdoor summer pond cultures at Rimrock, Arizona (Huesemann et al., 2017a&b). While the PNNL indoor ponds are reasonably accurate in simulating growth performance of microalgae in outdoor ponds, they are costly to build and operate, while the ePBRs predicted significantly slower growth than observed.

Furthermore, the ePBRs have several additional shortcomings, such as the inability to reliably achieve temperatures below 8 °C which is required for simulating cold season conditions, and, when operated in batch mode, insufficient culture volume (ca. 460 mL at 25 cm depth) for the periodic withdrawal of samples

for biomass and co-products analysis without significantly reducing the culture depth and thus changing the light regime. Therefore, there is a need for small-scale indoor photobioreactors that can accurately simulate the growth performance of microalgae in both the PNNL controlled climate simulation ponds and similar outdoor ponds.

The objective of this task was to develop and test of a new photobioreactor, the Laboratory Environmental Algae Pond Simulator (LEAPS). The specific objectives were to (a) design and build the LEAPS (ML 1.4), (b) evaluate its ability to accurately replicate incident light and culture temperature conditions observed in outdoor ponds (ML 1.5), and (c) validate its performance by comparing the biomass productivity of *Chlorella sorokiniana* and *Nannochloropsis salina* grown in outdoor ponds and in the LEAPS, using similar light, temperature, and culture conditions (ML 1.6). The results of this study have been published in Huesemann et al. (2017c).

Milestone Tasks, and Subtasks/ Purpose

Purpose: Develop laboratory and computer modeling methods capable of rapidly identifying high-productivity strains and optimal culture methods specific to locations. The Delhi location and *Chlorella sorokiniana* (DOE 1412) will be used in the current project.

+ ML1.0 Climate Model Output: Generate a year of daily sunlight and temperature scripts for the Delhi site. Three seasonal scripts (summer, fall/spring, and winter) will be defined (April 30, 2014).

+ ML1.1 Growth Model Output: Use the PNNL Biomass Growth Model (BGM) to predict the productivity of DOE 1412 at Delhi using the ML1.0 seasonal scripts (May 30, 2014).

+ ML1.2 pH Experiment for Growth Model Improvement: Report the maximum specific growth rate of DOE 1412 as a function of pH (6-9) (September 30, 2014).

+ ML1.3 Growth Model Improvement incorporating pH: Extend the BGM for DOE 1412 to account for pH effects based on ML1.2 results and generate new Delhi productivity predictions (December 31, 2014).

+ ML1.4 Develop Climate-Simulating Photobioreactors (csPBRs): Design and build, using off-the-shelf components, a benchtop photobioreactor system that accurately simulates the growth performance of outdoor pond cultures under fluctuating light intensity and water temperature (December 31, 2014).

+ ML.1.5 Initial Validation of csPBRs: Evaluate these climate-simulation photobioreactors (csPBRs) using DOE 1412 by comparing csPBR productivity data (to be collected under the current milestone using previously collected Arizona scripts) with previously collected DOE 1412 data from outdoor ponds in Arizona (March 31, 2015).

> **S1.5 Additional csPBR Experiments**: Use the ML1.4 validated csPBRs to predict the productivity of DOE 1412 at Delhi using the ML1.0 seasonal scripts or actual weather data from the Delhi site. Batch cultivation on defined media will be used. Two rounds of successful csPBR operation will be completed (June 30, 2015 and September 20, 2015).

+ ML1.6 Validation of Growth Model & csPBRs with Delhi Pond Data: Compare Biomass Growth Model predictions to pilot pond and csPBR productivity measurements. The BGM input will be actual weather data from the period of pilot measurements (ML2.3). DOE 1412 will be piloted on defined media at Delhi in batch mode. pH will be kept within a narrow band to make use of the pH-modified BGM of ML1.2 (December 21, 2015).

Methods

Preliminary modeling: Identification of optimal cultivation conditions (ML 1.0, 1.1)

Daily sunlight and water temperature scripts were generated for one entire year via PNNL's Biomass Assessment Tool (BAT) for different pond depths near the Delhi, CA, location. Wigmosta et al. (2011) describe the BAT in more detail. These light and temperature scripts, together with specific growth rate and dark biomass loss data that were measured earlier in the laboratory for *Chlorella sorokiniana* DOE 1412, were entered into the species-specific BAT to predict the monthly biomass productivities at different dilution rates.

Biomass Growth Model refinement: Including pH effects (ML 1.2, 1.3)

The maximum specific (exponential) growth rate of *Chlorella sorokiniana* (DOE 1412) was measured in Phenometrics photobioreactor (ePBR^{TM}) cultures at above saturating light intensity (>250 µmoles/m^2-sec) as a function of pH (6, 7, 8, and 9). To confirm reproducibility of the results, a total of 43 replicate exponential growth rates measurements were taken. After resolving reproducibility problems due to the formation of precipitates in the medium and eliminating partial growth inhibition by photosynthetically produced oxygen via the continuous sparging of all cultures with nitrogen, reliable growth rate data were obtained. Specific (exponential) growth rates were collected at the optimum temperature (36 ºC) of DOE1412 and were used to scale the maximum specific growth rate matrix that serves as input to the species-specific Biomass Assessment Tool (BAT). For example, to run the model at pH 9 instead of pH 7 (standard), the entire maximum specific growth rate matrix is multiplied by a "pH correction factor" of 0.72, which was calculated as 4.21 day^{-1} (the maximum specific growth rate at pH 9) divided by 5.83 day^{-1} (the maximum specific growth rate at pH 7).

The PNNL biomass growth model was run for the two pH 7 scenarios (at 15 and 30 cm depths) using the required input parameters (i.e., the maximum specific growth rate as a function of temperature and light intensity, the specific biomass loss rate in the dark as a function of temperature and the average light intensity during the preceding light period, and the scatter-corrected light attenuation coefficient) which were experimentally determined at pH 7. In order to run the model for the two pH 8.4 scenarios (at 15 and 30 cm depths), the entire maximum specific growth rate matrix $\mu(T,I)$ was multiplied by a "pH adjustment factor" of 0.79, i.e., the ratio of the maximum specific growth rate at pH 8.4, obtained by interpolation of the data shown in Figure 1.5, relative to the maximum specific growth rate at pH 7. It is implicitly assumed for growth modeling purposes that the $\mu=f(pH)$ relationship is the same at all temperatures.

Furthermore, it is assumed that the biomass loss rate and light attenuation data, which were experimentally determined at pH 7, are not affected by pH. The biomass growth model was run with BAT (Biomass Assessment Tool) generated light and temperature scripts for the month of May using 30-year average weather data for Merced, CA, the closest weather station Delhi, CA.

The climate-controlled LEAPS apparatus consists of an acrylic tank with six individual glass reactors, simulating pond water columns. Temperature is precisely regulated by a programmable recirculation bath and light is provided by a multi-color LED array suspended above the reactor columns. Calibrations to date have shown the LEAPS is able to use climate data to replicate light and temperature conditions well within a 5% error across all six individual columns (Huesemann et al. 2017a). The temperature bath can maintain anywhere between 10°C and 60°C with script time resolution down to the minute. The high-intensity LED panel simulates the solar spectrum and can deliver anywhere from 0 to 2,500 µmol photons/m^2/sec across all cylinders, with a script time resolution of 15 minutes.

LEAPs reactors were developed and validated by comparison to outdoor raceway pond growth trials conducted in Rimrock, AZ (Huesemann et al. 2017b) as described in Huesemann et al. 2017a. In brief, scripts with hourly light and temperature data from the Rimrock, AZ field trial were loaded as control scripts into the LEAPs interface. Water temperatures ranged from 15 to 30˚C, and light intensities reached a maximum of 2200 µmol/m^2-s. Reactors were filled to 25 cm depth, matching pond depth during the outdoor field trial, with modified BG-11 media. Inoculum was maintained in 1 L Roux bottles exposed to a constant 500 µmol/m^2-s on a 12:12 (day: night) photoperiod. Cultures were continuously stirred at 150 rpm, and sparged with humidified CO_2-enriched air via a fritted gas diffuser to maintain a pH 7.0 set point. Once inoculated into the LEAPs, evaporative losses were corrected with DI water, and volume removed for sampling was replaced with sterile BG-11 medium. Biomass concentration was measured daily in duplicate bioreactor samples, and the areal biomass productivity (g/m^2-day) was calculated by multiplying the volumetric biomass productivity (mg/L-day) by the culture volume.

Outdoor field experiments were conducted at the Delhi, CA field site to allow further comparisons of both LEAPS and the pH-refined biomass growth model to outdoor pond data. *C. sorokiniana,* initially cultivated in 15 L flat panel photobioreactors (12:12 day: night photoperiod), was used to inoculate triplicate raceway ponds (3.5 m^2 surface area each) located in Delhi, CA. Cultures were grown in batch, using on-site non-potable well water enriched with BG-11 nutrients, at a culture depth of 30 cm. Ponds were chlorinated with a dilute hypochlorite solution prior to nutrient addition, which induced formation of a dark brown precipitate. The precipitate was removed via cotton filters. Pond water temperature was logged hourly, and hourly irradiance was collected from a local weather station (Merced, CA). Pond pH was maintained at a pH 7.5 set point by injection of pure CO_2. Biomass concentration was monitored daily by duplicate ash-free dry weight determination, with samples collected after well-water makeup for evaporative loss. Light intensity and temperature profiles were input into the BGM after inclusion of pH-effects, and the output compared to the biomass productivity measured in the field. Growth conditions (light, temperature, depth, pH) were reproduced in the LEAPs for further validation of the laboratory scale reactors.

Results

Preliminary modeling: Identification of optimal cultivation conditions (ML 1.0, 1.1)

Figure 9 shows an example of predicted hourly pond water temperatures for a pond of 20.5 cm depth for the 10th day of January and July. As expected, pond water temperatures are on average 15 ºC higher in July than in January and increase during the daytime and decline at night. Figure 10 shows predicted monthly biomass productivities for 24 cm deep ponds operated near Delhi, CA. The predicted biomass productivities are zero or close to zero from November to March since *Chlorella sorokiniana* DOE 1412 does not grow below 13 ºC and is washed out. The highest predicted biomass productivity for the summer season was found to be around 25 g/m^2-day for dilution rates 0.3 and 0.4 day^{-1} (hydraulic retention times of 3.3 and 2.5 days, respectively). The predicted annual biomass productivities for the 0.1, 0.2, 0.3, and 0.4 day^{-1} dilution rates were 5.7, 7.5, 7.5, and 5.6 g/m^2-day, respectively.

Biomass Growth Model refinement: Including pH effects (ML 1.2, 1.3)

Figure 11 shows the average maximum specific growth rate as a function of pH for experimental runs 35 to 40. The maximum specific growth rates were highest (close to 6 day^{-1}) at pH 6 and 7 and declined to 4.9 day^{-1} at pH 8 and 4.2 day^{-1} at pH 9. These results indicate that pond cultures likely to achieve highest biomass productivities at pH 7. However, maintaining pH 7 in outdoor ponds is likely to result in significant CO_2 outgassing. A closer analysis of the trade-off between lower biomass productivities and greater CO_2 utilization efficiencies at higher pH (>7) is needed.

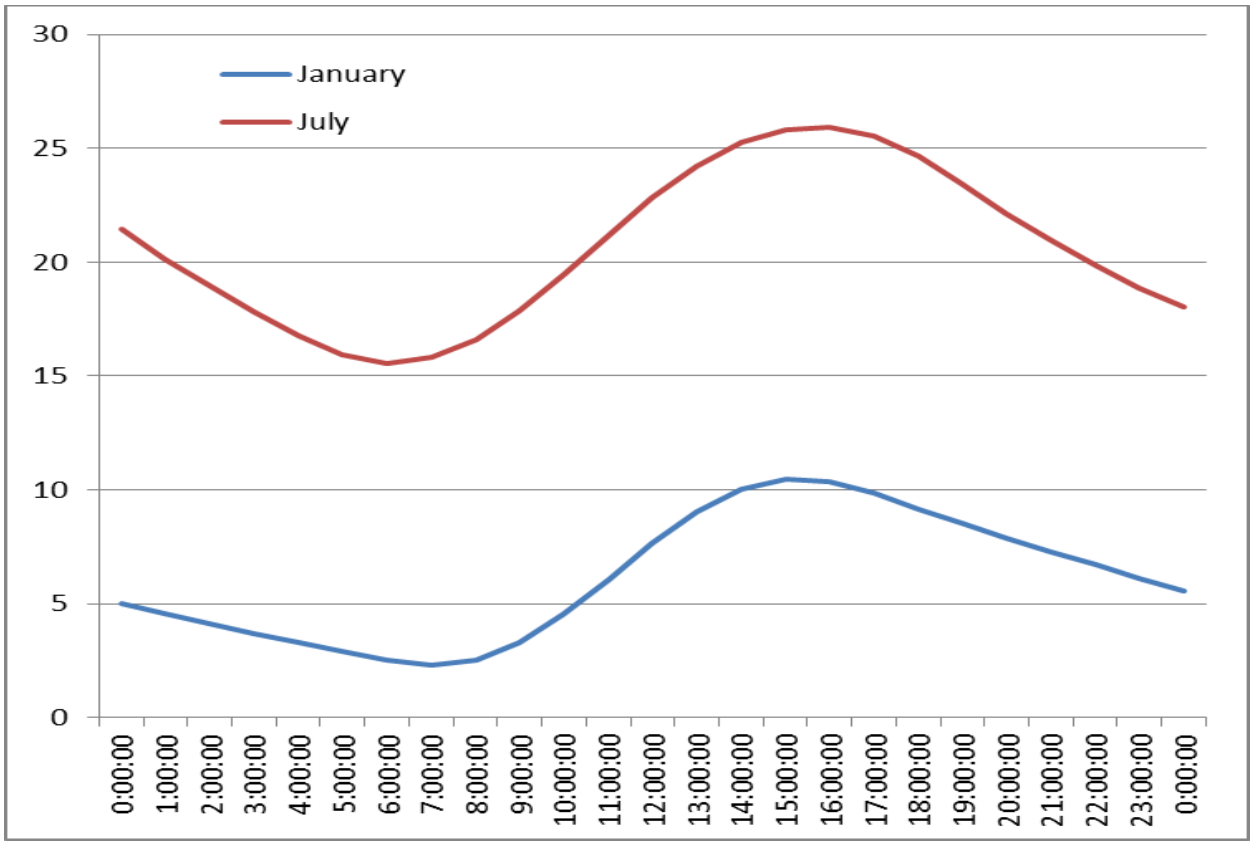

Figure 9: Representative BAT generated hourly pond water temperature "scripts" for a 20.5 cm deep pond for the 10th day of January and July near the Delhi, CA, location (Weather Station 45532, Merced, CA).

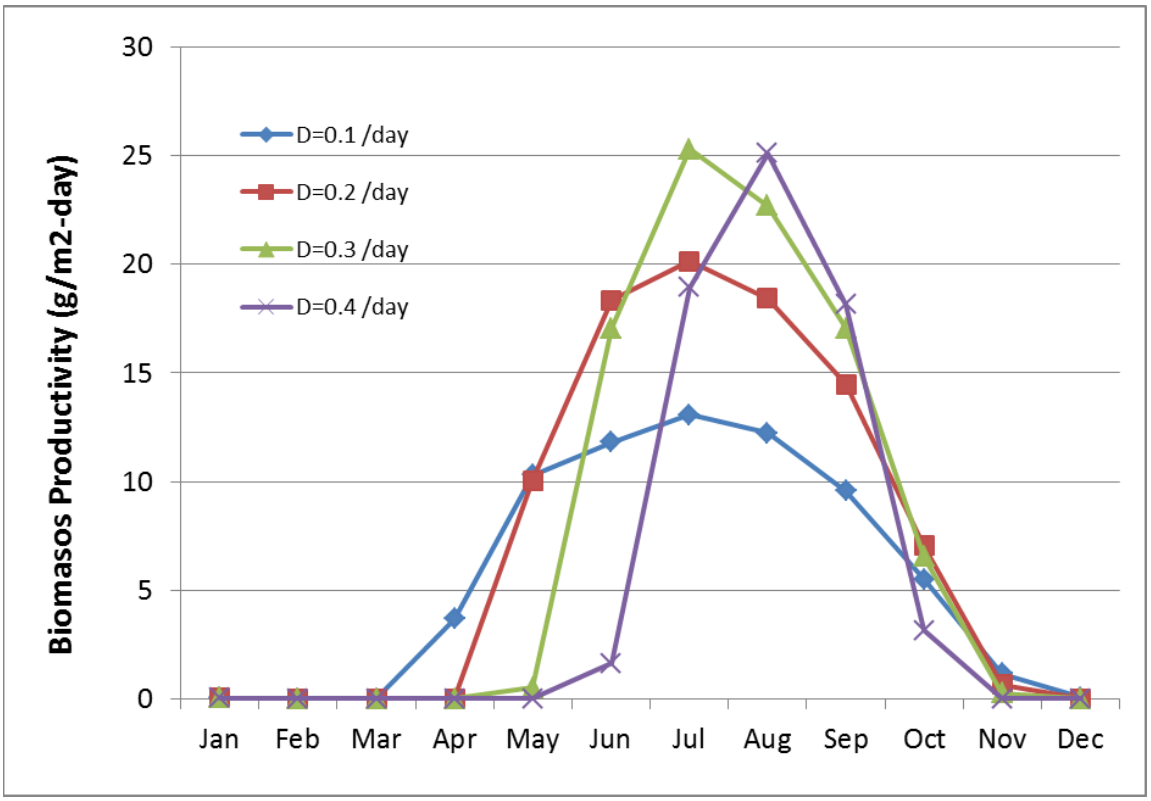

Figure 10: BAT generated monthly biomass productivity predictions for *Chlorella sorokiniana* DOE 1412 in 24 cm deep ponds operated at four different dilution rates (D) near Delhi (Weather Station 45532, Merced, CA).

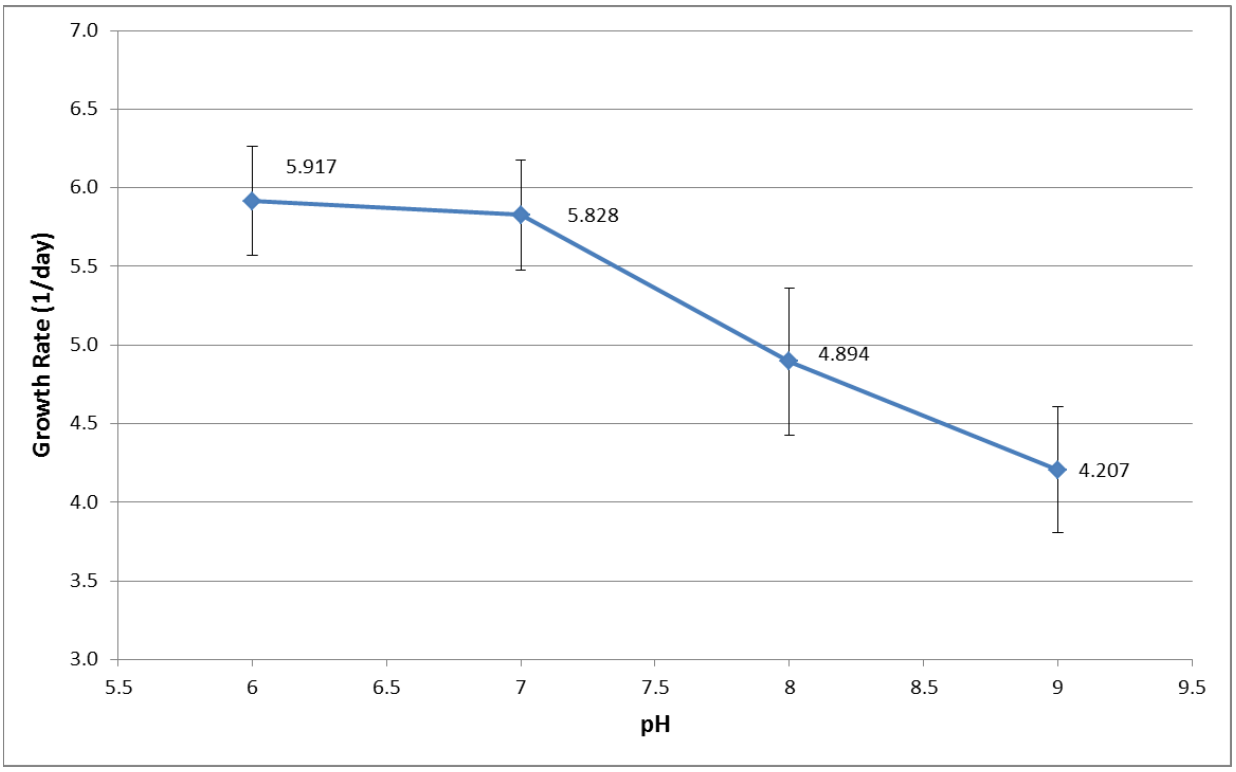

Figure 11: Average maximum specific growth rate of *Chlorella sorokiniana* (DOE 1412) at 36 ºC as a function of pH. Error bars represent one standard deviation. See 4QFY14 progress report for additional details.

The relationship developed between specific growth rate and pH was incorporated into the biomass growth model to predict monthly productivity as a function of pH. Productivity was calculated for 24 cm deep ponds operated at a daily dilution rate of 0.3 day^{-1} at four different pH set-points (6,7,8, and 9) at Delhi, using historical weather station data from nearby Merced, CA (Figure 12). A dilution rate of 0.3 day^{-1} was chosen since earlier BAT simulations had demonstrated that annual biomass productivities at Delhi, CA are highest at this dilution rate. The predicted monthly biomass productivities are greatest for the pH 6 and 7 pond cultures and decrease with increasing pH. The predicted annual biomass productivities are 7.9, 7.6, 5.4, and 3.4 g/m^2-day for the ponds maintained at pH 6, 7, 8, and 9, respectively. Given that the annual biomass productivity is only slightly higher at pH 6 than pH 7 and that significant amounts of CO_2 will outgas from ponds maintained at pH 6, it can be concluded that the optimum operating pH for outdoor pond cultures is around 7.

To guide pilot plant operations in Delhi, the biomass growth model was used to predict biomass productivity as a function of pond depth (15 and 30 cm) and pH (7 and 8.4) during the month of May. The BAT predicted wider diurnal temperature swings 15 cm deep ponds, reaching temperatures 5 ºC higher during the day and 3.6 ºC cooler at night than the 30 cm deep pond. Predicted AFDW versus time data for a typical modeling run (pH 7, 30 cm) shows higher biomass productivity over the first five days of growth than the last five. Since the modeling algorithm assumes that biomass is lost in the dark zone of the pond as the biomass concentration increases, the biomass productivity (slope) during the first 5 days is generally greater than the biomass productivity during the first 10 days.

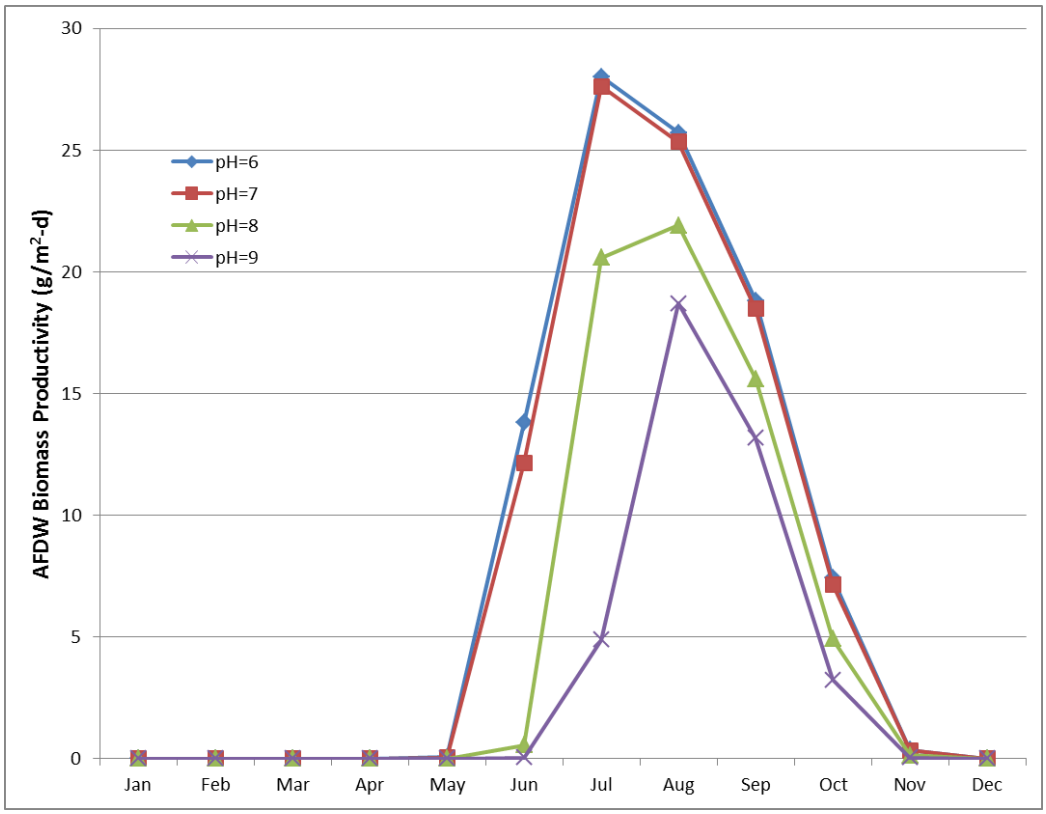

Figure 12: BAT generated monthly biomass productivity predictions for *Chlorella sorokiniana* (DOE 1412) in 24 cm deep ponds operated at four pH set-points at a daily dilution rate of 0.3 day-1 near Delhi, CA (Weather Station 45532, Merced, CA).

The discrepancy between 5 and 10-day biomass productivities is most pronounced for fast growing cultures where the high biomass density results in an earlier onset of biomass losses, presumably due to respiration with the decreasing light/cell in the culture. To account for this phenomenon, the average of the 5- and 10-day areal biomass productivity was determined for all four scenarios and plotted in Figure 13. For both pH 7 and 8.4, the predicted biomass productivity was higher in the 15 cm pond than in the 30 cm pond because higher daytime and lower nighttime temperatures in the 15 cm pond result in faster growth during the daytime and less biomass loss during the nighttime, as compared to the 30 cm pond. For a given depth, the biomass productivity at pH 8.4 was lower than at pH 7, due to the use of the "pH adjustment factor" of 0.79 in the modeling algorithm.

Based on a model-assisted evaluation of all four pond operation conditions, the highest biomass productivity (ca. 18 g/m^2-day) is expected to be achieved in 15 cm deep ponds operated at pH 7. There are many uncertainties in these models, such as use of 30 year historical weather data, assuming that temperature does not affect the μ versus pH relationship in Figure 11, assuming that pH does not affect the biomass loss rate and light attenuation, unknown biomass loss rates in the aphotic zone of a dense pond culture and differences in temperature swings in the indoor vs. outdoor cultures. Further validation of these model predictions with measured biomass productivities in outdoor Delhi, ponds is needed.

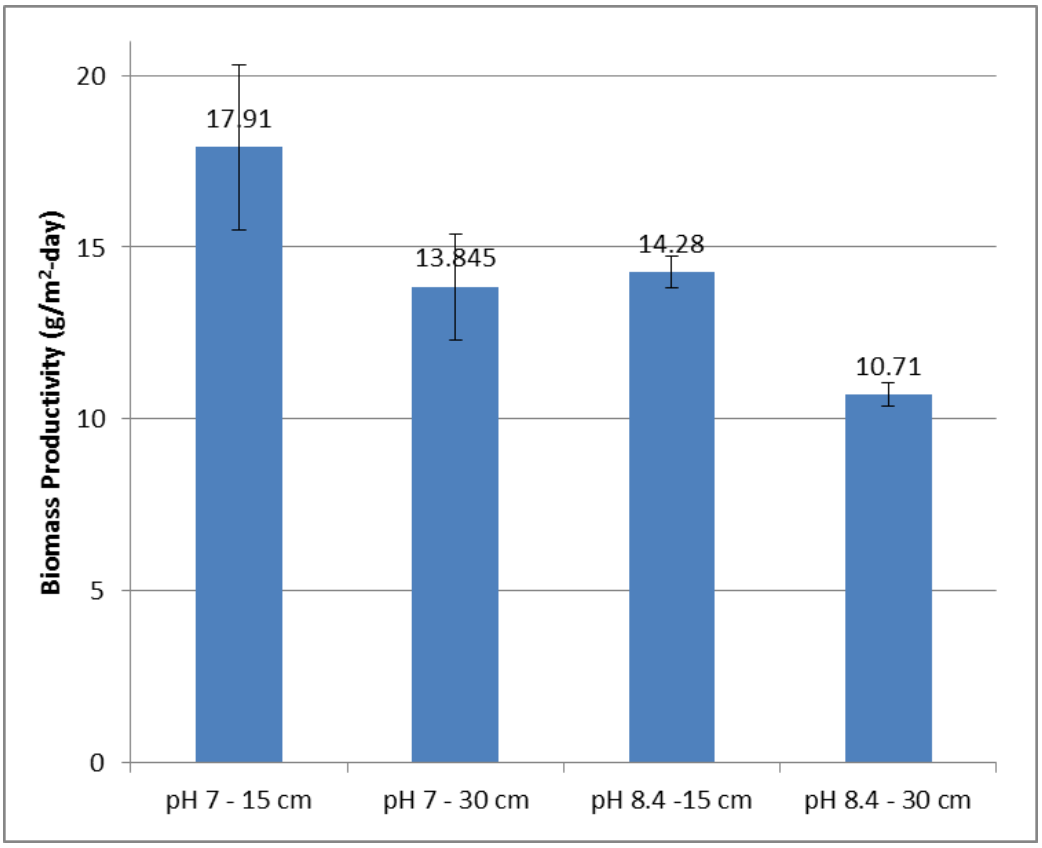

Figure 13: Model-predicted average biomass productivities for *Chlorella sorokiniana* (DOE 1412) pond cultures operated at the four different low/high pH and depths scenarios during the month of May. The height of each bar is the average of the predicted biomass productivities during the first 5 and 10 days. The top of the upper bar is the value of the 5-day biomass productivity, and the bottom of the lower bar is the value of the 10-day biomass productivity.

Development and validation of a laboratory-scale strain screening tool: The Laboratory Environmental Algae Pond Simulator (LEAPS) (ML 1.4, 1.5, s1.5, 1.6)

Preliminary cultivation trials in the LEAPS were conducted to refine and develop reactor management. Relative to the outdoor ponds, growth in the LEAPS cultures during initial trials was slower than anticipated. This was most likely due to problems related to vertical mixing and CO_2 limitation (i.e., too low gas flow rate and too large bubbles). Spargers with a smaller pore size and stir bars with improved vertical mixing were incorporated into subsequent trials. During another trial, biomass density increased unpredictably from one day to the next, likely due to washing the biomass that accumulated on the sides of the cylinder back into the columns instead of wiping it out as was done before. During the ninth validation run, biomass growth in the LEAPS column bioreactors was significantly faster than in the outdoor ponds because of excess light coming through the walls of the three unused columns in the acrylic tank. On day 8, the inactive cylinders were covered and there was an obvious and immediate change in the growth rate. During the tenth validation run, covers were used for the inactive cylinders to try to limit incidental light. Initial growth based on OD_{750} was much slower compared to the previous run. The LEAPS over-predicted growth based on OD_{750} by 22.7%, although when compared on an AFDW basis, the LEAPS over predicted biomass accumulation by only 11.4%.

We conducted one final validation experiment using climate data from Rimrock, AZ to confirm the reliability of the LEAPS. The run was conducted using two LEAPS cylinders with BG-11 medium, *C. sorokiniana* DOE 1412, and climate data from Rimrock, AZ. All cylinder walls were painted to eliminate extraneous light and a depth of 25 cm was maintained. In the eleventh, and final, validation run, the LEAPS over predicted growth based on OD_{750} by 3.5%. Based on AFDW, the LEAPS under predicted biomass productivity by 7.1% (Figure 14).

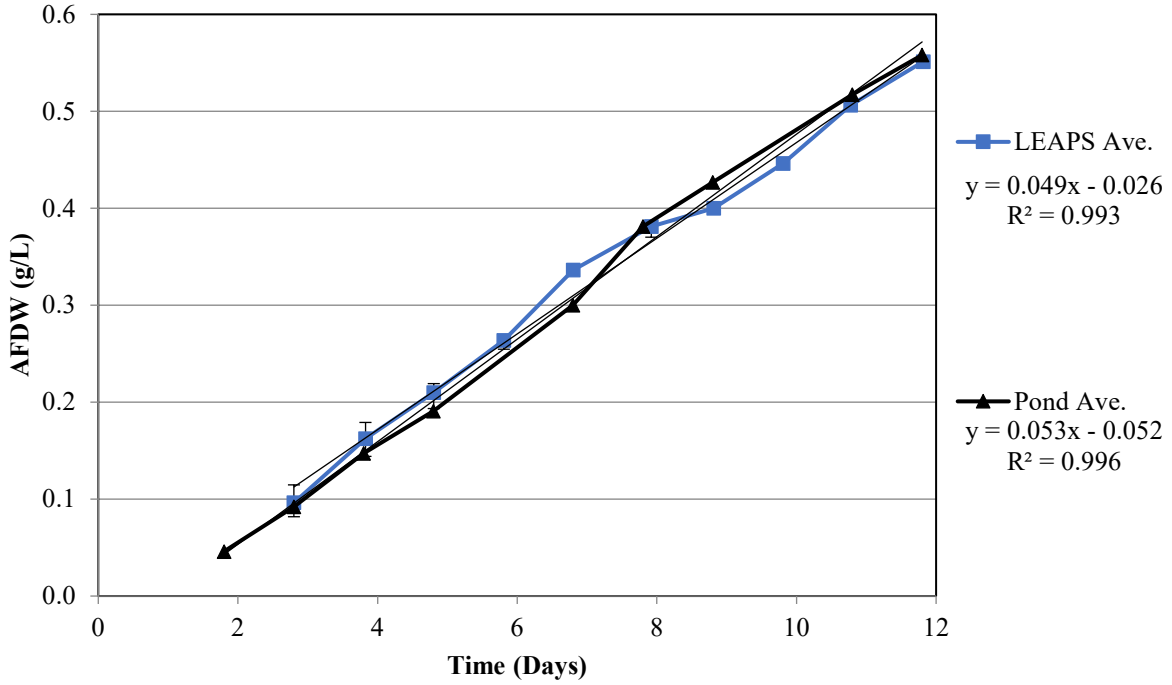

Figure 14: Volumetric biomass productivities calculated via linear regression of ash free dry weight versus time from run #11. The LEAPS data are blue solid line, the outdoor Arizona pond growth the black solid line.

Figure 15 shows the model-predicted versus measured AFDW concentration as a function of time for the Delhi outdoor ponds, LEAPS cultures, and biomass growth model predictions. Overall, the model was successful in predicting the overall growth performance of the triplicate outdoor pond cultures conducted at Delhi in June and July of 2015. The model- predicted biomass productivity is ca. 23% higher than was measured in the outdoor ponds. While this slight over-prediction could be caused by the inherent uncertainty of the species-specific model input parameters, it is also likely that the non-potable well water used for medium preparation, which was treated with Clorox prior to pond inoculation resulting in the precipitation of metals, could have slightly inhibited growth. Furthermore, the cultures may have been stressed given that after 10 days, the ponds started flocculating and biomass production slowed down.

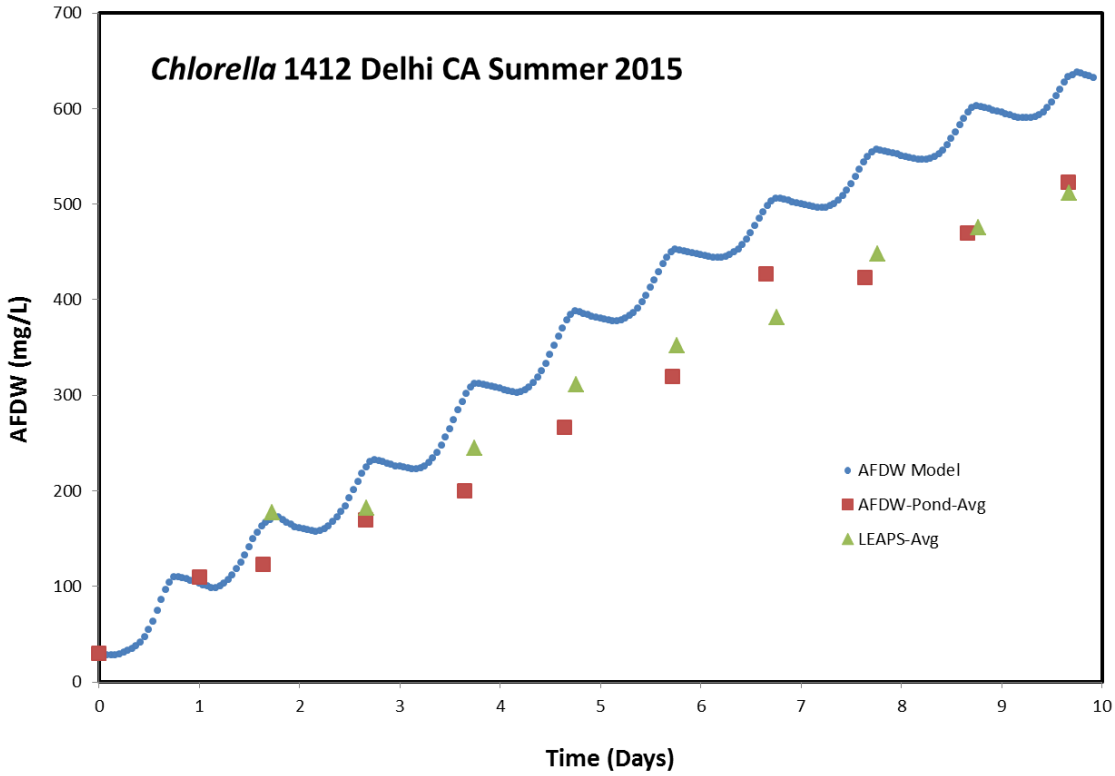

Figure 15: Model-predicted (blue line) versus measured AFDW concentration of *Chlorella sorokiniana* DOE 1412 as a function of time for the triplicate outdoor pond cultures in Delhi, CA (red squares), and the triplicate LEAPS climate-simulated cultures at PNNL (olive triangles).

Conclusions and Recommendations

LEAPS is a pond simulator that can out-perform ePBRs in reproducing pond algae growth rates. It has predicted biomass productivities within 10% of values measured in outdoor ponds using climate data from two geographically distinct locations. Currently the LEAPS is capable of simulating pond temperatures between 10 and 31°C and can deliver up to 2675µmol/m^2/s within 5% of set-point values. To our knowledge, this is the only bench-scale pond simulator that can replicate growth in outdoor algae ponds over a wide range of climatic zones, geographical locations, and at various depths (up to 35 cm) while being small enough to easily run up to six replicates but still large enough to take AFDW measurements without affecting operations.

In conclusion, the LEAPS was demonstrated to be a reliable photobioreactor system for quantifying the biomass productivity of microalgae under climate-simulated conditions. There are several key benefits of using the LEAPS photobioreactors, rather than outdoor ponds, for strain evaluation: First, using light and temperature scripts generated by PNNL's Biomass Assessment Tool for any geographic location on earth where meteorological data are available (Wigmosta et al. 2011), strains can be tested for any climate or season of choice at any time, without waiting for the desired season to arrive, thereby allowing for much faster throughput.

Second, testing in LEAPS photobioreactors is less capital and labor intensive, and therefore more cost effective. Third, it is easy to test different operational strategies for optimizing seasonal or annual biomass productivities, such as varying culture depth, changing dilution rates, or evaluating harvesting strategies.

Finally, strains can be objectively compared to each other by using the same seasonal light and temperature scripts, something that is very difficult to do in outdoor ponds due to the vagaries of weather.

Task 2: Maximize algal productivity and harvesting efficiency in Delhi pilot ponds

(Cal Poly and Todd Lane Lab Sandia National Lab, in consultation with MicroBio, PNNL, and Delhi County Water District)

Introduction, background, state of research

In this task, we researched algal cultivation and harvesting practices to maximize the outdoor biomass and biofuel productivity of wastewater grown polycultures to >2,500 gallons/acre-year and validated a biomass growth model and cultivation system with *Chlorella sorokiniana* strain DOE 1412. Research was performed in the inland community of Delhi, California at a 0.6 MGD full-scale wastewater treatment facility. The full-scale system consisted of two raceway ponds (3.2 and 3.4 acres) operated in series and was characterized to determine baseline productivity under the existing operational conditions. Nine 1,000-L pilot-scale raceways ponds were used to explore operational conditions including dilution rate and CO_2 addition that optimized biomass productivity and waste treatment. The work with the DOE 1412 was used to validate the Biomass Growth Model (BGM) and climate simulating reactors (LEAPS) developed by PNNL in Task 1. Finally, the samples were analyzed genetically to evaluate consortia and/or strains associated with superior treatment, settling performance, and biomass productivity.

Algae-based wastewater treatment systems are prevalent, with over 5,000 pond-based municipal wastewater treatment systems currently in use in the country (EPA 2002). Many, if not most of these pond-based systems, are not optimized for algae biomass production. They utilize deep facultative ponds (0.6 - 6m deep) without CO_2 addition. Typically, these systems are highly effective at removing suspended solids and biochemical oxygen demand (BOD) from wastewater at a relatively low energy input and low-cost when compared with conventional treatment systems but have more variable performance when it comes to nitrogen removal. Additionally, these systems typically also require substantial amounts of land and can produce significant amount of sludge or biomass, that was typically considered a liability in the past due to hauling and disposal costs.

In contrast, high-rate algae ponds (HRAPs) are simple, low-energy, and low-cost wastewater treatment systems that consistently produce high quality effluent, and biomass which can be used for fertilizer, feed, or biofuels (Craggs et al 2012, Park et al. 2011, Lundquist et al. 2010, Garcia et al. 2000, Oswald et al. 1957). High rate algae ponds (HRAP's) were developed by Oswald in the 1960's to treat wastewater while optimizing algal biomass production. HRAP's differ from conventional wastewater treatment ponds in several ways: they are much shallower with a typical depth of 0.3 - 0.6m, they utilize low intensity paddlewheel mixing, and CO_2 can be added to increase biomass yields. The shallower depth of HRAPS allows light to penetrate the depth of the ponds and the paddlewheel mixing agitates the culture so algal cells are cycled from the low-light bottom of the pond to the higher light top. CO_2 addition proves pH control and the critical carbon needed to maximize algae biomass yields. In an ideal system the CO_2 would come from a waste sources such as from the combustion of biogas from and anaerobic digester. Despite optimization, nutrient removal may still be variable especially during low light months (winter).

Coupling wastewater treatment with biomass production allows for the recycling and utilization of the water, carbon, and nutrients in the wastewater and substantially lowers the cost of biofuels production (see Task 5). Another benefit of optimized algae-based wastewater treatment is the potential for bioflocculation of the biomass into aggregated particles that settle by gravity without the aid of chemicals or energy intensive harvesting processes such as membrane filters or centrifuges for separation.

High-rate algae ponds and deep facultative ponds rely on a complex consortium of algae, bacteria, protozoans, fungi and more to treat the wastewater (Figure 16). The major processes are mediated by algae and bacteria with the algae utilizing sunlight to produce oxygen. This oxygen is then in turn utilized by the bacteria to degrade organic carbon to CO_2 which can then be utilized by the algae. Nutrients such as nitrogen and phosphorus are absorbed and incorporated into algae biomass and adsorbed to the cell walls. Bacteria called nitrifying bacteria may oxidize ammonia nitrogen to nitrate if the organic content is high and the dissolved oxygen is high. In HRAP's with high organic loads bioflocculation, or aggregation of algae and bacterial cells into larger flocs may occur and significantly reduce or eliminate the need for added chemicals or processes to remove the algae from the water at the end of treatment. The mechanisms and culture conditions that lead to good bioflocculation and gravity settling are typically poorly understood.

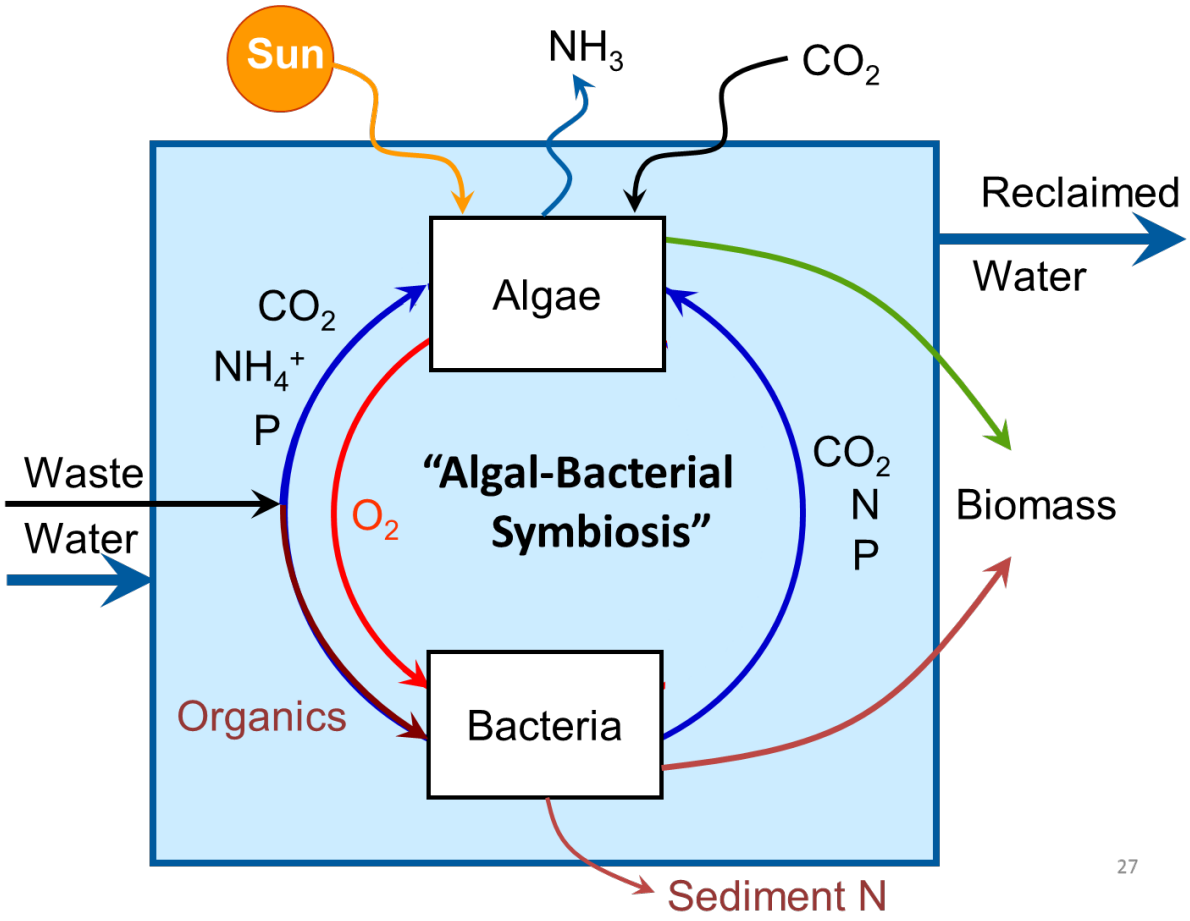

Figure 16: In a wastewater treatment pond organic carbon is consumed and converted to CO_2 by bacteria. This CO_2 is then utilized by the algae and they in turn produce O_2 that is consumed by the bacteria. Nutrients are also solubilized and recycled.

To optimize the cultivation and harvesting of algae biomass from algal wastewater treatment systems the prokaryotic and eukaryotic communities in the 10,000 L pilot ponds at the San Luis Obispo, California field station were studied. Traditionally, field station operators use visual observation via microscopy is used to provide qualitative descriptions of the eukaryotic pond community. The flocculated and filamentous nature of the native algal consortium typical of wastewater ponds presents difficulties when

quantifying population composition. Algal and bacteria assemblages clog tubing used in automated approaches, forcing the use of manual techniques. Operator subjectivity, as well as difficulty achieving enough counted cells to minimize statistical uncertainty, makes cell counts and biovolume estimates error prone. In the current work, we employed high throughput genetic sequencing to track the microbial community in ponds fed treated or untreated municipal wastewater. In addition to routine pond measurements to track biomass productivity and harvestability, samples were collected for analysis of the microbial communities at Sandia National Laboratories. These communities are correlated with the measured productivity and settling data to identify bacterial community members favorable for optimized biomass cultivation in the waste water systems. To perform these studies, we use amplicon sequencing of the 16s and 18s rRNA sub regions, followed by state-of-the-art metagenomics and amplicon sequencing pipeline (MAGPie) software to identify and characterize the prokaryotic and eukaryotic species present in the samples. Further, we use advanced statistical and data mining techniques to derive correlations between desired characteristics (i.e. biomass productivity, settling efficiency) and microbial ecology.

Milestones tasks and subtasks/ purpose

Purpose of Task 2: Develop cultivation and harvesting practices to maximize outdoor biomass/biofuel intermediate productivity for polyculture and a specific strain (targeting >2,500 gallons/acre-year). Generate pilot plant performance data to evaluate the Biomass Growth Model and the climate simulating photobioreactors of Task 1.

ML2.0 Characterize Existing Full-Scale System: Estimate baseline biomass productivity and settleability for the existing full-scale plant under two different process flow configurations.

ML2.1 Design & Install Pilot Plant: Design and install tank raceway ponds.

ML2.2 Shakedown Pilot Plant: Install controllers and demonstrate trouble-free operation of the pilot scale systems for algae growth and bioflocculation studies, settling tanks, pond water temperature monitors, pH controllers, and influent flow rate controllers.

ML2.3 Compare Strains: Compare biomass productivity of (1) a wastewater polyculture and (2) DOE 1412 grown on defined media. The DOE1412 data will also be used for ML 1.6 model and csPBR validation.

ML2.4 Dilution Study: Determine the effect of wastewater dilution rate on biomass productivity, treatment performance, nutrient assimilation, settling efficiency, and dewaterability with native polyculture.

ML2.7 Organism Identification (ID): Identify genetically strains or consortia, along with identification of other dominant organisms in the cultures, such as zooplankton. Look for relationships between dominant organisms and culture performance.

Methods

Full-Scale system description

The inland city of Delhi, California (population 10,000) operates a 0.6 MGD (2.4 ML/day) wastewater treatment plant on 48.3 acres. The treatment plant is located at a latitude of 37.4 N on Highway 99 and serves 7,500 residents and 2,300 residential and commercial connections (Figure 17, Figure 21). Plant effluent is collected from a deep sump located offsite of the wastewater treatment plant and then pumped to the headworks (Figure 18). The remainder of the wastewater treatment plant operates through gravity. The headworks consists of a bar screen and an inclined rotary screen that removes large debris and rags. From the inclined screen, the flow is split between two deep facultative ponds operating in parallel. The influent to the deep facultative ponds (4 m) enters in a deep trough (6 m) in the center of the ponds where the solids settle and digest. The facultative ponds also each contain two surface aerators and 1/3 of the

outer high rate pond is recirculated to the top of the facultative ponds to create an aerobic cover to combat odors. Overall the residence time in the facultative ponds is approximately 29 days. Some algae biomass grows in the facultative ponds but is generally restricted to the aerobic zone and/or first foot of depth due to light limitation at deeper depths.

From the facultative ponds the water travels to the first high-rate pond called the inner high-rate pond (HRPI). This pond is 3.2 acres (1.3 ha) with 2 - 3 ft depth (0.6 - 0.9m) and a residence time of 3.7-5.2 day from summer to winter. A large pipe near the paddlewheels allows the transfer of water from the inner to outer high-rate pond (HRPO). This pond is 3.4 (1.4 ha) with 2 - 3 ft depth (0.6-0.9m) with a residence time of 3.7 - 5.2 day from summer to winter. 1/8 of the flow from HRPO is recirculated back to the facultative ponds to form an aerobic cover and the remainder travels to a rapid mix tank where it is dosed with an aluminum chlorohydrate based coagulant at 20 - 100 mg/L depending on settling performance. From the rapid mix tank, the coagulated biomass travels to the algae settling ponds (ASP).

The ASPs consist of a deep (4 m) and 1,376 m^2 ponds and a one-day HRT. Typically, only one ASP is filled at a time with the other being drained and cleaned. Depending on the season and amount of biomass present this cycle happens every two to four weeks. Water leaving the ASP then travels to the maturation pond for polishing. The maturation pond is a deep-large pond with baffles to prevent short circuiting. The HRT is 14 days and little to no algae grows in the MP. From the MP waster is added to 11.5 acres of percolation basin to recharge the groundwater aquifer. No ponds receive CO_2 addition or pH control in the full-scale system.

Biomass from the ASPs are pumped to one of four drying beds. There are three sand drying beds and one concrete drying bed (Figure 19). A dewatering polymer is added in-line as the harvested biomass travels to the drying beds. Each drying bed has a sump and pump to remove water from the drying bed and this is returned to the HRPO.

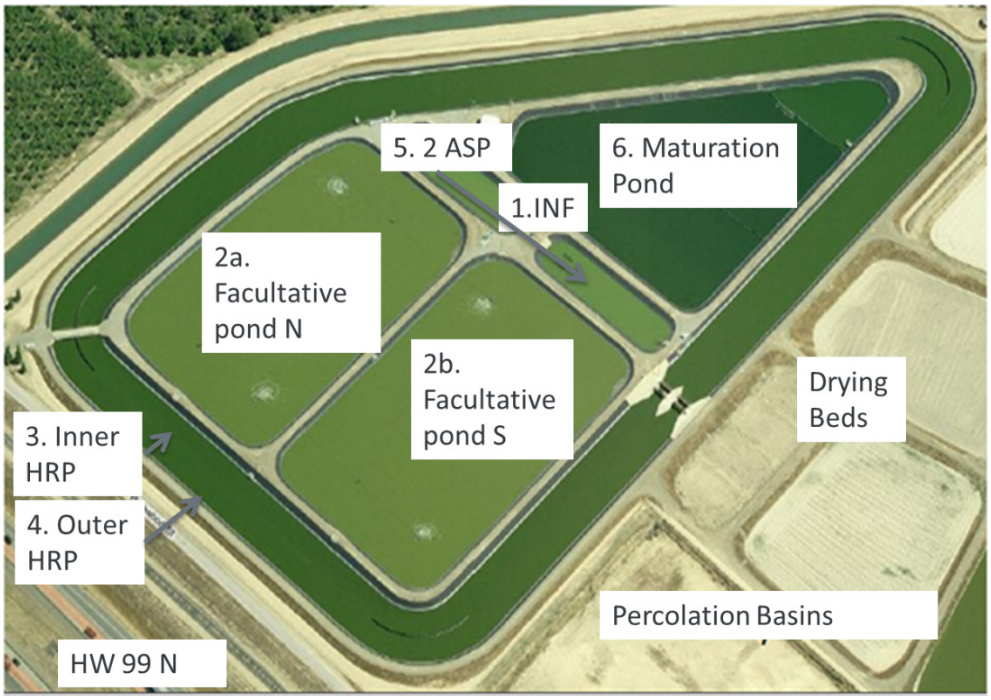

Figure 17: Plan view of the major unit processes at the Delhi wastewater treatment plant.

Figure 18: Major unit processes at the Delhi wastewater treatment plant including (1) the influent bar and rotary screen (2) a faculatative pond with a floating aerator (FAC), (3) the paddle wheels of the high-rate ponds (HRAP), (4) an empty algae settling pond (ASP) and (5)the maturation pond (MP).

Figure 19: Solids handling at the Delhi wastewater treatment plant including (1) Decanting the algae settling pond (2) the concerete drying bed, (3) and piles of solar dried biomass.

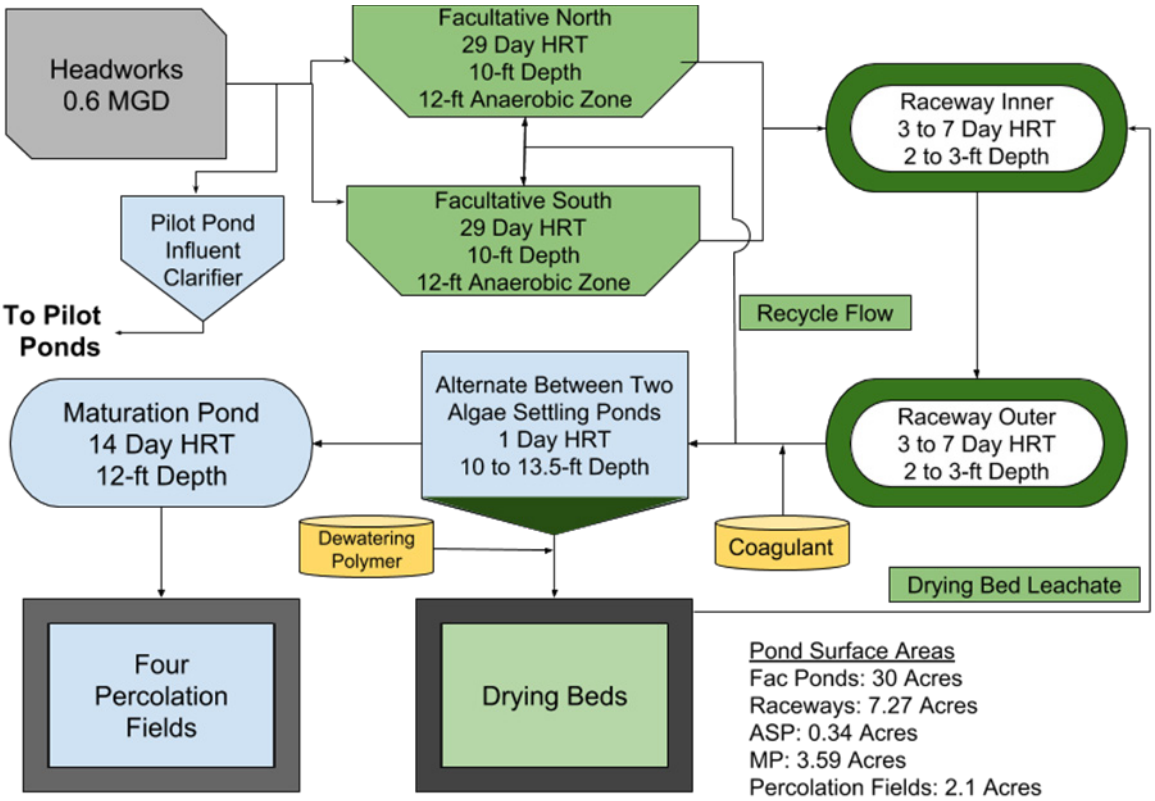

Figure 21: Process flow diagram for the Delhi wastewater treatment plant (Pittner 2018.)

Full-scale high loading experiment

The population of the community of Delhi, California is expected to increase in the coming years. Therefore, from 4/07/13 to 6/30/13 the Delhi full-scale wastewater treatment plant was operated under high loading conditions to verify that wastewater treatment plant could function properly if the flow to plant doubled. Typically, the facultative ponds operate in parallel and the high-rate ponds operate in series from the inner to outer HRAP (Figure 22a). To create the high loading conditions, the north facultative pond (FACN) and the outer high pond (HRPO) were operated in series (Figure 22b). This reduced the overall summer residence time through the facultative ponds and the high rate ponds from approximately 36 days to approximately 18 days and the residence time in the high rate ponds from 7.2 to 3.7 days. The remainder of the wastewater treatment plant was operated normally. Samples were collected to determine biomass productivity under the high loading conditions and compared to biomass productivity from the subsequent year under the normal loading conditions.

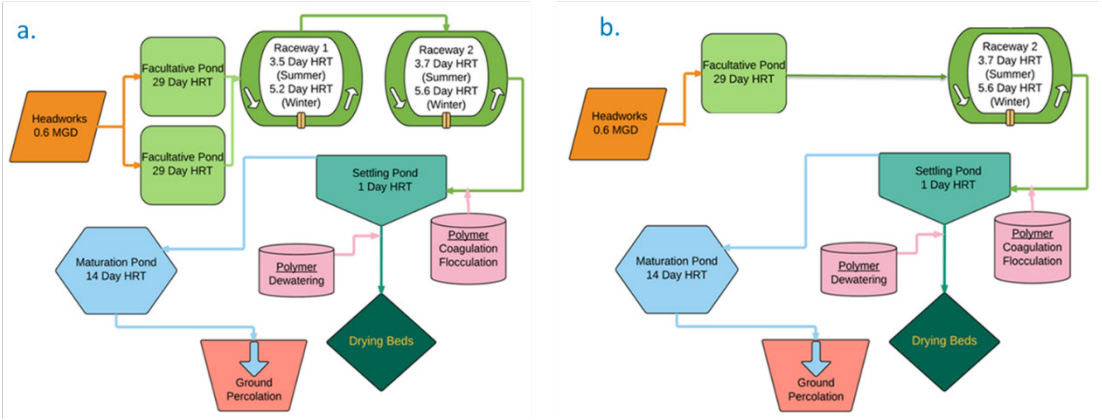

Figure 22: Process flow diagram of the normal (a) and high (b) loading conditions (Y. Suvorov et al. 2015).

Pilot-scale system description

The pilot-scale system consisted of nine 3.5-m^2 ponds (30 cm depth, 1,000 L) with automated controls, settling units and drying beds (Figure 26, Figure 27). The ponds were operated in triplicate and called the North (N1, N2, N3), Middle (M1, M2, M3) and South (S1, S2, S3) ponds. The ponds were located between the North FAC and ASP near the plant influent (Figure 23). The ponds were designed and built by MicroBio Engineering Inc. and they provided technical advice and service for the ponds over the duration of the project. One innovative aspect of the ponds was the clear paddlewheels that reduced light shading of the algae cultures (Figure 24).

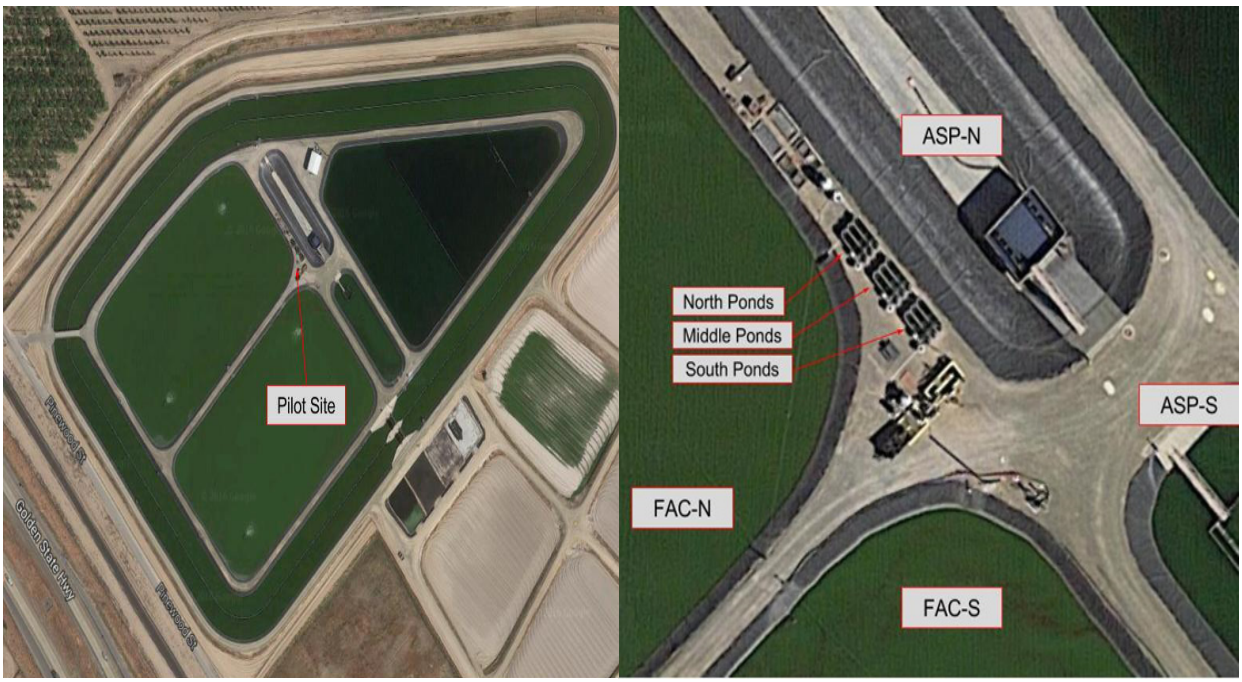

Figure 23: Plan view of pilot site. Image from Google Earth.

Figure 24: MicroBio Engineering Inc. 3.5-m^2 pilot ponds and settling tanks located in Delhi.

The experimental variables included hydraulic residence time (HRT) (Equation 2), CO_2 addition and water source (Table 2). The water sources consisted of primary clarified wastewater and the north facultative pond (FACN). Primary clarified wastewater was produced by pumping raw wastewater from the effluent of the full-scale inclined rotary screen to a 250-gallon (946-L) cone bottom tank with a 2-hour residence time. To remove accumulated solids from the clarifier the tank was drained each night with an automated valve. The tank was then allowed to fill and settle for two hours before the influent to the ponds started each day. Facultative pond water was pumped from the FACN by a 0.5 HP (100 GPM) sump pump suspended on a steel cable. The pump rested two feet below the water surface and 5 feet above the bottom of the FACN (Figure 25). Facultative pond water was pumped to a 55-gallon constant head tank that was wrapped in reflective material for insulation and to prevent growth in the tank. It was mixed with a sump pump to prevent the settling of any biomass removed from the facultative pond.

Equation 2: Hydraulic residence time

$$Hydraulic\ Residence\ Time = \frac{Pond\ Volume}{Influent\ Flow\ Rate}$$

Both source waters (primary clarified influent and facultative pond water) were delivered semi-continuously by gravity between 8:00 AM and 4:00 PM. Based on the timing in the control system

programming, a 1-inch actuated valve (Hayward Flow Control, Clemmons, North Carolina) was opened every hour and influent was added to a pond. Influent dosing for each pond was staggered to ensure that the starting head was constant in the primary clarifier and the facultative influent tanks. Flow rates into each pond were calibrated weekly using two 20-L buckets and a 4-L graduated cylinder to capture and measure the influent pulse volume. The valve open time was then adjusted in the control system programming to maintain the desired residence time and influent pulse volume.

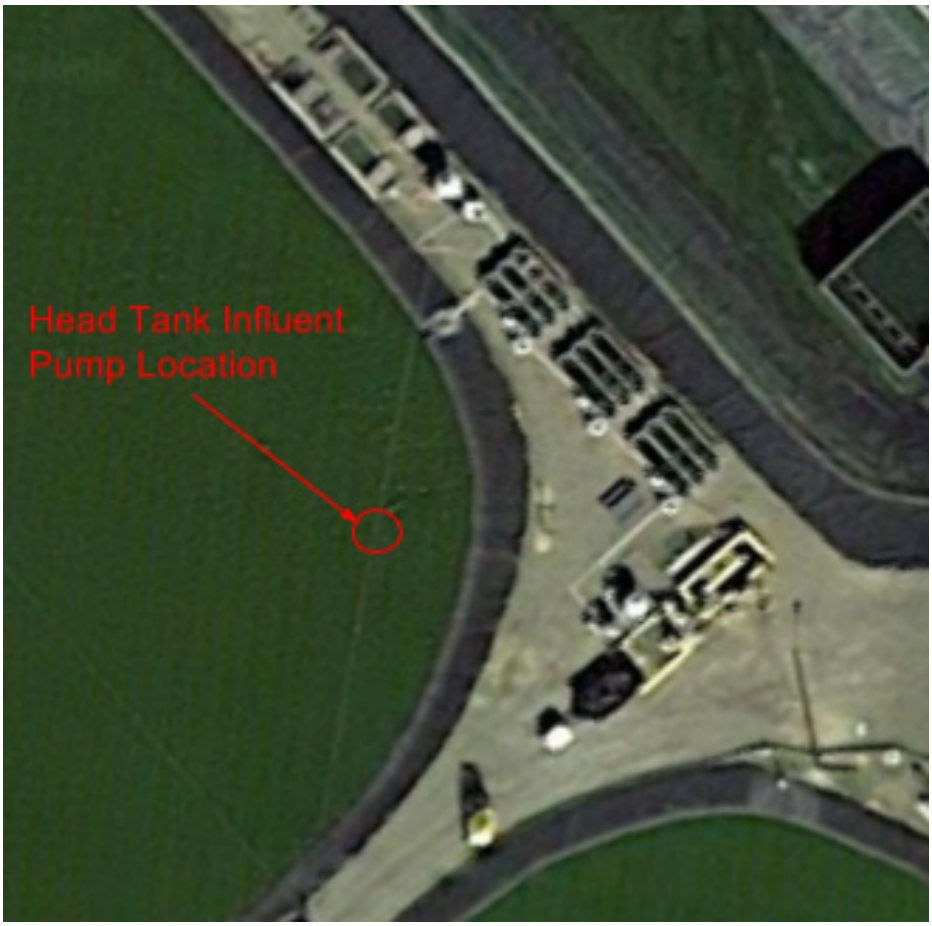

Figure 25: Location of the sump pump in the north facultative pond.

Effluent left the ponds over 4-inch vertical ramped standpipes that controlled the pond depth at 30 cm. The standpipes were designed to prevent straining of the flocculated biomass as it left the pond (Ripley 2013). Effluent flowed by gravity to a 65-gallon cone bottom tank. These tanks were decanted using a timed rubber impeller pump to the 150-gallon supernatant tank and the settled biomass was pumped with a rubber impeller pump to the 500-gallon subnatant tank. Settled biomass from the supernatant tank was pumped by a programed rubber impeller pump to the subnatant tank and clarified effluent from both the supernatant and subnatant tanks drained to FACN by gravity. To harvest biomass to the drying bed the subnatant tank the clarified water was manually decanted using a sump pump and the settled biomass drained by gravity from the boom of the tank to the drying beds. The drying system consisted of wooden frames with chicken wire support overlaid with an 18 x 16 mesh fiberglass window screen where the biomass was directly applied. These screens were placed over a lined pool to drain and dry.

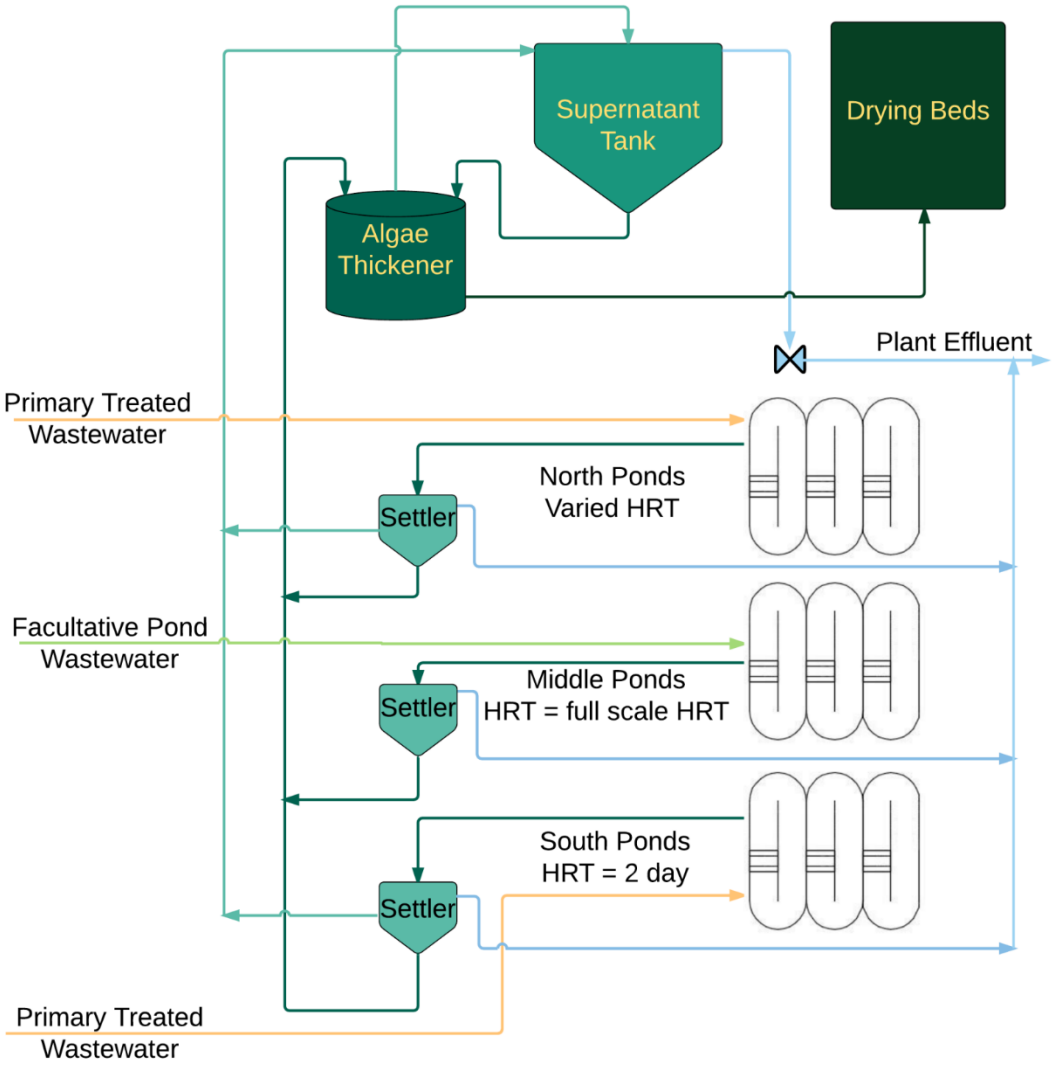

Figure 26: Process flow diagram of the pilot plant (Suvorov et al. 2015)

The 1,000 L (3.5-m^2) pilot ponds were constructed out of rotational-molded food-grade HDPE with UV stabilizer (Figure 27, Figure 28). The sides of the ponds were wrapped in reflective insulation to prevent light penetration through the sides of the ponds and additional photosynthesis. The ponds were placed on a metal frame so that they sat 0.3 m above the ground surface. This allowed for gravity drainage and easy to configure plumbing. The paddle wheels were made of transparent Plexiglas to reduce to reduce self-shading and were cleaned of biofilms weekly. A supervisory control and data acquisition (SCADA) unit (Neptune Systems, Morgan Hill, California) was used to control pond pH, pond influent pulse frequency and duration, and the settling tank pumps. Additionally, the pond pH, temperature and the dissolved oxygen were monitored and recorded on a ten-minute interval. Temperature and pH were collected in all ponds for the entire project and dissolved oxygen was collected in one pond from each triplicate set from October 2015 until the end of the project.

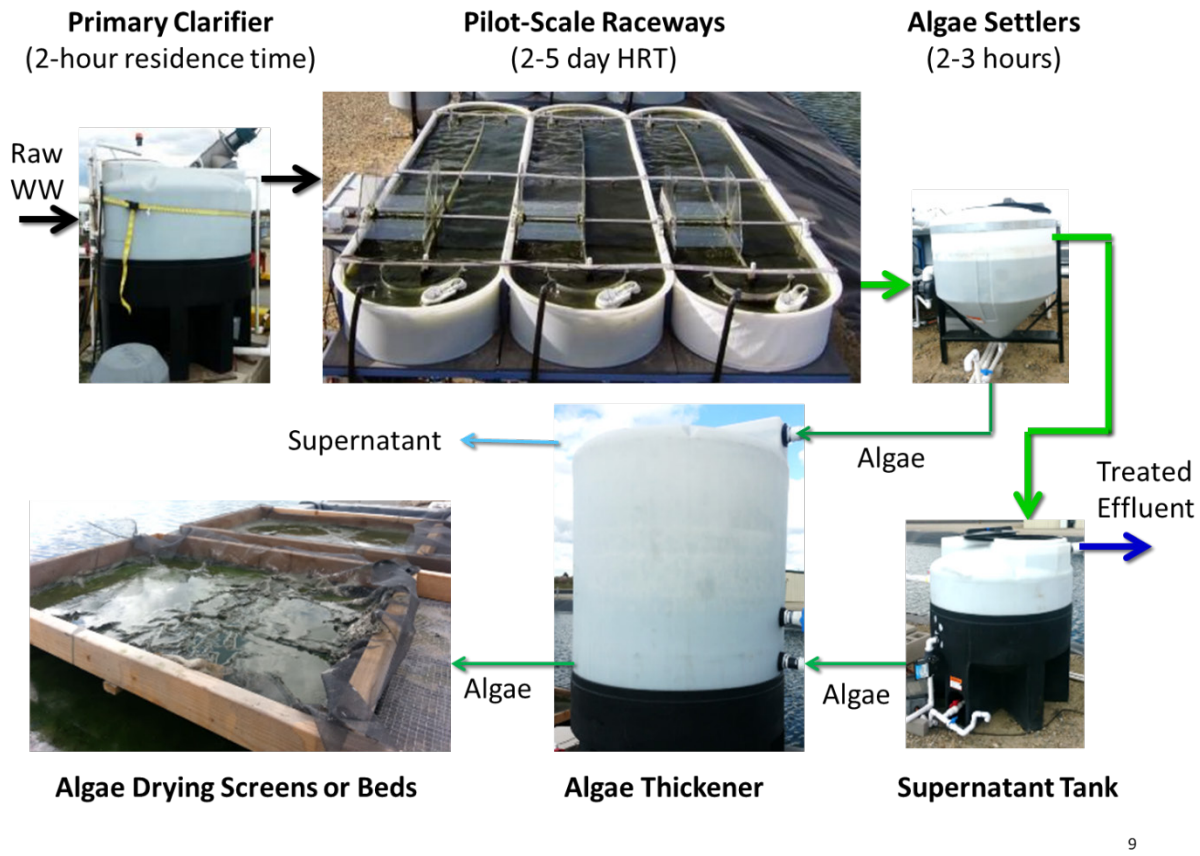

Figure 27: Pictographic process flow diagram for the ponds diluted with primary clarifier effluent.

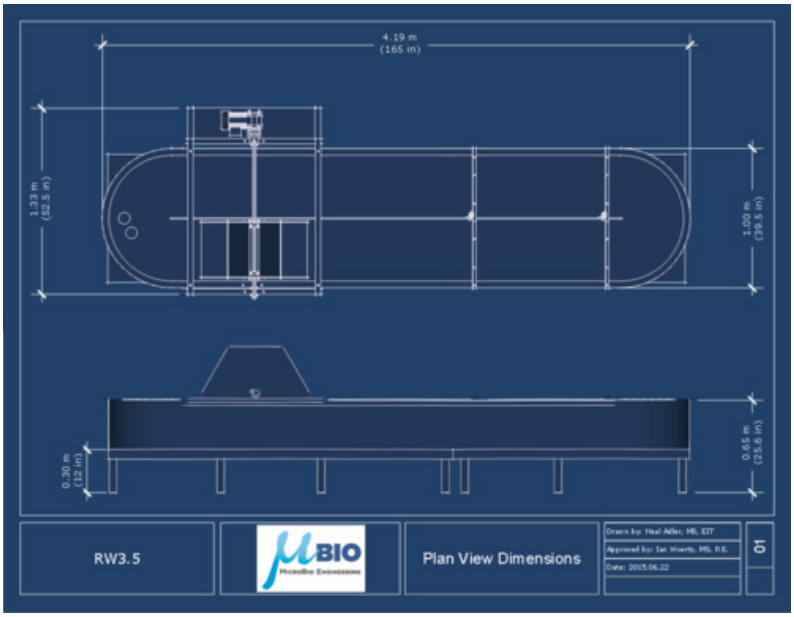

Figure 28: Plan and side view with dimensions of the MicroBio Engineering Inc. ponds used in this research. (Adler 2014)

For some experiments, carbon dioxide (CO_2) was added to the ponds to control pond pH and provide additional carbon. For the ponds with CO_2, the pH was initially controlled between 7.9 and 8.1 with a control system (Neptune Systems, Morgan Hill, California), compressed CO_2 (99.5% purity, Airgas), solenoid, and a calibrated pH probe (Sensorex, Garden Grove, California. On 9/19/2015 the set points were changed to 7.4 to 8.1.

Table 2: Description of pond conditions including HRT, feeding regime and pH set point for the ponds fed with primary clarified wastewater (Pittner 2018).

<table>
<tr><th rowspan="2">Start Date</th><th colspan="2">HRT (days)</th><th colspan="2">Feed Pulses Per Day</th><th colspan="2">pH Set Point</th></tr>
<tr><th>S</th><th>N</th><th>S</th><th>N</th><th>S</th><th>N</th></tr>
<tr><td>10/27/2014</td><td>2</td><td>4.5</td><td rowspan="4">8 - Hourly
8AM to 4PM</td><td rowspan="4">8 - Hourly
8AM to 4PM</td><td colspan="2" rowspan="4">Begin at 8.1
Down to 7.9</td></tr>
<tr><td>11/17/2014</td><td>1.8</td><td>4</td></tr>
<tr><td>11/24/2014</td><td>1.8</td><td>4</td></tr>
<tr><td>1/26/2015</td><td>2</td><td>4.5</td></tr>
<tr><td>2/2/2015</td><td>2</td><td>3</td><td>8 - Hourly
8AM to 4PM</td><td>8 - Hourly
8AM to 4PM</td><td colspan="2">Begin at 8.1
Down to 7.9</td></tr>
<tr><td>6/29/2015</td><td>2</td><td>-</td><td>8 - Hourly
8AM to 4PM</td><td>-</td><td>Begin at 8.1
Down to 7.9</td><td>-</td></tr>
<tr><td>7/13/2015</td><td>2</td><td>2</td><td rowspan="2">16 - Half-Hourly
8AM to 4PM</td><td rowspan="2">20 - Hourly
4AM to 12AM</td><td>Begin at 8.1
Down to 7.9</td><td>CO_2 Sparging Off</td></tr>
<tr><td>9/19/2015</td><td>2</td><td>2</td><td>Begin at 8.1
Down to 7.9</td><td>Begin at 8.1
Down to 7.7</td></tr>
</table>

Weekly pond maintenance activities included cleaning the paddle wheels, cleaning the pond walls, pH probe cleaning and calibration, dissolved oxygen (DO) probe cleaning and calibration, temperature probe cleaning and calibration, clarifier cleaning and flow rate testing and calibration. Other non-routine maintenance activities included cleaning the pump to the primary clarifier and the pump in the facultative pond to remove solids build-up and replacing impellers in the biomass harvesting impeller pumps as required.

Sampling from the full-scale system

Grab samples were collected from the full-scale wastewater treatment plant between 9 and 11 am weekly using a 500 mL polypropylene dipper attached to a 1.5-m pole. The dipper was dipped and dumped three times before collecting the sample to remove any residues from the cup, additionally the INF was sampled last since it contained fats oils and greases (FOG) that may have contaminated subsequent samples. The MP and ASP had their own sample cup since these sources were clean. In general, the sampling regime started with sampling the facultative ponds from their respective effluent weir gate prior

to entering HRPI. This was followed by sampling the HRPI at the submerged effluent pipe going into HRPO. HRPO was sampled as the effluent poured over the weir into the rapid mix chamber. Samples were collected from the ASP and MP as the clarified water flowed out the effluent weir (Figure 29). Finally, plant influent samples were collected before the rotatory screen while the offsite lift station pumps were running to ensure a well-mixed and representative sample. Dissolved oxygen, pH, temperature and time were recorded immediately for each sample and the samples were then refrigerated. Cool samples were packed in an ice chest with ice and shipped overnight from Delhi to Cal Poly in San Luis Obispo. Upon receipt of the samples at Cal Poly at approximately 8 AM the next day, the sample temperature was taken again to ensure that the sample remained below 4˚C. Occasionally the sample temperature exceeded 4˚C and the operators in Delhi were advised to add more ice in future shipments.

Figure 29: Sampling of the ASP over the overflow weir.

Sampling from the pilot-scale system

Grab samples were collected from the pilot-scale system from the overflow standpipe between 8 and 9 AM weekly using a 1-L sample cup. The 1-L bottle had a slightly smaller diameter than the standpipe, so it was inserted into the standpipe and allowed to fill. Care was taken to ensure that the sample cup did not overflow and concentrate solids. The entire sample was vigorously poured into a 1.5-L sample bottle until the bottle was full. Pond influent was added in pulses hourly, and samples were collected immediately after each influent pulse stopped. Dissolved oxygen, pH, temperature and time were recorded immediately for each sample and the samples were then refrigerated. Other sample cooling and shipping procedures were the same as for the full-scale system. Grab samples of the influent to the ponds were collected from the influent pipe to the ponds 30 seconds after the influent pulse started. Composite samples were also collected from the primary clarifier and the facultative pond constant head tank with an autosampler that collected 500 mL of sample each hour between the hours of 8 AM and 4 PM the day before the normal sample day. The autosamplers were shaded and cooled with ice to keep the samples cool. On sample day these samples were mixed into a composite sample.

Analytical tests

For the full-scale and pilot scale samples 2 and 24- hour settling efficiencies were measured in Delhi using Imhoff cones and a calibrated turbidimeter (Equation 3). Samples for settling efficiency were collected for HRPO, HRPI and all the pilot-scale ponds using the previously described sampling methods and locations. Immediately after the sample was added to the Imhoff cone a small sample was transferred to a clean turbidimeter cuvette and turbidity was immediately measured. Mixing and speed was essential to ensure the sample did not settle before it was measured. This was repeated at 2 and 24 hour intervals

from the Imhoff cone supernatant. The settling efficiency was calculated as the percent difference between the initial and two or 24-hour turbidity.

Equation 3: Settling efficiency

$$Settling\ Efficiency = \left(\frac{Turbidity_{initial} - Turbidity_{final}}{Turbidity_{initial}}\right) * 100\%$$

All other analytical tests were performed at Cal Poly using APHA standard methods on the day after they were collected in the field except for samples that could be preserved (APHA 1995) (Table 3, Figure 30). Preserved tests included chemical oxygen demand (COD), Total Kjeldahl Nitrogen (TKN), and Total Phosphorous (TP). Soluble samples were prepared by filtering the samples through a 1.2-µm glass fiber filter or 0.45 µM pore size nitrocellulose filter using a vacuum pump depending on the size specified in Standard methods. Gross and net algal areal productivity, as gram of biomass ash free dry weight per m^2 per day (AFDW/m^2-d), were determined using APHA standard methods 2540 D and 2540 E and Equation 4 (APHA 2005). Biomass net productivity was determined by subtracting the influent solids from the pond solids, while the gross productivity was determined from the pond solids alone. Net productivity indicates the amount of biomass grown in the ponds while the gross productivity indicates the total amount of mass harvested from the ponds that can be converted to fuel. Most productivities are reported as gross productivity.

Equation 4: Gross productivity

$$Productivity = \frac{VSS_{Pond} * Depth}{HRT}$$

Table 3: Analytical testing methods (Kraetsch, 2015)

Constituent	Analytical Method
Nutrients	
Total Ammonia Nitrogen	Ammonia Selective Electrode (APHA Method 4500-NH_3 D)
	Automated Selective Electrode (Based on APHA Method 4500-NH_3 D)
Nitrite	Colorimetric, Fisherbrand 0.45-µm Multiple Cellulose Ester filtration (APHA Method 4500-NO_2^- B)
Nitrate	Nitrate Ion Selective Electrode with Interference Suppression Solution (APHA Method 4500-NO_3^- D)
Total Kjeldahl Nitrogen	Macro-Kjeldahl and manual titration (APHA Method 4500-N_{org} B)

Dissolved Reactive Phosphorus	Ascorbic Acid, Fisherbrand 0.45-µm Multiple Cellulose Ester filtration (APHA Method 4500-P E)
Total Phosphorus	Vanadomolybdophosphoric Acid Colorimetric (APHA Method 4500-P C)
Total Nitrogen	Persulfate Digestion Method (HACH Method 10072)
Organics	
Total and Volatile Suspended Solids	Gravimetric with 1.2-µm Fisherbrand G4 Glass Fiber filters filtration (APHA Method 2540 D and E)
Total and Soluble Carbonaceous Biochemical Oxygen Demand	5-day with 20°C incubation, 1.2-µm Fisherbrand G4 Glass Fiber filtration (APHA Method 5210 B)
Other	
Microscopy for Algae ID and grazer counts	Selected Taxonomic References, Optical Microscope (Method 10900 E. 2.)
Alkalinity	Sulfuric Acid Titration (APHA Method 2320 B)

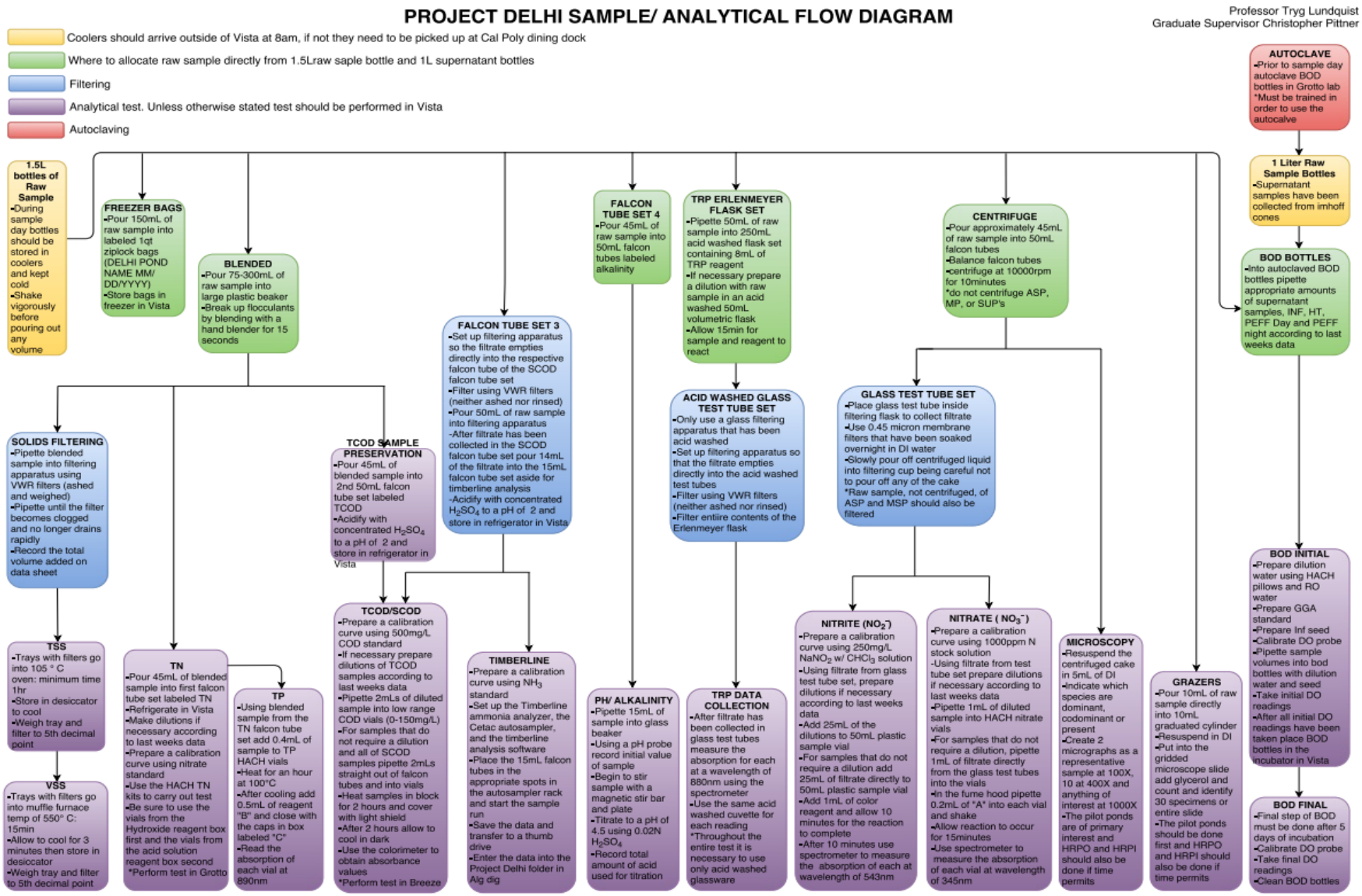

Figure 30: Sample flow diagram by Esme Diego 2016.

Methods for Organism Identification

Biomass concentration, productivity, and settling efficiency were measured five times per week in duplicate 33-m^2 pilot ponds in San Luis Obispo fed either primary clarifier effluent (containing organic carbon, ammonium-N as the dominant nitrogen form) or reclaimed water (near drinking water levels of organic carbon, nitrate-N as the predominate nitrogen form) from mid-July to late August 2015. Samples were subsequently persevered for genetic analysis. Influent was fed continuously throughout the day, with the flow rate averaging 2,500 L/day, equivalent to an HRT of 4 days. Biomass concentration was estimated as volatile suspended solids (VSS, Standard Method 2540D), and used to estimate productivity (g VSS/m^2-day) by dividing by the hydraulic retention time (HRT, days), then converting to an aerial basis by multiplying by the pond depth (0.3 m) (Equation 4). As primary clarifier effluent contains suspended solids (~50 mg VSS/L), these were subtracted from the respective ponds' biomass concentrations before calculating productivity. Settling performance was monitored by measuring supernatant biomass concentration after settling for two and 24 hours in an Imhoff cone and reported as the settling efficiency (100% * ($VSS_{initial} - VSS_{2hr}$) / $VSS_{initial}$).

Genetic material was collected from as grab samples from the primary clarifier influent and both pond treatments. No samples of the reclaimed water feed were collected for community ecology analysis, as it contains little to no suspended solids. Additionally, return activated sludge, the bacterial community responsible for secondary treatment in conventional wastewater treatment processes, was collected as a grab sample from aeration basins at the city of San Luis Obispo wastewater treatment facility. Samples for community analysis were collected by centrifugation of respective sample grabs in sterile 50 ml conical bottom centrifuge tubes, with the clarified supernatant removed by decanting. The resulting biomass pellet, along with up to 5 ml of residual supernatant, were preserved by submerging in RNAlater (Thermo AM702), then stored at -20˚ C until overnight shipment to Sandia National Laboratories for analysis.

Analysis of sequencing data sets was performed by the MetAGenomics and Amplicon sequencing PIpelinE (MAGPie), which consisted of various bioinformatics tools. The initial step, pairing of the paired reads used Paired-End reAd mergeR (PEAR), was followed by quality filtering. Quality filtering involves the removal of bad quality reads, the ends of the reads which have suboptimal quality, and primer sequence reads from the datasets. Reads passing the quality filter were subject to a dereplication processes using USEARCH (Edgar 2017). This process reduces the size of the database and computation time for the pipeline. Operational taxonomic unit (OTU) clustering was carried out on the dereplicated dataset, with OTUs comprised of sequences achieving 97% similarity clustered. The Silva and Green-genes database were used to identify the sequences and the abundance of each OTU. Using this mapping, we keep the counts of reads mapped to the OTUs and the OTUs identity to create the OTU table, which was the starting point for subsequent data analysis.

For the analysis of correlations between genetic data and pond performance (productivity, settling efficiency), both individual OTUs and OTUs grouped at the genus level were used. Both the sequence read counts and the $\log_{10}$ of the read count number (+1 to eliminate zero values) were checked for correlations. Any resulting Pearson's correlation coefficient that was greater than 70% or less than -70% was noted. A significance level of 95% was set and any correlations that had a p-value of less than 0.95 were rejected as statistically insignificant.

For analysis of the community structure, we computed the distances between the samples by calculating the correlation coefficient between the abundance profiles of the OTUs. The distances between the samples represented in the dendogram is calculated the "pdist" function in Matlab®. This calculates the co-occurrence correlation coefficient for all pairwise comparisons of identified OTUs. We computed

distances using the 1-correlation coefficient and visualized the resulting community network using Cytoscape. A heat map for clustering of genera was generated using the "clustergram" function in Matlab®, where correlation metrics were used to cluster genera.

Sample sets from 12 days were analyzed over the time interval from 7/22 to 8/11.

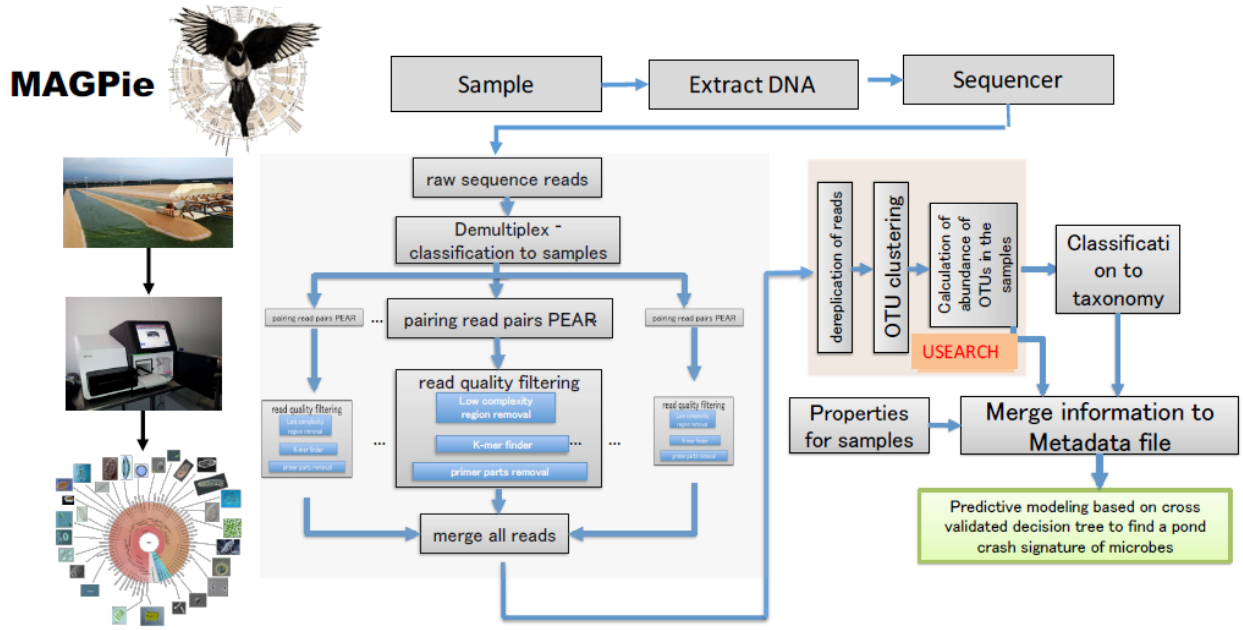

Figure 31: Metagenomics and Amplicon SequencinG Pipeline (MAGPie) process flow diagram. Each small subunit rRNA amplicon sequencing library contained nucleic acids from 96 samples. The sequencing reads were filtered for bad quality reads and further analyzed for OTU clustering. These OTUs were then classified to different taxonomic assignments using Silva and Green genes databases and further analyzed by machine learning.

Results

Characterization of the full-scale plant (ML 2.0)

Milestone 2.0 included the characterization of the full-scale plant in terms of baseline biomass productivity and settleability under two different process flow configurations. From 4/07/13 to 6/30/13 the Delhi full-scale wastewater treatment plant was operated under high loading conditions to verify that wastewater treatment plant could function properly if the flow to plant doubled. Typically, the facultative ponds operate in parallel and the high-rate ponds operate in series from the inner to outer HRAP (Figure 22a). To create the high loading conditions, the north facultative pond (FACN) and the outer high pond (HRPO) were operated in series (Figure 22b). This reduced the overall summer residence time through the facultative ponds and the high rate ponds from approximately 36 days to approximately 18 days and the residence time in the high rate ponds from 7.2 to 3.7 days. The higher organic loading rate and decreased residence time under the high loading experiment appeared to increase the areal productivity and variability of the HRPO pond by 20% from 16 to 19 g AFDW/m^2-day when compared to the low-loading conditions for the same date range in the subsequent year (Figure 32, Figure 33).

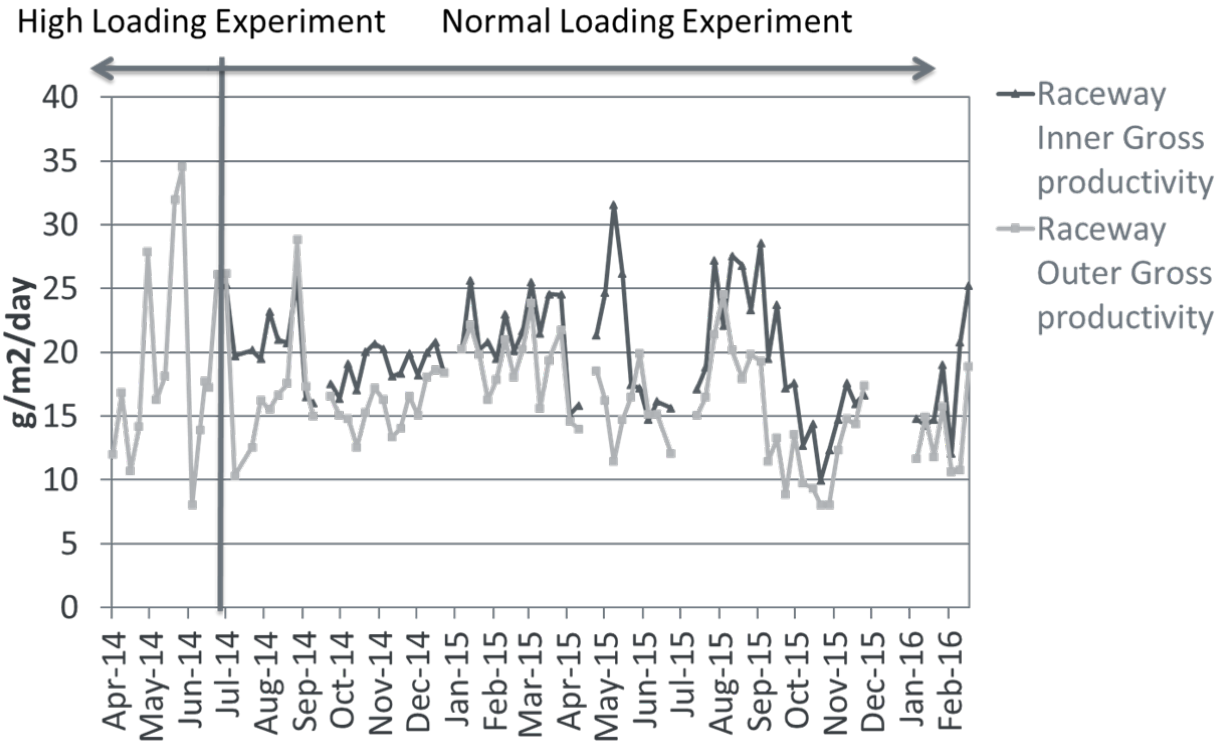

Figure 32: Time series of HRPO and HRPI gross productivity during the study. During the high loading experiment, a single facultative pond and HRPO received the entire plant flow.

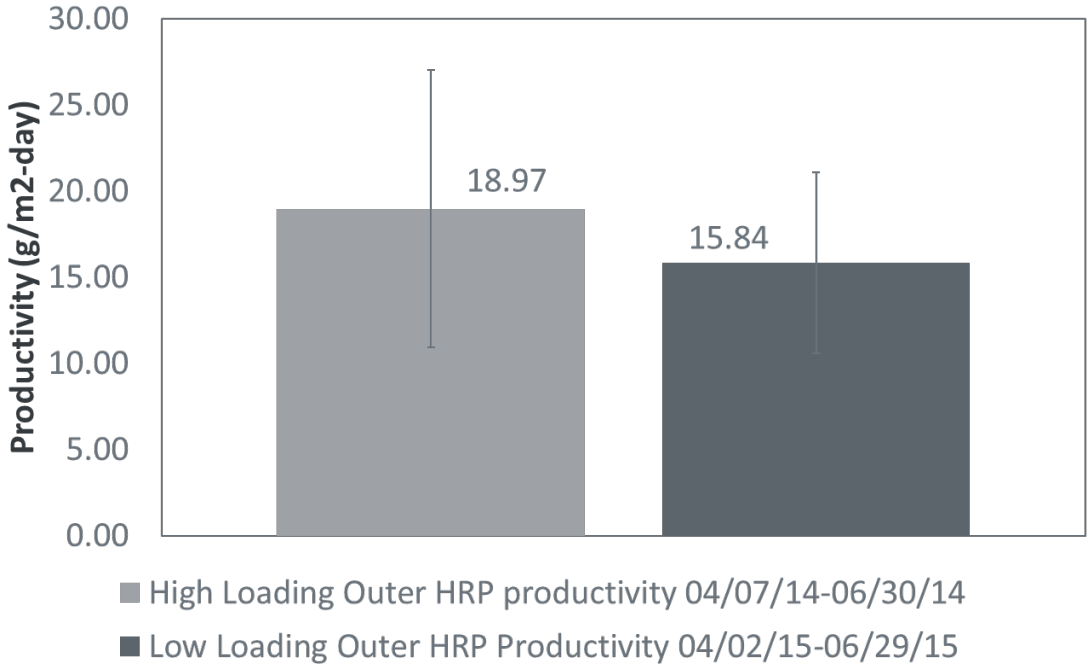

Figure 33: Productivity under the high and low (normal) loading conditions of the outer high rate pond in two sequential years.

Settling in the full-scale system under high and low loading conditions was also monitored by measuring the % VSS reduction from the HRPO to the algae settling ponds and by measuring the effluent solids (mf AFDW/L) from the ASP and MP (Figure 34). Measuring effluent solids from the ASP was important because it indicated the mass of solids not captured in the biomass harvest and measuring solids from the MP was important for meeting plant effluent discharge requirements. Aluminum chlorohydrate coagulant was added as the biomass laden liquid exited the HRPO under both the high and low loading conditions and coagulant dosage was adjusted as needed to meet effluent discharge requirements. Overall, the higher loading condition did not appear to significantly reduce overall volatile suspended solids reduction and the solids in the removal in the ASP was similar under both loading conditions. However, the high loading condition did increase effluent variability from the MP with 33% of the point exceeding 20 mg AFDW/L during the high loading condition and only 9% exceeding 20 mg AFDW/L for the low loading condition over the experiment duration (Figure 35). During the high loading condition, the effluent solids from the MP was consistently higher than the effluent solids from the ASP potentially indicating that additional biomass growth occurred in the MP after the algae biomass was harvested. These results indicate that under higher loading conditions and shorter residence times it may be beneficial to treatment and productivity to harvest between high-rate ponds in series.

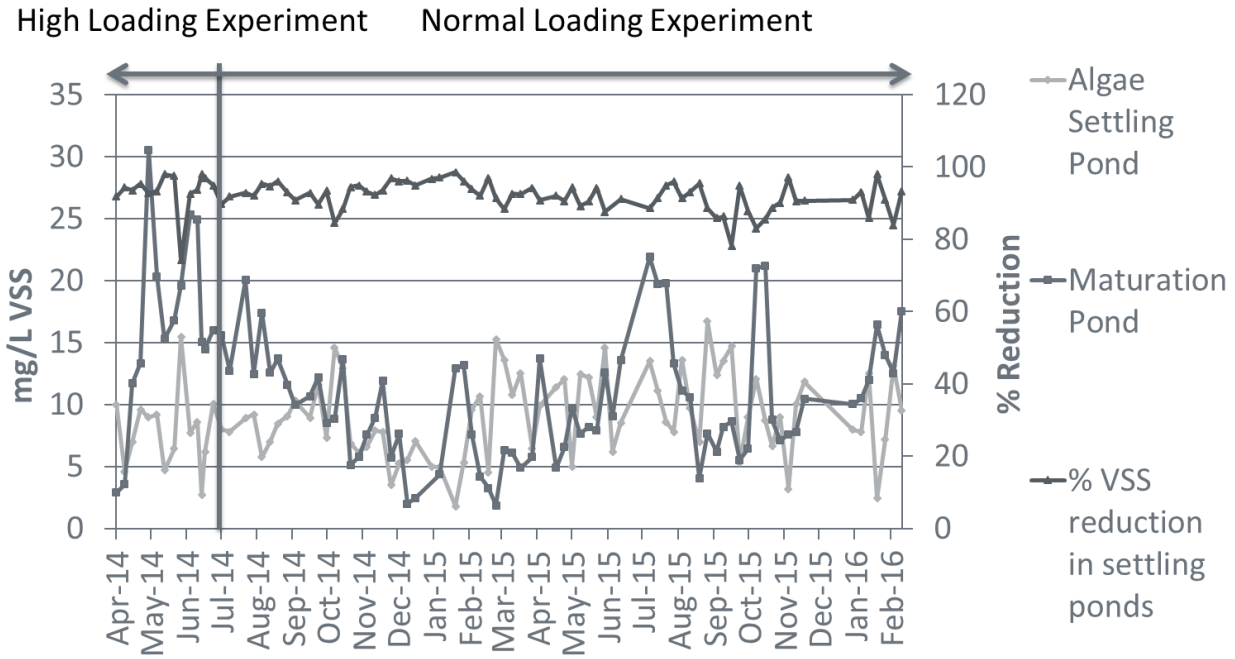

Figure 34: Effluent volatile suspended solids from the maturation pond and algae settling pond, and well as percent VSS reduction from the outer high rate pond to the algae settling pond under the high and low loading conditions.

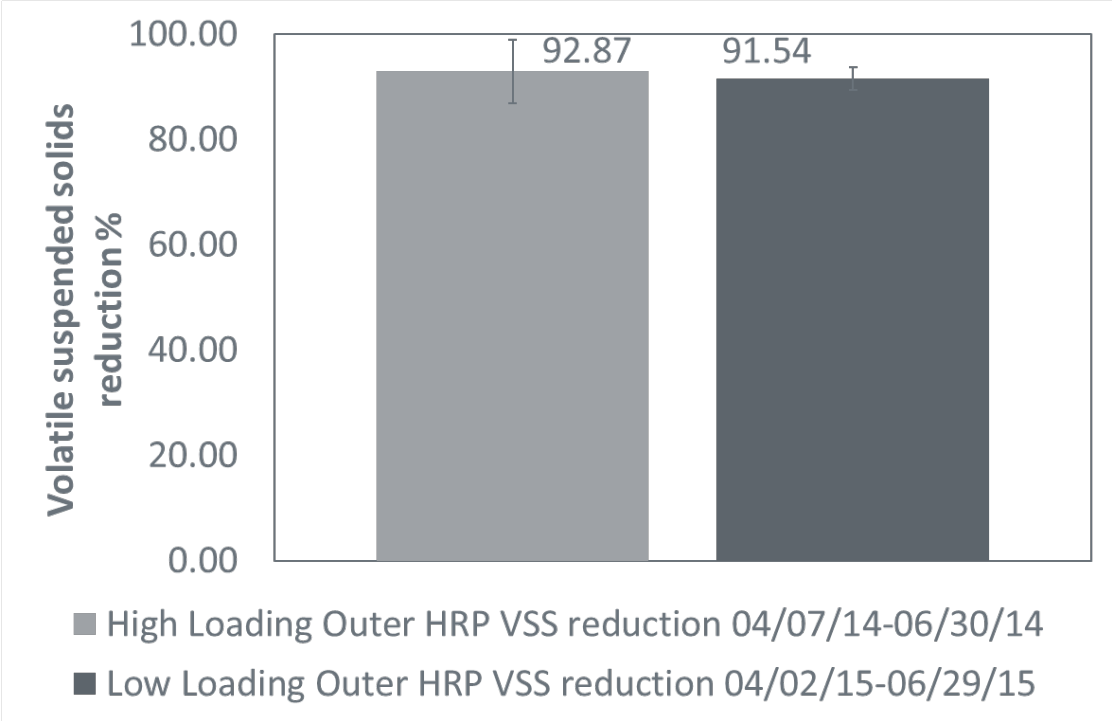

Figure 35: Settling under the high and low (normal) loading conditions of the outer high rate pond in two sequential years.

The high-loading experiment was only performed for approximately 3 months during the summer. Therefore, it was not possible to determine an annual average productivity for the high-loading experiment. Annual average productivities for HRPI and HRPO were calculated for the low loading experiment. From 12/01/14 to 12/01/15 the gross productivity for HRPI and HRPO was 20 g AFDW/m^2-day and 16 g AFDW/m^2-day, respectively (Figure 36). Productivity decreased slightly from the inner to the outer high rate pond indicating that respiration occurred in the second pond in series possibly due to carbon limitation (HRPI average pH, standard deviation and range 7.11±0.26: range 6.07-7.77, HRPO 7.28±0.38: range 6.01-10.00). Productivity decreases were likely not due to nutrient limitation in HRPO as total soluble nitrogen (NH_3/NH_4^+, NO_3^-, and NO_2^-) concentrations averaged 20.3±11.2 mg N/L (range 2.0-46.6 mg N/L) compared to HRPI with 25.5±9.6 mg N/L (range 5.7-54.1 mg N/L). Overall, coagulants achieved an AFDW removal greater than 90% over the same year that the annual average was achieved (Figure 37).

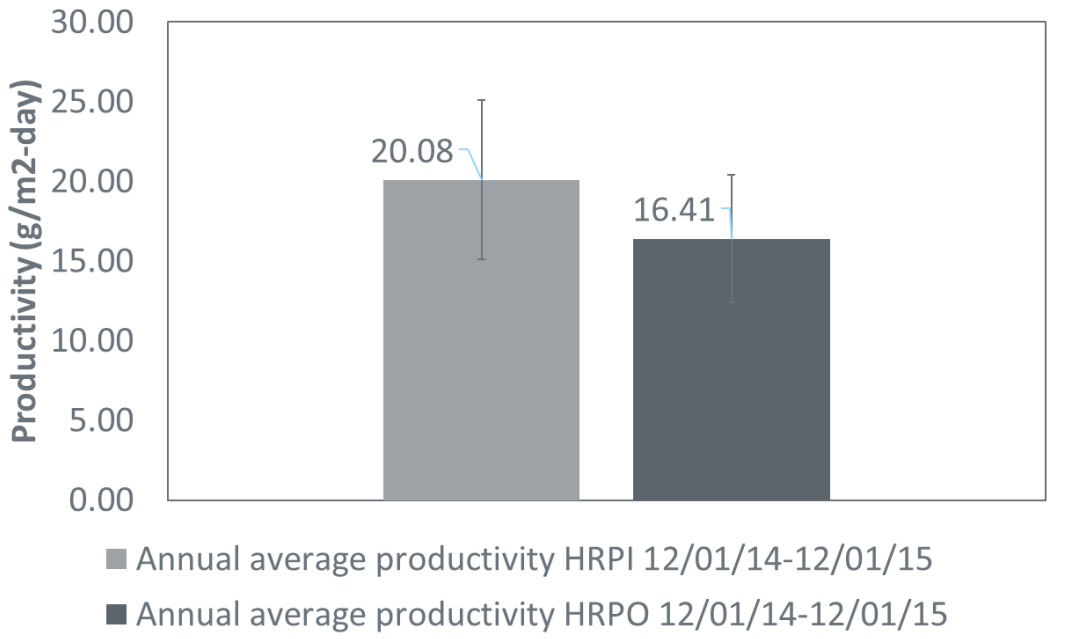

Figure 36: Gross annual average productivity between the full-scale HRPI and HRPO. The standard deviation is the standard deviation between all the productivity measurements collected over one year.

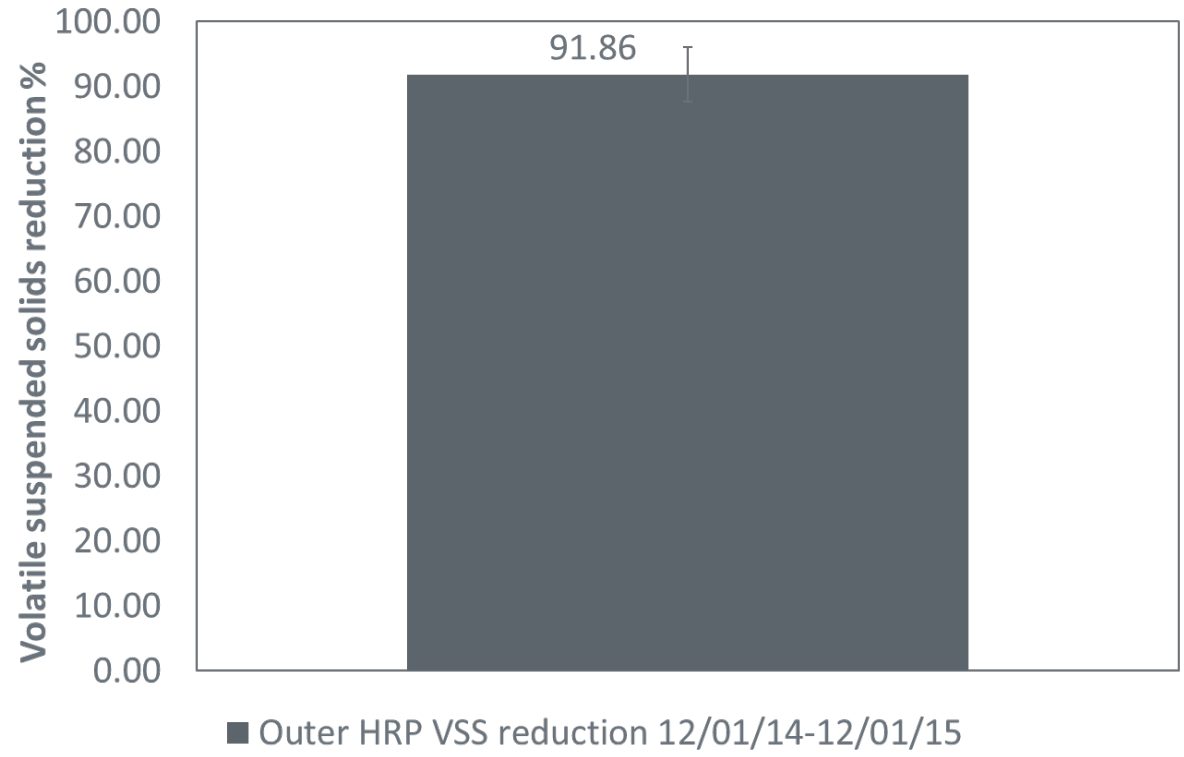

Figure 37: Average reduction in volatile suspended solids after coagulant addition over the course of one year.

A coagulant study was also performed to determine if bioflocculation reduces the amount of coagulant needed for 95% removal of biomass and to determine if the coagulant should be added before or after gravity settling. This study was performed using a jar tester apparatus with rapid mixing for 2 minutes followed by 20 minutes of gravity settling (Figure 38). For each test, three different coagulant doses and a control with no coagulant added were tested. For each pond set (S: 2 –day primary fed, N: 2-day primary fed with night aeration, and M: 4.5-day facultative fed with night aeration) coagulant was added before and after two-hour gravity settling to determine if presetting reduced coagulant dose for flocculated ponds. This was not performed for the full-scale ponds; as little biomass settles by gravity after two hours. Before coagulant was added initial turbidity was measured for all samples and after coagulant addition, rapid mixing, and 20 min of gravity settling the turbidity of the supernatant was measured to determine percent reduction in turbidity. Solids were performed on the two best coagulant doses (NTU <10) and the uncoagulated starting mixtures to determine total suspended solids removal.

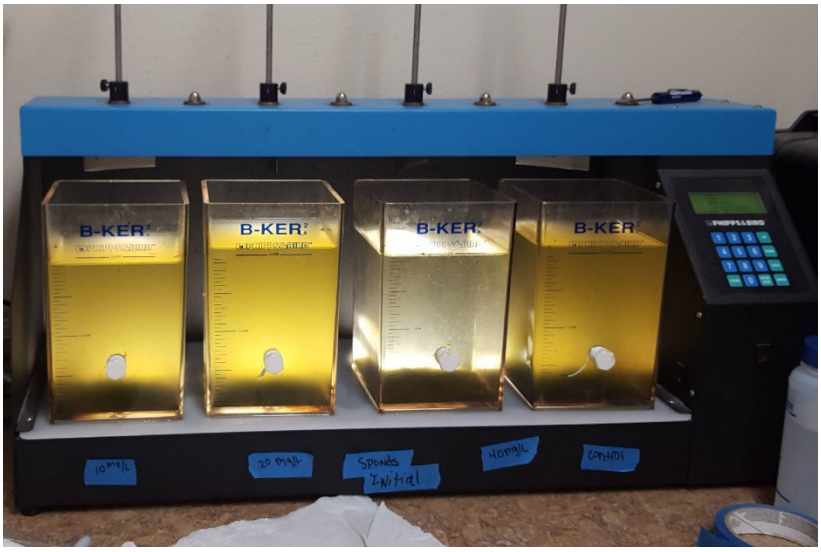

Figure 38: Settling after 20 min for the South pond set with no initial gravity setting. Coagulant doses from left to right are as follows – 10 ppm, 20 ppm, 40 ppm and the control. After this test an additional jar test was performed to further optimize the coagulant dose.

Gravity settling with bioflocculated algae biomass is frequently just as successful at removing suspended algal solids as coagulant addition (Figure 39). Suspended solids removal by gravity was assessed using an Imhoff cone. Suspended solids removal greater than 95% are common with 24 hours of gravity settling. However, pond upsets can sometimes result in poor gravity settling. Coagulants can be used in these cases before or after gravity setting to improve biomass removal and to meet wastewater treatment plant discharge requirements. On an annual average, bioflocculated ponds with gravity settling were able to meet discharge requirements 78% of the time. This indicates that bioflocculation and gravity settling could significantly reduce coagulant costs. Additionally, adding coagulant to bioflocculated unsettled ponds reduces the required coagulant dose by 50% (Figure 40). Finally, experiments showed that coagulant should be added to bioflocculated biomass before gravity settling to minimize required coagulant addition.

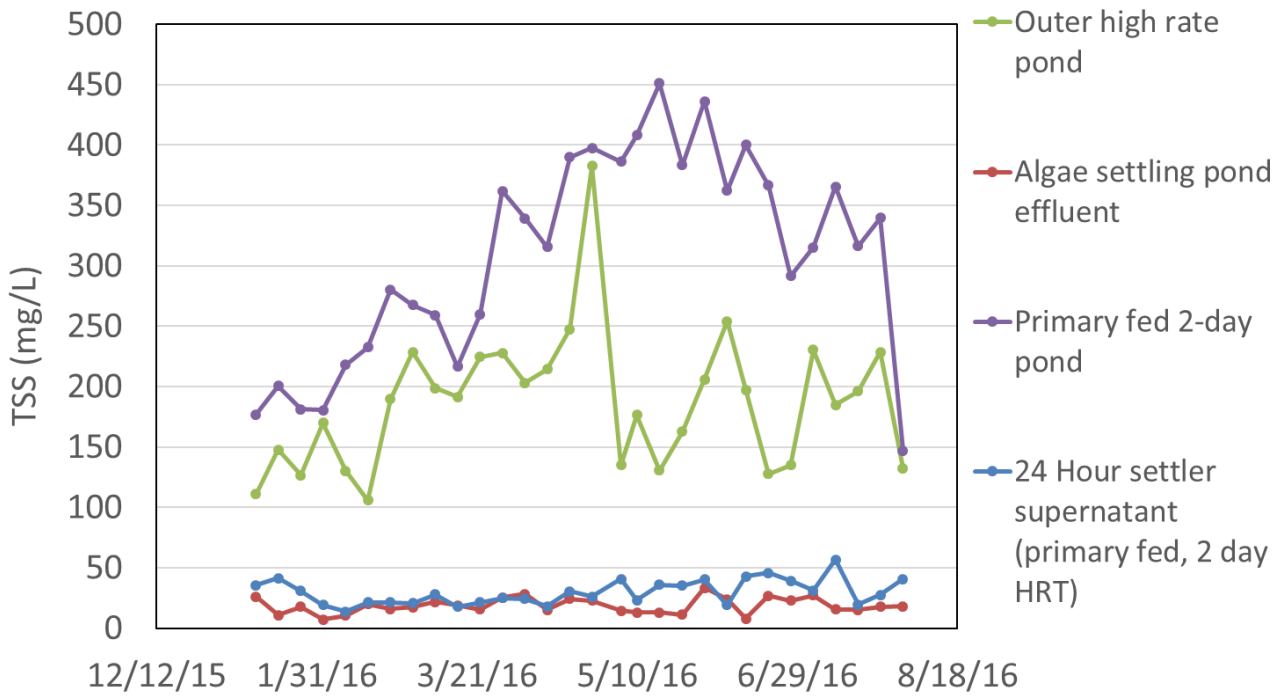

Figure 39: Total suspended solids removal with coagulants and with gravity settling. The green line shows that biomass concentration in the outer high rate pond. This pond biomass does not settle by gravity, so coagulants are dosed in the algae settling pond (red line). The purple line shows the primary wastewater fed 2-day residence time pilot pond biomass concentration. This pond showed significant and consistent bioflocculation and excellent gravity settling (blue line) for the experiment duration except for a few points (July 2016).

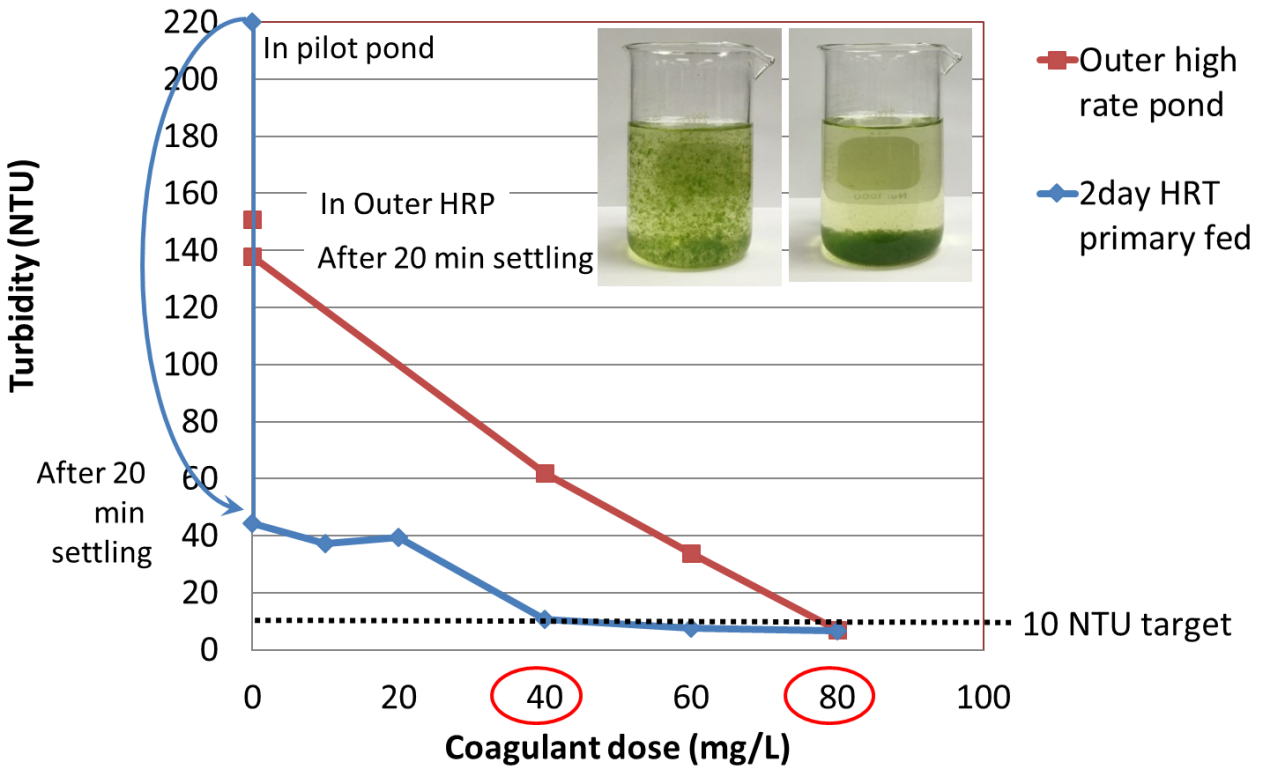

Figure 40: Comparison of setting efficiency and coagulant dose for bioflocculated ponds (2-day primary fed S ponds) and disperse full-scale ponds. 80% of the total solids settled by gravity in just 20 minutes of gravity settling in the control (no coagulant dose) for the ponds with bioflocculation. Coagulant dose was significantly reduced for the ponds with bioflocculation.

Design, Install, and Shakedown of the Pilot Plant (ML2.1 and 2.3)

Milestone 2.1 and Milestone 2.3 included the design, installation, and shakedown of the 1,000 L raceway ponds. This included the installation of actuated influent flow valves, pH controllers, and demonstration of trouble free operation of the pilot scale systems, settling tanks, pond water temperature monitors. The site was located on a berm near the influent screen of the Delhi Municipal wastewater treatment plant between the north ASP and facultative ponds (Figure 41). The 1,000-L, 3.4-m^2 ponds were constructed from opaque plastic. Three ponds were placed on a metal powder-coated frame with leveling legs. The paddlewheels were constructed from clear plastic to prevent shading and placed on a stainless steel shaft turned by a motor (Figure 42, Figure 43). Influent (clarified primary wastewater or facultative pond waster) was added to the ponds by gravity through an actuated valve connected to a smart plug that was programed to open the valve for the time required to deliver the volume required to maintain the appropriate residence time (Figure 44).

Figure 41: Planed location of the pilot site.

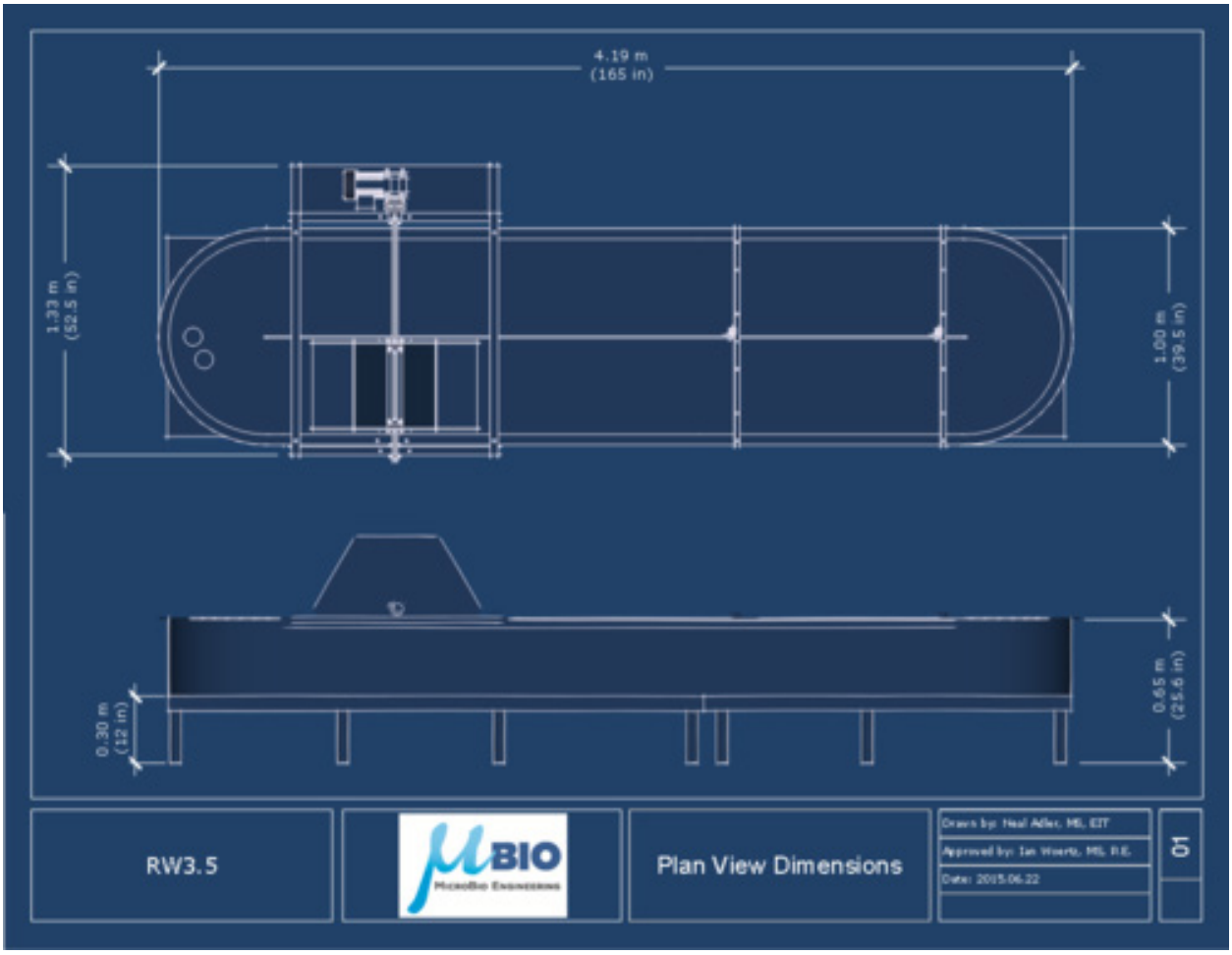

Figure 42: MicroBio Engineering Inc. ponds.

Figure 43: Installation of the pilot ponds started with the construction of the frames. Then the ponds and center baffles were installed. Finally, the paddle wheels were added.

Figure 44: Influent actuated valves.

The final site design consisted of 60-gallon gravity-fed cone bottom settling tanks and a harvesting system for harvesting, dewatering, and drying the biomass produced in the ponds (Figure 45, Figure 46). From the 60-gallon cone bottom tank the supernatant was pumped to the supernatant settling tank where any unsettled algae were given a second chance to settle. After decanting the algae remaining in the 60-L settling tank was pumped to the sludge settling tank for thickening. No coagulants were used in the

harvesting system and all pumping was performed with programmed timed impeller pumps. The algae thickener and supernatant tanks were decanted manually using a hose to the facultative pond. Sludge was added to a screen made with two by fours, a supportive metal mesh, and lined with fiberglass window screen (18 x 16 mesh). The screens were suspended over a shallow (12”) lined basin so water could drain from the screens.

A supervisory control and data acquisition (SCADA) unit (Neptune Systems, Morgan Hill, California) was used to control pond pH, pond influent pulse frequency and duration, and the settling tank pumps. Additionally, the pond pH, temperature, and dissolved oxygen were monitored and recorded on a ten minute interval. Temperature and pH were collected in all ponds for the entire project and dissolved oxygen was collected in one pond from each triplicate set from October 2015 until the end of the project (Figure 47, Figure 48). Dissolved oxygen, temperature, and pH probes were calibrated weekly if they were out of range and the flow rates were calibrated weekly if the hydraulic residence time was 10% different from the desired residence time.

Figure 45: Final site design.

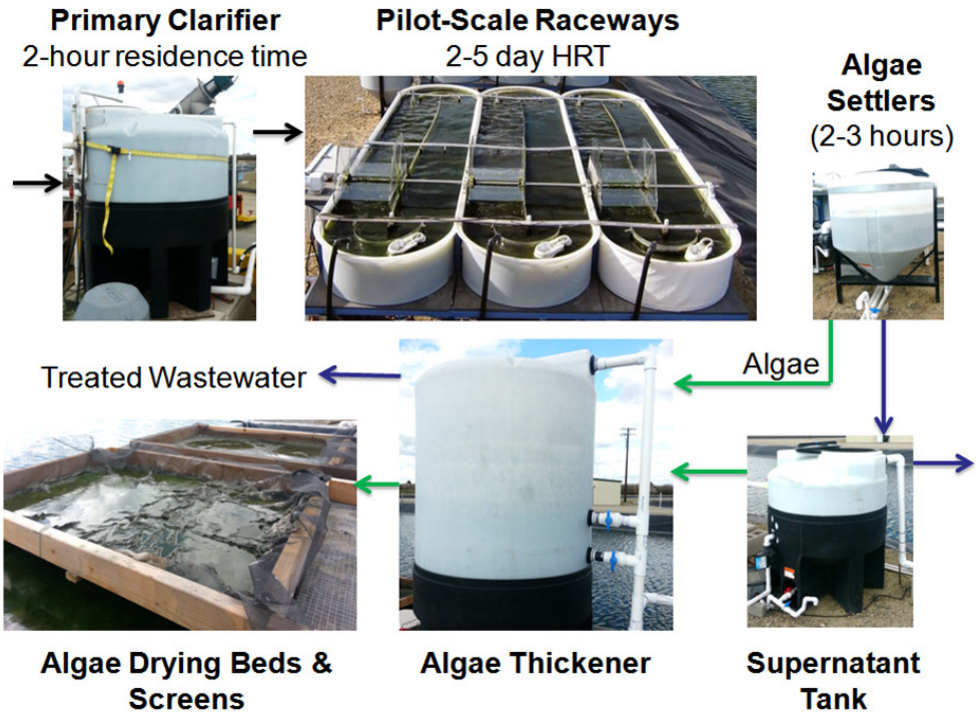

Figure 46: Process flow diagram for the ponds diluted with primary clarified effluent. The process flow was similar for the ponds diluted with facultative pond water.

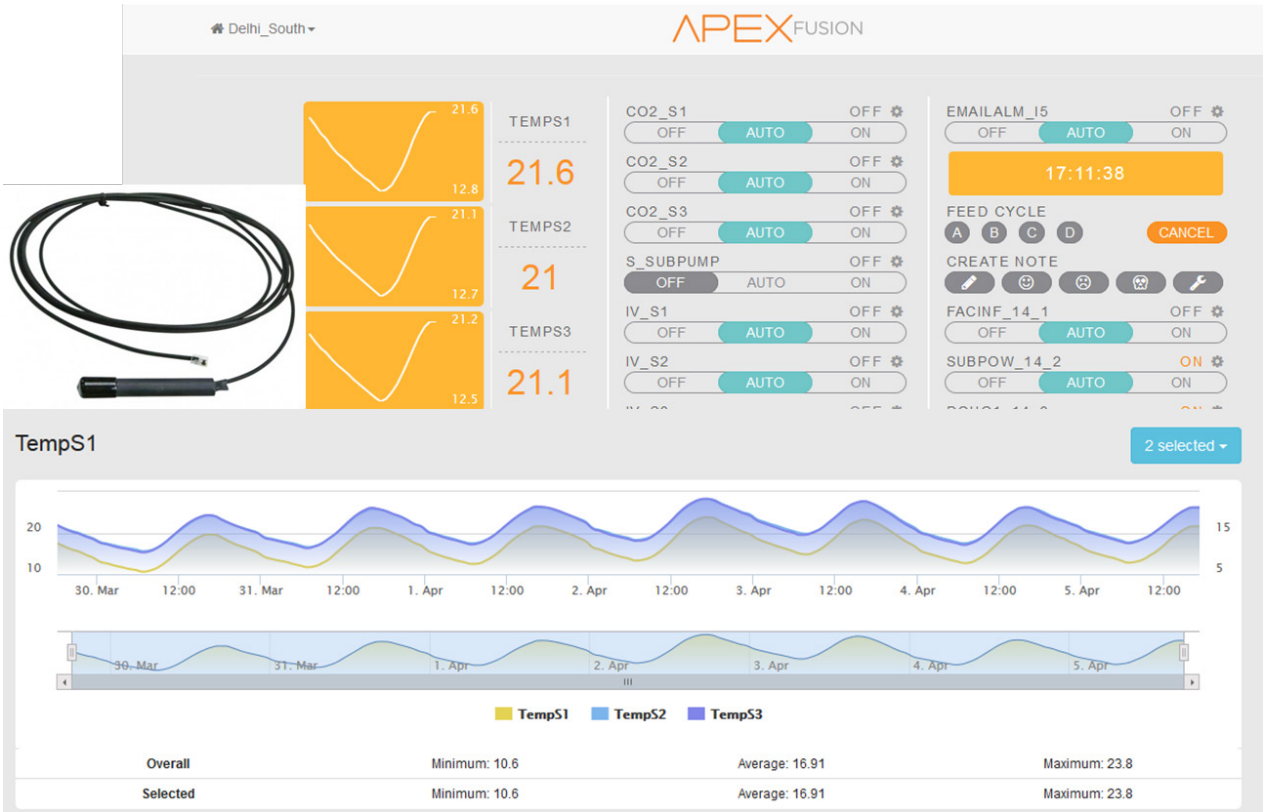

Figure 2: Output of temperature data through Apex Fusion. Top left example of a temperature probe.

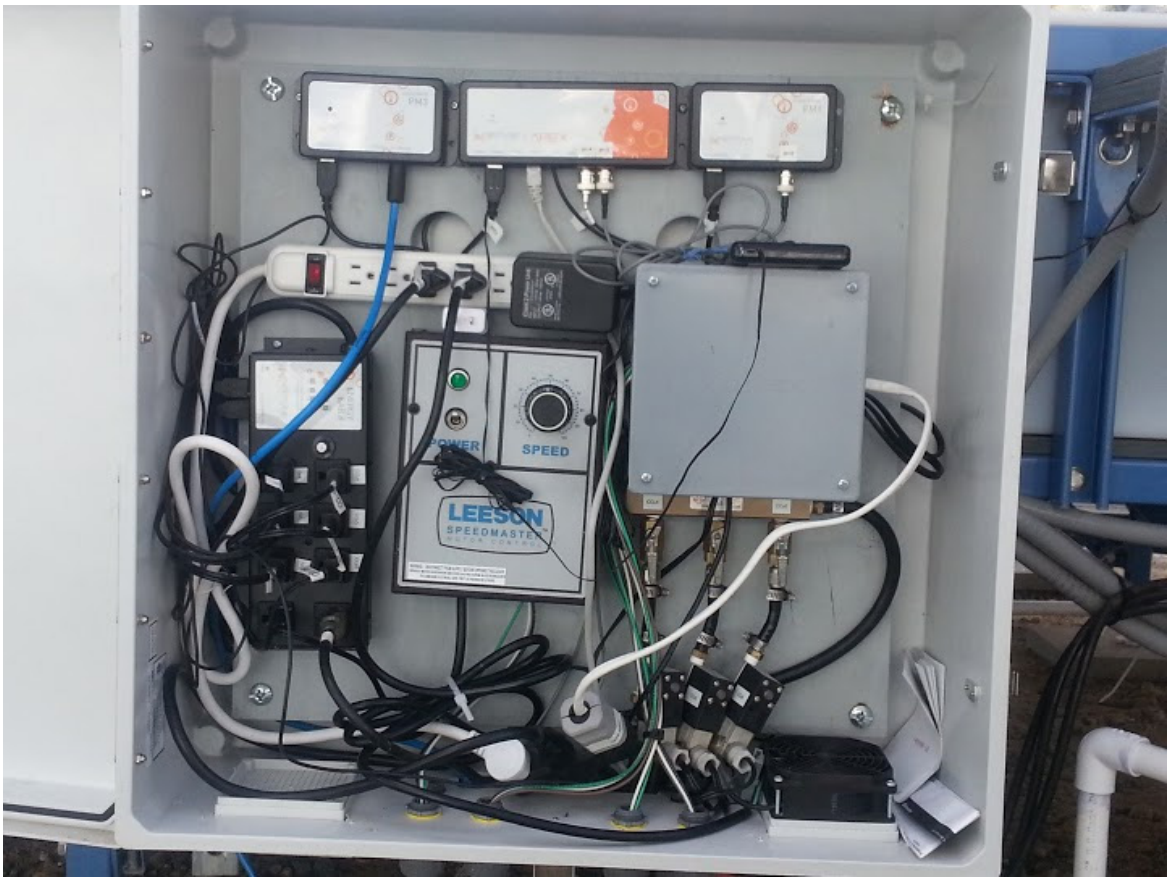

Figure 48: Control box, with CO2 solenoids, paddlewheel VFD, programmable outlets and probe input units.

Strain comparison of the wastewater polyculture to DOE 1412 (ML2.3)

A detailed description of the LEAPS system and validation experiments is included in the Task 1 section. A summary of the outdoor results with DOE 1412 compared to the LEAPS results is reproduced here. Outdoor field experiments were conducted at the Delhi field site to allow further comparisons of both LEAPS and the pH-refined biomass growth model to outdoor pond data. *C. sorokiniana,* initially cultivated in 15 L flat panel photobioreactors (12:12 day:night photoperiod), was used to inoculate triplicate raceway ponds (3.5 m^2 surface area each) located in Delhi. Cultures were grown in batch mode, using onsite non-potable well water enriched with BG-11 nutrients, at a culture depth of 30 cm. Ponds were chlorinated with a dilute hypochlorite solution prior to nutrient addition, which induced formation of a dark brown precipitate. The precipitate was removed via cotton filters. Pond water temperature was logged hourly, and hourly irradiance was collected from a local weather station (Merced, CA). Pond pH was maintained at a pH 7.5 set point by injection of pure CO_2. Biomass concentration was monitored daily by duplicate ash-free dry weight determination, with samples collected after well-water makeup for evaporative loss. Light intensity and temperature profiles were input into the BGM after inclusion of pH-effects, and the output compared to the biomass productivity measured in the field. Growth conditions (light, temperature, depth, pH) were reproduced in the LEAPs for further validation of the laboratory scale reactors.

Figure 49 shows the model-predicted versus measured AFDW concentration as a function of time for the Delhi outdoor ponds, LEAPS cultures, and biomass growth model predictions. Overall, the model was

successful in predicting the growth performance of the triplicate outdoor pond cultures conducted at Delhi in June and July of 2015. The model- predicted biomass productivity is about 23% higher than was measured in the outdoor ponds. While this slight over-prediction could be caused by the inherent uncertainty of the species-specific model input parameters, it is also likely that the non-potable well water used for medium preparation, which was treated with bleach prior to pond inoculation resulting in the precipitation of metals, could have slightly inhibited growth. Further, the cultures may have been stressed given that after 10 days the ponds started flocculating and biomass production slowed.

The biomass productivity of the pure culture DOE 1412 during cultivation was 15 g/m^2-day which was much lower than the polyculture strains under all conditions during the same period. For the ponds diluted with primary clarified wastewater on a two and three day residence time the productivity was 41 and 33 g/m^2-day, respectively, and the productivity in the polyculture ponds diluted with facultative pond water on a 3.7-day residence time the productivity was 20 g/m^2-day. Under all conditions, the polyculture ponds outperformed the pure culture (DOE 1412) ponds.

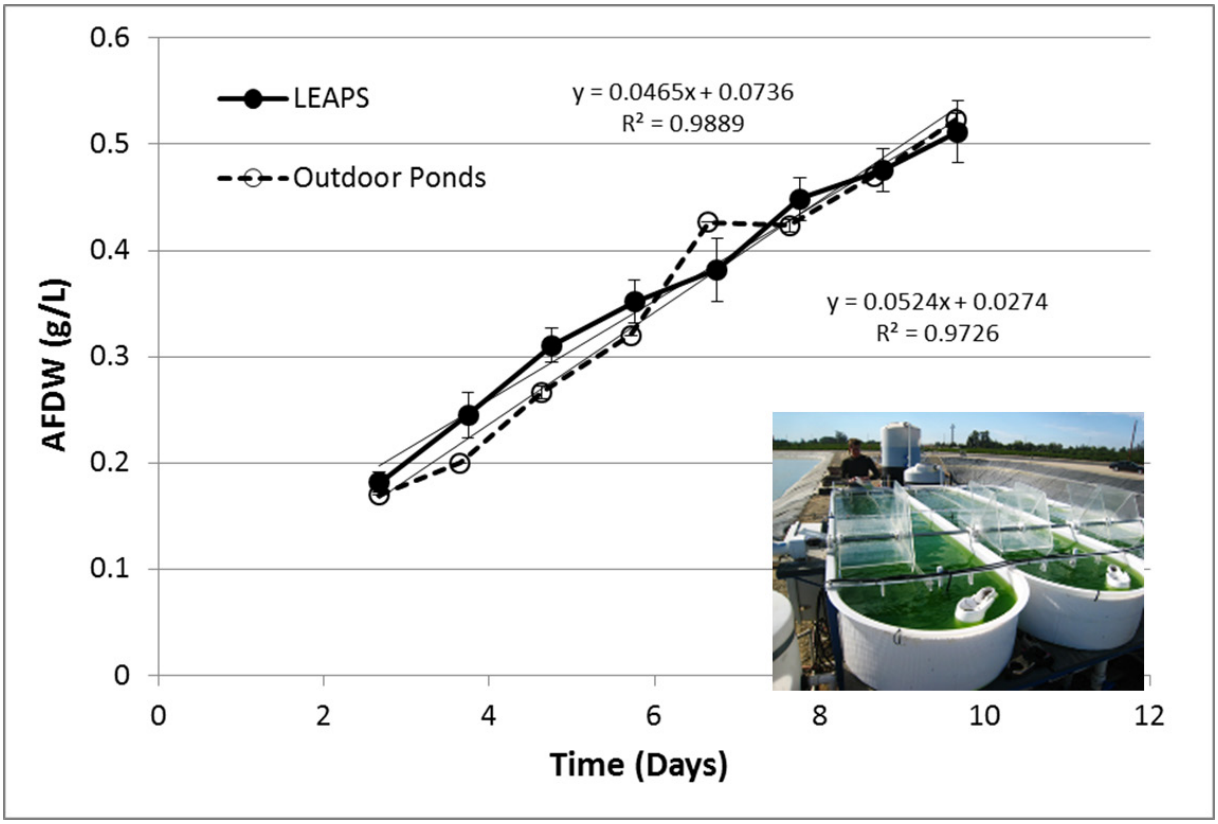

Figure 49: Volumetric biomass productivity of DOE 1412 cultivated in the LEAPS reactors and outdoors in Delhi CA.

Dilution Study (ML2.4) Determine the effect of wastewater dilution rate on biomass productivity, treatment performance, nutrient assimilation, settling efficiency, and dewaterability with native polyculture.

The effects of wastewater dilution rate (and source) were studied to determine the effect on biomass productivity, settling and wastewater treatment. In general, shorter residence times and higher strength wastewater resulted in higher productivity and better settling, while longer residence times resulted in

better wastewater treatment, especially in the winter. A detailed report of this milestone can be found in the Master's thesis produced from this work (Pittner 2018). The major results are summarized here.

Due to short changes in regional weather and longer term changes in seasons biomass productivity can be quite variable from week to week. Additionally, even though ponds were operated identically, the cultures in "replicate" ponds are often very different when observed by microscope (see ML 2.7). Despite these challenges, overall productivity trends in the replicate ponds tend to follow one another, indicating that weather (temperature and solar insolation) might influence overall productivity more than pond cultures, or that dips in productivity due to pond culture happen at a regular frequency independent of culture composition (Figure 50). Over the course of one year the productivity in the replicate south ponds (S) diluted with primary clarified wastewater at a two-day residence time was very similar with an average of 33 g/m^2-day (Figure 51).

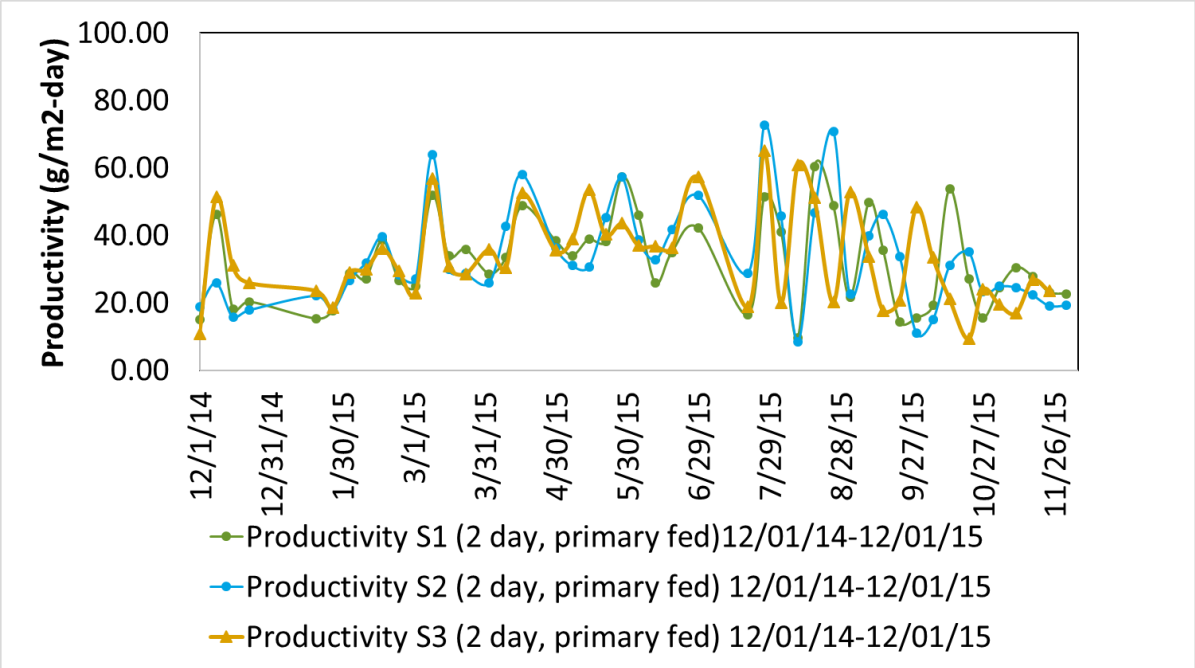

Figure 50: Annual average productivity for the ponds diluted with primary clarified wastewater on a 2-day hydraulic residence time.

Over the same year, the north ponds (N) were diluted with primary wastewater at a variable residence time (2 - 4.5 days) and compared to the south ponds (S). These ponds showed similar trends, the week to week variability in productivity was high, but the variability in productivity between the replicate ponds was low (Figure 52). Overall, the productivity in the ponds diluted at a two-day residence time was greater than the ponds with a longer residence time (Figure 53). Seasonally, the S-ponds with a 2-day residence time had an aerial productivity 24 - 55% greater than the N-ponds (4.5-3-day HRT) (Figure 53, Figure 54). This indicates that faster dilution rates generally result in higher productivities independent of season.

From 7/27/15 - 8/25/15 the North and South ponds were both set to a 2-day residence time, but the CO_2 was turned off in the north ponds. During this time the productivity in the CO_2 fed S-ponds was 24% higher than the N-ponds. After this experiment, the CO_2 was turned on to both ponds and they were diluted at 2-day residence times. Under these conditions, they demonstrated very similar productivities

(Table 4). This indicates that the CO_2 provided by bacterial respiration must be supplemented with gaseous CO_2 to maximize productivity in wastewater ponds.

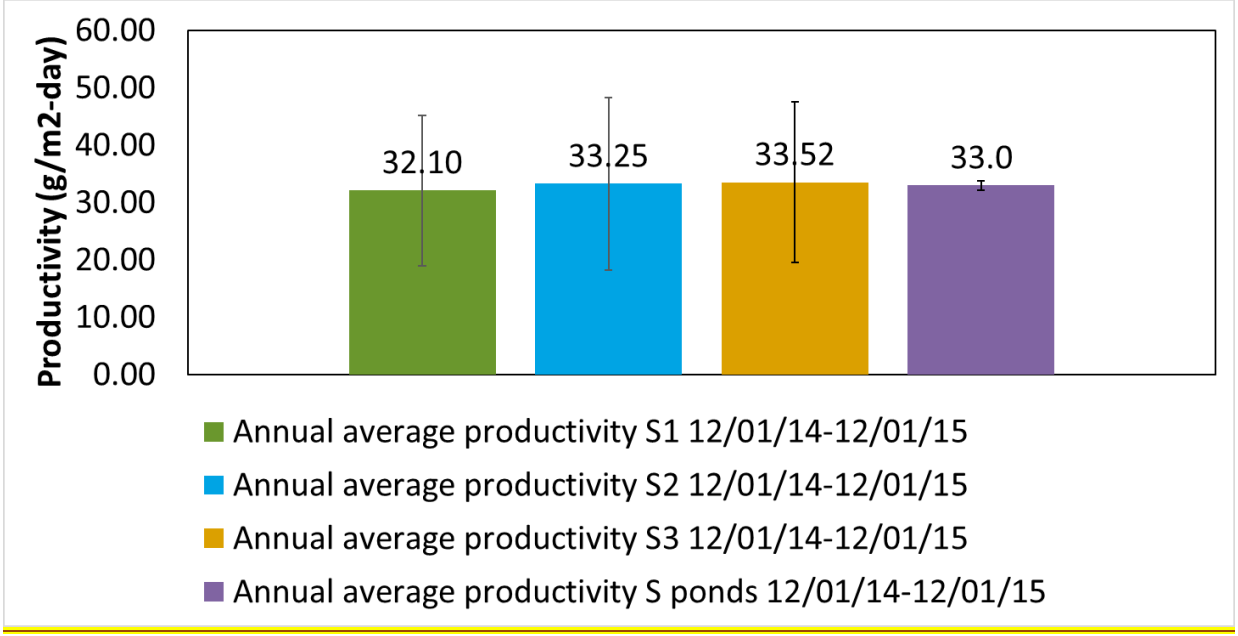

Figure 51: S ponds annual average productivity. The error bars for the individual ponds indicate the standard deviation of the productivity over 52 weeks and encompasses all four seasons. The error bar for the annual average productivity indicates the standard deviation between the annual average productivity of the three replicate ponds. As expected the week to week variability is high due to seasonal and daily weather changes, but magnitude of the variation is similar. Variability between the replicate ponds is low.

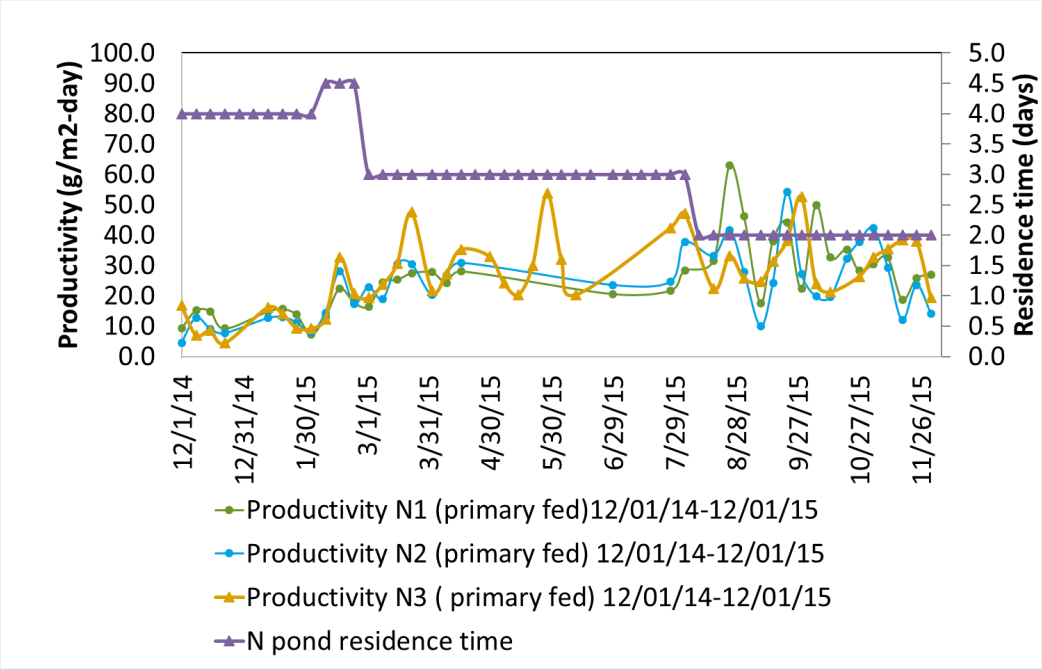

Figure 52: Annual average productivity for the ponds diluted with primary clarified wastewater on a 2-4.5-day hydraulic residence time.

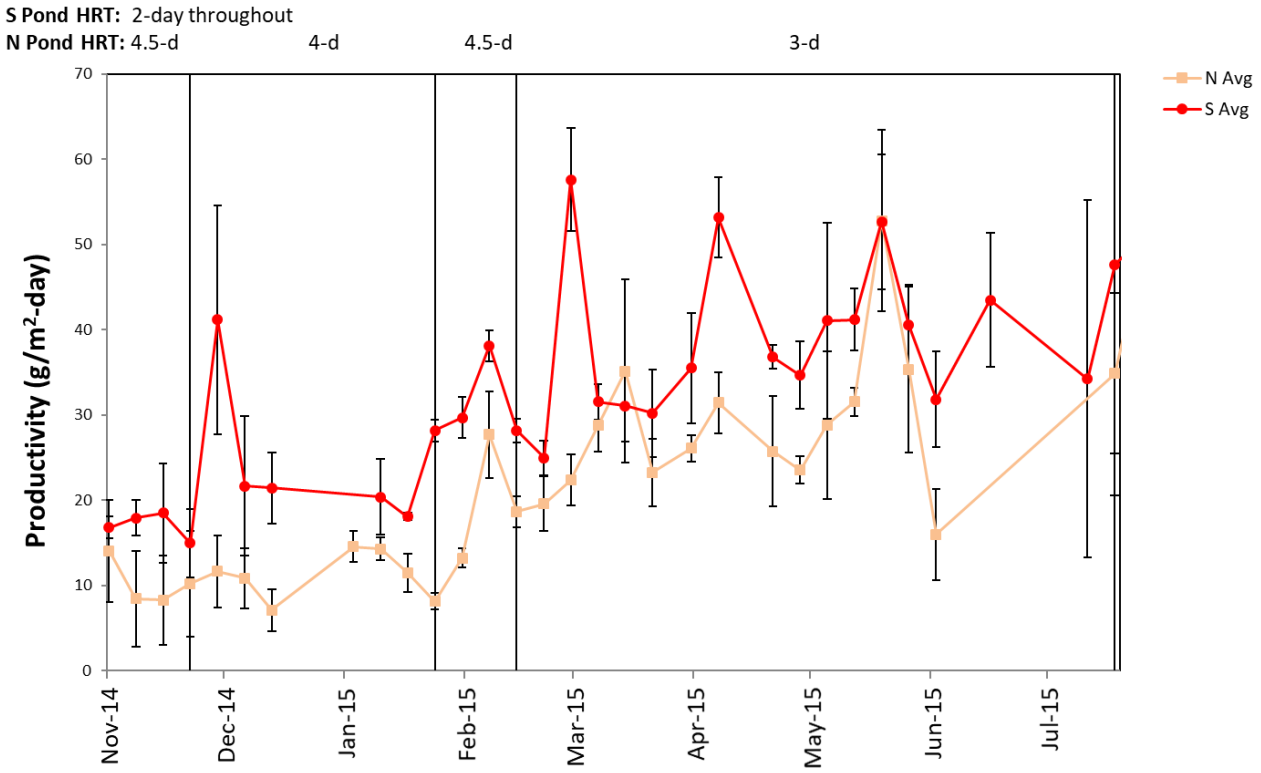

Figure 53: Comparison of the ponds diluted with primary clarified wastewater. Top axis indicates the residence time in the N-ponds while the S ponds were diluted on a 2-day residence time for the experiment duration (Pittner 2018). Error bars indicate the standard deviation between the replicate ponds.

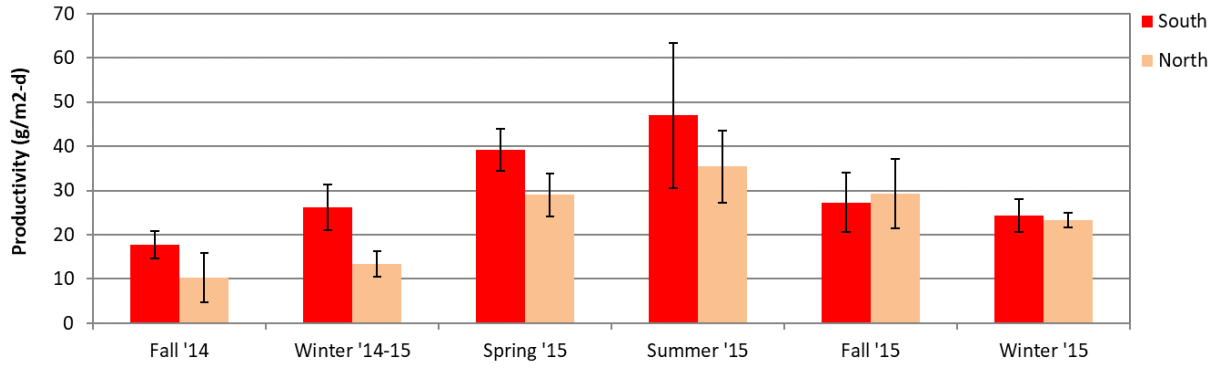

Figure 54: Average productivity for the N and S ponds. The S-ponds with a 2-day residence time had an aerial productivity 24-55% greater than the N-ponds (4.5-3-day HRT) (Pittner 2018). Error bars indicate the standard deviation between the average for each season for the replicate ponds.

Table 4: Productivity in the North ponds (primary, variable HRT) compared to the South ponds (primary, 2-day HRT). From 7/27/15-8/25/15 the HRT was the same in both pond sets, but the CO_2 was turned off to the North set. From 9/1/15 to the end of the experiment an influent dosing experiment was performed that had little to no effect on productivity.

Duration	Season	South (g/m^2-d)	North (g/m^2-d)	S HRT (day)	N HRT (days)	Percent Higher S Productivity
11/10/14 to 11/24/14	Fall '14	17.7	10.2	2.0	4.5	42.2
12/1/14 to 2/23/15	Winter '14-15	26.2	13.4	1.8	4.0	53.5
3/2/15 to 5/28/15	Spring '15	39.2	29.1	2.0	3.0	25.8
7/27/15 to 8/25/15	Summer '15	47.0	35.4	2.0	2.0	24.6
9/1/15 to 11/24/15	Fall '15	27.0	29.3	2.0	2.0 (D/N feed)	-8.5
1/12/16 to 2/23/16	Winter '16	24.3	23.4	2.0	2.0 (D/N feed)	3.9

The M-ponds were fed water from the full-scale facultative pond and diluted with a seasonal 3.7 - 5.4-day residence time based on the calculated residence time in the full-scale raceway ponds (Figure 55). The annual average productivity for the M ponds was 14.5 g/m^2 day (Figure 56). This productivity was only 43% the productivity of the S ponds (primary, 2-day HRT) and was also seasonally significantly less than the North ponds. These results indicate the importance of short dilution times and high organic loading to achieving high productivity in wastewater fed ponds. The facultative pond water typically contained significantly fewer solids and organic carbon then the primary wastewater because it was already partially treated in the deep facultative pond.

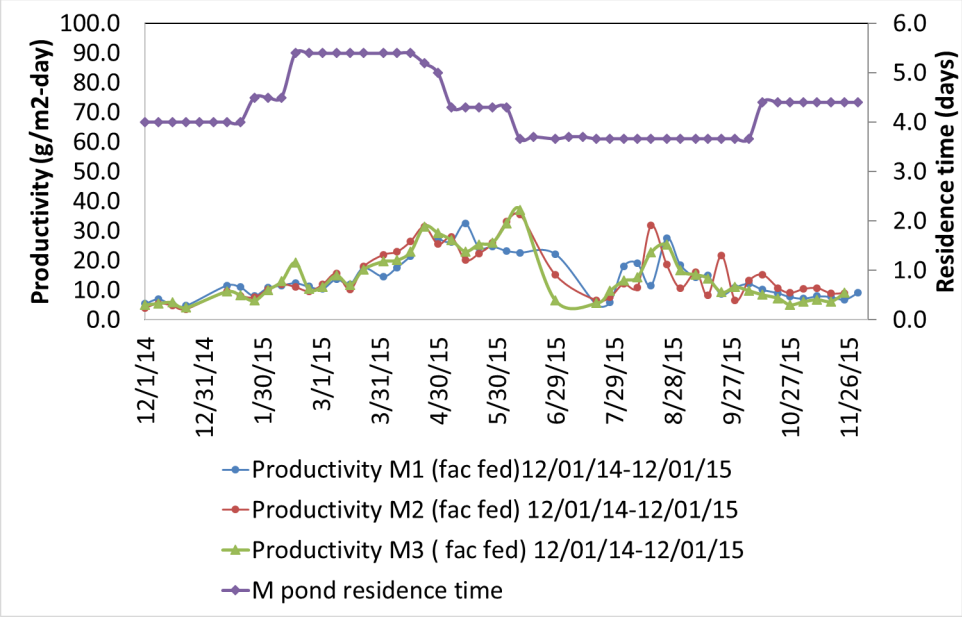

Figure 55: Productivity and hydraulic residence time of the middle ponds (M). These ponds were diluted with facultative pond water at a 3.7-5.4-day HRT to mimic the HRT changes in the full-scale system.

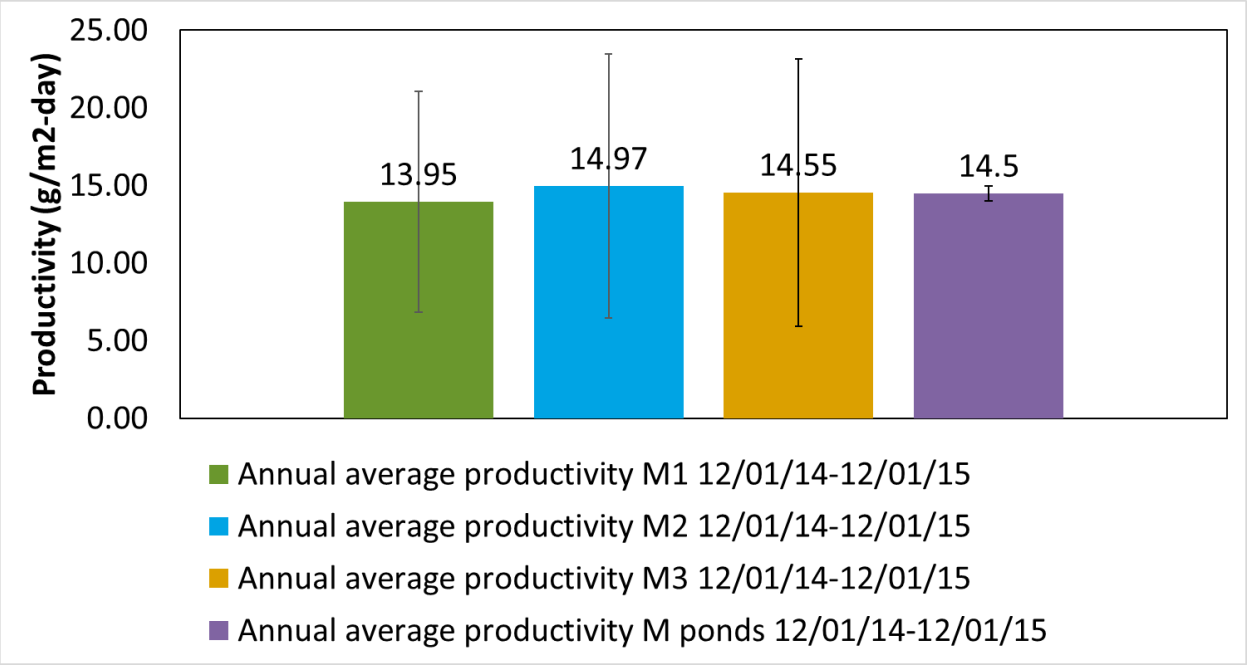

Figure 56: Annual average productivity for the ponds diluted with facultative pond water at a seasonal 3.7-5.4 -day HRT. The error bars for the individual ponds indicate the standard deviation of the productivity over 52 weeks and encompasses all four seasons. The error bar for the annual average productivity indicates the standard deviation between the annual average productivity of the three replicate ponds. As expected the week to week variability is high due to seasonal and daily weather changes, but magnitude of the variation is similar. Variability between the replicate ponds is low.

In general, the higher loaded primary diluted ponds had superior gravity settling when compared to the ponds diluted with facultative pond water. Removal of volatile suspended solids (AFDW) from the pond effluent by 24 hours of gravity settling from 08/03/15 - 03/22/16 was 88%, 87%, and 80% for the S-ponds, N-ponds and M-ponds respectively (Figure 57). For the same period, the average effluent AFDW was 22, 24, and 31 mg AFDW/L for the S-ponds, N-ponds and M-ponds respectively (Figure 58). This could be further rescued with the addition of coagulants, if needed, to meet waste discharge requirements. In general, the ponds diluted with primary clarified wastewater exhibited better bioflocculation than ponds diluted with more stable facultative pond water. These flocs led to better, and faster gravity settling. Additional data on the effect of residence time on treatment can be found in Pittner 2018.

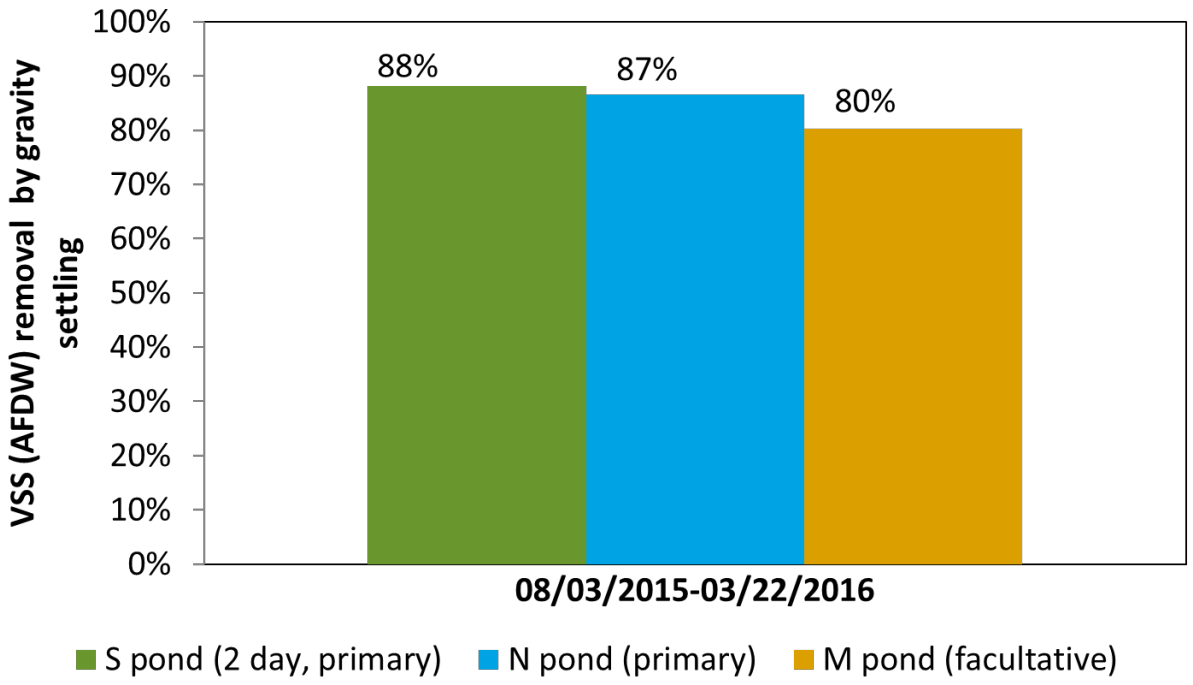

Figure 57: Percent removal of volatile suspended solids (AFDW) for the three pond set conditions.

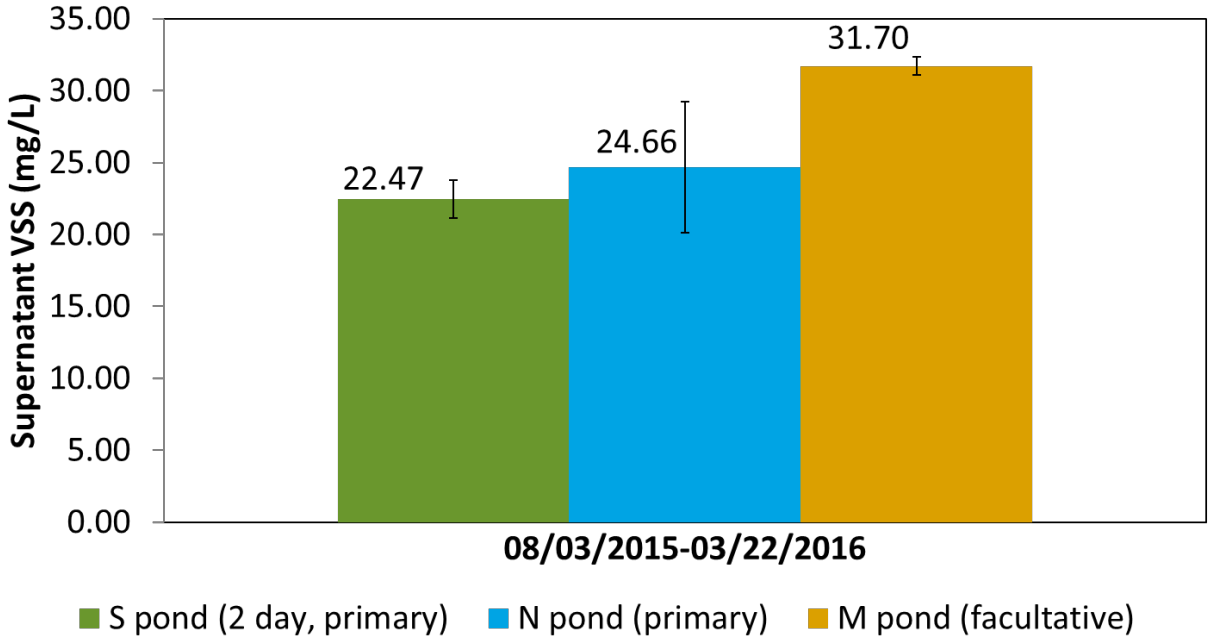

Figure 58: Supernatant volatile suspended solids (AFDW) after 24 hours of gravity settling.

ML2.7 Organism Identification (ID): Identify genetically strains or consortia, along with identification of other dominant organisms in the cultures, such as zooplankton. Look for relationships between dominant organisms and culture performance.

Biomass productivity in wastewater fed ponds can vary widely. Figure 59 shows the time-course evolution of biomass productivity in a primary clarifier effluent fed pond located in San Luis Obispo over a 19-month period. Two characteristics are apparent. First, biomass productivity shows a seasonal pattern, driven by changes in light intensity and temperature, reaching a maximum in late spring, and a minimum at mid-winter, with roughly a three-fold increase from the lowest to highest month. Second, biomass productivity is erratic, with fluctuations at times greater than those experienced seasonally. A host of variables are likely responsible, such as variations in weather patterns, pond operational parameters and fluctuations in influent wastewater flow rate or composition. However, measured values of the influent wastewater suggest that organic carbon, suspended solids, and nutrient concentrations are nearly constant over seasonal time scales. Sampling or pond influent dosing variability may also contribute to day-to-day variations in measured biomass concentration, and in effect productivity. Bias due to pond hydraulics and dilution is exacerbated by biomass morphology. Depending on whether the culture is predominately flocculated, colloidal, or filamentous, biomass may leave ponds via the overflow standpipe at a concentration not representative of the pond.

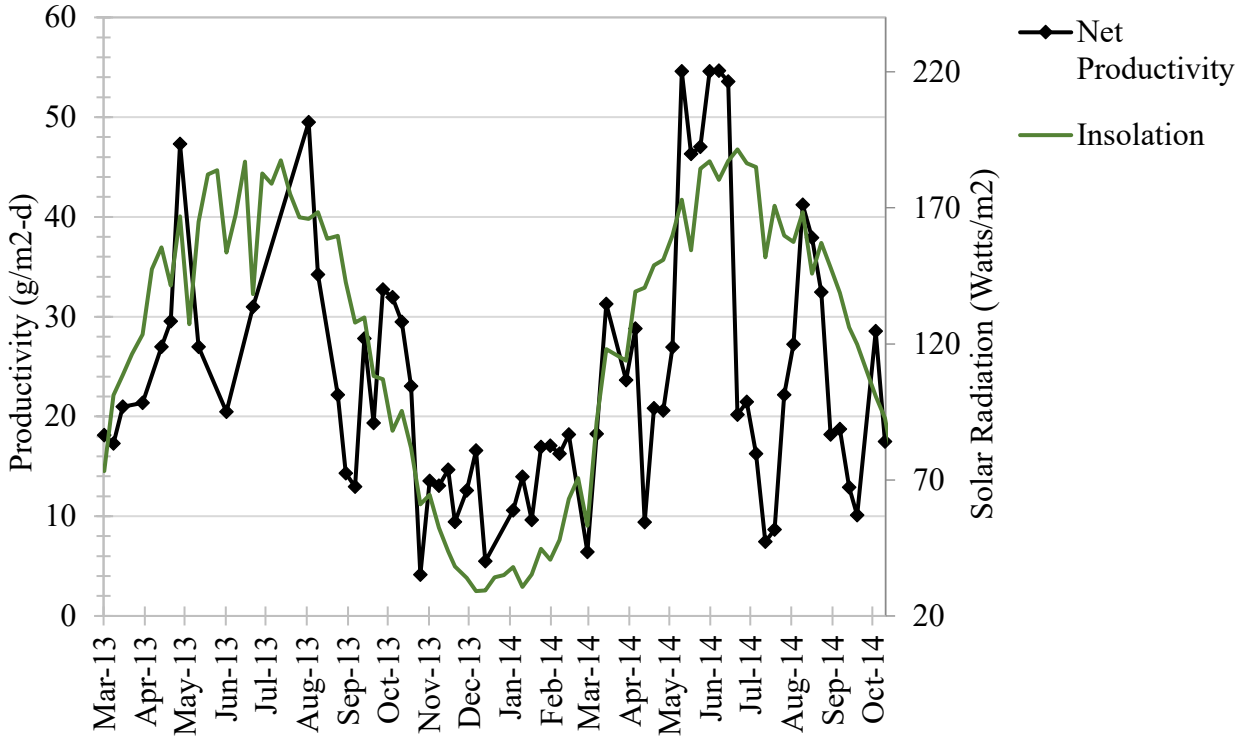

Figure 59: Net biomass productivity and insolation for ponds fed primary clarifier effluent at a 2-day HRT. Data span from March 2013 to October 2014.

Pond ecology is yet another factor contributing to pond performance. Pond cultures are traditionally monitored via microscopy, providing a qualitative estimate of presence or absence at the genus level. At the San Luis Obispo field site, genera including *Coelastrum*, *Chlorella*, *Chlorococcum*, *Closteridium*, *Cyclotella*, *Micractinium*, *Nitzschia*, *Oscillatoria*, *Pediastrum*, *Scenedesmus*, and *Stigeoclonium* are typically observed, although the relative proportion of each can vary widely. Biovolume estimates and cell counts can be used for more quantitative estimates of pond ecology, although are time intensive due

to the number of counts and measurements required to minimize statistical uncertainty. Culture morphology, namely the large flocs typically present in rapidly settling wastewater ponds, makes it difficult to mount representative sub-samples onto the microscope slide. Additionally, samples require pretreatment to break up algal-bacterial flocs, which would otherwise obscure identification and quantification. Utermohl chambers, in which a more representative (i.e. ~ 5 ml versus 10 µL) culture sample is allowed to settle, then examined using an inverted microscope to probe the settled biomass layer along the chamber bottom, have been used to provide monthly estimates, although more frequent analysis would be resource restrictive, particularly when considering multiple, replicated treatments. Additionally, microscopic techniques do not provide the resolution required to track the sub-micron community.

Recently, Next Generation DNA Sequencing (NGS) has been applied to outdoor ponds to monitor for organisms responsible for pond crashes (Carney et al. 2016), as well as analysis of the culture microbiome (Carny et al. 2014). These methods avoid sub-sampling bias by performing analysis on the bulk biomass, with samples collected by centrifugation of a sample volume sufficient to yield several milligrams of biomass. Genomic DNA is extracted from the dewatered biomass, and then characterized via high-throughput sequencing. Advanced datamining techniques are the applied to the data set, allowing a qualitative estimate of pond ecology.

In the present report, we apply genetic analysis and data mining techniques to better understand how pond ecology relates to biomass productivity and settling efficiency. Specific research questions include:

1. What are the principal algal and bacterial species in mixotrophic (i.e. primary clarifier effluent fed) and primarily phototrophic (reclaimed water) ponds?
2. Are there significant changes in the algal and bacterial pond ecology in ponds with either mixotrophic or predominantly phototrophic growth over day to week time-scales?
3. How does species composition compare in replicate ponds?
4. How does strain composition of algal pond wastewater treatment systems compare to that of biological assemblages traditionally used in wastewater treatment for settling processes, i.e. return activated sludge (RAS).
5. Are there bacterial or algal strains or communities that are positively or negatively correlated with biomass productivity or settling efficiency?

Biomass productivity measured in primary influent and reclaimed water fed algal ponds is reported in Figure 60. Biomass productivity was highest in the ponds fed primary clarifier effluent, reaching 27 g VSS/m^2-day, and a minimum of 2.7 g VSS/m^2-day, with changes in biomass productivity taking place over intervals ranging from two to twelve days. Short term productivity fluctuations were at times significant, decreasing by as much as three-fold (P1: 7/29 to 8/3, P2: 8/11 to 8/14) over four days, with changes of +/- 3 g VSS/m^2-day more typical. Rapid, short-term productivity changes were generally isolated to a single pond, suggesting a factor independent between ponds as likely responsible. More gradual biomass productivity fluctuations were also observed, with two to four-fold changes taking place over seven to twelve days. Gradual transitions were generally shared between replicate ponds. The pond fed reclaimed municipal wastewater (RmW) was nearly always less productive than the primary-influent fed counterparts. After a period of initially variable productivity from 7/21 to 7/29, productivity stabilized to between 7 to 10 g VSS/m^2-day for the remainder of the sampling period. The replicate reclaimed water-fed pond is not shown due to incorrectly recorded influent flow rates, a parameter required for the calculation of productivity.

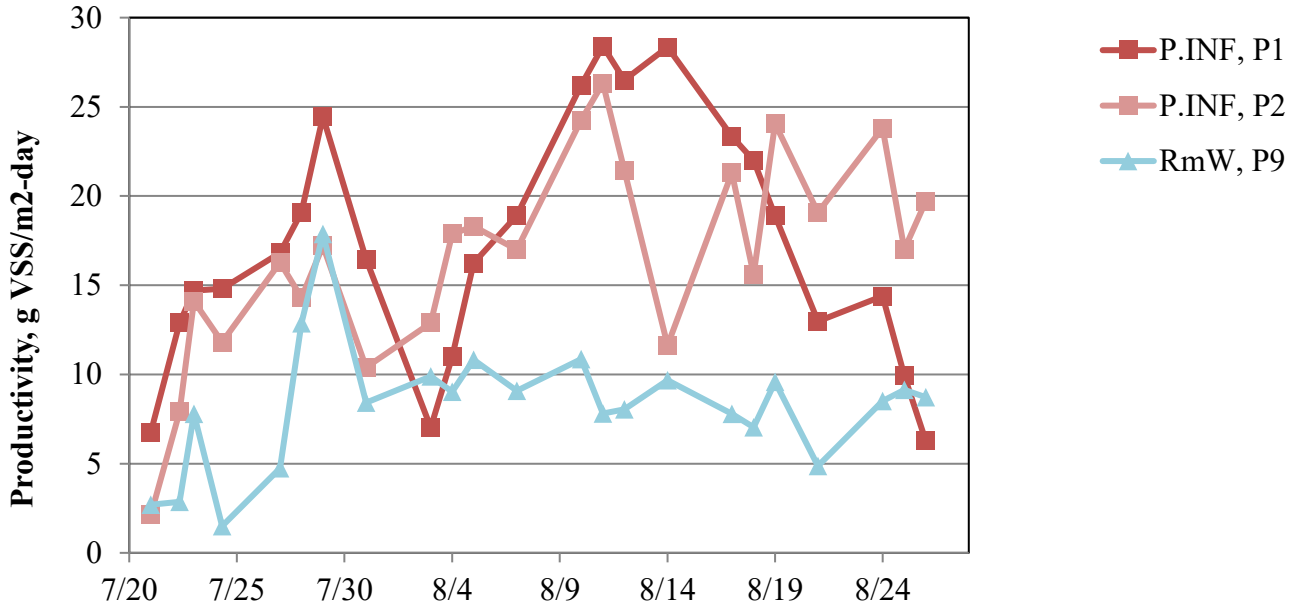

Figure 60: Productivity in raceways fed primary effluent (P. Inf, P1 and P2) and reclaimed water (RmW, P9).

Weather conditions, expressed as daily averages, are summarized in Figure 61. Insolation exhibited a gradual decline over the sampling period, with the daily average decreasing from 328 to 284 W/m^2. Air temperature varied more widely, reaching a high of 28˚C on 7/29 and 8/17, and a low of 21˚C on 8/4. Changes in weather conditions were buffered by the on-ground ponds, which remained relatively stable near and average temperature of 23˚C, exhibiting minor oscillations during periods of changing insolation and air temperature. Daily insolation decreased from 7/29 to 7/31 in response to local weather conditions, then more substantially from 8/3 to 8/6, then returned to seasonal norms on 8/7. This period of cloudy weather and was accompanied by a decrease in air temperature. In response, 24-hour average pond water temperature decreased by slightly over 2˚C.

Qualitative comparisons of the period of less-favorable growth (lower light intensity and temperature) to biomass productivity indicated that local weather conditions may in part be responsible for the decrease in productivity in all ponds from 7/29 to 8/3. When light intensity and pond water temperature increase to normal levels on 8/7, productivity in primary clarifier effluent ponds similarly increases. It is difficult to correlate weather conditions and biomass productivity during the slight increase in pond water temperature from 8/14 to 8/16 (23 to 25˚ C), as replicate primary clarifier effluent fed ponds performed differently, and the reclaimed water fed pond productivity remained stable.

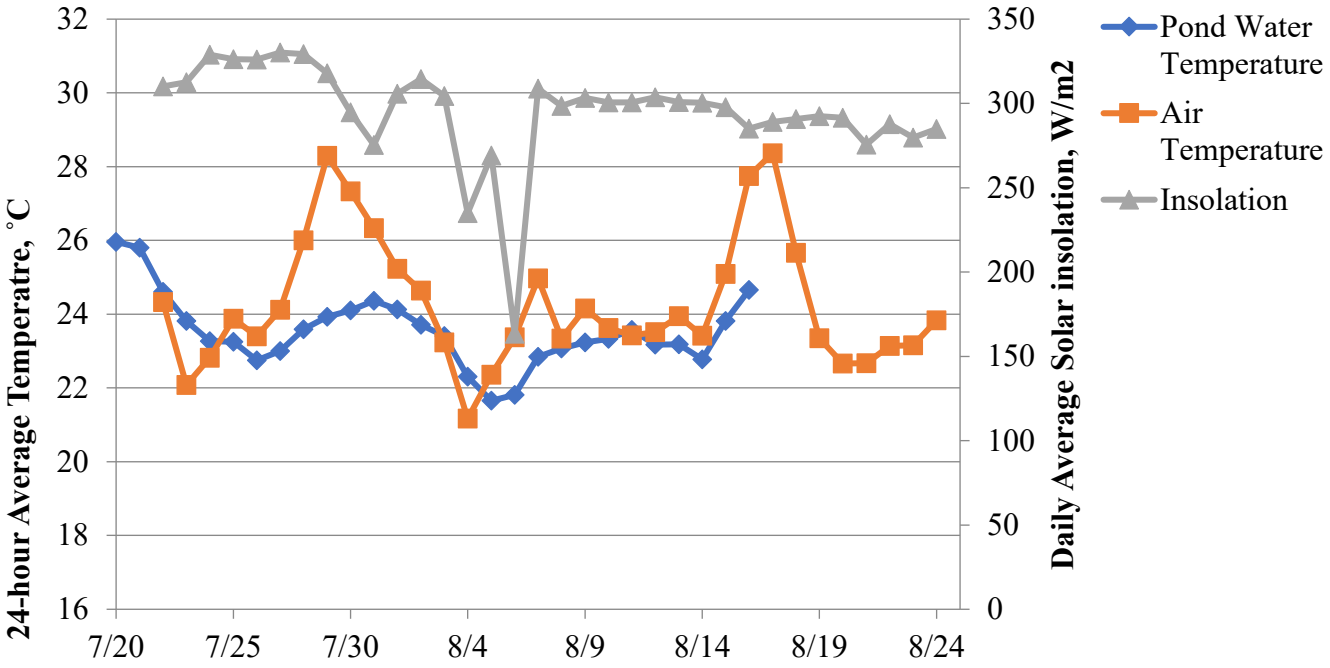

Figure 61: 24-hr averaged pond water temperature, air temperature, and insolation over the sampling period.

Reclaimed water fed cultures more consistently achieved a higher settling efficiency, a key metric for low-cost primary dewatering. Initially, settling efficiency in duplicate reclaimed water fed cultures varied, with the poor settling pond matching that of its replicate within a week (~95%, 7/29). At the beginning of the sampling period, both primary influent fed ponds settled poorly (~50% settling efficiency), although increased steadily over a three-week span to ~90%. Settling efficiency remained at 90% (primary influent fed ponds) for the remainder of the sampling period. Return activated sludge (RAS) samples nearly always settled with over 90% efficiency, with one sample (8/18) showing poor performance (40%).

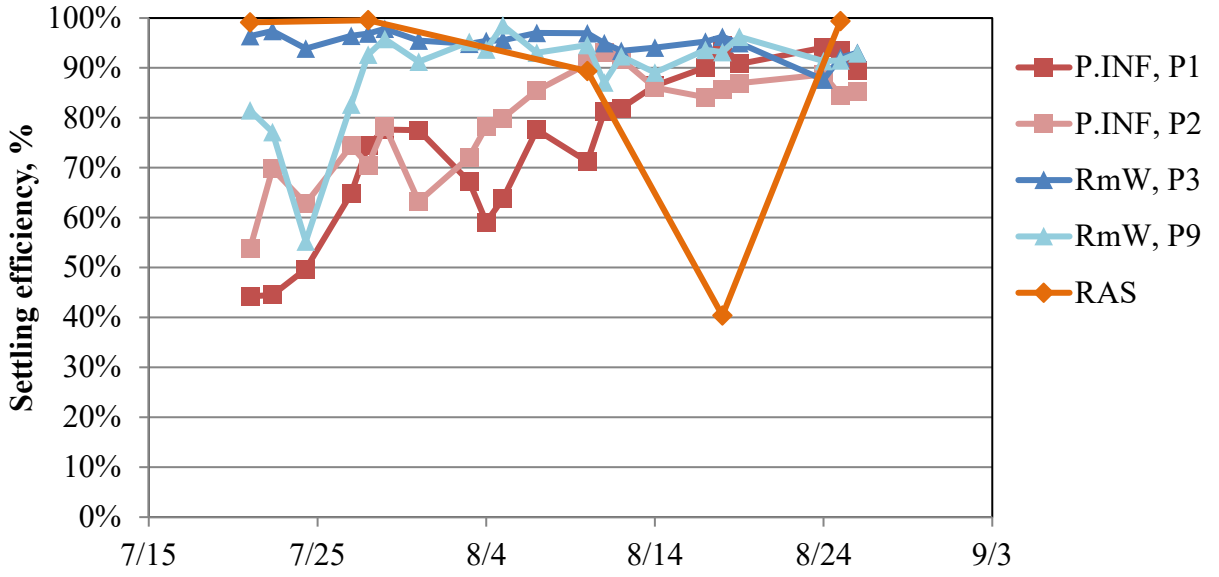

Figure 62: Daily Imhoff cone settling for raceways fed primary effluent (P1 and P2) and reclaimed water (P3 and P9). RAS is return activated sludge from the host site activated sludge system for comparison.

Metagenomic analysis and validation

Of the samples processed, there were 7,619,732 sequence reads for the eukaryotic small subunit rRNA (SSUrRNA) gene that were considered valid and distinct. Of the 858 different 18S sequences, 250 were identifiable in genomic databases. The identifiable eukaryotic taxa made up 76.5% of the read counts across all ponds. A higher percentage of identifiable operational taxonomic units (OTUs) were measured in samples containing less dissolved organic carbon. Primary clarifier effluent had the highest number of unknown assignments. Primary clarifier effluent fed ponds had a larger percentage of unknown organism counts then the reclaimed water fed ponds, 61.2% versus 3.8%. The primary clarifier effluent was the most diverse, with around 100 more OTUs than the experimental ponds across the sample period. Not all identified OTUs were algal or bacterial. *Mus musculus*, the house mouse, was found in primary clarifier effluent, with 361 read counts. For an overall view of pond composition, operational taxonomic units (OTUs) were grouped by higher taxonomic labels (Figure 63). Organisms were grouped to allow relevant trends to be identified. OTUs are listed by common names and by their role in the microbial community.

There were 31 OTUs in the eukaryotic SSUrRNA analysis that belonged to the domain Bacteria. They were Proteobacteria, Bacteroidetes, Firmicutes. Only ten of these OTUs were also found in the prokaryotic SSUrRNA analysis. Of the shared OTUs, different counts were measured in the prokaryotic and eukaryotic SSUrRNA data sets. Each rDNA sequence has a different affinity for binding by both eukaryotic and prokaryotic primers. In four instances, different OTUs were assigned to the same species. There were four OTUs for the species *Oocystis heteromucosa*, two OTUs for *Nannochloris sp.* SAG 251-2, two for *Chlorella sp.* MBIC10088, and three for *Desmodesmus sp. F2*, and in each case the online database accession number was matching among the repeats. Thus, they are most likely the same as the species in the database, but with point mutations or possibly some polymerase mistakes that were detected in sequencing.

Genera found in both primary influent and reclaimed water fed ponds include *Scenedesmus*, *Desmodesmus*, *Pediastrum*, *Tetraedron*, *Chlorella*, *Oocystis*, *Closterium*, *Chlorococcum*, *Tetradesmus, Oocystis*, *Pediastrum*, and *Scotiellopsis*, with minor but consistent levels of reads from golden algae and diatoms. Read counts of suspected pond pathogens were regularly detected, including rotifers, chytrids, and ciliates. Replicate primary clarifier effluent fed ponds maintained different genera composition. *Scenedesmus* gave the highest percentage of read counts in Pond 1, with *Chlorella*, *Desmodesmus*, and *Tetradesmus* as the primary secondary components. Pond 2 favored *Tetradesmus* and *Chlorella*, with the remaining genera constituting minor components (generally fewer than 5,000 reads). Given the morphological similarity of *Tetradesmus*, *Desmodesmus*, and *Scenedesmus*, the subtle difference in species composition went unnoticed by microscopy. The takeover of *Tetradesmus* in Pond 1 on 8/7 may more likely be a sample error. Unlike the primary clarifier effluent fed replicate ponds, reclaimed water fed ponds maintained a similar and consistent microbiome, primarily *Tetradesmus*.

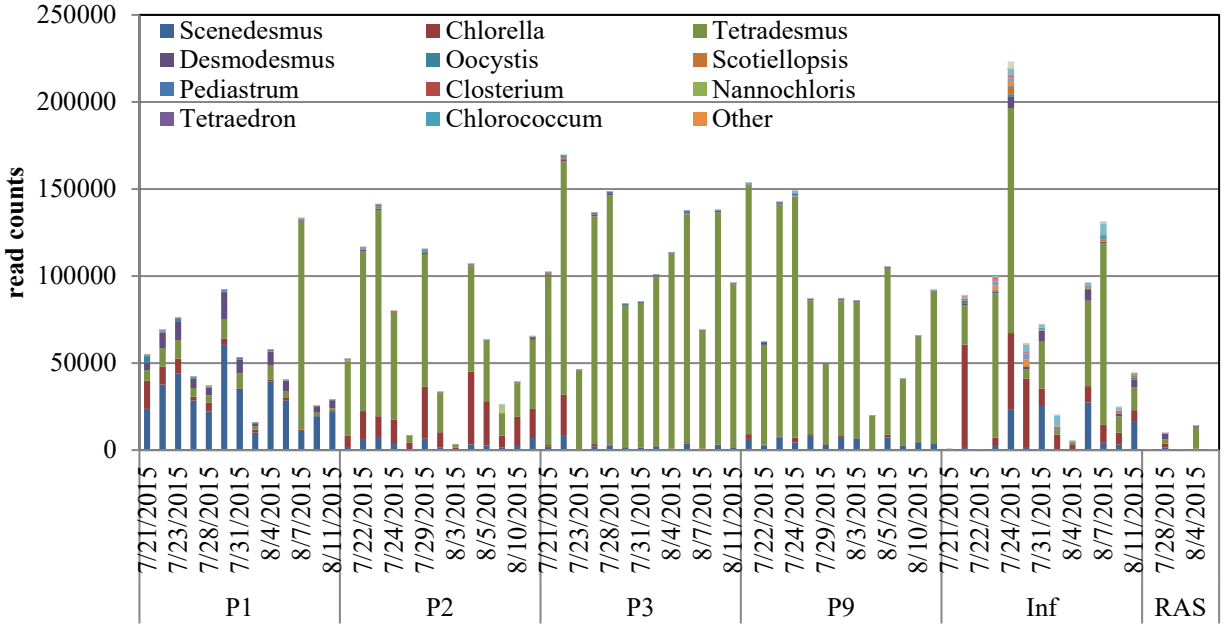

Figure 63: Summary of reads, grouped at the genus level, from the eukaryotic SSUrRNA dataset for primary clarifier effluent (Inf), primary clarifier effluent fed ponds (P1, 2), reclaimed water fed ponds (P3, 9), and return activated sludge (RAS). Counts of unassigned read are not shown.

In the prokaryotic SSUrRNA dataset, there were 718,465 sequence read counts. 590 different sequences were provided, 166 of which were recognizable in genomic databases. The prokaryotic SSUrRNA reads were only 41.2% identifiable. Proteobacteria were by far the largest group identified primary clarifier effluent, with the bacterial community structure increasing in diversity as it passed through the primary clarifier effluent fed ponds (P1, P2). Ponds receiving reclaimed water (P3, P9) showed some similarity to RAS, with bacteroidetes as a predominant and reoccurring group. Despite the very large amount of chloroplasts present in algal pond samples, the use of chloroplast excluding primers was largely successful; only two OTU's in the prokaryotic SSUrRNA dataset were identified as chloroplastic.

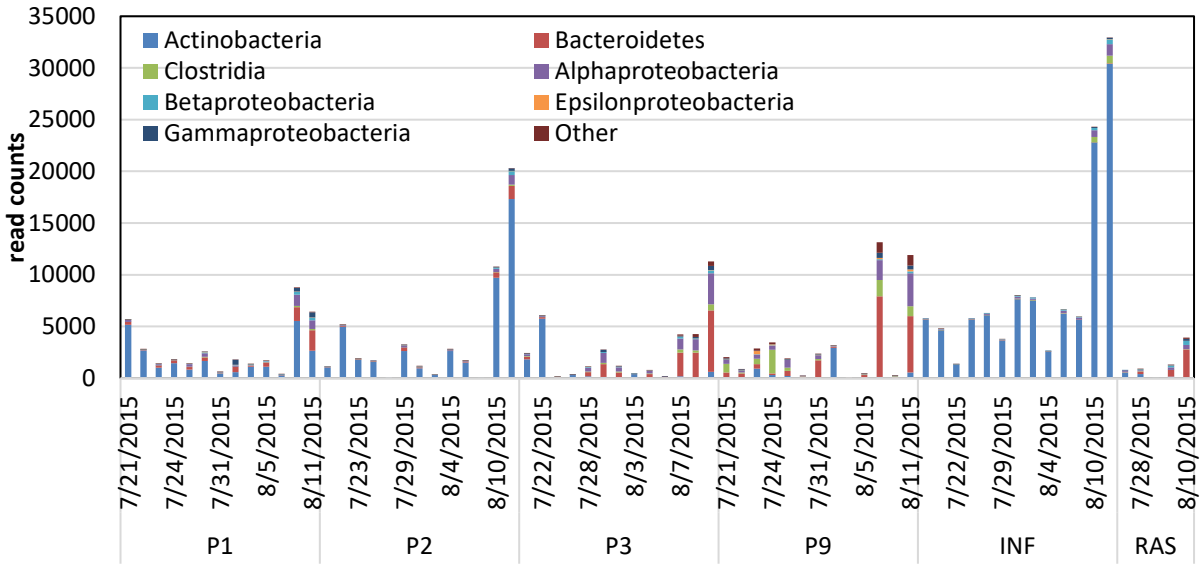

Figure 64: The 16S read count composition of the analyzed samples. Unidentified reads are not shown.

Return activated sludge and primary clarifier effluent maintained a more variable eukaryotic community than the ponds. *Tetradesmus* and *Chlorella* were routinely found in the primary clarifier effluent, likely contributing to their comparatively high counts in the ponds. Primary clarifier effluent was less likely to be dominated by a single component, with read counts of multiple genera reaching 15% of those assigned to an OTU. The number of assigned read counts in primary clarifier effluent was highly variable, anywhere from near zero to over 200,000, with the majority of the reads unassigned to an OTU. The eukaryotic community of RAS was variable, and comparatively few read counts measured relative to primary clarifier effluent or the algae ponds. From the prokaryotic SSUrRNA dataset, primary clarifier effluent was dominated by Actinobacteria, a group associated with decaying organic matter, while Bacteriodetes were generally favored in RAS.

For initial validation of the metagenomic dataset, taxonomic assignments were compared to pond micrographs (Table 1). Micrographs were compared with the sequence read counts of eukaryotic SSUrRNA OTUs grouped mostly at the genus level. In the example micrograph shown below (8/5, P1), metagenomics analysis appears to be well-matched. Cells resembling *Scenedesmus*, *Desmodesmus*, and *Tetradesmus* are clearly observed, which collectively account for the majority of read counts within the sample. Minor components such as *Chlorella, Oocystis* (not shown in the micrograph below, but found in others), and *Pediastrum* are similarly present in both the micrograph and genomic analysis. The 1 prokaryotic SSUrRNA OTU's consists almost exclusively of organisms that are too small be identified by microscope.

Table 5: Comparison of a pond microscopy-based identifications to dominant OTUs from the eukaryotic SSUrRNA dataset. Microscopic analysis compared well to OTUs reported from the genomic analysis (additional micrographs not shown), although in some instances the read counts did not appear well correlated to the general level of abundance from the micrograph.

Sample	Date	Read counts	Organism Category	Presence/absence	Representative Micrographs
P1	8/5/15	64172	Unknown	-	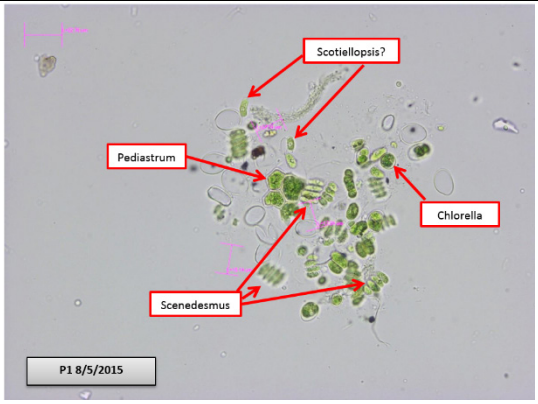
		28640	Scenedesmus	yes	
		6065	Desmodesmus	yes	
		3613	Tetradesmus	unclear	
		1270	Chlorella	yes	
		330	Oocystis	yes	
		248	Pediastrum	yes	
		92	Rotifers	not seen	
		66	Scotiellopsis	unclear	
		30	Diatoms	yes	
		18	Ciliates	not seen	
		14	Coelastrella	yes	

Identifying community networks

Microbial networks based on genus level assignments from the prokaryotic SSUrRNA gene sequence were formed by understanding the microbial co-occurrence within a given sample set, expressed numerically as a co-occurrence coefficient. Co-occurrence coefficients were calculated by comparing genera abundance as a profile in all the samples and time points. Genera simultaneously present at high abundance receive higher co-occurrence coefficients (regions of red in Figure 65 below). Conversely, genera present at high abundance only when other genera are absent, or at low abundance, are negatively co-correlated (regions of green in Figure 65 below). The heat map in Figure 65 is visualized as a microbial community network in Figure 66, with distinct communities present in primary clarifier effluent (red), primary clarifier effluent fed ponds (light green), reclaimed water fed ponds (blue), and shared groups between primary clarifier effluent and reclaimed water (green) highlighted. In Figure 66, the co-occurrence coefficient is represented spatially, with positively correlated genera positioned closer together, and negatively correlated genera further apart by calculating the pairwise distance calculated by 1- co-occurrence coefficients. The community networks of the three sample types (primary clarifier effluent, algal ponds fed primary clarifier effluent, and algal ponds fed reclaimed water) are consistent with initial expectations, that is, the community structure of the primary clarifier effluent fed ponds shares overlap between both the reclaimed water ponds and primary clarifier effluent, whereas fewer similarities exist between the reclaimed water ponds and primary clarifier effluent.

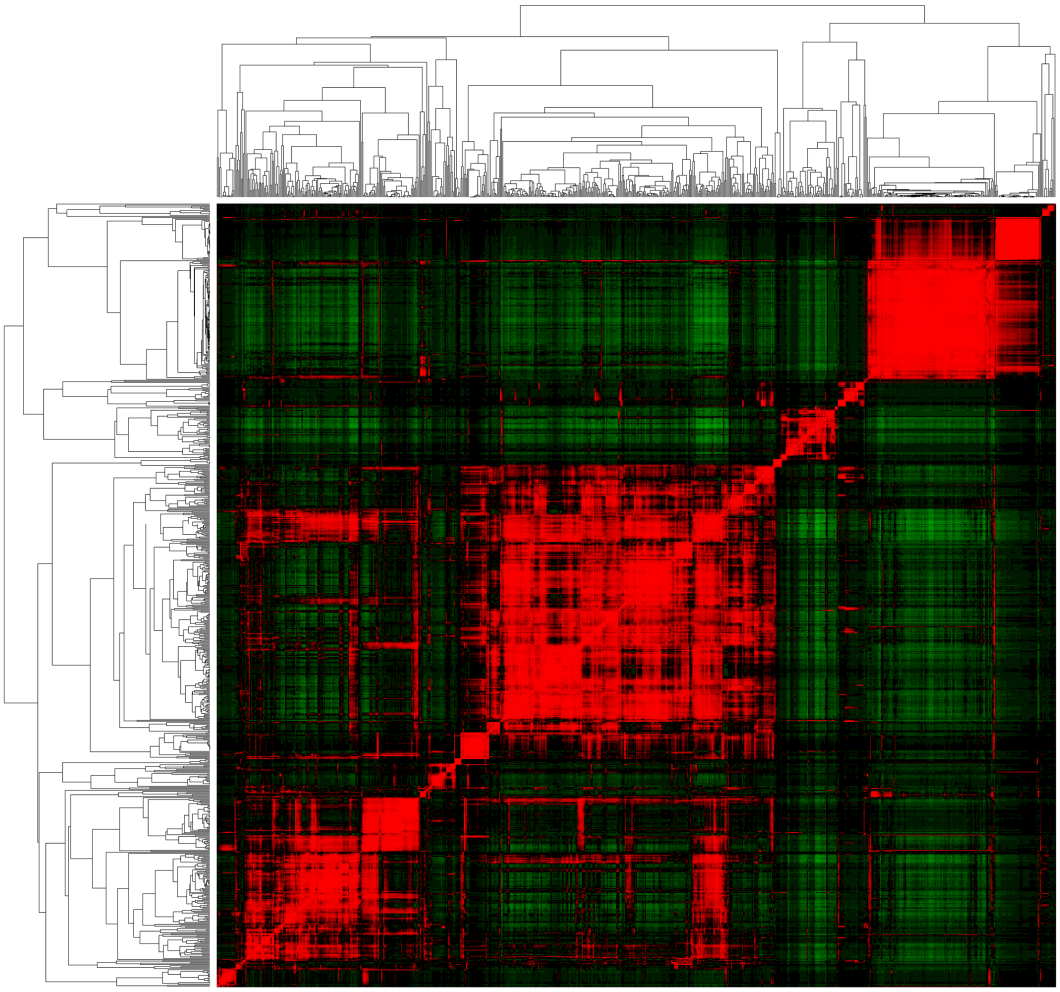

Figure 65: Heat map of the co-occurrence coefficient calculated from the time-course abundance between genera. Regions of red represent genera that are co-correlated, Green regions reflect negatively co-correlated genera.

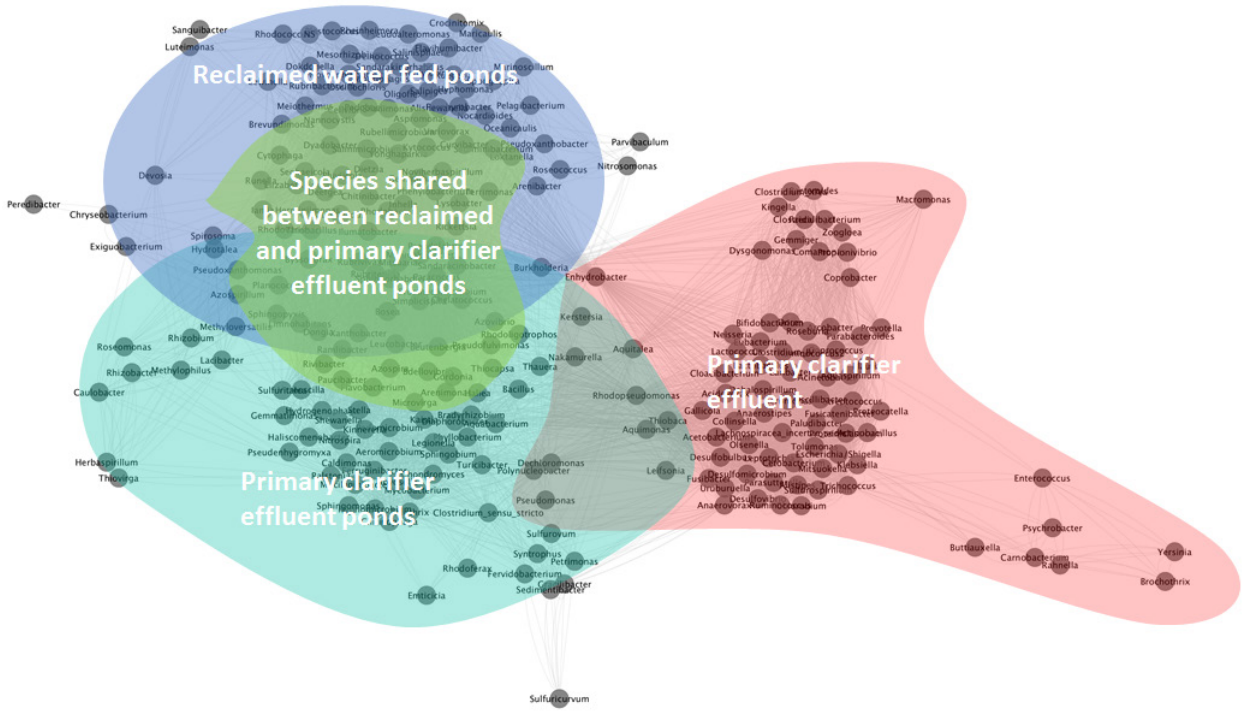

Figure 66: Microbial community network plot constructed by spatially arranging the data from Figure 65. From this analysis, three distinct communities emerge, consistent with the three sample types analyzed.

Relationships between community structure and pond performance

Canonical Correspondence Analysis (CCA) was performed to identify relationships between the microbial community and biomass productivity and settling efficiency. Correlation coefficients for the eukaryotic SSUrRNA left) and one prokaryotic SSUrRNA (right) communities are shown in Figure 67 below. Of the eukaryotes, CCA identified the ciliate *Loxophyllum* as the most likely to cause a decrease in settling efficiency, followed by the chyrsophyte *Ochromonadaceae*, while the chytrid *Rhizophydium* and chlorophyte *Botryococcus* were weakly (CCA coefficient ~0.5) associated with improved settling. Few eukaryotes were found to strongly influence biomass productivity, with the ciliate *Hemiophrys* showing a negative correlation (-0.50), and *Botryoccocus* as positively correlated (+0.5). Correlations below 0.5 were deemed unlikely to be significant. Of the prokaryotic community, the sphingobacterium *Algoriphagus* showed a negative correlation with settling efficiency and positive relationship with settling efficiency.

Pearson's correlation coefficients were calculated to check for possible linear correlations between pond performance and the microbiome. Of the metagenomic data compared, no correlations deemed statistically significant. The highest p-value was 0.5, which falls far below the threshold for significance ($p = 0.95$). Some correlation constants reached nearly 100%, but as the correlation increased for some organisms, the statistical significance decreased. Comparing read counts for dominant taxa to productivity and settling graphically, many of the top correlations with very low p-values appear at times well correlated, and then deviate suddenly. It would appear as if another factor in the pond might have changed, causing the organisms' population to fluctuate without impacting the measured productivity or settling data. Even though the sudden shift in taxa read count and productivity/settling correlation was observed in multiple taxa, there was no consistent time point at which the correlation deviated. It does not

seem likely that the many different points of drift-off could be attributed to a single recorded pond change, such as pH or temperature. It is more likely the influence of multiple factors and complex community dynamics in the ponds.

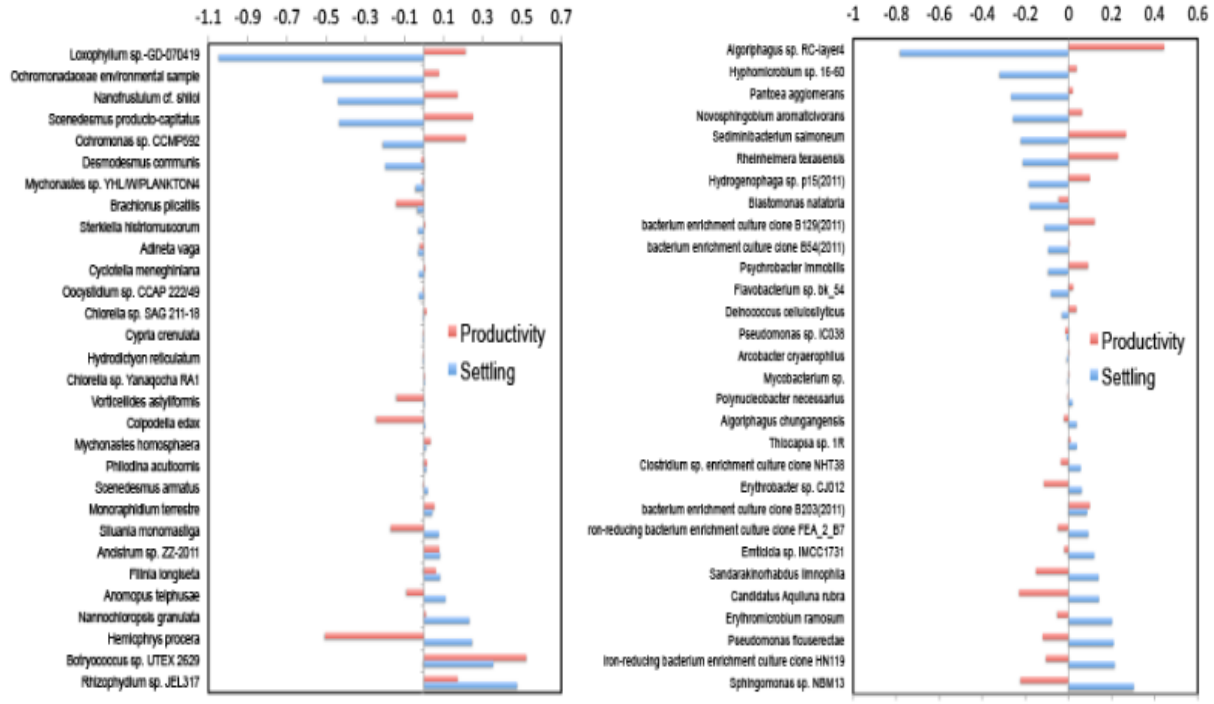

Figure 67: Canonical Correspondence Analysis (CCA) plot relating the 18s rRNA (Left) and 16s rRNA (Right) to biomass productivity (red bars) and settling efficiency (blue bars). Negative bars indicate the organism is generally present in higher abundance when productivity or settling efficiency is lower than the mean value.

The abundance of genera identified in CCA or Pearson's analysis are compared to pond performance parameters for qualitative assessment. *Oocystis,* identified via Pearson's analysis, shows a possible negative correlation to settling efficiency (Figure 68), even though the correlation coefficient and p-values suggest no correlation. In both primary clarifier effluent fed ponds (P1, P2), settling efficiency is initially low (i.e. ~40% in P1, 60% in P2), with a comparatively high read counts of *Oocystis* (log(readcount) > 2). Settling efficiency increased in both ponds to near 80% by the end of the genetic sampling period (8/11), eventually increasing to over 90%. In both ponds, *Oocystis* read counts drop from their initial values. Settling efficiency in ponds fed reclaimed water also appears negatively correlated with *Oocystis*. In RmW fed pond 3, settling efficiency is nearly always 90%, with a correspondingly low *Oocystis* count. Settling efficiency decreases from 95% to 55% in RmW fed P9 from 7/21 to 7/28, with a corresponding increase in *Oocystis* count. Similarly, settling improves when the log of *Oocystis* read counts drop below one. In RAS, *Oocystis* counts are consistently low, and settling efficiency is consistently high, although the sample size is limited. In other studies, we have noted high levels of *Oocystis* (identified from pond micrographs) during times of poor settling.

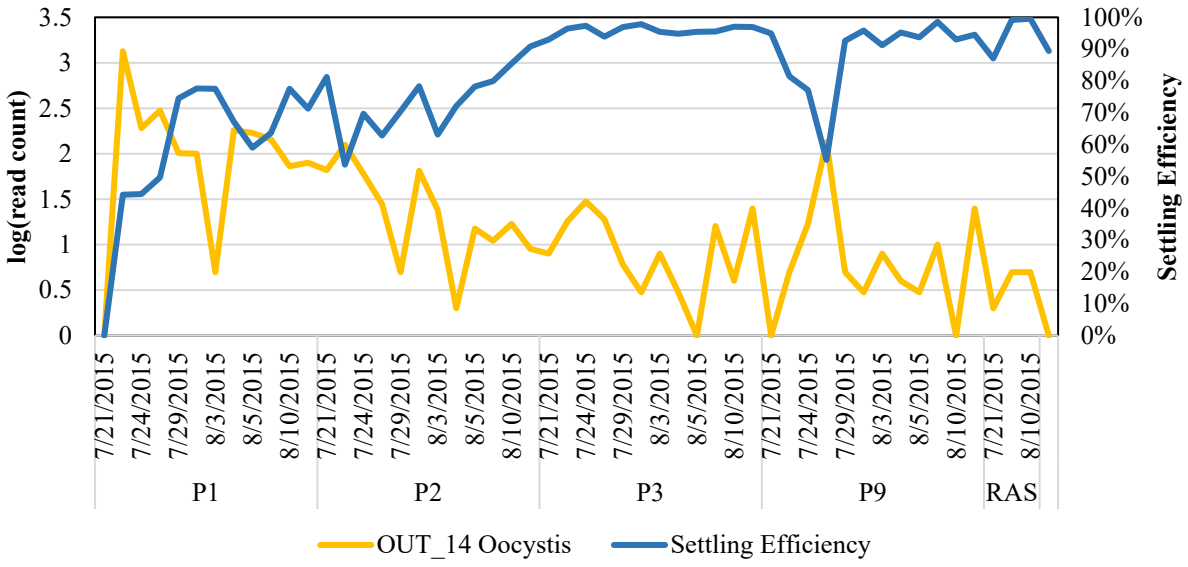

Figure 68: The correlation is statistically insignificant by its p-value, but the settling trend and the change in *Oocystis* read count agree with previous observations from field experiments.

Conclusions and Recommendations

The annual average productivity in the unoptimized full-scale system was 20 g/m^2-day. This productivity was optimized in the pilot scale system by reducing the residence time from 3.7 - 5.2 days in the full-scale system to two-days in the pilot system and controlling the pH in the pilot-scale system with CO_2 addition to a pH of 7.4-7.9. These changes increased the productivity 40% over the full-scale system to 33 g/m^2-day. In the pilot-scale system, along with CO_2 addition, higher organic loadings were found to result in the highest productivities. Therefore, short hydraulic residence times (2-days) and dilution with primary clarified wastewater were found to increase productivity compared to hydraulic residence times greater than 2-days and dilution with facultative pond water. These results were confirmed in a preliminary assessment with the full-scale system when it was operated under a higher organic load and shorter residence from 4/07/14 - 6/30/14. For this experiment, one facultative pond and raceway pond were bypassed, and the productivity increased to 18.97 ±8.1 g/m^2-day from 15.8 ±5.3 g/m^2-day for the same date range in 2015 under normal operating conditions. A longer duration experiment in the full-scale system would confirm these trends.

Additionally, the short residence times and high organic loads in the pilot ponds encouraged bioflocculation and reduced the required coagulant dose needed to meet permitted discharge requirements by half. 88% of the total pond biomass was removed by 24 hours of gravity settling alone. Reducing the coagulant dose has several benefits including reduced addition of ash and salts to the final biomass product which may improve the fuel yield and final fuel product when hydrothermal liquefaction is used, and reduced process costs. The positive effect of short hydraulic residence times, CO_2 addition, and high organic loading on productivity and biomass settling is confirmed in the literature (Park et al. 2011, Valigore et al. 2012, Park et al. 2010).

NGS was used to characterize the microbiome in continuously fed wastewater ponds, with the aim to derive correlations between pond performance and the ecological community. Eukaryotic SSUrRNA gene amplicon sequencing results were, for the most part, in agreement with observations from culture micrographs, at least on a presence and absence basis of genera easily identifiable from brightfield

microscopy. For example, tardigrades were observed in two of five images of RAS collected on 8/10/2015 while having the highest relative abundance in the eukaryotic SSUrRNA analyis. Detection of some samples via microscopy, but not in the genetic dataset, confirm that eukaryotic SSUrRNA rRNA gene characterization can misrepresent sample ecology. For example, despite observing *Closterium* protists (long, crescent shapped symmetric organelles) in the 8/10 Pond 2 sample, there are no corresponding sequences, even though two OTUs identified as *Closterium* were counted in other samples, confirming the genus as present in the database. Similarly, circular clusters of small round algae, visually identified as either *Westella* or *Dictyophaerium*, were also observed in Pond 2 micrographs, although not in the genomic analysis. Even so, for the majority of genera identified via brightfield microscopy, there are corresponding counts in the eukaryotic SSUrRNA dataset.

Correlations between of the percentage of read counts for a given genera to biovolume estimates from brightfield microscopy appear genera dependent. For some genera, relative read count appears well correlated with the relative abundance from micrographs. Members of the *Scenedesmaceae* family, for example, are often found in high abundance (by visual biovolume estimates) in the pond samples analyzed, in agreement with their high relative read count from the genetic analysis. In contrast, despite *Pediastrum* appearing as the dominant genera (on a biovolume basis) in several of the reclaimed water fed pond samples, its relative read count never reached above 0.5%. Bradley 2016 noted that the choice of primer set can influence the relative read count, with some species overrepresented by 4-5 times, while others were underrepresented by two orders of magnitude, and others not reported at all. Therefore, it is possible that a genus with a low relative read count may correlate to a high proportion of the culture on a weight or biovolume basis.

Genera with the highest relative abundance were nearly all confirmed by sample micrographs and showed similarities to wastewater algal ponds reported in literature. Chlorophytes of the family *Scenedesmaceae* were the predominate fraction in both pond sets, which are known to reach an outdoor areal productivity above 20 g VSS/m^2day (Huntley 2016, White 2017), and were also found with the highest percentage of read counts in the wastewater fed ponds from Carney 2014. The lack of diversity in both pond sets, comprising almost entirely members of the *Scenedesmaceae* family, is surprising considering the diversity of the 18s community in primary clarifier effluent. Similar trends were observed in Park 2011, with a single genera, *Pediastrum,* comprising nearly 80% of algal biovolume over a period of three consecutive months in unmanaged ponds, and nearly 100% in ponds with increased solids retention time. While the reclaimed water fed ponds were dominated by a single genera over the sampling interval, minor components, such as *Chlorella*, as well as small changes in the relative proportions of genera within the *Scenedesmaceae* family, were observed in the primary clarifier effluent fed ponds.

The eukaryotic community within each pond was remarkably stable over the 20 day sample interval. Replicate reclaimed water effluent fed ponds were nearly identical in eukaryotic SSUrRNA composition, while replicate primary clarifier effluent fed ponds maintained more varied eukaryotic communities. In one primary clarifier effluent pond, *Scenedesmus* remained the dominant genus, while *Tetradesmus* and *Desmodesmus* were persistent minor components, of mostly equal percentage. *Tetradesmus* dominated the other replicate pond, with *Chlorella* as a reoccuring minor component, and *Scenedesmus* even less so. Differences in influent composition may partly be responsible, with reclaimed water nearly absent of potential inoculum, whereas primary clarifer effluent continously seeded ponds with varied proportions of the predominant organisms: *Chlorella, Tetradesmus, Scenedesmus*. Wastewater derived algal communities reported in literature show similar stability, with *Desmodesmus/Sceneddesus* remaining dominant in the in Carney 2014 over 13 days of batch growth. In the wastewater ponds configured with continuous flow described in Park 2011, major shifts in primary producers take place over time scales

around one month. It is likely that the short sampling period of the present study did not capture a significant change in species composition.

NGS has facilitated the characterization of the bacterial community at various stages of traditional wastewater processes, and allow comparison to the return-activated sludge and primary clarifier effluent analyzed here. McLellan 2010 report high relative read counts of Actinobacteria in human fecal matter, with a shift to Proteobacteria after transit in the city sewer system to the wastewater treatment plant headworks. In contrast, high proportions (over 90% of read counts) of Actinobacteria were recorded in the primary clarifier effluent, which persisted in the primary clarifier effluent fed ponds. Phyla found in RAS were similar to those reported elsewhere (Ju and Zhang 2015), with bacteria from the classes alphaproteobacteria, actinobacteria, and betaproteobacteria predominant in most systems. RAS from San Luis Obispo contained a higher percentage of read counts of Bacteriodetes than literature values (Ju and Zhang, 2015; Sanapareddy et al. 2009; Xia et al., 2010), although the phylum was found at varying percentages in most systems. In the reclaimed water fed ponds, receiving influent after nearly complete biological organic carbon removal and nitrification, bacteroidetes and proteobacteria predominated, which have been shown to degrade a wide range of algal exudates (Ramanan 2015).

In addition to consistent nutrient and organic carbon removal, RAS consistently achieves high settling efficiency for efficient solids removal, and can be used as a reference point to understand the role of the bacterial community in settling performance in algal systems. Factors influencing settling properties of activated sludge include median floc size and floc heterogeneity (Sadalgekar, 1988; Andreadakis, 1993), growth of filamentous or zoogloeal bacteria (Jenkins, 1993; Wannder, 1994), and the amount and composition of extracellular polymeric subtances (Urbain, 1993). In a characterization of the bacterial community in well and poorly flocculating activated sludge from three wastewater treatment plants, Schmid 2003 found a unique response in each system, complicating the assignment of functional roles. At one treatment facility, *Beta* and *alpha-proteobacteria* decreased in poorly settling systems, while the opposite trend was found at another. Longer term studies (Ju and Zhang, 2014; Lee et al., 2002) monitoring the 16s community focus on correlations to nutrient removal only. In the current study, RAS and ponds fed reclaimed water consistently have higher proportions of read counts of *Bacteroidetes* than the primary clarifier effluent fed ponds. However, given that there is no clear model for an efficient settling RAS system, it is difficult to make further extensions to the algal pond systems investigated here.

Cannonical correspondance analysis revealed few correlations between pond productivity and genera read count. Deleterious organisms reported as pond crash agents or responsible for reductions in productivity, such as Cryptomycota infections of *Scenedesmus* cultures (Letcher 2013), predation of *Chlorella* by the flagellate *Poteriochromonas sp.* (May 2017), or grazing by zooplankton (2017 Montemezzani), were found in most samples, although were not found correlated with changes in biomass productivity. Only the ciliate *Hemiophyrs procera* was found to be negatively correlated (-0.5 CCA factor) with productivity, while the ciliate *Loxophyllum* was weakly positively correlated (0.2 CCA). Additionally, it was surprising to see *Botrycoccos sp*., an organism with generally low reported biomass productivity in outdoor raceway pond settings (Benemann 2013), as the most strongly positively correlated (CCA 0.5) with biomass productivity.

In contrast to weak interactions between the microbiome and productivity, the genetic community appears to have a more significant influence on settling efficiency. Positively correlated predatory organisms, including *Rhizophydium* and the ciliate *Hemiophyrs procera*, have been shown to induce defensive responses in primary producers, ranging from an increase in the number of cells per colony and spine generation (*Pediastrum*, *Desmodesmus*) to colony clumping (*Micractinium*), resulting in a more readily settleable culture (Montemezzani 2017). Curiously, another ciliate, *Loxophyllam*, had the strongest

negative correlation with settling efficiency (CCA -1.1), suggesting diverse roles within the microbiome. Small, round, and nuetrally bouyant, *Chlorella* is generally difficult to settle. Despite a significant relative read count of *Chlorella*, Pond 2 achieved over 90% settling efficiency by the end of the sampling period. Looking for insights into the settleability, Lee 2013 found that while axenic *Chlorella* cultures remained colloidal, settling performance improved in xenic cultures, and identified *Sphingomonas* a primary component of the within the bacterial community. Similarly, *Sphingomonas* showed one of the strongest positive correlations to setting efficiency here. Of the negatively correlated bacteria, *Algoriphagus sp.* (Bowman 2003) potentially discourages floc formation, with filamentous bacteria notorious in activated sludge systems for disrupting settling performance.

Interesting global trends emerge from the CCA (Figure 10). Of strains with moderate negative correlations to settling (~0.5 CCA), most are weakly positively correlated with biomass productivity (~0.2 CCA). By comparison, only one strain (*Hemiophyrs procera*) shows the opposite influence with any confidence; it is positively correlated with settling performance, but negatively influences biomass productivity. Only two members of the 18s community *Botryococcus sp.* (UTEX 2629) and *Rhizophydium sp.* JEL317 were positively correlated to both productivity and settling. Few genera exist with positive correlations to both productivity and settling efficiency. Most genera positively correlated to biomass productivity appear detrimental to settling efficiency, and, conversely, those that are positvely correlated to settling efficiency are detrimental to biomass productivity. This suggests that unique bacterial consortia may exist in highly productive, poor settling, and poorly productive, highly settleable cultures.

Ultimately, longer term studies are required to make stronger correlations relating the microbiome to productivity and settling efficiency, such as that of the activated sludge system from Ju and Zhang 2015. For example, in their characterization of activated sludge samples from traditional wastewater treatment plants, Ju and Zhang 2015 sampled monthly for five years. Observations of reoccurring trends in the microbiome during periods of fluctuating pond performance are required for more thorough identification community roles within the microbiome. Additionally, a more in-depth analysis of the sequencing accuracy and of alpha/beta diversity is required.

TASK 3: Full-scale raceway hydraulic characterization

(Cal Poly and MicroBio Engineering, in consultation with the Delhi County Water District)

Introduction, Background, and State of Research

Mixing of raceway ponds makes up most of the electricity consumption in past technoeconomic assessments of algae production (Neenan 1986, Hreiz 2014). Technoeconomic assessments (TEAs) for algal biofuels production have assumed a raceway mixing energy intensity of 2.0 kW/ha for 20-25 cm/sec pond channel water velocity (Lundquist et al 2010), but this intensity was based on measurements from small 1000-m^2 raceway ponds.

Mixing energy input is required to sustain enough velocity in raceway channels to blend the supply of nutrients and CO_2 with the media, promote off gassing of excess O_2, minimize in-pond algae settling, reduce thermoclines, and thereby optimize productivity. The hydraulic power required for mixing a raceway is the product of volumetric flow rate, specific weight of water, and head loss. Total power input for raceway mixing also includes power loss due to motor, gear drive, bearing friction, and paddle wheel inefficiencies. Manning's equation for open channel flow expresses head loss as the product of the square of velocity, the square of roughness, and depth to the negative four-thirds power. Combining hydraulic power and Manning's equations (Equation 6, Equation 7) shows that the mixing input power should vary

with the cube of velocity (Weissman & Goebel 1987). This present report aims to confirm current assumptions for mixing velocity and power use.

Facility Description

The Delhi County Water District Wastewater Treatment Facility (WWTF) is a series of deep ponds and raceway ponds, with the final effluent percolated to the groundwater. The WWTF treats an average of 2300 m^3/d municipal wastewater from the community of Delhi, Calif. (population 10,755 as of 2010). The WWTF consists of headworks, two advanced facultative ponds, two raceways, two settling ponds, a maturation pond, and four percolation basins totaling 4.7 ha.

The inner and outer raceways have areas of nominally 1.3 and 1.4 ha, respectively (Figure 69). Their depths are gradually and linearly seasonally, with a minimum in winter of 62-65 cm and a maximum of 92-97 cm in summer (Table 6). The dimensions of the water channels for both raceways change depend on operating depth. The raceways are adjacent and symmetrical in cross-section, separated by a vertical concrete barrier. Their outer edges are earthen berms with 2:1 (horizontal: vertical) slopes, which are covered with smooth 60-mil HDPE liner. The pond floors are asphalt that has been rolled smooth, like roadway construction.

Figure 69: Aerial View of the Delhi, Calif. Wastewater Treatment Facility. The facility has two algae raceway ponds surrounding it, an inner and outer.

Table 6: Dimensions of inner and outer raceways at the Delhi County Water District Wastewater Treatment Facility. Both raceways are operated at shallower depths in summer and deeper in winter. Depth is average of four measurements along width of the channel where velocimetry was performed.

		Summer		Winter	
	Units	Inner	Outer	Inner	Outer
Measured Values					
Average Channel Depth	m	0.620	0.646	0.965	0.920
Average Channel Width at Surface	m	11.6	11.7	12.3	12.4
Raceway Length	m	1125	1212	1125	1212
Calculated Values					
Raceway Surface Area	ha	1.32	1.44	1.38	1.51
Cross Section Area	m^2	6.81	7.12	10.95	10.55
Wetted Perimeter	m	12.38	12.47	13.49	13.52
Hydraulic Radius	m	0.550	0.572	0.812	0.781
Raceway Volume	m^3	7,660	8,630	12,320	12,790

Figure 70: Paddle wheel station. Each raceway is mixed by paddle wheels 2.4-m in diameter and 6.1-m long.

The motors (Sew Eurodrive DFT90L4-KS) are nominally rated for 1.5 kW, 3 phase, and 60 Hz and are operated at a nominal 460 volts. The variable frequency drives (VFD) used in the original construction were removed years ago, and consequently the motors operate at full speed, which provides only a relatively low channel velocity. The power factor at full load is 0.76, and the manufacturer claims the motors are 79.9% efficient (Sew Eurodrive). The manufacturer claims the gear drive (Sew Eurodrive Type R137R77, 564.0:1 Gear Ratio) is around 96% efficient.

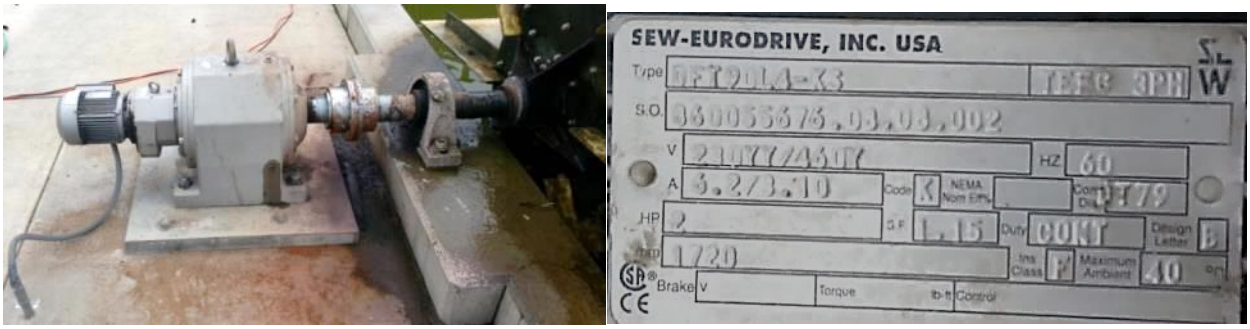

Figure 71: Motor, gear drive, and paddle wheel connection (left). Motor Plate (right).

The following sections outline the methods for the various measurements taken in summer and winter.

Milestone Tasks, and Subtasks/ Purpose

Purpose: Preliminary operation and hydraulic characterization of the full-scale raceways.

> **S3.0 Plan Hydraulic Study:** Develop the detailed methods for hydraulic characterization of the Delhi raceways (April 30, 2015).
>
> **S3.1 Determine Friction Factor:** Measure velocity and water surface elevation profile to determine hydraulic friction factors (July 31, 2015).
>
> **S3.2 Mixing Study:** Characterize mixing and flow short-circuiting with dye tracer studies (November 30, 2015).

+ ML3.3 Mixing Power Determination: Develop velocity versus energy consumption relationship for 3-acre raceways (December 31, 2015).

Experimental Goals and Methods

The raceways were studied at their seasonal extreme operating depths of 62-65 cm and 92-97 cm in summer and winter, respectively. The following were measured:

1. Head loss in the raceway, by measuring the difference in water surface elevation upstream and downstream of the paddle wheel.
2. Channel velocity by acoustic doppler velocimetry.
3. Electrical power consumption by the paddle wheel motors.
4. Tracer dispersion.

Head Loss

Observing head loss, or lift, indicates the hydraulic power imparted by the paddle wheel to the raceway water to overcome the drag caused by the channel floor and walls and other obstructions (bends, contrary wind, etc.). Head loss measurements, adapted from methods in Green et al. 1995, were observed by measuring surface water elevation upstream and downstream of the paddle wheel station using stilling

wells, an autolevel, a Philadelphia rod, and measuring sticks with 1/16-inch (1.6 mm) markings. Stilling wells dampen the wave oscillation to permit precise surface water elevation measurement. The stilling wells were made from round galvanized trash cans, each 520 mm in diameter, with several large holes cut in the bottom and one 2.5-cm hole cut in the side at mid-depth of the water. This side hole was oriented perpendicular to flow direction (USBR 2001). During measurement, two stilling wells were placed, one 15 m upstream and one 15 m downstream of the paddle wheels, in the center of the channel width. The stilling wells could have been placed closer to the paddle wheel but were set back by 15 m for to maintain a safe distance from the paddle wheel. Steel angle bar was laid across each stilling well mouth for the Philadelphia rod to rest on during measurement. The autolevel was placed approximately midway between upstream and downstream stilling wells and was used for differential leveling between stilling wells. The difference between the angle bar and the water surface in the stilling well was measured using the meter stick and was approximated to the nearest 1/32-inch (0.8 mm) in between 1/16-inch markings.

Figure 72: Differential leveling to measure head loss (i.e., paddle wheel lift) as change in water surface elevation before and after the paddle wheel.

Channel Velocity

A Sontek Flowtracker Acoustic Doppler Velocimeter was used to observe the X and Y horizontal components of velocity (Figure 73). Mean velocity was calculated using the Mean-Section method, which divides the channel cross section into several imaginary segments. The intersection of the segments forms a "vertical," where velocity measurements are made at various depths. Measurements were taken at different depths at four verticals locations per channel, spaced 2.6 m apart. Mean velocity for each vertical was calculated from two measurements at different depths (about 30-33% and 70-77% depth). The total depth at each vertical was measured using a meter stick, and that, combined with the distance between verticals, allowed for calculation of the segment cross section area. The segment area was multiplied by the average of the two bounding vertical velocities to estimate the segment flow rate. The segment flow rates were summed for each channel to calculate channel flow rate. The channel flow rate

was divided by total channel cross section area to calculate mean velocity. The outer segment areas were assumed to linearly decrease to zero from the nearest vertical to the channel edge.

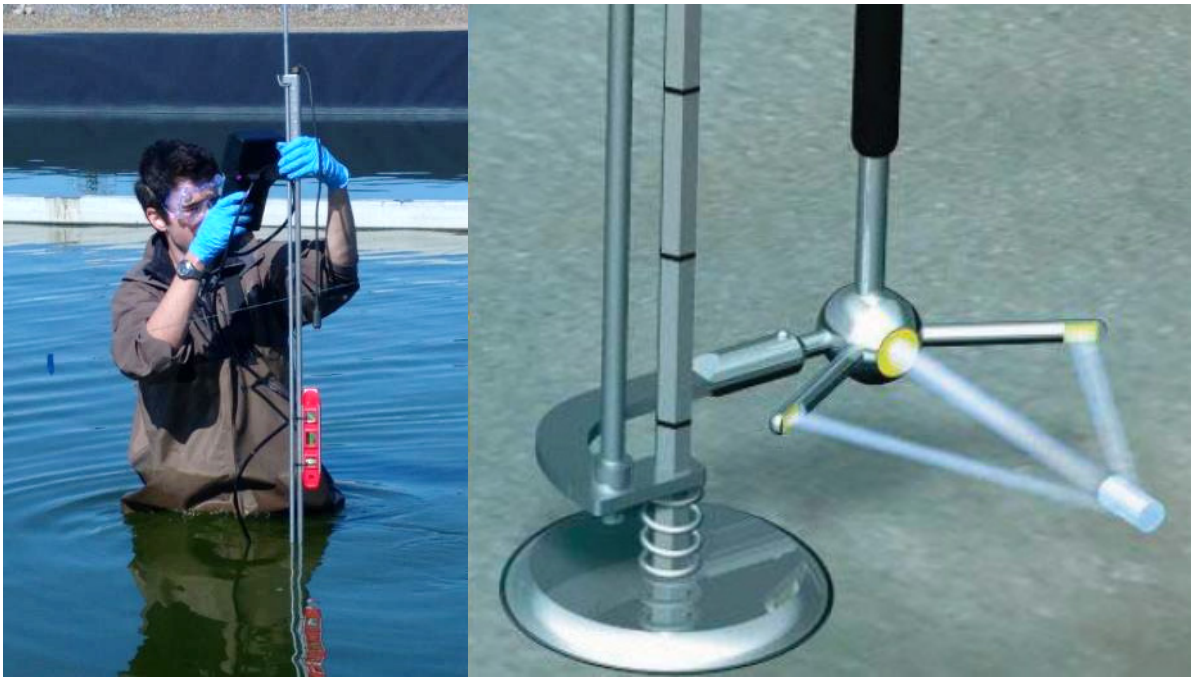

Figure 73: (left): Reading x and y velocity from the Sontek Flowtracker. (right): Visualization of the Sontek Flowtracker Acoustic Doppler Velocimeter. Reprinted from "Automated Quality Control in the SonTek® FlowTracker®", by SonTek, Retrieved December 12, 2015, from https://ysi.actonsoftware.com/acton/attachment/1253/f-0163/1/-/-/-/-/Automated%20Quality%20Control%20in%20the%20SonTek%20FlowTracker%20-%20SmartQC.pdf. Reprinted with permission.

Power Consumption

Paddle wheel electrical motor power was calculated by measuring amperage and voltage of each phase, estimating power factor from manufacturer specifications, and using Equation 5 below

Equation 5: Power consumption

$$P = \frac{VI(PF)\sqrt{3}}{1000}$$

where

P = three-phase power (kW)
V = voltage mean line-to-line of 3 phases (v)
I = current, mean of 3 phases (A)
PF = power factor, dimensionless.

Power factor (PF) was provided by the motor manufacturer and was not directly measured. According to the manufacturer, at full load, the power factor is 0.76, and at 75% load the power factor is 0.6. For each

calculation, PF was estimated by linear interpolation depending on estimated power draw as a fraction of "full load", and iterations were performed.

Water Power and Manning's Roughness Coefficient

Water power imparted by the paddle wheel to the raceway was estimated by the hydraulic power Equation 6 below:

Equation 6: Hydraulic power

$$P_w = \gamma Q h$$

where

P_w = theoretical water power (w)
γ = specific weight of water (N/m^3)
Q = mean channel flow rate (m^3/s)
h = head loss (m).

Manning's roughness coefficient, a dimensionless factor that quantifies the roughness of the raceway channel, was derived by rearranging Manning's equation to Equation 7 below:

Equation 7: Manning's equation

$$n = \left(\frac{1.00}{Q}\right) A R^{\frac{2}{3}} \sqrt{S}$$

where

n = dimensionless Manning's roughness coefficient
Q = mean channel flow rate (m^3/s)
A = area of raceway channel cross section (m^2)
R = hydraulic radius, ratio of cross section area over wetted perimeter (m)
S = surface water slope along length of channel, ratio of head loss over channel length (m/m).

Dispersion Study

A tracer study was performed on the inner raceway to characterize the extent of mixing in terms of (1) mean hydraulic residence time, which indicates the extent of plug-flow behavior, and (2) the Peclet number and axial dispersion coefficient. While dispersion vertically in the water channel and along the channel width are topics that warrant future study, this present analysis focuses on axial dispersion along the length of the raceway circuit.

Rhodamine WT dye was used as the tracer because it is fluorescent in a spectrum different than common materials found in wastewater (USGS 1986). The dye was instantaneously poured into the influent weir box of the inner raceway to simulate a discrete pulse of influent wastewater. During the first 8 hours, samples were taken by hand every 2 minutes initially and then at 8-minute intervals. Afterwards, samples were collected by a Hach Sigma 900 Max autosampler every 30 minutes. Samples were transported to a lab where their temperature stabilized to 24°C before dye concentrations were determined. Samples were manually shaken and then fluorescence was measured in a fluorometer (Turner Designs Model 7200, Trilogy Module Model 42). A week prior to the study, a calibration curve was created by preparing standard dilutions with pond water and known concentrations of Rhodamine WT. To correct for

interference caused by turbidity in pond water samples, standard dilutions were created with pond water diluent instead of de-ionized water. Figure 74 below shows tracer addition point and sample location at the effluent port of the inner raceway.

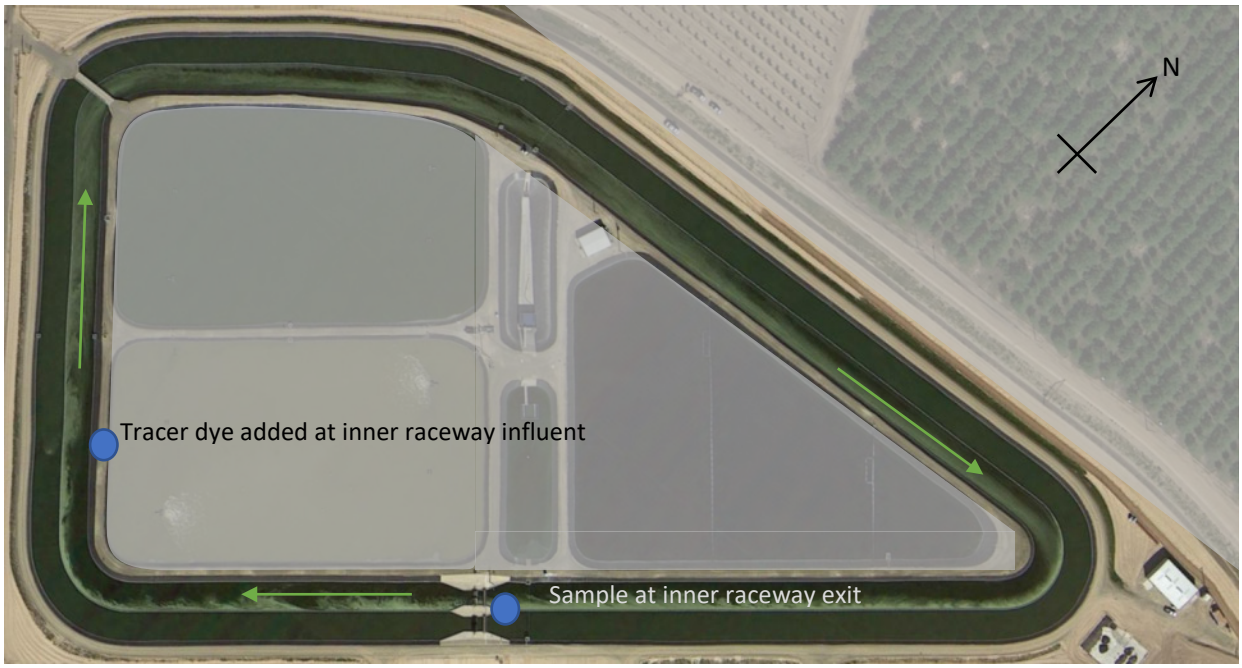

Figure 74: Tracer experiment injection point, flow direction, and sample point.

Figure 75: Tracer plume addition to the inner raceway via the weir box at right. Influent is piped underground and upwells at mid-width of the channel.

The axial dispersion coefficient, **D**, was calculated from Equation 8 after fitting Equation 9 to an experimental tracer response curve with the Peclet number as the fitting parameter by minimizing the sum of the square of the differences between the data and the model (Voncken et al. 1964). The Peclet number (Pe) can be used in single-parameter models as a comprehensive measure of dispersion (MWH 2005):

Equation 8: Axial dispersion coefficient

$$D = \frac{V_1 L}{Pe}$$

where

D = dispersion coefficient, (m^2/s)
V_1 = mean channel velocity, (m/s)
L = length of raceway loop, (m)
Pe = Peclet number, dimensionless.

The follow equation for dispersion in a recirculating system was used to estimate Pe from the tracer dye concentration (C) pattern (Voncken et al. 1964):

Equation 9: Tracer dye concentration pattern

$$\frac{C}{C_\infty} = \left(\frac{Pe}{4\pi\theta}\right)^{\frac{1}{2}} \sum_{x=1}^{\infty} exp\left[-\frac{Pe}{4\theta}(x-\theta)^2\right]$$

where

C = concentration of tracer in the reactor effluent
C_∞ = "cumulative" concentration leaving the reactor after an infinite time
θ = dimensionless time (= t/t_c, where t_c is average circuit time around raceway)
x = dimensionless circuit number indicates *n*th pass by the exit of raceway

C_∞ was determined by Equation 10 below

Equation 10: Cumulative concentration leaving the reactor

$$C_\infty = \int_0^\infty C * d\left(\frac{t}{t_{avg}}\right)$$

Where t_{avg} is the mean residence time in reactor for the dataset used to derive the dispersion coefficient. t_{avg} was calculated using Equation 11 below

Equation 11: Mean residence time

$$t_{avg} = \frac{\int_0^\infty Ct\ dt}{\int_0^\infty C\ dt}$$

To compare mean residence time in the reactor with a generic theoretical residence time, Equation 12 was used to calculate theoretical residence time:

Equation 12: Theoretical residence time

$$\tau = \frac{V}{Q}$$

where

τ = theoretical residence time (days)
Q = daily average system influent flow rate (m^3/d)
V = raceway volume (m^3)

Results, Discussion, and Significance

The summary of results from flow velocimetry, power consumption, and head loss measurements are tabulated below, along with the raceway dimensions used for calculated values.

Table 7: Summary of measured and calculated results from the hydraulic studies on the inner and outer raceways at the Delhi wastewater treatment facility, at 60- and 90-cm depths.

	Units	60 cm Inner	60 cm Outer	90 cm Inner	90 cm Outer
Measured Values					
Channel Velocity	m/s	0.12	0.13	0.11	0.11
Head Loss	m	0.021	0.021	0.013	0.016
Channel Flow Rate	m^3/s	0.81	0.91	1.20	1.17
Calculated Values					
Hydraulic Power	kW	0.17	0.19	0.15	0.18
Electrical Power Demand	kW	1.6	1.6	1.1	1.2
Wire-to-water efficiency	%	10%	12%	14%	15%
Area Normalized Power	kW/ha	1.21	1.11	0.80	0.79
Manning's Roughness Coefficient	-	0.024	0.022	0.027	0.028

All head loss values were relatively low compared to expected values in a system with shallower channel depths and higher channel velocity. While it may appear counterintuitive, raceways operating at 60-cm depth have a higher head loss than 90-cm. A higher required water energy input at shallower depth is partly attributed to the slightly higher channel velocity measured at the shallower depth, and from an inspection of Manning's equation, it can also be attributed to the reduced hydraulic radius (Equation 13). Channels with larger hydraulic radii have less water in contact with the channel surfaces and thus less energy is required to overcome those frictional losses. In other words, a larger hydraulic radius means the channel cross section has a higher efficiency.

Equation 13: Hydraulic radius

$$R = \frac{A}{P}$$

R = hydraulic radius, ratio of cross section area over wetted perimeter (m)
A = area of raceway channel cross section (m^2)
P = wetted perimeter (m)

Manning's roughness coefficients ranged between 0.022 and 0.028, which are equivalent to straight uniform earthen channels with some gravel (Chow, 1959). In actuality, the floor of each raceways is lined with asphalt, and the berms are lined with smooth HDPE plastic liner. When new and clean in 1998, the overall Manning's coefficient was very likely closer to 0.016. Some patches of accumulated sediment,

and scattered gravel were observed lying throughout the bottom of the raceways, which would support the idea that the Manning's roughness coefficient changed with time.

The Area Normalized Power ranged from 1.21 to 0.79 kW/ha which represent the mixing energy input requires per hectare of raceway surface area. The Lundquist et al. (2010) techno-economic assessment report assumes 2.0 kW/ha mixing energy input required when mixing channels 0.30 m deep, at 0.25 m/s for 14 hours/day during daylight and 0.20 m/s for 10 hours/day during the night. The velocities observed at the Delhi raceway ponds were only 0.13 to 0.11 m/s.

While apparently counterintuitive, Area Normalized Power was estimated to be 35% lower during 92-97 cm depth operation in winter versus 62-65 cm depth operation in summer. Several factors may contribute to lower energy demand at higher channel depths:

1. The channel cross section becomes more hydraulically efficiency (larger hydraulic radius).
2. The raceway surface area increases marginally with increasing depth due to the sloped sidewall, which will reduce the resultant Area Normalized Power.
3. Ambient temperatures were upwards of 38 °C during 62-65 cm depth observations in summer, and the gearmotors are in direct sunlight, both of which would contribute to higher temperature. Higher motor temperatures may reduce efficiency and increase power demand.
4. The observed velocity was slightly lower with the larger depth, which will reduce the channel flow rate, which reduces the hydraulic power demand.

The hydraulic power required for mixing a raceway is the product of volumetric flow rate, specific weight of water, and head loss. Total power input for raceway mixing also includes power loss due to motor, gear drive, bearing friction, and paddle wheel inefficiencies. Manning's equation for open channel flow indicates head loss as the product of the square of velocity, the square of roughness, and depth to the negative four thirds power. Combining hydraulic power and Manning's equations indicates that the mixing input power varies with the cube of velocity (Weissman & Goebel 1987).

The factors in deciding an optimum mixing velocity include the need to prevent algal cell sedimentation, allow off-gassing of excessive dissolved oxygen while retaining CO_2 if possible, and providing sunlight to the cells in a mode that optimizes productivity. Studies have shown that high mixing intensities do not necessarily increase productivity and that it may be a detriment due to greater outgassing of CO_2 (Weissman et al. 1988; Asadollahzadeh et al. 2014). However, the velocity in the Delhi channels might be too low, as indicated by sludge accumulation after channel bends and along the banks. While the Delhi raceways have normal algae concentrations in suspension, these would be only the algae for which the velocity is sufficient to maintain suspension. When bioflocculated cultures are to be maintained, higher velocity (~20 cm/sec) is needed to keep the flocs suspended, and this velocity will have higher power demand than observed at Delhi. Unfortunately, the current effluent weirs at Delhi do not allow for the target 30-cem depth for optimal algae production, and the paddle wheel motors do not allow the testing of higher velocities. Thus, the present study provides valuable information on power use and channel roughness but does not cover the target conditions for algae biofuel feedstock production.

Dispersion Study

Figure 76 shows the measured normalized tracer dye concentration curve in blue versus the axial dispersion model (Vonckens et al 1964) for a recirculating reactor.

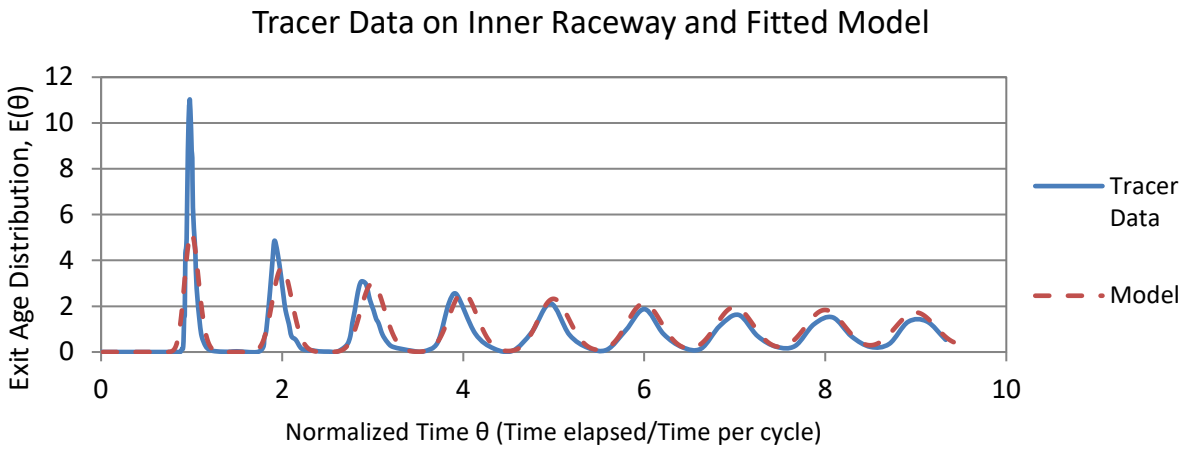

Figure 76: Normalized Measured Tracer Dye concentration vs. axial dispersion model (Equation 9). Tracer dye concentrations were measured at raceway exit and are an indication for both axial dispersion along the length of the raceway, and for the residence time in the raceway system.

The axial dispersion model along the raceway circuit was fitted to the measured tracer data by using least squares approximation. The Peclet number was calculated to be 340 and the dispersion coefficient was 0.43, which are important single parameter mixing characteristics that can help compare hydraulic systems of different geometries. The degree of axial dispersion is important to study for both wastewater treatment applications and for algae producers for considering fertilizer addition. Faster axial dispersion could lead to greater short circuiting and shorter mean hydraulic residence times where more partially treated wastewater exits the raceway. Placement of CO2 sumps in very large-scale systems might depend on these dispersion numbers as well. Mean cycle time was calculated as average time between peak of tracer concentration and was 0.10 days. Cumulative concentration at infinite time was 106 ug/L dye.

The mean residence time for the full dataset was estimated to be 4.4 days from Equation 11. However, the theoretical residence time (Equation 12), was only 3.7 days, based on the inner raceway volume being 7660 m^3 during the study and the mean influent wastewater flow rate being 2050 m^3/day. The mean residence times are normally less than the theoretical. To have a longer mean residence time would require an unlikely circumstance such as absorption of the dye on biofilm followed by slow release that would increase dye concentrations at the tail end of the tracer study curve, skewing the mean residence time higher than the theoretical. The unusual result could have been caused by not modeling exactly the diel variation in the influent wastewater flow or by errors in sampling or measurement. The conclusion is that the actual mean hydraulic residence time is essentially the theoretical residence time, which would not be surprising in a mixed reactor such as a raceway pond.

Conclusions and Recommendations

Maintaining channel velocity of as little as 0.11 m/s has been enough for operating the nominally 1.3- and 1.4-ha raceways at the Delhi County Water District Wastewater Treatment Plant of non-settling algae in paddle-wheel mixed raceway ponds. For algae cultures grown in raceways that can settle on their own, 0.20 to 0.25 m/s is still recommended to reduce biomass accumulation in ponds, but no more than 0.25 m/s should be considered to keep raceway mixing operating costs to less than 5% of annual costs.

Power demand in the Delhi raceways was determined to trend higher with shallower depth and indicate that the power demand of 30-cm depth raceways used for optimal biofuel production will be higher than values measured in present study.

The raceways at Delhi have strong plug flow characteristics and axial dispersion of the influent water occurs slowly, which is good indication for low short circuiting of partially treated wastewater leaving the system. For algae producers growing algae on fertilizers, this is another reason to bleed in fertilizer gradually versus rapidly.

While the calculated wire-to-water efficiencies are relatively low (10-15%), the Area Normalized Power is the key factor in evaluating different mixing methods. Other mixing methods, like a transfer pump, may have a higher efficiency but the entire channel flow must be constricted through pipes to achieve this higher velocity, sharply increasing the friction losses of the system and in turn increasing overall Area Normalized Power demand.

TASK 4. Biomass processing to biofuel intermediates

(Doug Elliott Lab and Cal Poly, in consultation with MicroBio Engineering)

Introduction, background, state of research

A substantial volume of research has been conducted on hydrothermal liquefaction and it is well documented in the literature. However, HTL processes are highly feedstock-dependent and information on HTL processing of whole cell algal biomass is not abundant. In fact, due to the highly interrelated nature of feedstock quality and conditioning and HTL processing, research and development on algae HTL processing is ideally done in tandem with feedstock research. In its 2014 update of the Multi-Year Program Plan (US Department of Energy, 2014), BETO expressed interest in the co-development of algae cultivation and R&D technologies:

> *"…HTL R&D is an area of interface tasks between Thermochemical Conversion R&D and Algal Feedstocks R&D."*

This theme has been reflected in recent research funding opportunities from BETO (US Department of Energy, Office of Energy Efficiency and Renewable Energy, 2016).

Researchers in the DOE ecosystem, including agency staff, national laboratory staff, and research awardees, have driven the development of this technology in pursuit of cost per gallon goals. In a 2014 publication, Pacific Northwest National Laboratory detailed the current state of the conversation technology and established future values needed to achieve the $3 per gallon of gasoline equivalent goal (Jones, et al., 2014). A related report published around the same time considered the process design and cost aspects of algae biomass fuel via the HTL pathway. This work identified several critical research and development needs to be addressed in pursuit of the DOE-established $3 per gallon of gasoline equivalent goal (Jones, et al., 2014):

1. Maximize yield and optimize oil quality through improved AHTL reaction conditions for a variety of different algal feedstocks,
2. Optimize phase separation of the AHTL oil from the aqueous product, solids and gas,
3. Optimize AHTL aqueous phase treatment to reduce costs and enhance carbon recovery, and,
4. Better characterize the AHTL oil and hydrocarbon products.

The work described here collected real world information and operational data supporting these critical areas of improvement. Task 4 was organized into three milestones, which were developed specifically to

characterize and optimize the HTL process. Feedstock considerations are addressed elsewhere in this report.

Milestones tasks and subtasks/purpose

The Task 4 workplan was broken down into three milestones.

ML4.1 HTL Run 1: Deliver first biomass samples to PNNL for hydrothermal liquefaction (HTL) and biofuel intermediate analyses (April 30, 2014).

> Milestone 4.1 included Subtask 4.1: "Evaluate the effect of thickening on HTL yield". This subtask was completed by Q2 of CY14. A preliminary sample, referred to as Sample 1 in this report and also known as "HTL-Poly" in PNNL HTL reporting was tested in the HTL system. Milestone 4.1 was completed in Q2 of CY14 when the first Sample 1 materials were delivered form Cal Poly to Pacific Northwest National Laboratory for testing.

ML4.2 Hydrotreating: Conduct hydrotreating and distillation tests. Characterize the biofuel intermediate for downstream upgrading requirements. Report mass balances and fuel yield (September 30, 2014).

> This milestone was completed in Q4 of CY14. It comprised the hydrotreating analyses undertaken on Sample 1.

ML4.3 HTL Runs 2-5: During Year 2, conduct at least four HTL runs on wastewater-derived biomass, while characterizing air emissions on at least one run (December 31, 2015).

> This milestone was completed in Q4 of CY15 and when the last of Samples 2 through 5 were treated and analyzed by the Pacific Northwest National Laboratory/Cal Poly team.

Throughout this report, the activities undertaken in Task 4 are discussed in terms of sample runs rather than by milestone.

Experimental goals, methods

The purpose of the biomass processing task was to explore the conversion of wastewater grown microalgal feedstock into a biofuel intermediate suitable for further upgrading. Factors that may impact the applicability of that process, such as air emissions, fuel quality, and treatment of waste fractions from the process were considered. Five algae biomass samples of varying origin and pretreatment condition were delivered to Pacific Northwest National Laboratory. For all samples, process performance was characterized by mass (C, N, P, S, H, and O).

Sample 1 was processed in a preliminary HTL run: HTL-Poly. This initial test that was used to optimize the process parameters for HTL, including the solids content that would be targeted for future HTL feed materials in the studies. One major outcome of the early work was the determination that the optimal percent solids for HTL was 20% or greater – a value that was approached in other tests for the remainder of the project. AGCal-02 through AGCal-05 were HTL runs completed under Task 4 and are described in detail here. The schedule, feed origin, and preprocessing of the five tests AGCal-01 through AGCal-05 are summarized here:

Table 8: Summary of HTL Testing Campaign

Sample	Sample 1	Sample 2	Sample 3	Sample 4	Sample 5
Associated HTL Run	**HTL-Poly**	**Cal-01 Cal-02**	**Cal-03**	**Cal-04**	**Cal-05**
Received	**7/19/13**	**5/8/14**	**10/29/14**	**7/16/15**	**9/10/15**
HTL Test Date	**8/7/13**	**Cal-01 5/15/14 Cal-02 5/20/14**	**5/19/15**	**7/30/15**	**9/17/15**
Material Description	Source: SLO ponds; Scenedesmusmicractinium, chlorella, filamentous cladophora, bacteria ~15 gal, 6.7 to 9.4 wt%	Source: SLO ponds. Algae harvested April and early May 2014. 5 gal of SLO ponds Biofloc slurry (~10% solids) 10 gal of algae chips (~50% solids) harvested from SLO primary fed ponds. Settled in tube settlers, harvested, placed in 55 gal drums and buckets, thickened and decanted, transferred to screens for drying.	Source: Delhi full s (0.6 MGD) Delhi WWTP. Sludge was harvested ~10/27/14. Primary wastewater is screened then split between two facultative ponds. From the facultative ponds the wastewater goes to two raceways operated in series. The effluent from the second facultative pond is dosed with an aluminum chlorohydrate polymer (60ppm) and taken to one of two settling units. Each settling unit is operated for about two weeks, then decanted, and the slurry is pumped to a concrete drying bed. A dewatering polymer is added as the sludge goes to the bed. 10 gal: The sludge is then dried by the sun for about three weeks to create paste. 5 gal: Slurry s from the settler after it was decanted for harvest, but before the dewatering polymer was added. The slurry did not experience any solar drying.	Source: Delhi full scale. 10 gal are thick sludge from Delhi full-scale system (harvested from concrete drying bed 5/25/15) with both coagulant and dewatering polymer added. 5 gal: from the ASP (harvested 6/25/15) with coagulant added but collected before dewatering polymer added	Source: Delhi pilot scale algae Harvested by gravity and placed in drying bed. 10 gal: 10% TS slurry 5-gal: 90% TS chips. Slurry collected 9/1/15 and the chips were collected 7/28/15.

			Due to the polymer addition ash content expected to be ~30% of TS. 15-20% higher than the ash content in SLO algae.		
Pretreatment	No autoclaving. As received feed mixed with overhead mixer. No dilution required.	No autoclaving. 9 kg of chips added to 5 gal of slurry and mixed in high sheer homogenizer. Final slurry passed through 20 mesh inline filter.	Feed stored frozen until 5/6/15. Feed process through two 6- h cycles in autoclave (May 7 and May 11, 2015). Autoclaved/thickened sludge was homogenized, and size reduced on 5/15/15 in the sheer mixer. Prepared sludge was passed through a 20-mesh inline strainer.	Cal Poly autoclaved the feed (at 121°C) before sending and noted that algae exhibits a jelly-like consistency after autoclaving at PNNL, clumps were present; therefore, feed was homogenized in the high sheer mixer (7/27/15). Sheering was continued for 45 minutes after last feed addition. Prepared sludge was passed through a 20-mesh inline strainer.	Cal Poly autoclaved the feed (at 121°C) before sending. Received material was placed in the homogenizer and mixed for about 1 hour on 9/15/16. Material was allowed to stay in the homogenizer tank overnight to help rehydrate it.

Sample 1

Sample 1 consisted of algae biomass from the ponds at the Cal Poly-operated San Luis Obispo Algae Field Station. The field station's nine algae raceway ponds were connected to tube-type lamella settlers for the continuous removal of algal solids. The sample was collected from the tube settlers at about 2% solids and then thickened in the field by centrifugation to roughly 7 to 10% solids. It was package on ice and transmitted to PNNL in July of 2013. The feedstock is shown here.

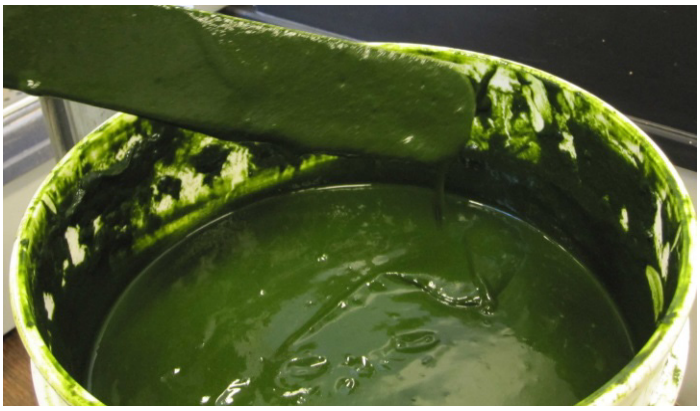

Figure 77: Sample 1 Feedstock

PNNL homogenized a portion of the sample and returned it to Cal Poly for biochemical analyses of the biomass feed. Upon receipt, Cal Poly staff freeze dried the sample and stored it at -20 C prior to testing. Moisture/ash, carbohydrates, lipids (as FAMEs), elemental nitrogen, and elemental carbon were measured. Samples were measured in triplicate for each analysis, except nitrogen and carbon. The following results are expressed in terms of % dry weight and % ash free dry weight.

Table 9: Sample 1 Feedstock Composition

Sample	**Moisture content, % dw**		**Ash content, % dw**		**FAME Lipids, % dw**		**Carbohydrates, % dw**		**N-content, % dw**	**Protein content, % dw**	**C-content, % dw**	**Mass closure, % dw**
	Average	RSD	Average	RSD	Average	RSD	Average	RSD				
July 2013*	97.8	0.32 %	12.4	1.20 %	5.9	8.83 %	16.1	2.16%	7.2	34.6	47.8	69.0
May 2014**	95.0	0.16 %	14.9	1.69 %	3.6	1.11 %	10.0	2.18%	8.3	39.6	47.7	68.1

*Centrifuge thickened Cal Poly tube settler sludge
**Solar dried Cal Poly tube settler sludge homogenized with tube settler sludge before HTL

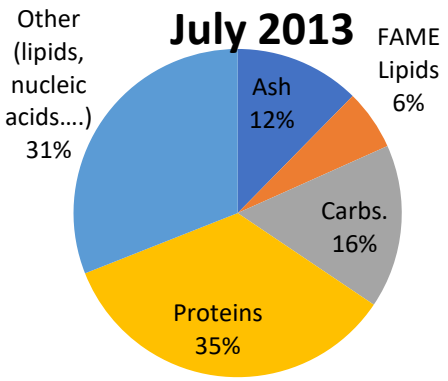

Figure 78: Sample 1 Feedstock Biochemical Analysis (July)

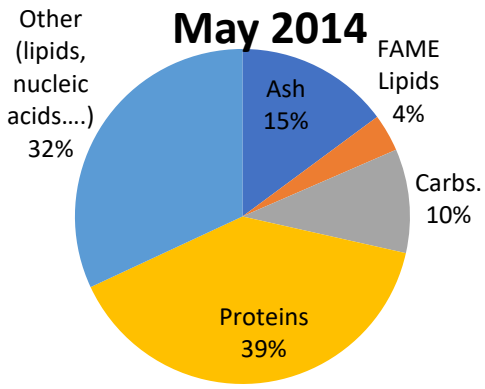

Figure 79: Sample 1 Feedstock Biochemical Analysis (May)

These analyses were conducted according to the standard methods of the National Renewable Energy Laboratory, which have been disseminated for researchers undertaking research in this area:

- Moisture/ash (Van Wychen & Laurens, 2013)
- FAME lipids (Van Wychen, Ramirez, & Laurens, Determination of Total Lipids as Fatty Acid Methyl Esters (FAME) by in situ Transesterification Laboratory Analytical Procedure (LAP), 2013)
- Carbohydrates (Van Wychen & Laurens, 2013)
- N and C-content (Laurens, 2018)
    - N and C content measured by combustion
    - Protein content determined by multiplying N-content by 4.78

The hydrothermal liquefaction studies were undertaken by PNNL with the setup operated in a hybrid configuration.

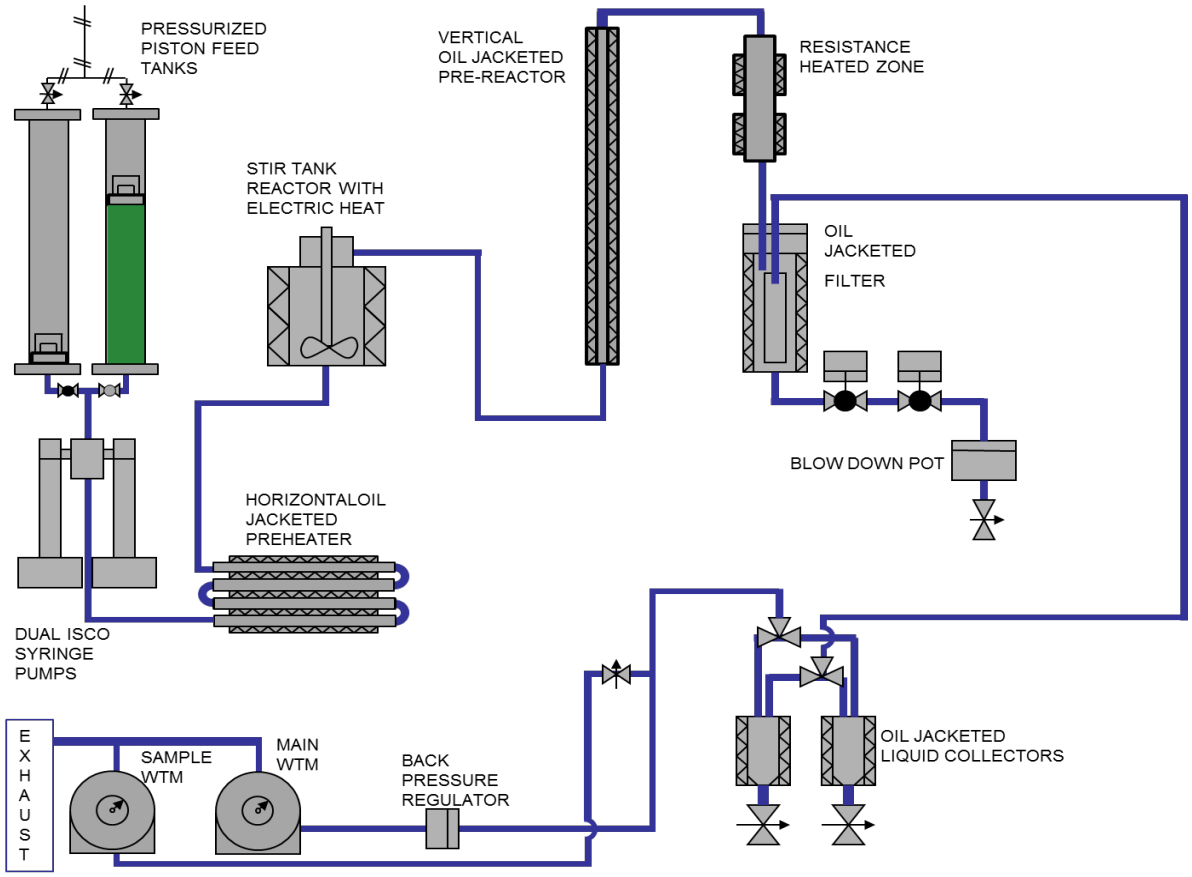

Figure 80: Sample 1 HTL Configuration

Table 10: Sample 1 HTL Parameters

Run Parameters		
Rxt Config	Unit	Hybrid
Sample Count	number	5
HOS (@ steady state)	hour	3.3
Reactor Temperature	C	348
Pressure	psig	2930
Vol at Temp	mL	682
Feed Rate	mL/h	1500
LHSV	L/L/h	2.2

Air emissions measurements were collected from this test.

A small-scale hydrotreater run was conducted with the bio-oil produced in the HTL process. The system was operated at 1,500 psi hydrogen and 400°C nominal bed temperature. A Ketjen CoMoF/Al_2O_3 (30-60 mesh) sulfided catalyst was used. The study was configured as follows:

- 20.0 cm^3 bed volume
- 16.0 g catalyst

- Catalyst bed heated from 250°C to 400°C; sulfiding agent run for 2 hr at 400°C prior to run to re-sulfide catalyst
- Bio-oil feed rates 0.080 mL/min (bio-oil $\rho_{40°C}$= 0.984 g/cm^3)
- LHSV tested: 0.24 cm^3/ cm^3-cat/hr
- WHSV tested: 0.30 g/g-cat/hr
- H_2 Flow = 91 scc/min
- Test duration was 7.0 hr (reactor plugged)
- The bio-oil had high (1.19 wt%) filterable solids content (0.1 wt% is typical).

The hydrotreating setup is detailed and photographed here.

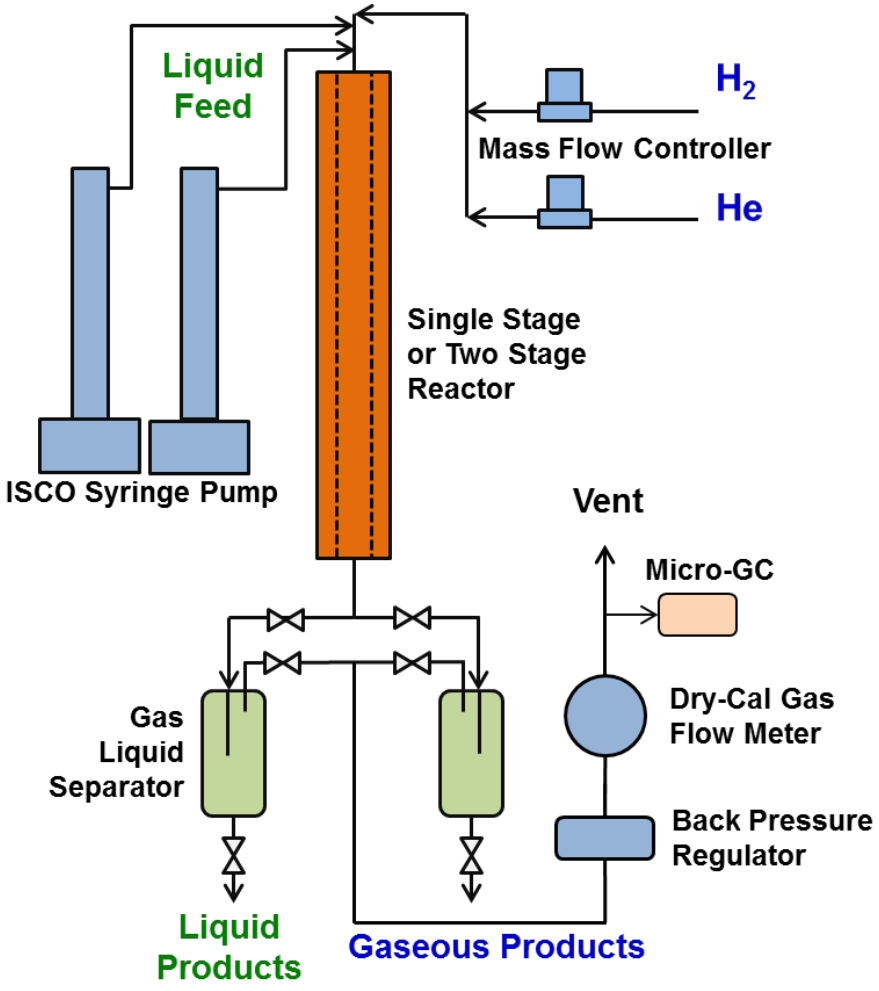

Figure 81: Hydrotreating System Configuration

Figure 82: Hydrotreating System

This is a dual zone hydrotreating system. The first zone consists of 2 mm extrudates as a guard bed to remove iron. The second zone contains granules of nominal 30-60 mesh size $CoMo/Al_2O_3$ (Alfa-Aesar). The catalyst was sulfided before feeding under the following sulfidation parameter: Room temp to 150 ºC in H_2, hold 150 oC for 2 h in H2 and sulfiding agent (35% DTBDS in decane); 150 to 400 ºC in 3 h then hold at 400 ºC for 4 h in H_2 and sulfiding agent; Pressure: 1540 psi; Sulfiding agent LHSV: 0.1 L/L cat/h for total; H_2/liquid: 1890 L H_2/L sulfiding agent.

Sample 2

Sample 2 consisted of bioflocculated algae biomass collected from the San Luis Obispo project site over a period of about three weeks from mid-April to early May of 2014. One five-gallon bucket of slurry (~10% solids) and two five-gallon buckets of dried algae chips (~50% solids) were harvested from algae raceways fed primary wastewater effluent. The biomass was settled in tube settlers, harvested, placed in 55-gallon drums and buckets, thickened, and decanted. The chipped biomass was transferred to screens for drying.

Figure 83: Sample 2 Dried Biomass Feedstock

Figure 84: Sample 2 Homogenized, 17.6% Solids Feedstock

Biochemical analyses were undertaken. These data were collected in the same manner as those described in Sample 1.

Table 11: Sample 2 Feedstock Composition

Sample	Moisture content, % dw		Ash content, % dw		FAME Lipids, % dw		Carbohydrates, % dw		N-content, % dw	Protein content, % dw	C-content, % dw	Mass closure, % dw
	Average	RSD	Average	RSD	Average	RSD	Average	RSD				
July 2013*	97.8	0.32%	12.4	1.20%	5.9	8.83%	16.1	2.16%	7.2	34.6	47.8	69.0
May 2014**	95.0	0.16%	14.9	1.69%	3.6	1.11%	10.0	2.18%	8.3	39.6	47.7	68.1

*Centrifuge thickened Cal Poly tube settler sludge

**Solar dried Cal Poly tube settler sludge homogenized with tube settler sludge before HTL

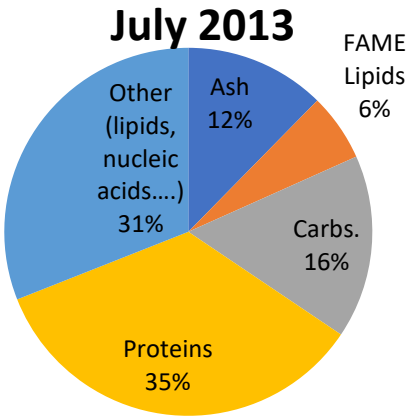

Figure 85: Sample 2 Feedstock Biochemical Analysis (July)

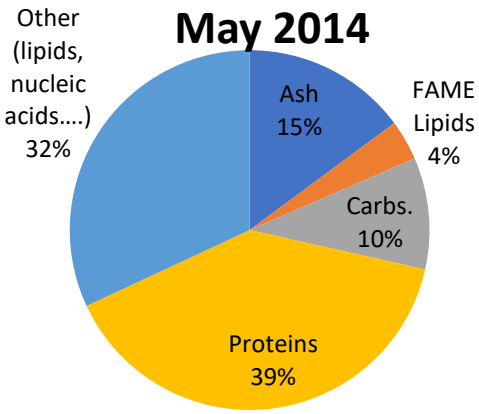

Figure 86: Sample 1 Feedstock Biochemical Analysis (May)

The biomass was reconstituted upon receipt by Pacific Northwest National Laboratory:

- 1 bucket slurry (wt % solid)
- 2 buckets of dried chips (15 kg @ 50% solids)
- Chips to slurry mix ratio determined by lab tests:
- max solids in pumpable slurry
- Slurry (20 kg) + Chips (9.2 kg) placed into high sheer mixer 4 to 5 h to add chips, ~1 h of mixing after all chips added.
- Homogenized mixture passed through 20 mesh inline screen while pumping mixture to 5 gal buckets.

This resulted in the following HTL feedstock:

Table 12: Sample 2 HTL Feedstock Composition

Parameter	Wt %
Total Solids in Feed Slurry	17.6
Ash in Dried Solids	13.6

Ash in Slurry	2.4
Ash Free Solids	15.2
Density of feed slurry, g/ml	1.03

These materials were processed in two HTL runs (Cal-01 and Cal-02). Cal-01 was terminated early after being interrupted by a fire alarm, which required the system to be stopped and then restarted. The hydrothermal liquefaction system was configured as follows.

5/15/14: Run 1

- Liquid hourly space velocity: 2.2 l/l/h
- 7.1 liters processed
- 450 g (wet) biocrude collected.
- Before early end, solids accumulation in CSTR was noted

5/20/14: Run 2

- CSTR insert removed: LHSV = 1.2 l/l/h
- 7.6 L processed;
- 550 g (wet) biocrude collected.
- Run terminated due to building evacuation (fire alarm)
- Overall, material processed well.
- Several posttest steps conducted to reduce water content of biocrude (settling, filtration attempted, but abandoned, and centrifugation.

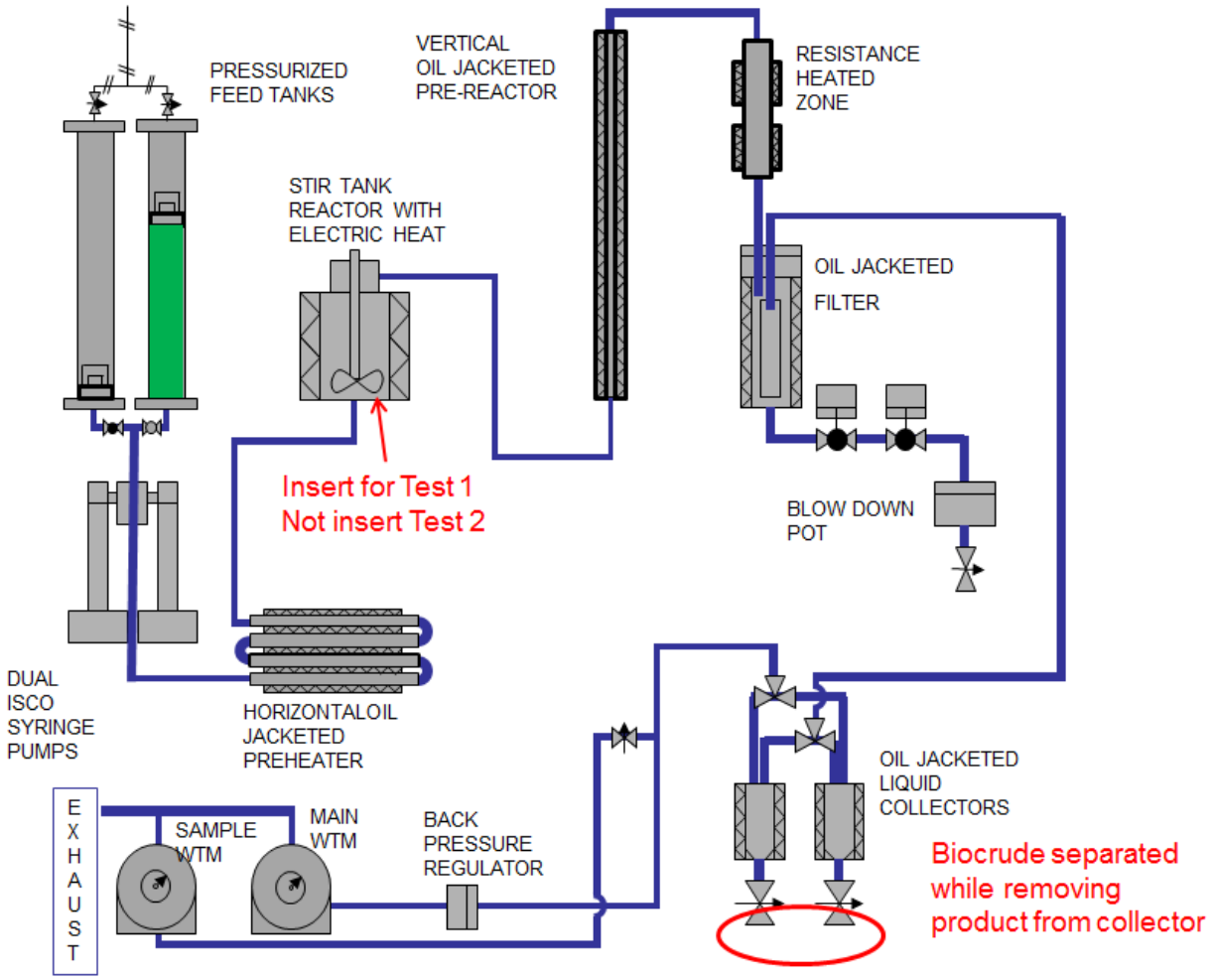

Figure 87: Sample 2 HTL Configuration

Sample 3

Algal biomass was harvested from the full-scale wastewater treatment at Delhi, California around October 27, 2014. In that 0.6 MGD system, primary wastewater is screened before being split between two facultative ponds. From there, it flows into two raceway ponds that are operated in series. The effluent from the second facultative pond is dosed with an aluminum chlorohydrate polymer (60 ppm) and taken to one of two settling units. Each settling unit is operated for about two weeks and then decanted. Slurry from the decanting process is pumped to a concrete drying bed. A dewatering polymer is added as the sludge goes to the bed. The sludge is dried by the sun for about three weeks.

The material used in the third sample processed by Pacific Northwest National Laboratory was collected from the settler after it was decanted for harvesting and before the dewatering polymer was added. The slurry did not undergo any solar drying.

Due to the chlorohydrate polymer addition, it was estimated the ash content would be somewhere around 30% of total solids. This is 15-20% higher than the ash content than the San Luis Obispo sourced algae. Pacific Northwest National Laboratory staff froze the buckets. Buckets were then defrosted, autoclaved, and strained prior to the May 19 HTL run.

Figure 88: Collecting Algal Biomass Feedstock for Sample 3

Figure 89: Sample 3 Algal Biomass Feedstock on Arrival at PNNL

This sample had a solids content in the ideal range, but had a relatively high ash content. These ash content derived from coagulating agents and also likely dust at the Delhi wastewater treatment plant.

Table 13: Sample 3 Feedstock Composition

	Unit	Cal 03 5/19/15
Total Solids in Feed	**wt%**	**20.1%**
Ash in Dry Feed	**wt%**	**28.4%**
Ash in Slurry Feed	**wt%**	**5.7%**
AF Solids in Slurry Feed	**wt%**	**14.4%**

Average Feed density	**g/ml @20C**	**1.070**
Feed Rate	**g (AFDB)/h**	**231**
Carbon	**wt%**	**32.9%**
Hydrogen	**wt%**	**5.7%**
Oxygen	**wt%**	**29.7%**
Nitrogen	**wt%**	**6.0%**
Sulfur	**wt%**	**0.64%**
COD	**mgO/L**	**173,400**
pH	**pH unit**	**6.3**

The aluminum chlorohydrate coagulant was a major contributor to the high ash content of the sample. The aluminum concentration in the Sample 3 HTL feedstock was well over an order of magnitude higher than typical San Luis Obispo grown algae.

Table 14: Sample 3 Feedstock Metals Analysis

	Dry Feed Basis	**Cal 03** **5/19/15**
Ash (in dry feed)	Wt%	**28%**
Al	ppm	52550
Ca	ppm	10320
Cr	ppm	< 35
Cu	ppm	89
Fe	ppm	1095
K	ppm	5469
Mg	ppm	4026
Mn	ppm	279
Na	ppm	5862
Ni	ppm	< 35
P	ppm	32920

Sr	ppm	169
Si	ppm	15100
S	ppm	6427

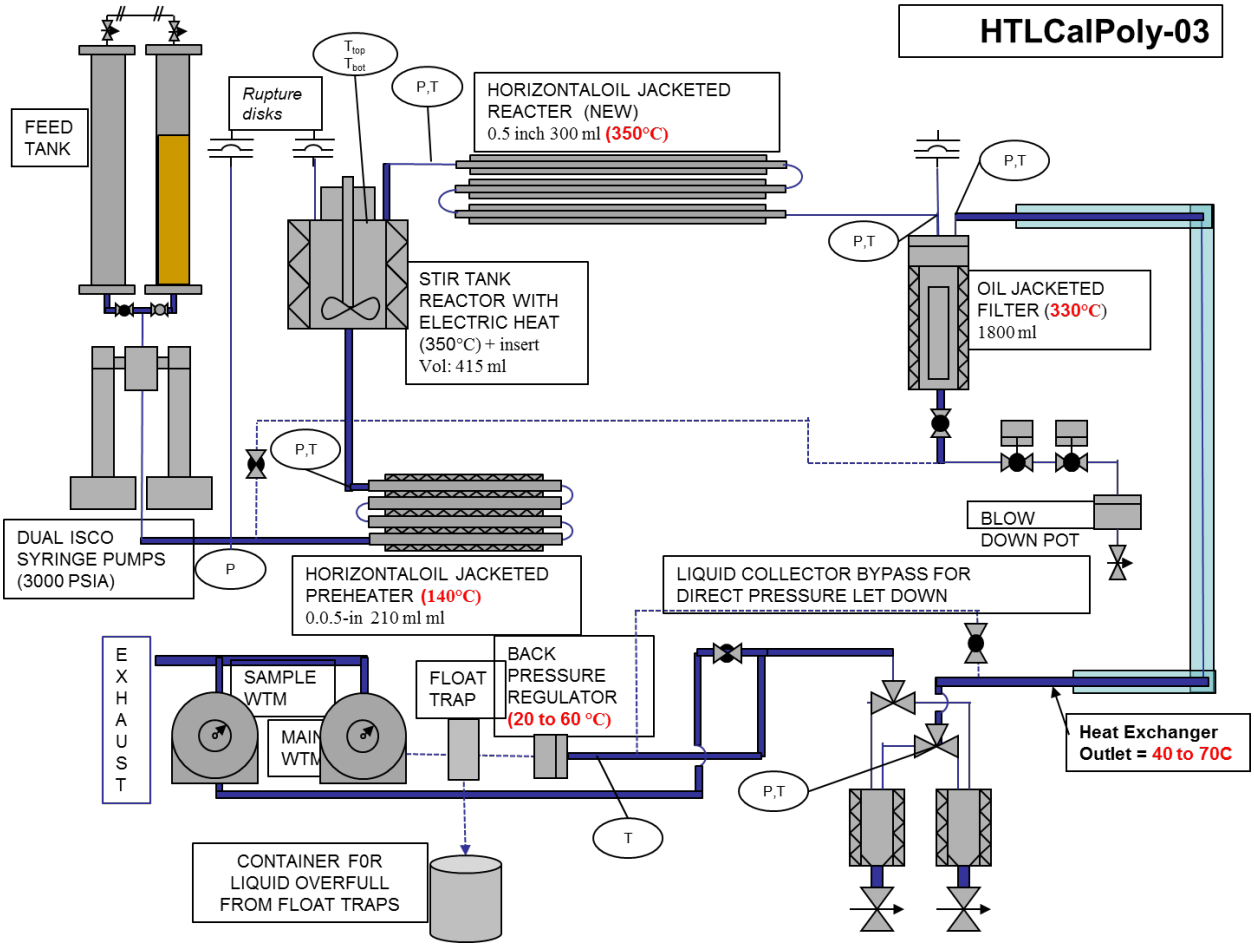

Figure 90: Sample 3 HTL Configuration

Table 15: Sample 3 HTL Parameters

	Unit	**Cal 03** **5/19/15**
Sample Count (steady state)	**number**	**4**
HOS at SS	**hour**	**2.7**

Reactor Temperature	**C**	**329**
Pressure	**psig**	**2897**
Vol at Temp	**ml**	**715**
Filter house volume	**ml**	**1800**
Feed Rate	**ml/h**	**1500**
LHSV	**L/L/h**	**2.1**

This sample was hydrotreated in the same system as Sample 1 and under the same operating conditions. In this sample, HTL feed from Sample 3 was combined with HTL feed from Sample 4. They are reported under Sample 3. Additionally, when the Sample 3 and 4 material had been consumed, HTL materials from Sample 1 were added to allow the test to continue. The bulk feed material of this test is detailed in the Sample 3 results section.

Sample 4

Sample 4 biomass consisted of algae solids collected from the full-scale Delhi wastewater system. Two buckets were harvested:

- one from the concrete drying bed (5/25/15) with both coagulant and dewatering polymer added and,
- one of slurry from the settling pond (6/25/15) with coagulant added but no dewatering polymer.

Both samples were autoclaved by Cal Poly staff in San Luis Obispo, resulting in a jelly like material that was transmitted to Pacific Northwest National Laboratory for HTL studies.

Sample 4 materials are shown here as received by PNNL and after homogenization by PNNL in a high shear mixer.

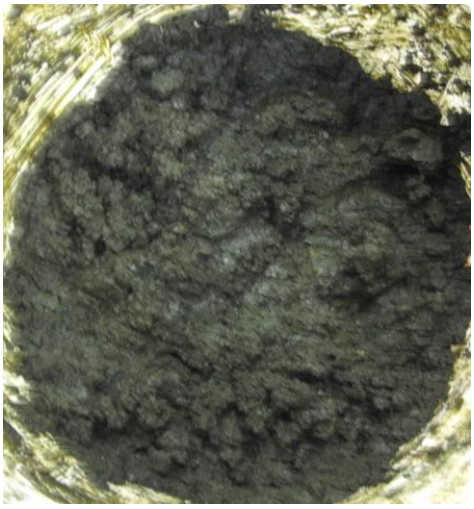

Figure 91: Sample 4 Feedstock on Arrival at PNNL

Figure 92: Homogenized Sample 4 Feedstock Ready for HTL Run

The HTL feedstock was characterized after homogenization. This sample had a relatively low solids concentration and a relatively high as content. Ash in the sample resulted from the addition of coagulating agents at the point of origin at the Delhi wastewater treatment plant.

Table 16: Sample 4 HTL Feedstock Composition

	Unit	Cal 04 7/30/15
Total Solids in Feed	wt%	15.2%
Ash in Dry Feed	wt%	28.8%
Ash in Slurry Feed	wt%	4.4%
AF Solids in Slurry Feed	wt%	10.9%
Average Feed density	g/ml @20C	1.073
Feed Rate	g (AFDB)/h	175
Carbon	wt%	34.1%
Hydrogen	wt%	5.8%
Oxygen	wt%	28.0%
Nitrogen	wt%	5.7%
Sulfur	wt%	0.70%
COD	mgO/L	157,400

pH	pH unit	6.3

As in Sample 3, the coagulant used at Delhi was a major contributor to the high ash content of the sample. The aluminum concentration in the Sample 4 HTL feedstock was well over an order of magnitude higher than typical San Luis Obispo grown algae.

Table 17: Sample 4 Metals Analysis

	Dry Feed Basis	**Cal 04** **7/30/15**
Ash (in dry feed)	Wt%	**29%**
Al	ppm	59415
Ca	ppm	11505
Cr	ppm	< 35
Cu	ppm	46
Fe	ppm	1831
K	ppm	3587
Mg	ppm	2469
Mn	ppm	177
Na	ppm	1868
Ni	ppm	< 35
P	ppm	25230
Sr	ppm	117
Si	ppm	138
S	ppm	6907

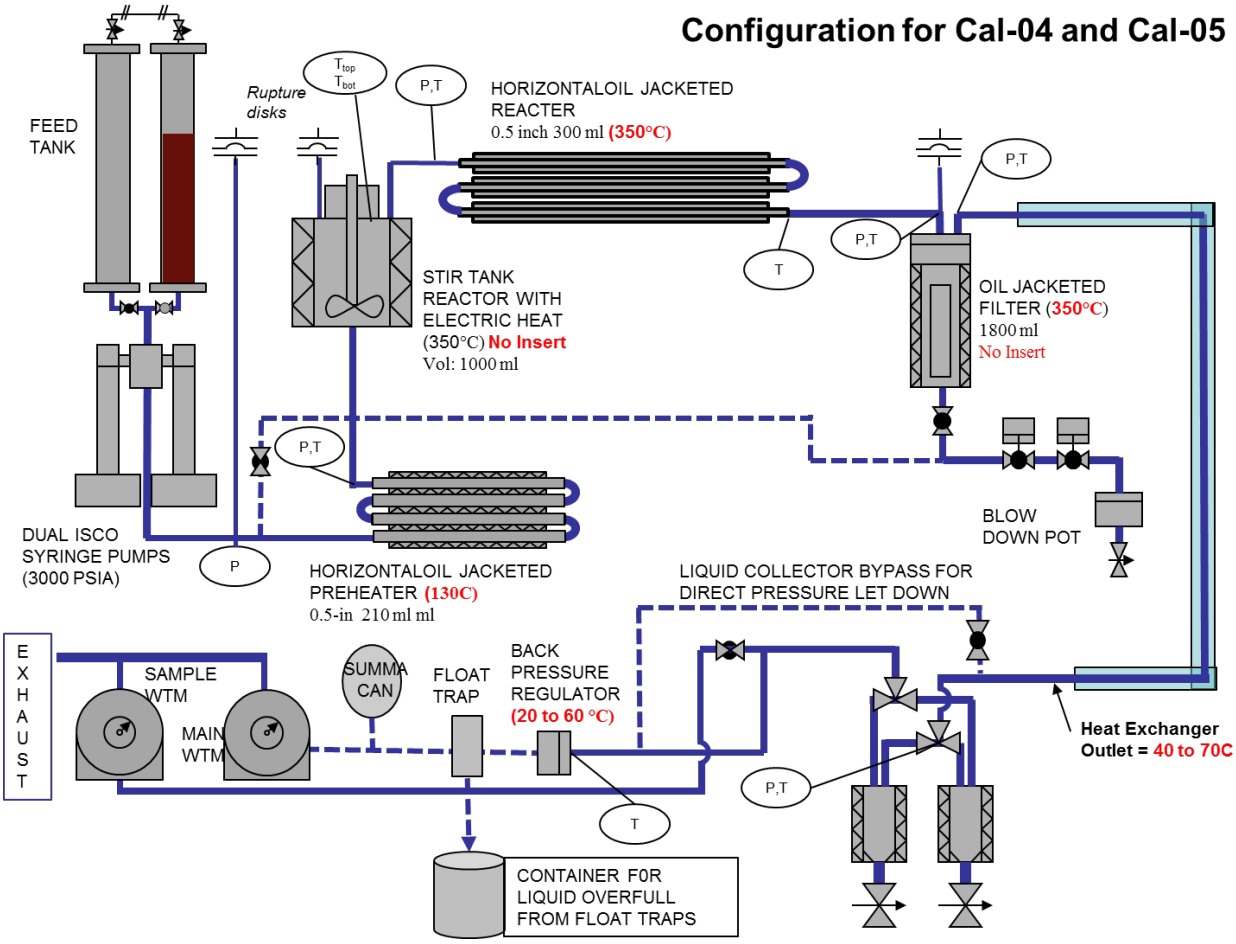

Figure 93: Sample 4 HTL Configuration

Table 18: Sample 4 HTL Parameters

	Unit	Cal 04 7/30/15
Sample Count (steady state)	number	3
HOS at SS	hour	2.0
Reactor Temperature	C	341
Pressure	psig	2866
Vol at Temp	ml	1300

Filter house volume	**ml**	**1800**
Feed Rate	**ml/h**	**1500**
LHSV	**L/L/h**	**1.2**

Sample 5

Sample 5 consisted of algal biomass collected from the Delhi pilot scale system. The sample was harvested by gravity and placed in a drying bed. The first two buckets contained a 10% total solids slurry and the third bucket contained roughly 90% solids chipped biomass. The slurry was collected on 9/1/15 and the chips were collected on 7/28/15. All samples were autoclaved at Cal Poly in San Luis Obispo before being transmitted to Pacific Northwest National Laboratory.

The chipped biomass is shown here as received (autoclaved chips of ~90% dry matter) and after homogenization in high shear mixer.

Figure 94: Sample 5 Dried Biomass

Figure 95: Sample 5 Feedstock Ready for HTL Run

Table 19: Sample 5 Feedstock Composition

	Unit	Cal 05 9/17/15
Total Solids in Feed	**wt%**	**21.2%**
Ash in Dry Feed	**wt%**	**41.8%**
Ash in Slurry Feed	**wt%**	**8.9%**
AF Solids in Slurry Feed	**wt%**	**12.4%**
Average Feed density	**g/ml @20C**	**1.084**
Feed Rate	**g (AFDB)/h**	**235**
Carbon	**wt%**	**30.6%**
Hydrogen	**wt%**	**4.6%**
Oxygen	**wt%**	**18.5%**
Nitrogen	**wt%**	**4.5%**
Sulfur	**wt%**	**0.69%**
COD	**mgO/L**	**134,700**
pH	**pH unit**	**6.3**

Table 20: Sample 5 Feedstock Metals Analysis

	Dry Feed Basis	Cal 05 9/17/15
Ash (in dry feed)	Wt%	**42%**
Al	ppm	4181
Ca	ppm	20910
Cr	ppm	186
Cu	ppm	76
Fe	ppm	2361

K	ppm	6972
Mg	ppm	4867
Mn	ppm	88
Na	ppm	18625
Ni	ppm	19
P	ppm	14595
Sr	ppm	160
Si	ppm	2315
S	ppm	8147

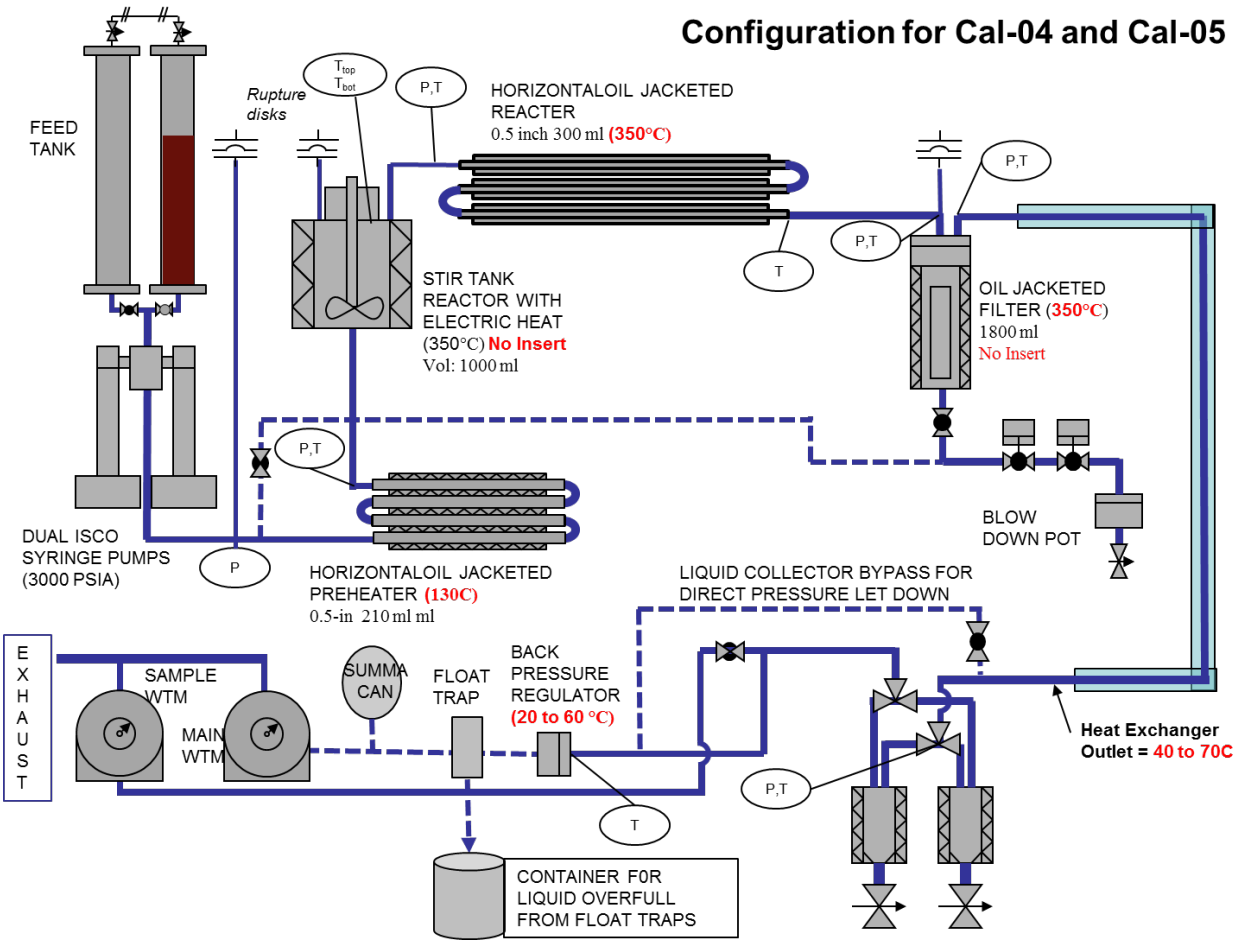

Figure 96: Sample 5 HTL Configuration

Table 21: Sample 5 HTL Parameters

	Unit	Cal 05 9/17/15
Sample Count (steady state)	number	2
HOS at SS	hour	1.3
Reactor Temperature	C	344
Pressure	psig	2884
Vol at Temp	ml	1300
Filter house volume	ml	1800
Feed Rate	ml/h	1755
LHSV	L/L/h	1.4

Results

HTL Results

Results of the tests are summarized here. Mass balances near 100% reflect the efficacy of the tests. Normalized mass yields of oil ranged from about 17% to 36%. Normalized mass yields of carbon in the bio-oil product ranged from about 33% to 55%.

Table 22: HTL Mass and Element Balances and Yields

	Unit	HTL Poly 8/7/13	Cal 01 5/15/14	Cal 02 5/20/14	Cal 03 5/19/15	Cal 04 7/30/15	Cal 05 9/17/15
Mass Balance	%	98%	99%	100%	104%	101%	98%
C-Balance	%	69%	95%	102%	110%	100%	77%
H-Balance	%	91%	103%	105%	108%	106%	100%
O-Balance	%	100%	99%	100%	103%	101%	100%
N-Balance	%	90%	91%	103%	89%	96%	96%
P-Balance	%	nd	69%	118%	118%	92%	95%
Mass Yields Normalized							

Oil Yield, Mass (N)	**g_{oil}/g_{fd}**	**17%**	**35%**	**36%**	**32%**	**27%**	**16%**
Solid Yield, Mass (N)	**g_{solid}/g_{fd}**	**5%**	**3%**	**4%**	**11%**	**9%**	**7%**
Gas Yield, Mass (N)	**g_{gas}/g_{fd}**	**2%**	**6%**	**5%**	**12%**	**14%**	**12%**
Aq Yield, Mass (N)	**g_{aq}/g_{fd}**	**76%**	**56%**	**55%**	**45%**	**50%**	**65%**
Carbon Yields - Normalized							
C-Oil Yield (N)	**%**	**34%**	**55%**	**53%**	**52%**	**45%**	**32%**
C-Water Yield (N)	**%**	**53%**	**36%**	**37%**	**32%**	**37%**	**45%**
C-Gas Yield (N)	**%**	**2%**	**3%**	**2%**	**7%**	**9%**	**9%**
C-Char Yield (N)	**%**	**11%**	**6%**	**8%**	**9%**	**9%**	**14%**

The highest yields were obtained in samples deriving from the San Luis Obispo system, suggesting that some feature inherent to Delhi-grown algal biomass may limit the HTL process' performance. The sample with the highest normalized carbon yield in the bio-oil also had the lowest ash content. Delhi derived samples had high levels of ash owing to aluminum chlorohydrate addition and possibly to dust, which is more abundant by observation than at the San Luis Obispo site. It is likely the ash content had a deleterious effect on the HTL process.

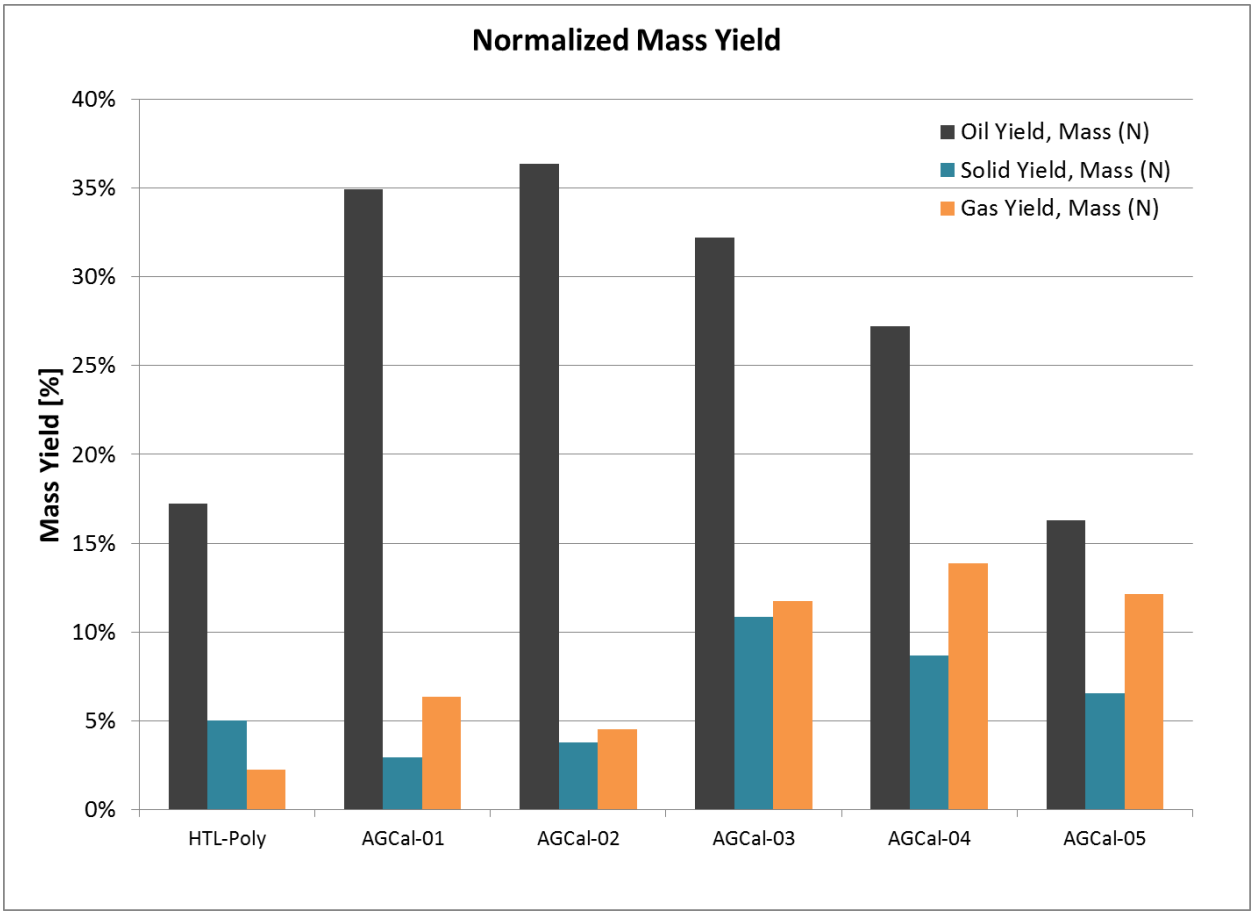

Figure 97: Normalized Mass Yields

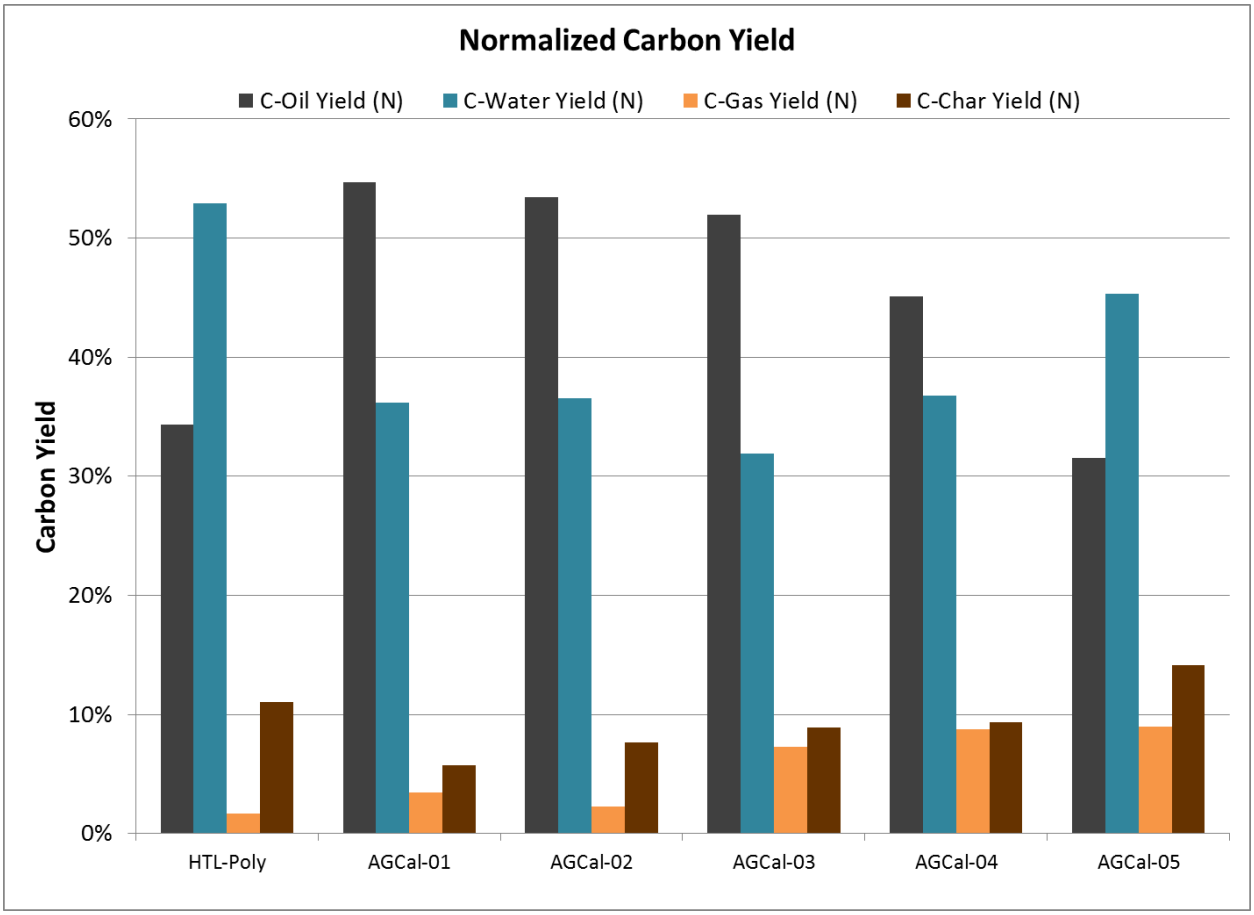

Figure 98: Normalized Carbon Yields

The graph of Normalized Carbon Yields illustrates how samples with higher ash contents resulted in HTL runs in which less of the carbon was recovered in the bio-oil fraction. In Sample 5, with a particularly high ash content of 41.8%, the result was especially poor. In Samples 2 and 3, a low ash content was obtained along with an ideal solids content of around 20%. These samples were the most successful in terms of carbon yield in the HTL product.

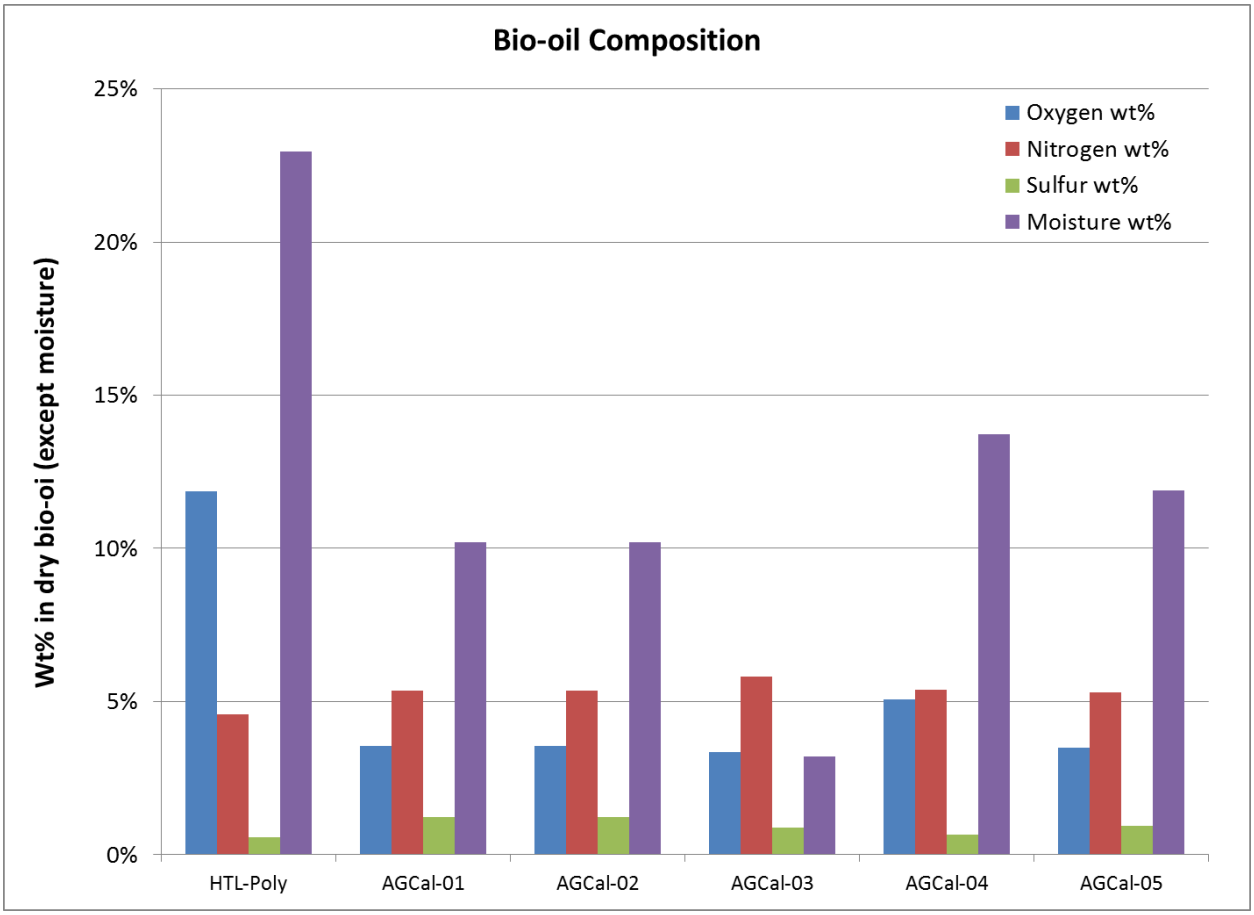

Figure 99: Bio-oil Elemental and Moisture Composition

Across Samples 1 through 5, the proportion of oxygen, nitrogen, and sulfur was relatively consistent. Samples 4 and 5, with their relatively high ash contents, contained significantly more moisture in the oil fraction.

Table 23: HTL Biocrude Analysis (Dry Basis)

	Unit	HTL Poly 8/7/13	Cal 01 5/15/14	Cal 02 5/20/14	Cal 03 5/19/15	Cal 04 7/30/15	Cal 05 9/17/15
Carbon, wt%	wt%	74%	79%	79%	80%	79%	78%
Hydrogen, wt	wt%	8.1%	10.2%	10.2%	10.0%	10.1%	9.9%
H:C, mol ratio	ratio	1.31	1.53	1.53	1.50	1.53	1.52
HHV	MJ/kg	34.1	39.2	39.2	39.3	38.8	38.6
Oxygen	wt%	11.9%	3.6%	3.6%	3.3%	5.1%	3.5%
Nitrogen	wt%	4.6%	5.4%	5.4%	5.8%	5.4%	5.3%

Sulfur	wt%	0.6%	1.2%	1.2%	0.9%	0.7%	1.0%
TAN	mg_{KOH}/g_{oil}	47	39	39	27	33	41
Density	g/ml	0.98	0.98	0.99	0.98	0.98	0.99
Viscosity	cSt@40C	725	165	346	355	371	3298
Moisture	wt%	22.9%	10.2%	10.2%	3.2%	13.7%	11.9%
Ash	wt%	0.78%	0.60%	1.12%	0.22%	0.15%	1.93%
Filterable Solids	wt%	1.2%	0.39%	0.72%	0.18%	0.13%	2.09%

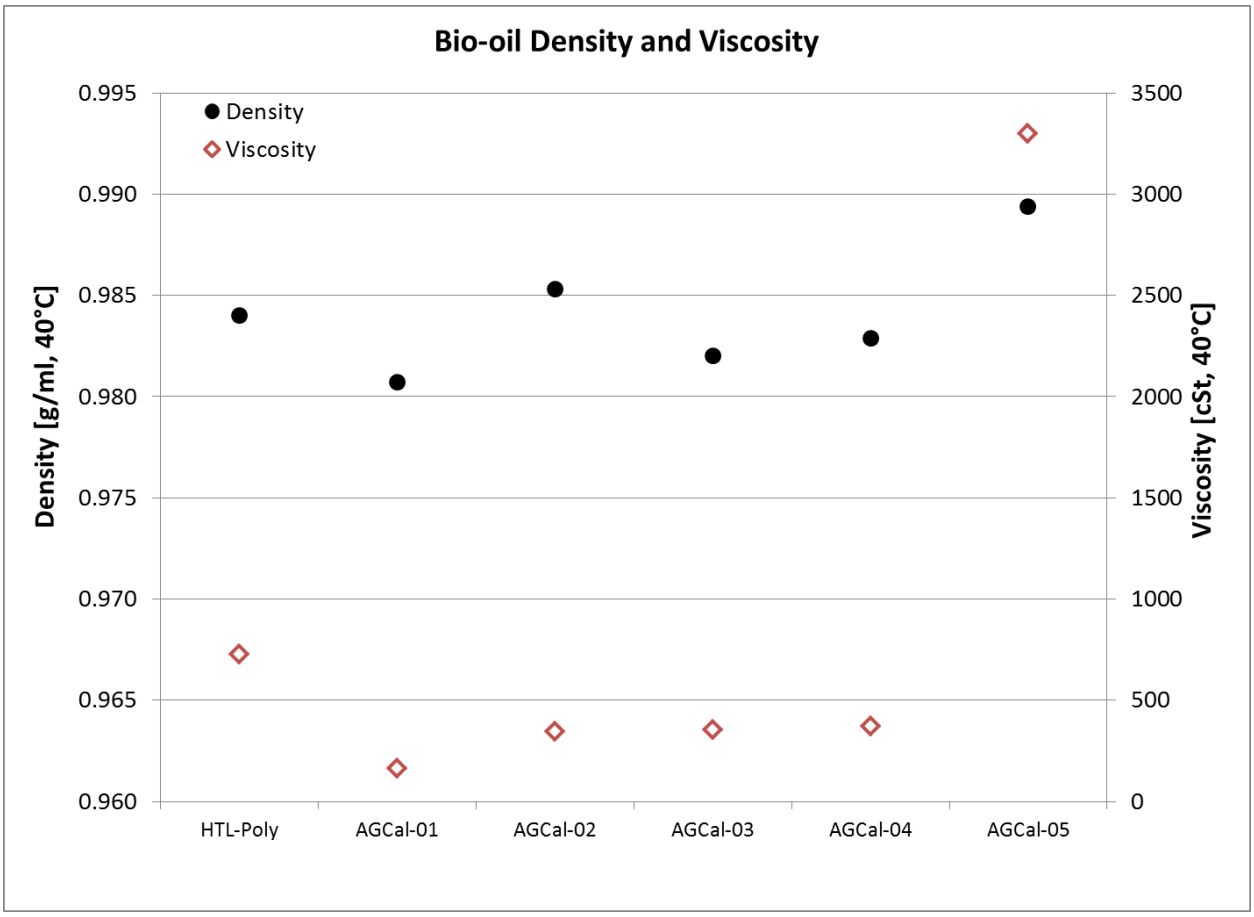

Figure 100: Bio-Oil Density and Viscosity

The density of the bio-oil fraction ranged from about 0.981 to 0.986 g/mL among Samples 1 through 4. Sample 5 had a higher density of nearly 0.99 g/mL, reflecting its especially high moisture content. The viscosity of the Samples 1 through 4 was relatively consistent between about 200 and 400 cSt. Sample 5 stood out again, with a much greater viscosity of around 3,300 cSt.

Hydrotreating studies

Hydrotreating studies were conducted on the bio-oil fractions resulting from Sample 2, 3, and 4 HTL runs. These were compared to a diesel standard in a distillation study. The materials from the tests had very consistent boiling curves. Overall, the bio-oil was lighter than diesel. About 30% of the bio-oil samples were in the gasoline range and about 50% were in the diesel range.

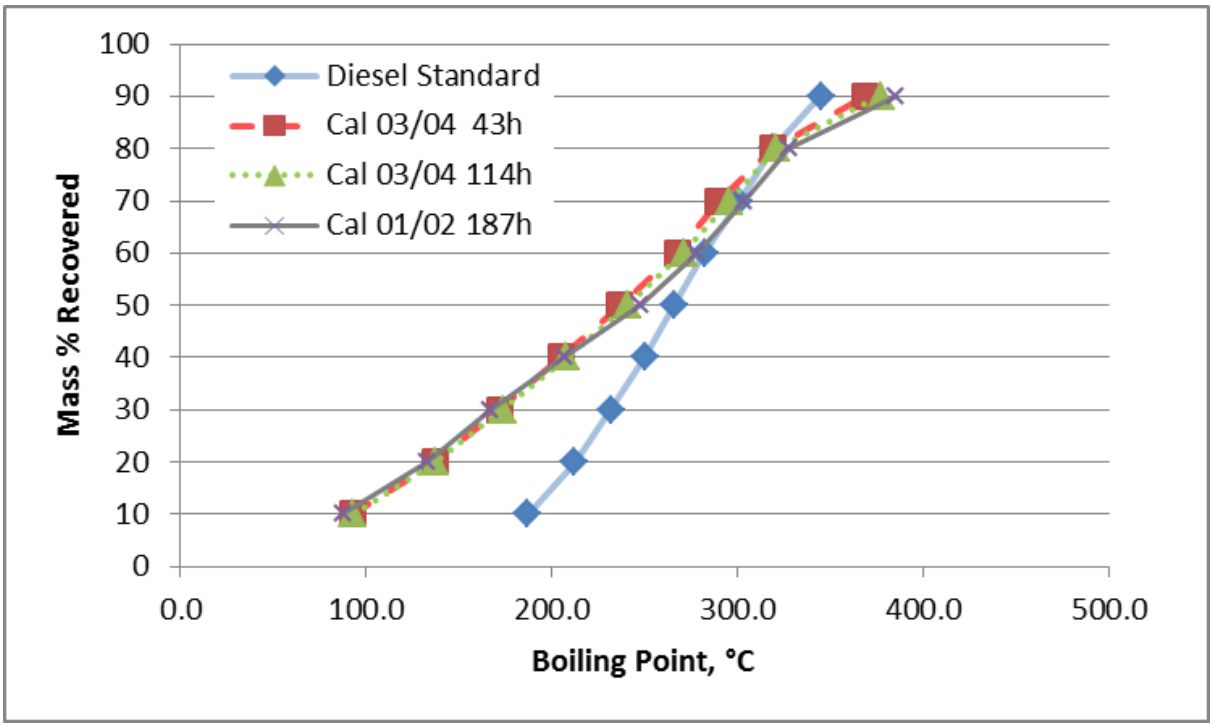

Figure 101: Boiling Point of Sample 2, 3, and 4 Bio-Oil Compared with Diesel Standard

Mass Fraction of product cuts were generally stable as function of time on stream.

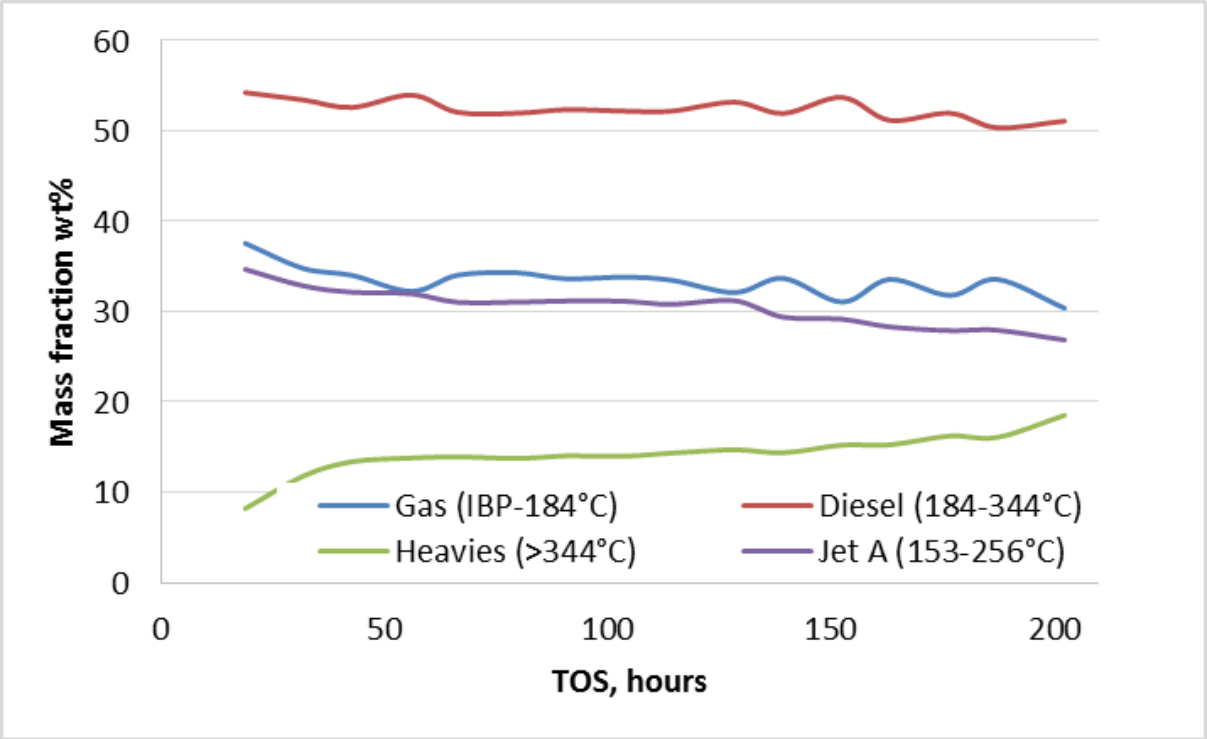

Figure 102: Mass Fraction of Hydrotreated Samples as Function of Time on Stream

Air emissions studies

Air emissions from HTL fuel processes derive from two sources:

1. reactor effluent from heating and pressurizing the biomass to reaction temperatures
2. process heating equipment

Only lab-scale data is available on the gas composition of HTL exhaust. Emissions from process heating technologies are well characterized.

Air emissions for a theoretical HTL unit at the Delhi Wastewater Treatment plant would be regulated by the San Joaquin Valley Air Pollution Control District (SJVAPCD). Regulated emissions include nitrogen and sulfur oxides, volatile organic compounds (VOCs), particulate matter under ten microns (PM10), and carbon monoxide. Requirements for emissions control are unique to each pollutant and dependent on the rated heat input of the process unit (btu/hr), with an HTL system likely subject to Rules 4306/5 (NOx, CO), 4307, 4308, or 4320 for boilers, steam generators, dryers, and process heaters.

Anticipated gaseous emissions were estimated from steady-state in-line gas composition analysis collected during HTL processing campaigns of the Delhi full-scale system biomass (Table 24). During initial runs, HTL exhaust was diluted during collection, as gas collection vessels were pre-filled with nitrogen gas and are not shown.

Table 24: HTL effluent gas phase composition, as well as the anticipated daily mass flow at Phase 2 (1.2 ha of cultivation area). Depending on unit emissions, daily mass flows greater than 2 lb./day of a given component may trigger Best Available Control Technology (BACT) requirements.

Component	Mass % in HTL gas phase[i]	Mass flow at Phase 2 (3 acre, 1.2 ha), lb./day
H_2	0.07	0.02
N_2	3.45	0.75
H_2S	0.25	0.06
CO_2	91.14	19.77
CH_4	0.85	0.18
Ethane, Ethylene	0.72	0.16
Propane	0.71	0.15
C_4 (butane, …)	1.29	0.28
C_5 (pentane, …)	1.51	0.33

[i] Average value of samples collected from the Delhi full scale system.

HTL exhaust gas is approximately 91% (by mass) carbon dioxide, with small amounts of hydrogen, nitrogen, hydrogen sulfide, and various VOCs making the balance. Using the exhaust gas composition in Table 24, as well as the yield of gas per unit of algal slurry feed, the estimated gas-phase mass flows (in lbs./day, as regulated by SJVAPCD) are shown in Table 24 for the Phase 2 design case (1.2 ha of cultivation area, 20 g VSS/m^2-day).

The only component above the 2 lb./day trigger for emissions control is carbon dioxide, which is not regulated at this time. VOC (methane, ethane, and C4 and C5 organic compounds) emissions amount to 1 lb./day, less than half of the regulatory limit, although VOC's emitted via other facility processes or the process heater could approach the regulatory threshold. An incinerator or recycle flow exhaust gas into the process heater intake, may be required for emissions control. HTL gas phase nitrogen and sulfur oxide emissions were estimated based on mass balance, subtracting the expected sulfur or nitrogen mass flows of the HTL biocrude and aqueous phase from the incoming minerals from the reactor feed, and give values on the order of magnitude of the regulatory limit. These constituents will need further characterization as upgrades to the HTL apparatus allow measurement of target components via methods and equipment approved by SJVAPCD. Exhaust PM10 content was not measured, although expected to be minimal as the exhaust gas is water-washed by the aqueous phase.

Initial implementation of an HTL system at the Delhi site would likely be regulated by "Rule 2021, Experimental Research Operations", which allows a temporary exemption from permitting requirements for experimental process units operating less than 180 days per year, although only after prior written approval by SJVAPCD (District, San Joaquin Valley APCD List of Current Rules, 1992). Under this rule, criteria pollutants (including NOx, SOx, CO and PM10) could be independently measured using approved methods by a certified testing laboratory. A full scale unit will require an Authority to Construct permit, after which SJVAPCD has 180 days after receiving a completed permit to review the design. In addition to emissions related permits, requirements for the storage of organic liquids in tanks greater than 1,100 gallons are governed by Rule 4623 (District, 2005). For the Phase 2 design case, biofuel intermediate production approaches 9,000 gallons per year.

Sample 1

Figure 103: Sample 1 HTL Product

During the first HTL run some plugging occurred downstream of the CSTR. Blowdowns alleviated the plugging, but it recurred. When the blowdown pot was unrecoverable (the outlet was plugged), the runs were ended. A plug was located at the exit of CSTR (soft tar/oil plug). It was determined that the plugging may have been due to high ash content or may have simply been an anomaly.

Data are plotted here for COD, pH, NH_3 and wet oil rate as function of run time during the run. The green block shows the steady state window used for data analysis.

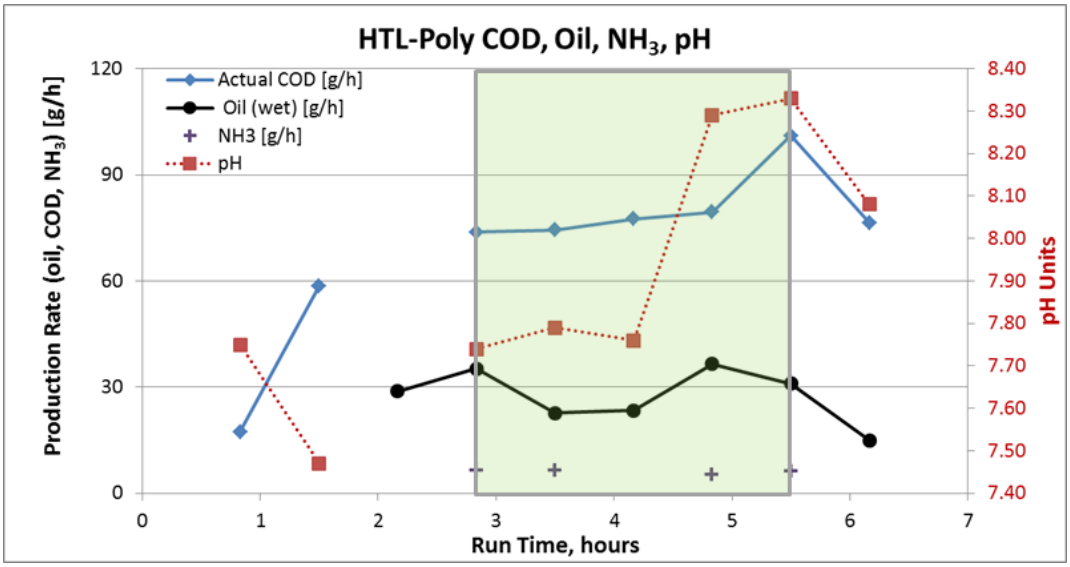

Figure 104: Oil Production Rate Over Time

Separation of the oil and water phases was found to be difficult. This was likely due to an overabundance of organic material lost to the water phase.

Figure 105: Sample 1 Oil-Water Phase Separation

The separation was improved with centrifugation, resulting in roughly 25% of the volume of the emulsified oil/water phase being recovered in oil phase.

Figure 106: Sample 1 Oil-Water Partition in Centrifuge Tubes

The mass balance was satisfactory at 98%, though a relatively low bio oil yield of about 15% was obtained. A relatively low carbon balance of 68% was obtained. Pacific Northwest National Laboratory reported carbon balances are typically >90%.

Table 25: Sample 1 Mass Yields

Mass Yields (Dry, Ash Free, Normalized)		
Mass Balance	%	98%
Oil Yield, Mass (N)	g_{oil}/g_{fd}	15%
Solid Yield, Mass (N)	g_{solid}/g_{fd}	5%
Gas Yield, Mass (N)	g_{gas}/g_{fd}	2%
Aq. Yield, Mass (N)	g_{aq}/g_{fd}	78%

Table 26: Sample 1 Carbon Balance and Yield

Carbon Balance and Yield		
C-Balance	%	68%
H-Balance	%	91%
O-Balance	%	100%
N-Balance	%	89%
C-Oil Yield, (N)	%	34%
C-Water Yield (N)	%	53%
C-Gas Yield (N)	%	2%
C-Char Yield (N)	%	11%

Table 27: Sample 1 Bio-Oil Composition

Bio-oil Composition		
Carbon, wt%	wt%	83%
Hydrogen, wt%	wt%	9.1%
H:C, mol ratio	ratio	1.31
Oxygen	wt%	1.3%
Nitrogen	wt%	5.2%
Sulfur	wt%	0.6%
TAN	mg_{KOH}/g_{oil}	47
Density	g/mL	0.98
Viscosity	cSt@40°C	725
Moisture**	wt%	32.7%**
Ash	wt%	0.78%
Filterable Solids	wt%	1.19%

Metals in the oil phase were analyzed by ICP. These values are typical of other Pacific Northwest National Laboratory HTL runs on other feedstock materials. All values reported in PPM.

Table 28: Sample 1 Bio-Oil Metals Analysis

Bio-oil Composite					
Metal	Fe	K	Na	Ni	S
Concentration (PPM)	1202	306	76	129	3326

Table 29: Sample 1 HTL Emissions

	61573-22-2

LHSV (WHSV)	0.24 (0.30)
Gas Flow Rate, scc/min	74.8
H_2, vol%	96.2
CH_4, vol%	1.3
Ethane, vol%	0.9
Propane, vol%	1.0
Butane (iso- and n-), vol%	0.3
Pentane, vol%	0.0
NH_3, vol%	0.0

The hydrotreating upgrading tests resulted in one steady state sample being collected between 114 and 202 hours on stream. This sample was the second attempt at a hydrotreating run of these materials, as the first was terminated in under 12 hours due to bed plugging. For the final sample, a relatively poor mass balance of 79.7% was obtained, which is not typical for low solids bio-oils. It is postulated that this resulted from phase separation of the feed materials during the test. Results are reported here for a sample collected at 187 hours on stream.

Table 30: Sample 1 Hydrotreating Product

Stream Parameter	**Cal-01/02 Biocrude (dry basis)**	**HT Product at 187 h**
Carbon, Wt%	80	84.5
Hydrogen Wt%	10.1	14.6
H:C	1.5	2.05
Nitrogen, Wt%	5.5	nd
Oxygen, Wt%	3.11*	0.97
Sulfur, ppm	11,000	43
Wt% Moisture	10.6	~0
Density, g/cm3	0.98	0.79
Viscosity, cSt	320 (@ 40°C)	2.02 (@20°C)
nd = not detected *O in biocrude determined by difference		

Distillation of the upgraded product was simulated for comparison to conventional fuels. This resulted in a high yield of distillate range hydrocarbons. The compounds were 20% lighter than kerosene with some material in diesel range.

Table 31: Sample 1 Distillation Study

Sample Recovered, wt%	61573-22-2
0.5	48.5
5	87.0
10	114.0
20	153.0
30	176.0
40	215.0
50	258.5
60	288.0
70	303.0
80	319.5
90	357.5

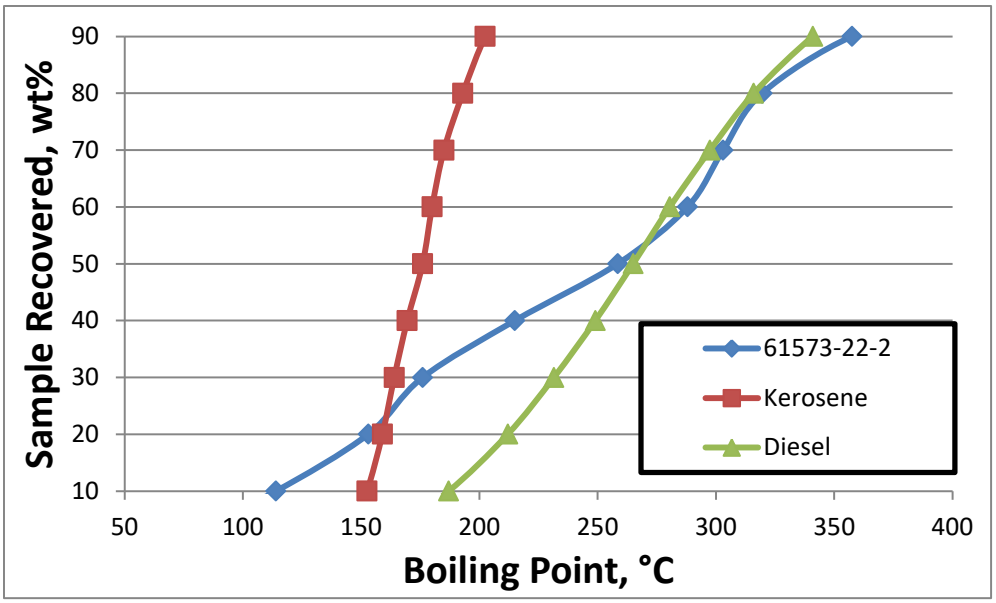

Figure 107: Sample 1 Distillation Study with Kerosene and Diesel Standards

Sample 2

In the first run of Sample 2 materials, challenges were again encountered in oil water separation. The phase separation is clearly depicted here.

Figure 108: Sample 2 HTL Product

Figure 109: Sample 2 HTL Product Phase Separation

Oil droplets are apparent in the aqueous phase in the cone bottom flask. Separation was found to be improved by centrifugation. The first run had to be halted due to solids accumulation in the CSTR. A mineral encrusted paddle is shown here. These solids would ideally have been deposited downstream at the filter housing rather than collecting here.


Figure 110: Mineral Encrusted CSTR Paddle

The second test was run at a lower space velocity and resulted in an aqueous phase of similar appearance to the first. With a clean CSTR impellor, most of the solids in this test were deposited at the filter stage.

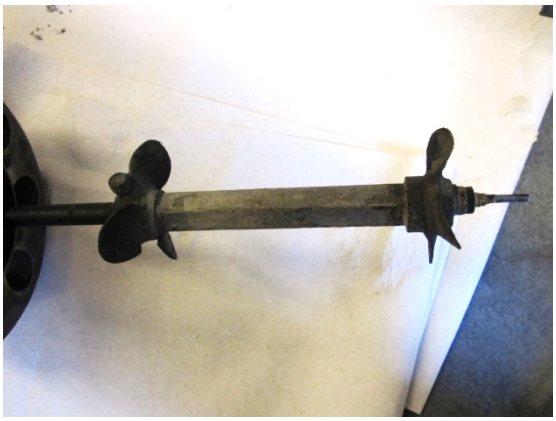

Figure 111: Cleaned CSTR Impellor

Figure 112: Mineral Deposits on Filter

The product distribution and process results from the two days of testing was as follows:

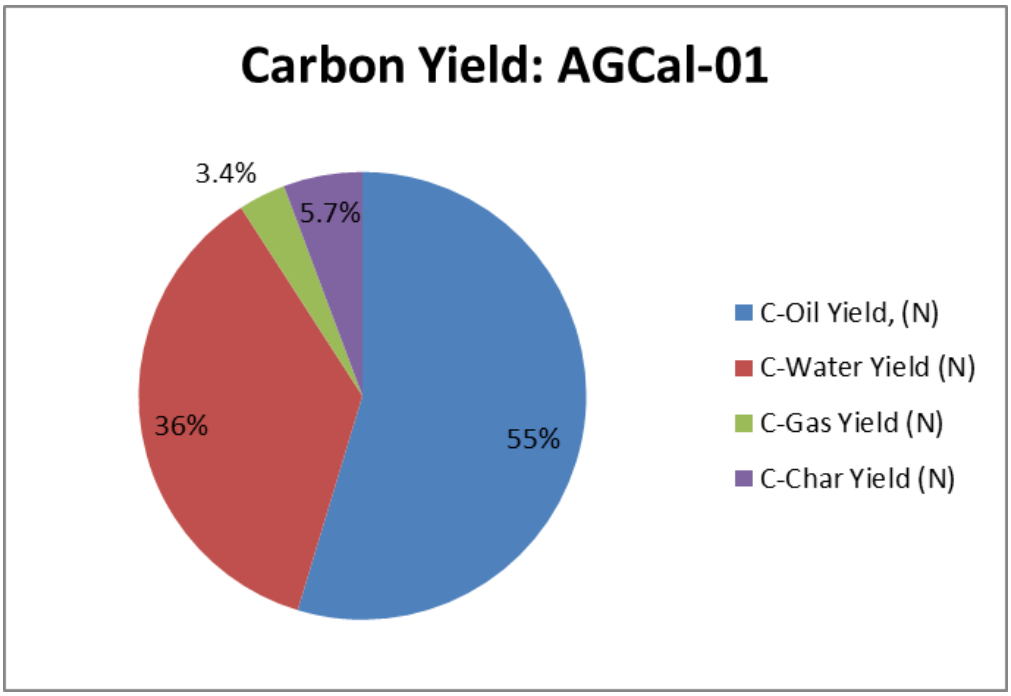

Figure 113: Sample 2 Run 1 Carbon Yield

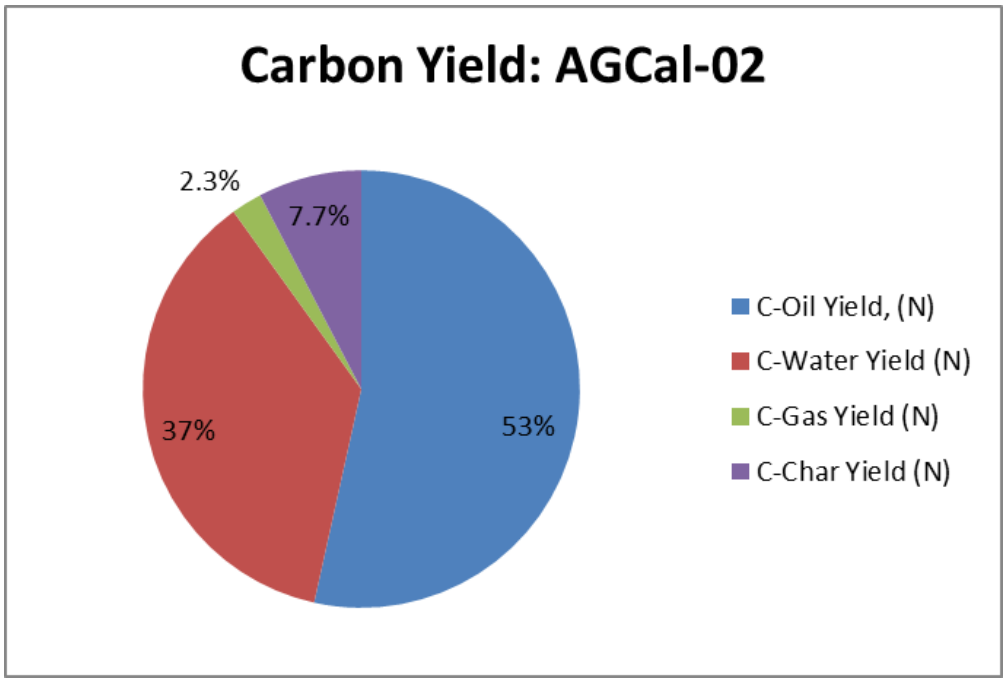

Figure 114: Sample 2 Run 2 Carbon Yield

Table 32: Sample 2 Mass Yields

Mass Yields (Dry, Ash Free, Normalized)			
Mass Balance	%	99%	100%
Oil Yield, Mass (N)	g_{oil}/g_{fd}	35%	36%
Solid Yield, Mass (N)	g_{solid}/g_{fd}	3%	4%
Gas Yield, Mass (N)	g_{gas}/g_{fd}	6%	5%
Aqu Yield, Mass (N)	g_{aqu}/g_{fd}	56%	55%
C-Balance	%	95%	102%
H-Balance	%	103%	105%
O-Balance	%	99%	100%
N-Balance	%	91%	103%
C-Oil Yield, (N)	%	55%	53%
C-Water Yield (N)	%	36%	37%
C-Gas Yield (N)	%	3.4%	2.3%
C-Char Yield (N)	%	5.7%	7.7%

Table 33: Sample 2 Bio-Oil Composition

Bio-oil Composite for Upgrading		
Mass	g	550
Carbon, wt%	wt%	78.9
Hydrogen, wt%	wt%	10.2
H:C, mol ratio	ratio	1.53
Oxygen	wt%	3.6
Nitrogen	wt%	5.4
Sulfur	wt%	1.2
TAN	mg_{KOH}/g_{oil}	38
Density	g/mL	0.98
Viscosity	cSt@40°C	320
Moisture	wt%	10.2
Ash	wt%	0.75%
Filterable Solids	wt%	0.72%

Sample 3

For the Sample 3 HTL run, the insert for the CSTR was reinstalled to prevent the issues of the Sample 2 run. During the run a small pressure differential developed across the preheater and remained essentially constant throughout the run. Operations were smooth during the test. However, after switching to water, issues with the CSTR were again encountered, including pressure differential and loss of mixing. Post-run disassembly revealed CSTR packed with solids. The test resulted in a mass balance of 104%.

Table 34: Sample 3 HTL Mass Balance

	Unit	**Cal 03**

		5/19/15
Mass Balance	**%**	**104%**
C-Balance	**%**	**110%**
H-Balance	**%**	**108%**
O-Balance	**%**	**103%**
N-Balance	**%**	**89%**
P-Balance	**%**	**118%**
Mass Yields Normalized		
Oil Yield, Mass (N)	g_{oil}/g_{fd}	**32%**
Solid Yield, Mass (N)	g_{solid}/g_{fd}	**11%**
Gas Yield, Mass (N)	g_{gas}/g_{fd}	**12%**
Aq Yield, Mass (N)	g_{aq}/g_{fd}	**45%**
Carbon Yields - Normalized		
C-Oil Yield (N)	**%**	**52%**
C-Water Yield (N)	**%**	**32%**
C-Gas Yield (N)	**%**	**7%**
C-Char Yield (N)	**%**	**9%**

Table 35: Sample 3 Bio-Oil Composition

	Unit	**Cal 03** **5/19/15**
Carbon, wt%	**wt%**	**80%**
Hydrogen, wt	**wt%**	**10.0%**
H:C, mol ratio	**ratio**	**1.50**
HHV	**MJ/kg**	**39.3**
Oxygen	**wt%**	**3.3%**
Nitrogen	**wt%**	**5.8%**

Sulfur	**wt%**	**0.9%**
TAN	**mg_{KOH}/g_{oil}**	**27**
Density	**g/ml**	**0.98**
Viscosity	**cSt@40C**	**355**
Moisture	**wt%**	**3.2%**
Ash	**wt%**	**0.22%**
Filterable Solids	**wt%**	**0.18%**

Table 36: Sample 3 Bio-Oil Composition

	Wet Crude Basis	**Cal 03**
Ash (in biocrude)	Wt%	0.22%
Cu	ppm	74
Fe	ppm	853
K	ppm	107
Mg	ppm	88
Na	ppm	423
Ni	ppm	< 45
P	ppm	< 45
Zn	ppm	< 45
Si	ppm	941
S	ppm	2200

Steady state gas production and composition was measured. The N_2 is likely to have been a residual added to the test system (unlikely to be a produced gas). These analyses were done by micro GC with TCD detector.

Table 37: Sample 3 HTL Emissions

	Unit	**Cal 03**

Gas Rate	L/h	17.2
Gas Rate	L/Kg-dry feed	53
Gas Rate	L/Kg-ash free dry feed	74
Gas Composition		
CO_2	Mol %	84%
H_2	Mol %	1.6%
N_2	Mol %	5.0%
CH_4	Mol %	1.9%
H_2S	Mol %	0.4%
C2	Mol %	1.1%
C3	Mol %	0.7%
C4	Mol %	1.0%
C5	Mol %	1.0%

At 14:00, product collection mode switched to rapid letdown. In this mode, N_2 is purged from the gas system with increased sensitivity for gas composition measurements

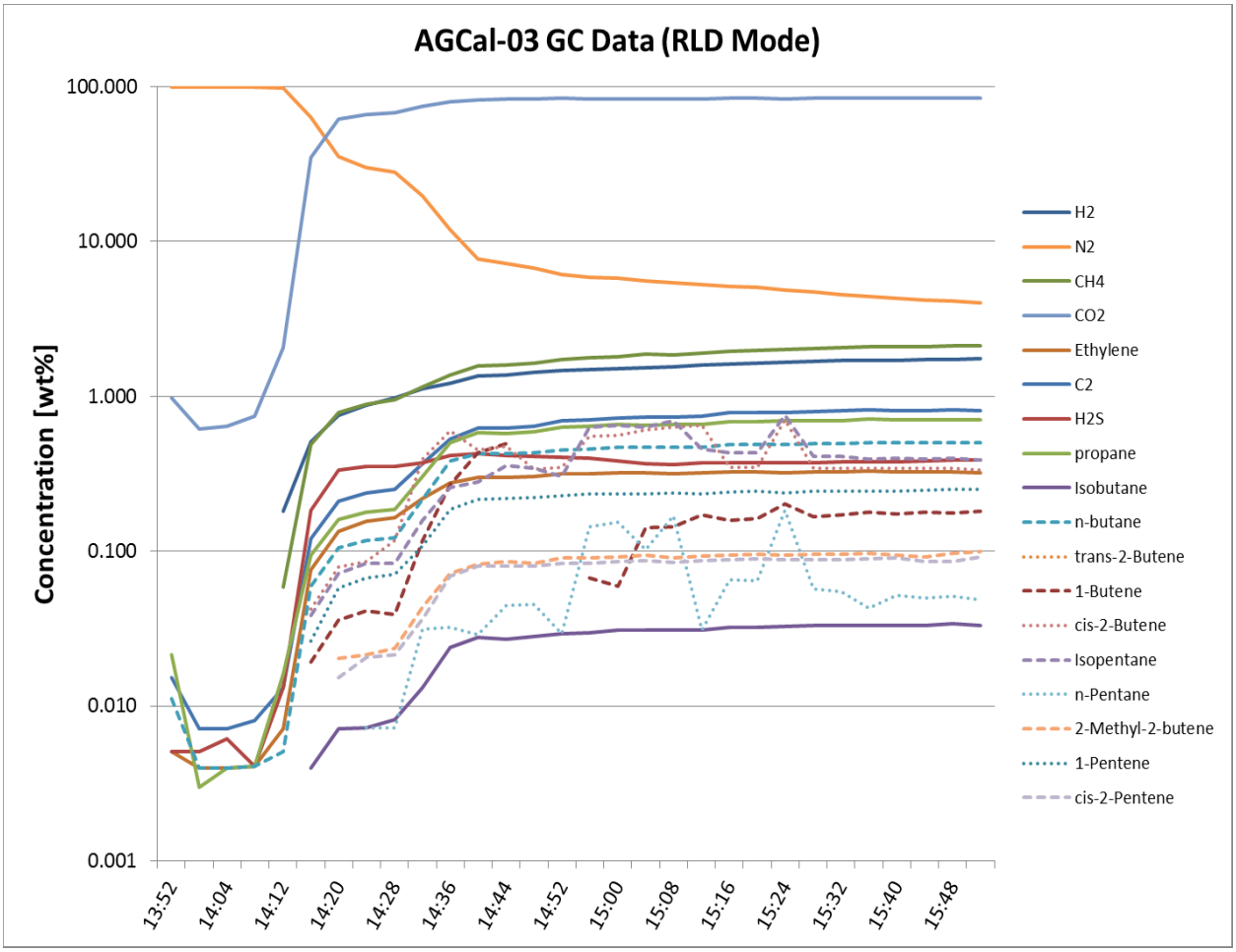

Figure 115: Sample 3 Gas Emissions Over Time

The results of the hydrotreating run are included here. The sample was collected at 114 hours on stream.

Table 38: Sample 3 Hydrotreating Composition

Stream Parameter	Cal-03/04 Biocrude	HT Product (at 114h)
Carbon, Wt%	81	84
Hydrogen Wt%	10.0	14.5
H:C	1.5	2.04
Nitrogen, Wt%	5.8	nd
Oxygen, Wt%	2.2*	1.18
Sulfur, ppm	6,900	66

Wt% Moisture	5.03	~0
Density, g/cm3	0.99	0.79
Viscosity, cSt	370 (@ 40°C)	2.5 (@20°C)
nd = not detected *O in biocrude determined by difference		

Sample 4

For Sample 4, the CSTR insert was removed. A pressure shift at 08:30 occurred due to increasing pressure on the dome-loaded BPR by 100 psig. Cyclical fluctuations in pressure differential occurred due to a leaking valve of BPR seal issue during product collection. Towards end of run, the pressure differential increased due to solids accumulating in the filter. No filter blowdown conducted during this run. The test resulted in a mass balance of 101%.

Table 39: Sample 4 HTL Mass Balance

	Unit	**Cal 04** **7/30/15**
Mass Balance	**%**	**101%**
C-Balance	**%**	**100%**
H-Balance	**%**	**106%**
O-Balance	**%**	**101%**
N-Balance	**%**	**96%**
P-Balance	**%**	**92%**
Mass Yields Normalized		
Oil Yield, Mass (N)	g_{oil}/g_{fd}	**27%**
Solid Yield, Mass (N)	g_{solid}/g_{fd}	**9%**
Gas Yield, Mass (N)	g_{gas}/g_{fd}	**14%**
Aq Yield, Mass (N)	g_{aq}/g_{fd}	**50%**
Carbon Yields - Normalized		
C-Oil Yield (N)	**%**	**45%**

C-Water Yield (N)	**%**	**37%**
C-Gas Yield (N)	**%**	**9%**
C-Char Yield (N)	**%**	**9%**

Table 40: Sample 4 Bio-Oil Composition

	Unit	**Cal 04** **7/30/15**
Carbon, wt%	**wt%**	**79%**
Hydrogen, wt	**wt%**	**10.1%**
H:C, mol ratio	**ratio**	**1.53**
HHV	**MJ/kg**	**38.8**
Oxygen	**wt%**	**5.1%**
Nitrogen	**wt%**	**5.4%**
Sulfur	**wt%**	**0.7%**
TAN	**mg_{KOH}/g_{oil}**	**33**
Density	**g/ml**	**0.98**
Viscosity	**cSt@40C**	**371**
Moisture	**wt%**	**13.7%**
Ash	**wt%**	**0.15%**
Filterable Solids	**wt%**	**0.13%**

Table 41: Sample 4 Bio-Oil Metals Analysis

	Wet Crude Basis	**Cal 04**
Ash (in biocrude)	Wt%	0.15%
Cu	ppm	79
Fe	ppm	1091
K	ppm	36

Mg	ppm	< 25
Na	ppm	29
Ni	ppm	82
P	ppm	< 25
Zn	ppm	50
Si	ppm	42
S	ppm	5588

Steady state gas production and composition was measured. Again, the N_2 is likely to have been a residual added to the test system (unlikely to be a produced gas). These analyses were done by micro GC with TCD detector.

Table 42: Sample 4 HTL Air Emissions

	Unit	**Cal 04**
Gas Rate	L/h	15.2
Gas Rate	L/Kg-dry feed	62
Gas Rate	L/Kg-ash free dry feed	87
Gas Composition		
CO_2	Mol %	84%
H_2	Mol %	1.4%
N_2	Mol %	5.0%
CH_4	Mol %	2.4%
H_2S	Mol %	0.2%
C2	Mol %	1.0%
C3	Mol %	0.6%
C4	Mol %	0.8%
C5	Mol %	0.7%

At 13:01, product collection mode switched to rapid letdown. In this mode, N_2 is purged from the gas system with increased sensitivity for gas composition measurements

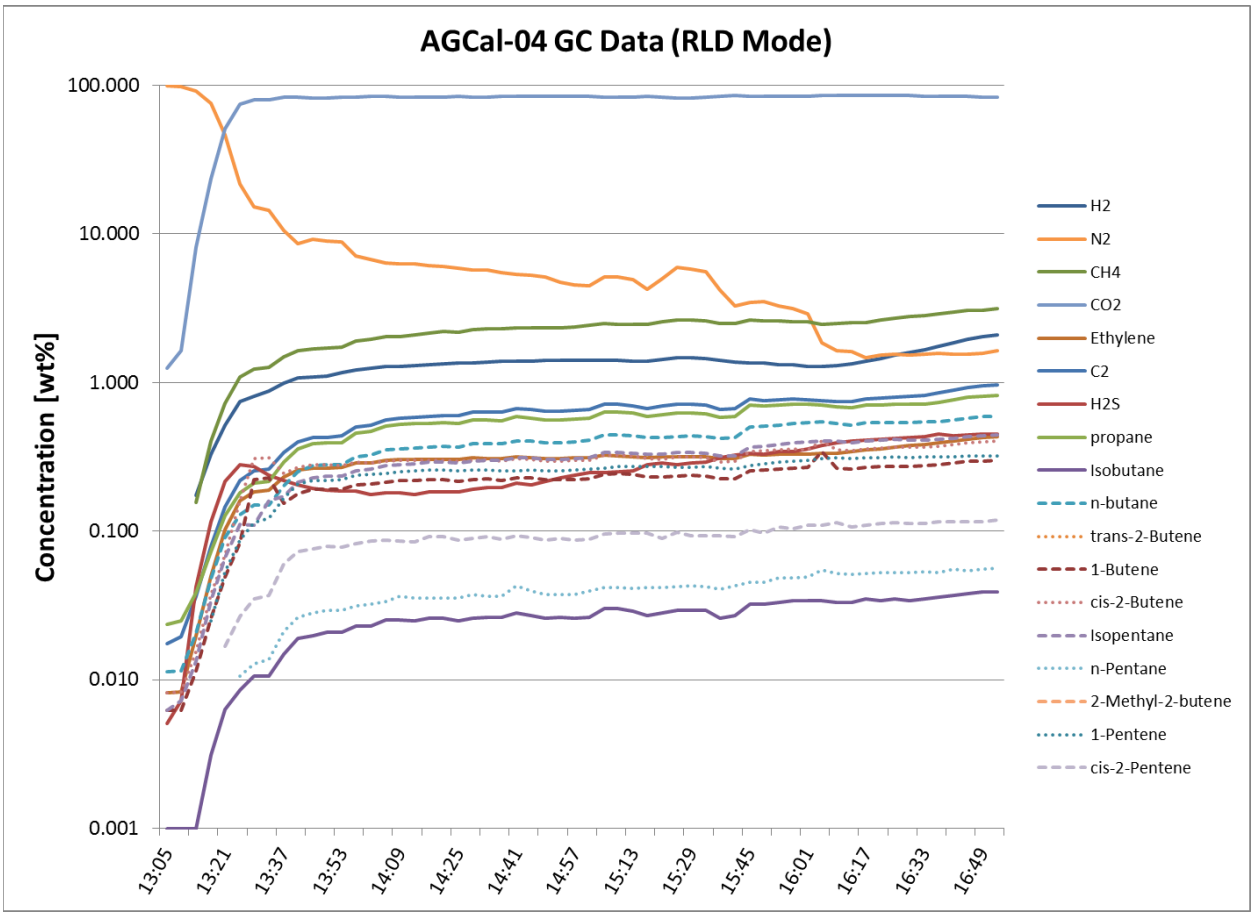

Figure 116: Sample 4 HTL Air Emissions

Sample 5

The HTL operation of Sample 5 – a particularly high ash sample – is detailed here. Spikes in both the temperature and pressure records reflect repeated clogging events. The feed material for this sample contained about 41% ash. This led to the repeated need for blowdown events during the HTL run. This made data acquisition challenging. Due to the frequency of overpressure events, the HTL system switched to water at 12:33, before operating in RLD mode.

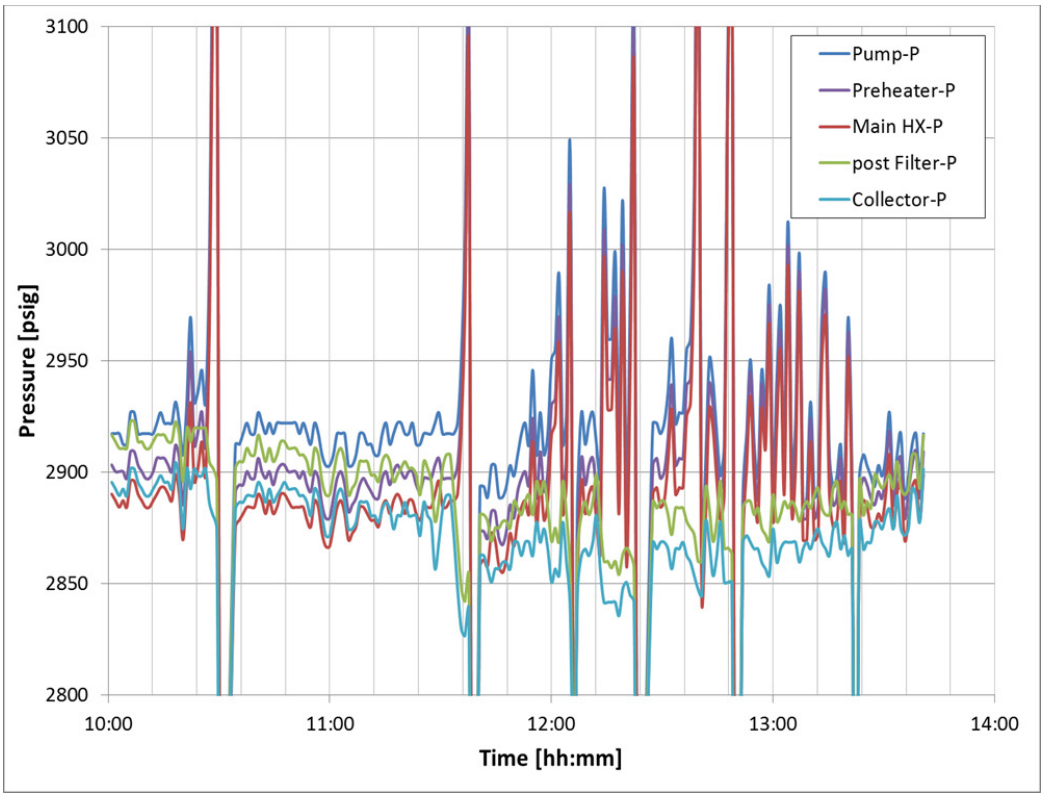

Figure 117: Sample 5 HTL Operating Pressure Over Time

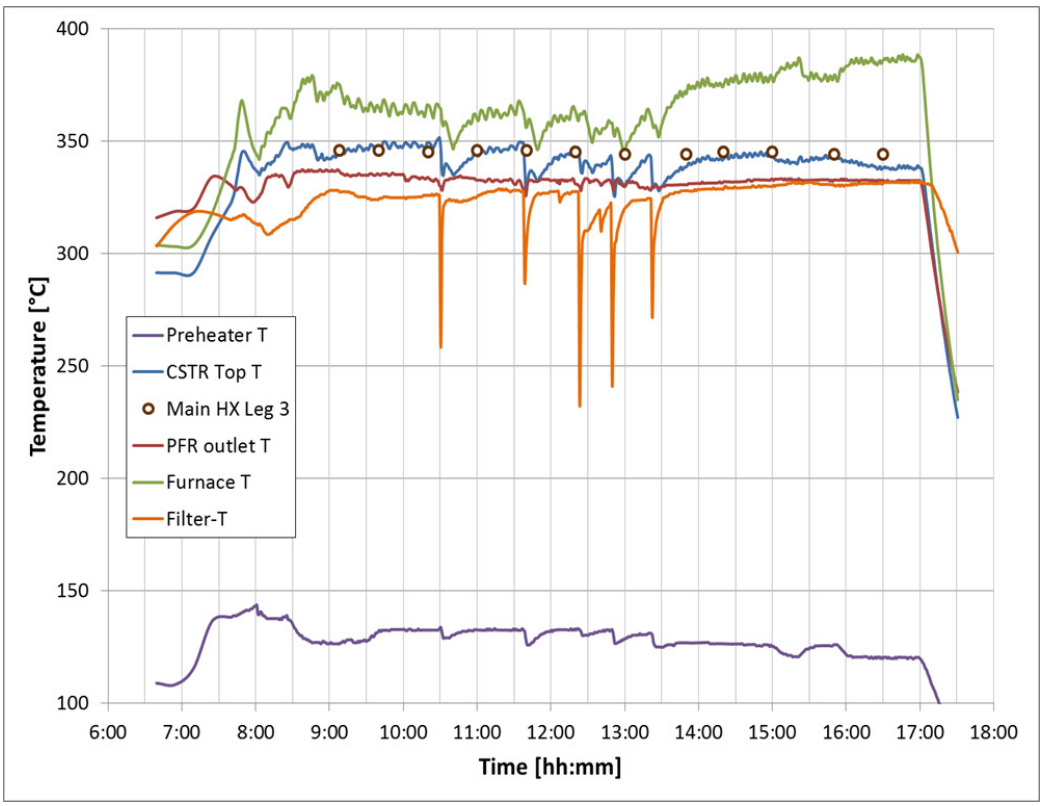

Figure 118: Sample 5 HTL Operating Temperature Over Time

Table 43: Sample 5 HTL Mass Balance

	Unit	Cal 05 9/17/15
Mass Balance	**%**	**98%**
C-Balance	**%**	**77%**
H-Balance	**%**	**100%**
O-Balance	**%**	**100%**
N-Balance	**%**	**96%**
P-Balance	**%**	**95%**
Mass Yields Normalized		
Oil Yield, Mass (N)	**g_{oil}/g_{fd}**	**16%**
Solid Yield, Mass (N)	**g_{solid}/g_{fd}**	**7%**
Gas Yield, Mass (N)	**g_{gas}/g_{fd}**	**12%**
Aq Yield, Mass (N)	**g_{aq}/g_{fd}**	**65%**
Carbon Yields - Normalized		
C-Oil Yield (N)	**%**	**32%**
C-Water Yield (N)	**%**	**45%**
C-Gas Yield (N)	**%**	**9%**
C-Char Yield (N)	**%**	**14%**

Table 44: Sample 5 Bio-Oil Composition

	Unit	Cal 05 9/17/15
Carbon, wt%	**wt%**	**78%**
Hydrogen, wt	**wt%**	**9.9%**
H:C, mol ratio	**ratio**	**1.52**

HHV	**MJ/kg**	**38.6**
Oxygen	**wt%**	**3.5%**
Nitrogen	**wt%**	**5.3%**
Sulfur	**wt%**	**1.0%**
TAN	**mg_{KOH}/g_{oil}**	**41**
Density	**g/ml**	**0.99**
Viscosity	**cSt@40C**	**3298**
Moisture	**wt%**	**11.9%**
Ash	**wt%**	**1.93%**
Filterable Solids	**wt%**	**2.09%**

Table 45: Sample 5 Bio-Oil Metals Analysis

	Wet Crude Basis	**Cal 05**
Ash (in biocrude)	Wt%	1.9%
Cu	ppm	76
Fe	ppm	1009
K	ppm	222
Mg	ppm	
Na	ppm	663
Ni	ppm	37
P	ppm	< 25
Zn	ppm	49
Si	ppm	3415
S	ppm	8250

Conclusions and Recommendations

The five HTL runs were completed on algae biomass samples derived from wastewater at several different sites in California. Studies of HTL bio-oil upgrading and of HTL process emissions were

completed. In addition to achieving the immediate goals of the project, these activities resulted in substantial advances in the knowledge of whole algae biomass conversion via HTL

The mass balances in the five tests were around 100%, indicating a high level of fidelity in the results of these studies. Over five tests, the normalized mass yield of oil ranged from 17% to 36%. In other words, the tests resulted in a mean yield of about 0.3 grams of crude bio-oil per gram of dry algae feed. It is understood from these tests that values in the higher reaches of the oil yield range are consistently obtainable with ideal solids contents and low-ash concentrations in the feed materials. 20% solids feed material was found to be ideal for producing high bio-oil yields. Samples in which the ash content was smaller tended to have higher bio-oil yields, with better partitioning of products and better oil quality. Low ash feed material has another important benefit of reducing operational challenges such as filter clogging, pressure control difficulties, and HTL operation interruptions. The normalized carbon yield ranged from 33% to 55%. Again, low ash in the feed material was found to improve this carbon yield.

Some samples were hydrotreated for comparison with conventional fuels. The products of these studies contained a range of oil compounds. Distillation studies of those products revealed them to contain roughly 30% by mass materials in the gasoline range and 50% by mass in the diesel range. This indicates that the product could be suitable as a liquid fuel for a range of applications or as a blendstock for the adjustment of conventional petroleum fuels.

The gaseous emissions from the HTL comprised 93% CO_2. The remaining fraction consisted of hydrogen, nitrogen, methane, ethylene, carbon monoxide, hydrogen sulfide, isobutene and n-butane.

HTL is an intriguing fuel conversion pathway for aquatic biomass since it is not reliant on complete drying of the feedstock. Additionally, HTL does not require that algal biomass be especially high lipid materials as do other conversion pathways. The studies described here generated process knowledge and fed into technical, economic, and lifecycle considerations that are detailed elsewhere in this report. An oil yield of 30% was assumed in those models, which was based on the studies described here, though the studies yielded knowledge that may make possible consistently higher oil yields than that.

Long term, repeated studies are needed to gain more knowledge of the HTL conversion process and of the upgrading process. These must involve larger scale HTL systems to project accurately the at-scale process inputs, outputs, and parameters. In particular, larger scale, continuously operating HTL systems and hydrotreating systems will refine the process outputs.

Such investigations should be conducted in tandem with algae biomass production studies, as the interplay between feedstock and HTL processing is not yet well understood. Studies of HTL wastes have been considered in a related project and may be beneficial in improving sustained biomass yields. Such studies should continue along with consideration of feedstock production and HTL operation.

Several critical feedstock features were identified in the studies that can inform the operation of algae ponds producing biofuel feedstock. Ash content in feedstock was found to be a critical parameter in determining HTL process and product quality. Dust abatement may be useful for minimizing the ash in algae biomass. Ash-containing flocculants should be avoided to the greatest extent possible in collecting algal biomass. These materials are costly and will have a negative impact on the bio-oil product. Further, solar drying to achieve to ideal moisture content may have limited applicability due to the risk of dust contaminating the feedstock materials. Feed phase separation negatively impacted the HTL process. The application of mixing in the HTL feedstocks will be critical to the outcomes of the process. As will the phase separation of the HTL effluent materials, which can be improved dramatically by limiting ash content in the feedstock.

TASK 5. Scale-up engineering analysis, modeling, and planning (MicroBio Engineering and Cal Poly, in consultation with Delhi County Water District, PNNL, and SNL)

Executive Summary: Introduction, background, state of research

Techno-economic analysis (TEA) and life cycle assessment (LCA) are tools used to determine the economic viability and environmental impact of a fuel product. The results of these analyses are compared to conventional fossil fuel products to calculate the relative reduction of environmental impacts, specifically the GHG emissions and the potential for economic competitiveness. The following sections outline the methods used to determine the minimum fuel selling price (MFSP) and the GHG emissions of a biodiesel blendstock produced by hydrothermal liquefaction (HTL) of 20% ash-free-dry-weight (AFDW) algal biomass paste. Below is a list of subtasks covered in this section.

Milestones tasks and subtasks/ purpose

Purpose: Develop refined engineering models of the process developed and evaluate its projected costs and net greenhouse gas emissions. Prepare the Phase 2 scale-up preliminary engineering plan, evaluate additional sites for Phase 2 and full-scale facility implementations (Fresno, Hilmar, and other promising sites), and a Stage Gate review of these issues.

S5.0 Gather Design Information: At conferences, meetings, and interviews, gather and disseminate information relevant to the design of the Phase 2 scale-up of the biofuel-wastewater process (February 28, 2016).

S5.1 Assess Scale-Up Sites: Identify and assess locations for the Phase 2 scale-up and additional full-scale implementations of wastewater-based algae biofuels (e.g., Hilmar, Fresno) (February 28, 2016).

S5.2 Process Engineering Model: Create a process engineering model for the Delhi Phase 2 design (January 30, 2016).

+ ML5.3 Harvesting and Dewatering Study: Prepare an engineering study on algae harvesting, dewatering, and drying to the level required by HTL (June 30, 2015).

S5.4 Facility Improvements Study: Prepare an engineering study on any facility improvements needed to meet Regional Water Quality Control Board discharge standards while simultaneously producing biomass sufficient to produce the equivalent of 2500 gallons per acre per year of biofuel intermediate. Gather information on permissions needed from water regulators to conduct Phase 2 (February 28, 2016).

S5.5 Air Permitting Study: Prepare an engineering report on air permitting and HTL flue gas clean-up technology expected to be needed (October 31, 2015).

+ ML.5.6 Economics and Lifecycle Study: Prepare facility economic and LCA analyses for the algae wastewater treatment/biofuels process for conditions in California's Central Valley (February 28, 2016).

Methods

Engineering Model Refinement and Full-Scale Evaluation (ML5.3, 5.6; S5.0, 5.1, 5.2, 5.4 5.5)

Scale-Up Engineering Analysis, Modeling, and Planning

A techno-economic analysis (TEA) and life cycle assessment (LCA) was prepared for the present project to estimate the minimum fuel selling price (MFSP) and the carbon balance of a projected large-scale algal biofuels production facility. The system was modelled using MBE's Environmental Sustainability and Process Economics (ESPE) model. The facility consists of large (4 ha) open-pond paddle wheel raceway

ponds, with the algal biomass produced harvested by gravity settling ('bioflocculation') and centrifugation, and then subjected to hydrothermal liquefaction (HTL) for conversion to liquid biofuel intermediates. Colocation of biomass production with the HTL process allows for nutrients recycling and treatment of the HTL effluents in the algal production ponds. A block diagram of the process is shown in Figure 119.

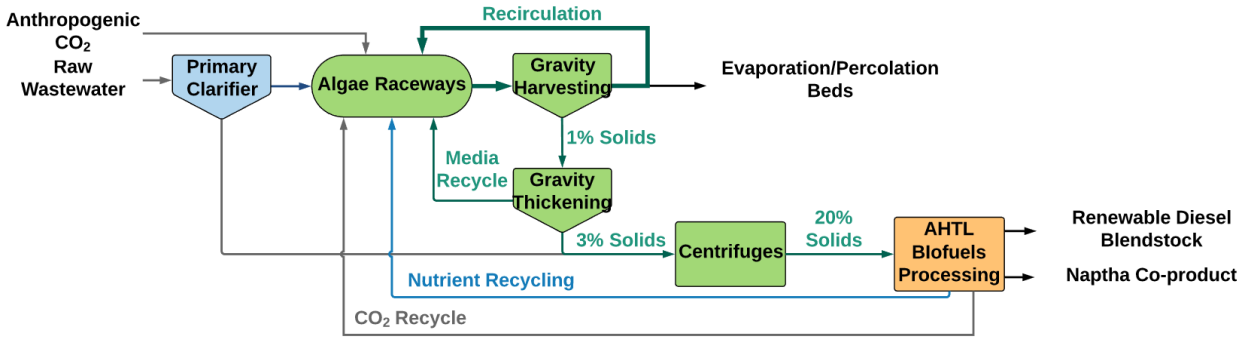

Figure 119: A process flow diagram for the proposed biofuels facility.

The HTL processing facility mass balance, energy consumption, and economics were modeled following the process described in Jones et al, 2014. A block diagram of the HTL process with major flows identified is shown in Figure 120.

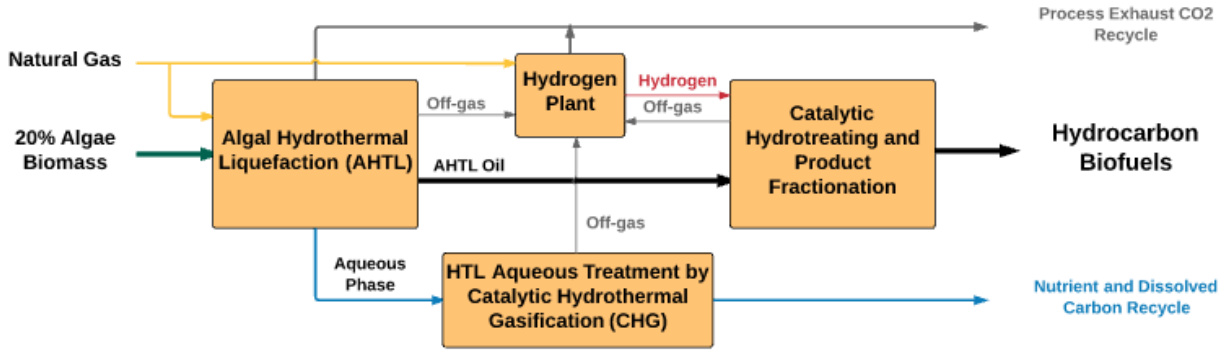

Figure 120: Process flow diagram of the algal biomass HTL to biofuels processing facility (adapted from Jones et al. 2014).

The San Joaquin Valley of California was chosen for the location of the facility, due to its mild climate (annual average of 64° F, minimum monthly average of 45° F in December and maximum monthly average of 84° F in July), abundant flat land, and native clay soils. Clay soils can be used as in situ liners instead of plastic liners, greatly reducing capital cost of the ponds. Data collected in the present study Delhi Wastewater Treatment Plant is deemed representative of such a full-scale facility, due to its proximate location in the San Joaquin Valley. Several municipalities in this region have both available land and sufficient wastewaters to supply the nutrients and water to such a large-scale biofuels facility. However, the Delhi and nearby Hilmar wastewater treatment plants have insufficient flow (< 1 MGD, or <4 million L/d) to provide the required make-up (for evaporation) required for a large (400 ha, or 1,000 acre) biofuels plant, requiring at least ten-times this flow. The modeled facility is thus based on co-locating with the 80 MGD Fresno-Clovis Regional Wastewater Reclamation Facility (RWRF) Figure 121.

Figure 121: An aerial image of the Fresno-Clovis Regional Wastewater Treatment Facility. As shown, the facility is surrounded by open agricultural land. A 500-ha lot is highlighted to demonstrate a hypothetical location for the collocated algae biofuels production facility.

The MBE ESPE model is based on several input assumptions, which can be varied depending on the specific process. In this case, one major input to the model is a projected total biomass productivity of 33 g/m^2-d. This was demonstrated at the Delhi facility by using primary effluent (settled municipal wastewater) and recycling of HTL effluents as main inputs to the algal ponds. This high level of projected productivity has a major impact on the MFSP of the biofuel product. It must be noted that this a 'mixotrophic' process, which combines the entire gamut of both algal metabolic processes, from photo- to photohetero- to hetero-trophic. Further, a substantial fraction of the biomass produced in the ponds (measured as ash-free dry weight) is produced by heterotrophic bacteria, not algae, and some even derives directly from the inflow settled wastewaters.

The wastewater inflows also supply a considerable fraction of the C required for algal growth, thus reducing the need for CO_2 supply. The C flux in the ponds is complex (involving C recycling between the algal and bacterial populations, as well as losses of CO_2 to the atmosphere). However, this model balances inputs and outputs in terms of C and suspended solids, without need to address the internal pond processes. Other sources of C in the process are the organic C and CO_2 recycled from the HTL process, both as liquid and gaseous products (see Figure 120). Additional CO_2 could come from the wastewater treatment plant, which digests the primary solids to biogas, or other local sources, such as landfill gas. Additionally, a 400 MW natural gas-fired power station is located at the Panoche Energy Center in Firebaugh, CA, about 40 miles from the Fresno facility, which can potentially provide supplemental concentrated CO_2 through amine-based flue gas scrubbing.

Carbon dioxide produced from the breakdown of organic substances in wastewater was estimated at 1.2 g CO_2/g BOD (biological oxygen demand), based on a wastewater composition of $C_6H_{11}ON_2$ (Woertz et al., 2009). It was assumed that the algae did not assimilate any of the inorganic carbon in the influent wastewater. In addition, solids in the recirculation and recycling streams increase the raceway effluent suspended solids. The estimated distribution of suspended solids is shown in Figure 122. Raceway

effluent suspended solids were approximated using theoretical equations for heterotrophic growth on wastewater as shown below (Metcalf and Eddy 2003).

Equation 14: Heterotrophic yield

$$Y_{obs} = \frac{Y}{1 + (k_d)HRT} + \frac{(f_d)(k_d)(Y)HRT}{1 + (k_d)HRT}$$

Where;

$Y_{obs} = Observed\ Heterotrophic\ Yield$
$Y = Heterotrophic\ Synthesis\ Yield = 0.8\ gVSS/gBOD$
$k_d = Endogenous\ Decay\ Factor = 0.06\ \ gVSS/gVSS * d$
$f_d = Heterotrophic\ Fraction\ of\ Biomass\ that\ Remains\ in\ Cell\ Debris = 0.125\ gVSS/gVSS$
$HRT = Hydraulic\ Residence\ Time = 4\ days$

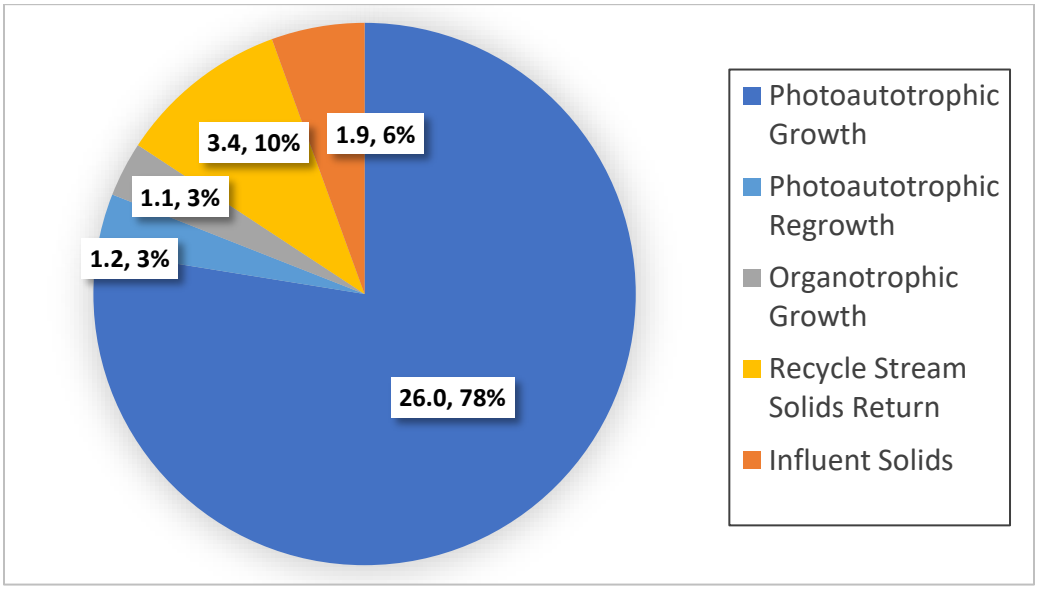

Figure 122: The distribution of the biomass composition is shown: photoautotrophic growth (algae grown on supplemental CO_2), photoautotrophic regrowth (algae grown on CO_2 produced by heterotrophic organisms), organotrophic growth (aerobic bacteria growth), recycle stream solids return, and influent solids.

Harvesting and Dewatering Study

Harvesting and dewatering methods must achieve the target solids content of 20% for HTL processing. The two options evaluated were for initial gravity settling to 3% solids, with and without coagulant addition. Capital and operating costs along with CO_2 life cycle assessment (LCA) were compared.

Coagulant addition requires minor additional capital costs for dosing station, but operating expenses increase significantly with polymer addition. The polymer KlarAid is used for gravity settling in Delhi, CA, added at 40 mg/L of pond effluent, costing approximately $700 per million gallons of flow treated.

Solutions for dewatering from 5% to 20% included, centrifugation, screw press and solar drying. For 400 hectares of ponds, producing 33 g/m^2-d, or 133 Mg/d of biomass, a 5% solids concentration would

represent at flow of 2,660 m^3/day. Allowing for down-time and peak flows, this would need to be processed in about 10-hours per day, or 266 m^3/hr.

The calculation and results of the harvesting and dewatering study are given below in the results section.

Facility Design

The proposed facility is divided into six areas; Area 100: Production Ponds, Area 200: Utility Distribution, Area 300: Make-up Water, Area 400: Dewatering, Area 500: Biofuels Processing. The following sections describe in detail the design assumptions made for modeling the process.

Area 100: Production Ponds

The site consists of 100 4-ha raceways. The design of the raceways was based on the comprehensive design work to scale-up currently operational ponds (Lundquist 2010). The raceways are partially lined at areas of high erosion potential. In-situ clay soils minimize groundwater infiltration. The raceways are 690 m long and 60 m wide. The raceways operate with an average hydraulic residence time of 4 days, which varies seasonally from 2 to 6 days. The ponds have two CO_2 sumps each and one paddle wheel station, which are of concrete construction. The power for mixing the raceway ponds was determined using Manning's equation for head loss with an assumed mixing efficiency of 25% (including hydraulic and motor efficiencies). The raceway effluent flows by gravity, continuously to the algae settlers. Key parameters for the sizing and operation of the raceways are shown in Table 46.

Table 46: Algae raceway production pond geometry and operational parameters used to calculate power requirements, capital costs, and operating costs.

Parameter	Value	Units
Average Hydraulic Residence Time	4	days
Channel Width	30	m
Channel Length	630	m
Surface Area	4	ha
Water Depth	0.3	m
Freeboard Height	0.61	m
Daytime Channel Velocity	0.25	m/s
Nighttime Channel Velocity	0.2	m/s
Daytime Operation	12	hr
Nighttime Operation	12	hr
Paddlewheel Mixing Efficiency	25	%

Area 200: Utility Distribution

Anthropogenically generated CO_2 is provided by the locally operated natural gas fired power station approximately 40 miles from the proposed facility. At this distance, concentration by amine absorption is less expensive than flue gas transport. The delivered price of the concentrated CO_2 is set at $80/Mg at 40 miles (Mostertz et al. 2014). The price assumes that this farm draws from a pipeline network capable of providing 10,000 Mg/day, as this is the scale at which a pipeline system becomes economical. The amine

absorption system and pipeline are considered outside the boundary limits of the economic calculations. However, the energy impact and LCA global warming potential are considered in the energy and carbon balances. Amine extraction energy requirements were taken from literature values (Ramezan 2007, IEAGHG 2012). Pressure drop, and compressor power was calculated assuming isothermal compressible flow. Table 47 lists the parameters used as input to the model.

Table 47: Modeling inputs used to calculate the pressure drop and compressor power for the concentrated CO2 transport pipeline.

Parameter	Value	Units	Notes
Distance to CO_2 Point Source	40	Miles	
Energy consumed through MEA Regeneration	2.7	MJ/kg	IEAGHG 2012
Cost of CO_2 at 40 Miles	$80.00	USD/mt	Mostertz 2014
Peak flow of supplemental CO_2 Required	20,000	m^3/hr	Calculated by peak hourly productivity
Average flow of supplemental CO_2 Required	185,700	m^3/d	Calculated by annual average productivity
Compressor Efficiency	75%		Low range of typical efficiency (Green 2008)
Motor Efficiency	92%		NEMA Design B Criteria
Peak Compressor Power	1080	HP	Isothermal compressible flow
Average Compressor Power	172	HP	Isothermal compressible flow

CO_2 and electrical utility lines deliver utilities to their point of use throughout the facility. The design follows the comprehensive facility design previously developed and published (Lundquist 2010).

Area 300: Makeup Water Delivery

Screened wastewater is utilized to make-up water and nutrients. The characteristics of the wastewater are based on typical medium strength wastewater and are listed in Table 48.

Table 48: Water quality characteristics assumed for the influent to the facility, taken from Metcalf & Eddy 2003.

Component	Value	Units
Total Dissolved Solids (TDS)	500	mg/L
Total Suspended Solids (TSS)	210	mg/L
Total Volatile Suspended Solids (VSS)	160	mg/L
Biochemical Oxygen Demand (BOD_5)	190	mg/L
Total Nitrogen (TN)	40	mg/L-N
Total Phosphorus (TP)	7	mg/L-P

Screened wastewater is pumped from the existing public owned treatment works (POTW) to the facility's primary clarifiers at a rate of 53,500 m^3/d (14.5 MGD). Friction losses are calculated using the Darcy-Weisbach equation, with the Swamee-Jain equation used for calculating the friction factor. Pumping power is then estimated assuming an average pump efficiency of 65% and an average motor efficiency of 92%.

The clarifiers are v-shaped, in-ground units with plastic lined sides and a concrete center channel. The center channel is sloped to a sump to allow sludge pumping. The clarifiers operate with a 2-hour retention time and solids are settled at a rate of 8,027 kg/d, based on a typical value of 150 kg/1000-m^3 (Metcalf and

Eddy 2003). The settler subnatant has a solids concentration 6%, which is combined with the thickened algal biomass before dewatering by centrifugation. The supernatant of the clarifiers flows by gravity to the site make-up water distribution system. Water is distributed throughout the site via distribution canals. The water flows from the canals through gate valves to individual raceways.

Area 400: Harvesting and Dewatering

The algae settlers are V-shaped, in-ground type settlers. The effluent of five raceways feed one settler for a total of 20 settlers. Settlers have a depth of 5 m and surface dimensions of 19 m wide by 71 m long with side slopes of 1.7:1. The sides of the settlers are plastic lined, and the bottom channel of the settlers are sloped concrete with a sump on one end. This allows biomass to be continuously scraped to the sump, where the subnatant is continuously pumped to the gravity thickeners. The settlers have a 6-hour retention time and are assumed to remove 95% of the biomass. The subnatant solids concentration is 2%. 90% of the supernatant is recirculated to the raceway make-up water distribution canals. The remaining 10% of the flow is discharged to 150 ha of evaporation ponds. The residual dried solids are hauled for landfill disposal at a rate of 27.3 Mg/day.

The gravity thickeners are similarly designed to the settlers but with smaller dimensions of 14m wide, 50 m long and 3.5 m deep. The thickeners are semi-continuously batch operated with a retention time of 18 hours. Semi-continuous operation allows the biomass to settle undisturbed after which the supernatant is decanted, and the sludge is pumped to the anaerobic digesters. Supernatant is discharged into the distribution canals for recirculation back to the algae raceways. The settlers are assumed to remove 95% of the influent suspended solids, and the subnatant has a solids content of 5%. There is a total of five gravity thickeners located centrally with the centrifuges.

The biomass is further dewatered by centrifugation. Continuously operated horizontal solid wall bowl centrifuges are utilized, which are designed for dewatering of municipal and industrial wastewater sludges. The system consists of 4 centrifuges with a combined rated capacity of 50 m^3/hr. Multiple smaller centrifuges are used to accommodate fluctuations in biomass production. The biomass is dewatered to 20% AFDW for feedstock to the HTL biofuels processing system. Centrifugation was evaluated as a dewatering technology alongside screw pressing and solar drying. Centrifugation was chosen due to the level of technology maturity and lab-scale demonstration of dewatering without the need of chemical coagulants. This analysis is further detailed in the Harvesting and Dewatering Study segment of the Results section below.

Area 500: Biofuels Processing

An annual average flow of 127 mt/d AFDW biomass feeds the HTL system to produce HTL crude oil. Further refining of the crude takes place onsite to allow the reuses of nutrients and carbon dioxide in exhaust streams. The HTL system was modeled based on the parameters from the comprehensive analysis of an algae HTL system performed by Pacific Northwest National Laboratory (Jones 2014). Table 49 lists the parameters used as inputs to the MBE model for modeling.

Table 49: Hydrothermal liquefaction biofuels processing assumptions used to calculate mass balances, power requirements, and nutrient recycling streams.

Parameter	Value	Units	Notes
Peak Capacity	210	mt/d	
Average Capacity	130	mt/d	
Electrical Consumption	0.52	kW/mt/d	Jones 2014 (Most electricity is generated onsite)

Diesel Fuel Yield	122	US gal/mt	Jones 2014
Naphtha Co-product Yield	25	US gal/mt	Jones 2014
Nitrogen Recovery	90%		Jones 2014
Phosphorus Recovery	90%		Jones 2014
Carbon Recovery Aqueous Phase	9%		Jones 2014
Carbon Recovery in Exhaust	21%		Jones 2014
Natural Gas Requirement	685	MMBTU/d	Scaled from Jones 2014

The seasonality of algal biomass production creates logistical issues with the sizing of the HTL fuel conversion system. Storage of biomass during the peak system requires additional chemicals for acidification and biomass degradation. The decomposition of biomass during storage, which occurs during the warm season, can lead to fugitive greenhouse gas emissions (methane and carbon dioxide) as well. Additionally, biomass storage creates a nutrient recycle deficit during the summer months as well as a surplus during the winter months. Therefore, for the current study, a system sized to handle the peak flow of biomass is considered. HTL conversion of other waste streams can be used during the winter months to offset the cost of the oversized biofuels processing system.

Economics

Facility capital and operating costs were estimated using MicroBio Engineering's ESPE model. Raceways, storage ponds, and gravity settling ponds are designed and estimated by materials and labor. The centrifugal dewatering, biofuels production, and refining system costs were estimate based on previously published data and cost curves (Jones 2014, Loh 2007). These systems were scaled to the size of this facility using the following equation;

Equation 15: Cost scaling

$$Cost\ B = Cost\ A * \left(\frac{Capacity\ B}{Capacity\ A}\right)^{\boldsymbol{n}}$$

The cost scaling exponent, *n*, typically ranges from 0.4 to 0.9, with 0.7 being a typical value for an average process plant. A value of 0.7 was used in this estimate. All costs were adjusted to 2011 dollars using RSMeans 2015 Heavy Construction Cost Data Historical Cost Indexes. 2011 was chosen as a baseline year to align with recent NREL reports to allow easy comparison of MBSP and MFSP (ANL 2012, Davis 2016). Electrical consumption was calculated by summing pump, compressor and other equipment power requirements or by using literature values based on system capacity (Jones 2014, Ramezan 2007). The model estimates the costs of the algae growth and biofuels production system using "nth-plant" design assumptions, which is a future plant construction reflects a future facility at which point n facilities have already been successfully constructed and are in operation. This reduces inflated costs due to first-of-a-kind facility design and construction (Davis, 2016).

Total Capital Investment

The total capital investment (TCI) was computed similar to the methods outlined in Process Design and Economics of Algal Biomass, Davis et al 2016. This method was chosen to harmonize capital and finance calculations so that MFSPs can be compared. Assumptions made in the techno-economic assessment can have a large effect on the MFSP and this reduces variability between studies.

The total installed costs of the facility are divided into the 6 process areas as described in the previous section. Various factors are applied to determine additional direct costs. The direct costs are the summed to calculate Total Direct Costs (TDC). Further factors are applied to the TDC of each area to determine

the indirect costs, which are then summed to calculate Total Indirect Costs (TIC). The TDC and TIC are added together to calculate the Fixed Capital Investment (FCI). Finally, the land costs and a working capital amount of 5% of FCI are added to the FCI to calculate the Total Capital Investment (TCI).

A few differences were made in the TCI calculation to better fit this study. Site development was calculated using RSMeans 2015 values in place of an applied percentage. This calculation method resulted in much higher site development costs, which were chosen to be specific to the chosen location of the San Joaquin Valley. The areas listed as outside boundary limits (OSBL) in the Davis 2016 report are labeled as "other" here since they include some equipment that would be included inside the boundary area such as distribution piping, water storage tanks, and clarifiers. Also, biofuels processing costs are included as an additional area here and have the same applied cost factors as Area 500: Dewatering, which is identical to the Biorefinery Standard. Table 50 summarizes the applied cost factors by area.

Table 50: Indirect cost factor table adapter from Davis 2016.

Item	Description	A100 & A200	A500 & A600	A300 & A400
	Additional Direct Costs (Applied to area subtotals)			
Warehouse	Includes on-site storage of equipment and supplies.	1.2%	4%	0%
	Indirect Costs (Applied to TDC)			
Prorateable expenses	Includes fringe benefits, burdens, and insurance of the construction contractor.	4%	10%	1%
Field expenses	Consumables, small tool and equipment rental, field services, temporary construction facilities, and field construction supervision.	5%	10%	1%
Home office & construction	Engineering plus incidentals, purchasing, and construction	10.3%	20%	1%
Project contingency	Extra cash on hand for unforeseen issues during construction.	10%	10%	10%
Other costs	Start-up and commissioning costs; land, rights-of-way, permits, surveys, and fees; piling, soil compaction/dewatering, and unusual foundations; sales, use, and other taxes; freight, insurance in transit and import duties on equipment, piping, steel, and instrumentation; overtime pay during construction; field insurance; project team; and transportation equipment, bulk shipping containers and plant vehicles.	10%	10%	1%

The following sections summarize the methods and assumptions used to calculate each functional area.

Area 100: Production Ponds

Production pond construction and material costs were estimated primarily using RSMeans 2015 values as well as vendor quotations. Table 51 summarizes the major assumptions made in this cost estimation.

Table 51: Cost assumptions used to calculate capital costs associated with the raceway production pond construction.

Name	Value	Units	Source
HDPE Plastic Liners	$4.00	/m^2	Vendor Provided Quote
Fine Grading	$4.68	/m^2	RSMeans 2015 scaled to 2011 USD
Compaction	$0.22	/m^2	RSMeans 2015 scaled to 2011 USD
Paddle Wheels	$30,525	ea.	MBE fiberglass paddle quotation
Concrete for Paddle Wheel Stations and CO_2 Sumps	$278	/m^3	RSMeans 2015 scaled to 2011 USD

The majority of the raceway construction cost is due to fine grading and liners. The cost is substantially reduced by the assumption that ~75% of the raceway pond bottom can be unlined by utilizing native clay soils. Liner is provided at raceway bends to prevent erosion. Table 52 summarizes the raceway construction cost calculation.

Table 52: Calculation summary of capital costs for Area 100.

Description	Qty	Unit	Unit Rate	Total
Raceway Fine Grading	400	ha	$46,806	$18,691,151
Raceway Liner Trenching	156000	m	$3.18	$496,844
Raceway Compaction	400	ha	$2,220	$886,537
Raceway Liner	1236126	m^2	$4.00	$5,249,243.82
Raceway Paddle Wheels	100	ea.	$30,525	$3,052,540
Raceway Concrete for Paddle Wheel Stations and CO2 Sumps	5300	m^3	$278	$1,470,769
			Subtotal	$29,847,084

Area 200: Utility Distribution

The utility distribution cost calculation was based on previously published work (Lundquist 2010). The cost of utilities was scaled on a per hectare basis. Table 53 summarizes the total utility distribution costs.

Table 53: Area 200 capital cost calculation based on the detailed design of an algae raceway farm in Lundquist 2010.

Description	Qty	Unit	Unit Rate	Total
CO_2 Distribution	400	ha	$6,370	$2,543,686
Electrical Distribution	400	m	$20,171	$8,055,066
			Subtotal	$10,598,693

Area 300: Make-up Water Storage and Delivery

Storage, primary treatment, and distribution of make-up water to raceway ponds are accomplished using a system of lined ponds and canals. Construction and material costs were estimated using RS MEANS 2015 values and vendor quotations. Major assumptions for this estimation are summarized in Table 54.

Table 54: Cost assumptions made for the calculation of make-up water storage and delivery capital costs.

Name	Value	Units	Source
HDPE Plastic Liners	$4.00	/m^2	Vendor Provided Quote
Fine Grading	$4.68	/m^2	RSMeans 2015 scaled to 2011 USD
Excavation	$8.24	/m^3	RSMeans 2015 scaled to 2011 USD
Compaction	$0.22	/m^2	RSMeans 2015 scaled to 2011 USD
24-inch Make-up Water Piping	$207,895	/km	RSMeans 2015 scaled to 2011 USD
Gate Valves	$648	ea.	RSMeans 2015 scaled to 2011 USD
Concrete	$278	/m^3	RSMeans 2015 scaled to 2011 USD
Sludge Scraper	$31,849	ea.	Vendor Provided Quote
Sump Station	$26,541	ea.	Vendor Provided Quote
Weirs	$21,233	ea.	Vendor Provided Quote

Pipe work and excavation have the highest contribution to the total cost. The in ground lined pond type of primary settler chosen here has been successfully used for decades at Delhi, CA as well as many other sites and significantly less costly than conventional concrete primary clarifiers. Table 55 summarizes the total cost of the make-up water system.

Table 55: Calculation summary of capital costs for Area 300.

Description	Qty	Unit	Unit Rate	Total
Distribution Canal Excavation	19500	m3	$8.24	$160,716
Distribution Canal Fine Grading	19500	m2	$4.68	$91,271
Distribution Canal Compaction	19500	m2	$0.22	$4,329
Distribution Canal Liner	19500	m2	$4.25	$82,807
Distribution Gate Valves	100	ea.	$648	$64,751
24-inch Source Water Pipework (PVC)	1.64	km	$207,895	$340,812
Primary Clarifier Excavation	21693	m2	$8.24	$178,787
Primary Clarifier Fine Grading	2667	m2	$4.68	$12,482
Primary Clarifier Compaction	2667	m2	$0.22	$592
Primary Clarifier Trenching	696	m	$3.18	$2,215
Primary Clarifier Liner	2667	m2	$4.25	$11,324
Primary Clarifier Concrete	111	m3	$278	$30,873
Primary Clarifier Sludge Scraper	2	ea.	$31,849	$63,698
Primary Clarifier Sump Stations	2	ea.	$26,541	$53,082
Primary Clarifier Weirs	2	ea.	$21,233	$42,465

	Subtotal	$1,140,205

Area 400: Harvesting and Dewatering

The first step of the dewatering is constructed of lined settling ponds similar nearly identical in construction to the primary clarifiers described in Area 300. The recirculation pumps that return the supernatant from gravity harvesting are included in this section as well. Further dewatering to 20% AFDW, as required for HTL processing, is accomplished by centrifugation. Cost for this system was scaled based on a publicly available technical memorandum (Perinpanayagam 2013) of a 30 MGD wastewater sludge dewatering system. Cost was scaled based on the flow. For the algae facility flow capacity value, the combined influent and recirculation flow (93.5 MGD) was used since 90% of the flow post harvesting is recirculated. Table 56 summarizes the cost of the dewatering systems.

Table 56: Calculation summary of capital costs for Area 400.

Description	Qty	Unit	Unit Rate	Total
Settler Excavation	75508	m2	$8.24	$622,327
Settler Fine Grading	38476	m2	$4.68	$180,090
Settler Compaction	38476	m2	$0.22	$8,542
Settler Trenching	4292	m	$3.18	$13,671
Settler Liner	34835	m2	$4.25	$147,927
Settler Concrete	783	m3	$278	$217,359
Settler Sludge Scraper	20	ea.	$31,849	$636,979
Settler Sump Stations	20	ea.	$26,541	$530,816
Settler Weirs	20	ea.	$21,233	$424,653
Settler Recirculation Pumps	40	ea.	$35,613	$1,424,519
Thickener Excavation	5413	m2	$8.24	$44,614
Thickener Fine Grading	3988	m2	$4.68	$18,668
Thickener Compaction	3988	m2	$0.22	$885
Thickener Trenching	641	m	$3.18	$2,042
Thickener Liner	3467	m2	$4.25	$14,723
Thickener Concrete	159	m3	$278	$44,196
Thickener Sludge Scraper	5	ea.	$31,849	$159,245
Thickener Sump Stations	5	ea.	$26,541	$132,704
Thickener Weirs	5	ea.	$21,233	$106,163
Centrifuge system	93.5	MGD	-	$2,834,102

Description	Qty	Unit	Unit Rate	Total
			Subtotal	$7,564,226

Area 500: Biofuels Processing

The capital costs of the HTL processing and biofuels refining systems were all scaled based on values provided in Jones 2014. The system was sized to accommodate peak flows of biomass during the summer months as previously described. Table 57 summarizes the biofuels processing cost calculation.

Table 57: Calculation summary of capital costs for Area 500.

Description	Qty	Unit	Unit Rate	Total
HTL Oil Production	209	mt/day	$101,800,000	$27,739,829
CHG Water Treatment	209	mt/day	$81,400,000	$22,180,963
HTL Oil Upgrading	209	mt/day	$24,700,000	$6,730,587
Hydrocracking	209	Mg/day	$5,700,000	$1,553,212
Hydrogen Plant	209	Mg/day	$28,600,000	$7,793,311
Steam Cycle	209	Mg/day	$3,600,000	$980,976
Balance of Plant	209	Mg/day	$6,800,000	$1,852,955
			Subtotal	$68,831,834

Summary of Total Capital Investment Calculation

As previously described, cost factors are applied to the subtotals of the functional areas to calculate total direct cost, total indirect costs, fixed capital investment, and finally total capital investment. This calculation is summarized in Table 58.

Table 58: Total Capital Investment (TCI) calculation worksheet.

Process Area	Cultivation	Dewatering and Biofuels Processing	Other	Total Installed Cost (TIC)
Area 100: Production Ponds	$29,847,084			$29,847,084
Area 200: CO_2 & Electrical Distribution			$10,598,693	$10,598,693
Area 300: Make-up Water			$1,140,205	$1,140,205
Area 400: Dewatering		$7,564,226		$7,564,226
Area 500: Biofuels Processing		$68,831,834		$68,831,834
Subtotals	$29,847,084	$76,396,061	$11,738,897	$117,982,042
Warehouse	$358,165	$3,055,842	$0	$3,414,007
Site Development	$4,580,243	$4,580,243	$4,580,243	$13,740,728
Total Direct Costs (TDC)	$34,785,492	$84,032,146	$16,319,140	$135,136,777
Prorateable Expenses	$1,391,420	$8,403,215	$163,191	$9,957,826
Field Expenses	$1,565,347	$8,403,215	$163,191	$10,131,753
Home Office & Construction Fee	$3,582,906	$16,806,429	$163,191	$20,552,526
Project Contingency	$3,478,549	$8,403,215	$1,631,914	$13,513,678
Other Costs (Start-up, permits, etc.)	$904,423	$8,403,215	$163,191	$9,470,829
Total Indirect Costs (TIC)	$10,922,644	$50,419,287	$2,284,680	$63,626,611
Fixed Capital Investment (FCI)	$45,708,136	$134,451,433	$18,603,819	$198,763,389
Land				$10,697,740
Working Capital (5% of FCI)				$9,938,169
Total Capital Investment (TCI)				$219,399,299

Financing

This analysis assumed that the facility would be 20% equity financed at a rate of 5% over a term of 20 years. A detailed analysis including an initial construction period where only interest is paid on the borrowed amount was not deemed necessary for the level of detail of the TCI estimate. Table 59 summarizes the financing and repayment calculation.

Table 59: Calculation summary of the bond repayment.

Financing	
Capital Required	$219,399,299
Percentage of Capital financed by debt	80%

Percentage of Capital financed by equity	20%
Equity	$43,879,860
Total Borrowed	$175,519,439
Bond Length (yr.)	20
Interest Rate	5%
Bond Repayment	$14,084,134

Depreciation

A simple straight-line depreciation calculation was performed to calculate equipment depreciation expenses. The salvage value of the equipment was set to zero. No interest was accumulated on the initial depreciation expense, and no tax deductions were calculated. This simplified analysis provides a transparent calculation that conservatively over estimates the actual costs. Table 60 summarizes the depreciation calculation.

Table 60: Calculation summary of depreciation costs. Straight-line depreciation with no salvage value was used for simplicity and transparency.

Item	Capital Expense	Useful life	Depreciation/year
Area 100: Production Ponds	$29,847,084	20	$1,492,354
Area 200: CO_2 Delivery	$10,598,693	15	$706,580
Area 300: Make-up Water	$1,140,205	15	$76,014
Area 400: Dewatering	$7,564,226	15	$504,282
Area 500: Biofuels Processing	$68,831,834	15	$4,588,789
Roads	$1,145,719	15	$76,381
Warehouse	$3,414,007	20	$170,700
Fencing	$339,812	15	$22,654
		Depreciation Expense	$7,637,754

Variable Operating Costs

Variable operating costs are costs that will vary throughout the seasons due to the variable productivity of the algae. These costs include CO_2, electricity, natural gas, chemicals, and solids hauling. In addition to the variability of the algal productivity, electrical costs vary seasonally due to peak generation costs during the summer. Also, as noted earlier, the hydraulic retention time of the raceway ponds will vary seasonally, which affects the recirculation water pumping power. Operating costs are provided as annual averages for simplicity. Operating costs were calculated based on an annual average productivity of 33 g/m^2-d. Variable operating costs for the biofuels production were scaled from literature values (Jones 2014) based on system capacity with a scaling factor of n=0.7. Variable operating costs are summarized below in Table 61.

Table 61: Calculation summary of variable operating costs.

Description	Value	Units	Unit Rate	Total Cost
Make-up Water Pumping	3,178,324	kWh	$0.120	$381,717
Primary Clarifier and Pumping	62,714	kWh	$0.120	$7,532
Raceway Mixing	7,418,892	kWh	$0.120	$891,009

Settler Harvesting and Pumping	5,371,758	kWh	$0.120	$645,148
Thickener Harvesting	221,700	kWh	$0.120	$26,626
Biofuel Processing	581,547	kWh	$0.120	$69,844
Natural Gas				$1,275,982
Catalysts and Chemicals				$1,643,310
Solids Hauling	9,969	Mg	$30	$299,069
CO2	90,948	mt	$80.00	$7,275,834
Total Variable OPEX				$12,516,070

Fixed Operating Expenses

Fixed operating expenses are expenses that occur regardless of the seasonal productivity variation. These expenses include labor, overhead, depreciation, property insurance & taxes, and maintenance. Labor rates were taken from Davis et al 2016, which were sourced from the Bureau of Labor Statistics. The labor rates for engineers, supervisors, operators, and technicians were simplified by taking averages of the role specific rates given in the 2016 Davis report, and full-time equivalent quantities were generally scaled down linearly and rounded up to the nearest whole number. Equipment maintenance at 3% of FCI was based on the higher end of the range for mature fossil fuel technology (Short 1995). This is considered to be conservative given that a large portion of the FCI is liner and excavation costs. However, there are considerable unknowns of maintaining a facility of this scale. An additional labor burden of 90% is applied to the salary total to account for overhead expenses such as safety, general engineering, general plant maintenance, payroll overhead (including benefits), plant security, janitorial and similar services, phone, light, heat, and plant communications (Davis 2016). Table 62 and Table 63 summarize the computation of fixed operating expenses.

Table 62: Summary of the salaries and positions of staff at the algae biofuels production facility. Adapted from Davis 2016.

Position	Salary	Source
Plant Manager	$155,400	2016 Davis NREL based on BLS data
Plant Engineer	$82,590	Average of engineers, 2016 Davis NREL, based on BLS data
Lab Manager	$59,200	2016 Davis NREL based on BLS data
Plant Supervisor	$55,500	Average of supervisors, 2016 Davis NREL, based on BLS data
Plant Technician	$42,286	2016 Davis NREL based on BLS data
Plant Operator	$36,482	2016 Davis NREL based on BLS data
Clerks and Secretaries	$38,057	Average of operators, 2016 Davis NREL, based on BLS data

Table 63: Calculation summary of fixed operating costs.

Description	Qty	Unit	Unit Rate	Total
Plant Manager	2	ea.	$155,400	$310,800
Plant Engineers	3	ea.	$82,590	$247,769
Lab Manager	1	ea.	$59,200	$59,200
Plant Supervisors	5	ea.	$55,500	$277,500
Plant Operators	18	ea.	$36,482	$656,676

Plant Technicians	5	ea.	$42,286	$211,430
Clerks & Secretaries	5	ea.	$38,057	$190,285
Labor Burden (90%)				$1,758,293
Depreciation				$7,637,754
Property Insurance & Tax (0.7% of FCI)				$1,391,344
Equipment Maintenance (3% of FCI)				$5,962,902
Total Fixed OPEX				$18,703,952

Cash Flow Analysis

A simplified cash flow analysis was performed in this study to estimate the MFSP. Due to level of variability in the TEA, a more detailed analysis does not add value. Instead, conservative estimates were made to estimate reasonable cash flow from an n^{th} plant scenario.

The internal rate of return (IRR) for the project was set to 20% with a plant life time assumed to be 30 years. The IRR was increased from the BETO standard of 10% (Davis 2016) to account for corporate taxes, technology leasing, and other "costs of doing business" that are not accounted for in this simplified analysis. The required net cash inflow to achieve an IRR of 20% was back calculated using the following formula.

Equation 16: Net present value

$$NPV = \sum_{t=1}^{N} \frac{C_t}{(1+r)^t} - C_0 = 0$$

Where;

$$C_0 = Initial\ investment\ costs$$

$$C_t = Net\ cash\ inflow\ during\ period\ t$$

$$r = discount\ rate\ (equal\ to\ IRR\ when\ NPV = 0)$$

$$T = number\ of\ time\ periods$$

A 6-month start-up period was assumed where no revenue was generated. The cash flow equation was modified as follows:

$$\sum_{t=2}^{30} \frac{C_t}{(1+0.2)^t} + \frac{0.5C_1 - 0.5(OPEX + Bond\ Repayment)}{(1+0.2)^1} + -C_0 = 0$$

The equation was solved iteratively in MS Excel using the goal seek function to calculate the required cash inflow. A summary of the cash flow analysis is given in Table 64.

Table 64**: Summary of cash flow analysis calculation.**

Description	Value
IRR	20%

Plant Life	30 years
NPV	$0.00
Start-up Time	6 months
Revenue During Start-up	25%
Net Cash Inflow Required	$17,493,718
Bond Repayment	$14,084,134
Variable Operating Costs	$12,516,070
Fixed Operating Costs	$18,703,952
Total Cash Inflow Required	$62,797,874

Additional Revenue

Besides the revenue provided from biofuels sales, the envisioned facility will have two coproducts: naphtha from the refining of HTL biocrude and wastewater treatment. The naphtha coproduct yield and selling price of $3.24/gallon was based on previously published modelling (Jones 2016). The facility will reduce loading on the connected POTW, which will in turn reduce operating costs and/or replace the need to expand the existing POTW due to population growth. A revenue stream of $2,406 per million gallons treated, based on a national average for wastewater treatment operations and maintenance costs (NACWA 2015), is assumed. The flow to the facility varies seasonally due to varying of evaporation and precipitation, so as with operating costs, an annual average value was calculated to compute waste water revenue.

In addition to wastewater revenue and fuel sales, the facility would also collect revenue from the US EPA Renewable Identification Numbers (RINs) as part of the Renewable Fuel Standard Program (RFS) as well as credits from California's Low Carbon Fuel Standard (LCFS) program. Values were taken from the summer of 2016 and converted to 2011 dollars based on the energy unit of MMBTU using the higher heating value of diesel fuel at 45.8 MJ/kg. These credits are traded on government run markets and are historically highly variable in price. In addition, these credits would be collected at any biofuels facility. Therefore, their value here is not for comparison to other reports, but rather to show that the selling price of the fuel could be reduced substantially to make the product more competitive with conventional fossil fuels. Revenue sources are summarized in Table 65.

Table 65: Summary of revenue streams from potential co-products and carbon credit markets.

Revenue Source	Unit Value	Units	Unit Rate	Total Value
Wastewater Revenue	5,161	MG WWT	$4,054	$12,416,242
Naphtha Co-product	1,165,427	Gallons	$3.25	$3,787,637
LCFS Credits	776,935	MMBTU	$5.46	$4,240,176
RIN Credits	776,935	MMBTU	$8.55	$6,639,829
			Total	$27,083,887

Life Cycle Assessment

Life cycle assessment (LCA) is a comprehensive, structured, and standardized method to quantify the environmental impacts of goods and services. The assessment considers the full life cycle of a product from resource extraction from the environment to final use and disposal (European 2010). The following sections outline the analysis of the biodiesel blendstock product produced from the envisioned facility described in previous sections.

Goal and Definition

The focus of this LCA is on GHG emissions. Therefore, this analysis only is a streamlined GHG emission LCA as opposed to a full environmental impact LCA, which analyzes multiple impact factors such as those defined by the United States Environmental Protection Agency (US EPA) Tool for Reduction and Assessment of Chemicals and Other Environmental Impacts (TRACI). The goal of the assessment is to identify the reduction of CO_2 emissions compared to conventional diesel fuel. This methodology is like the standardized methodology required by the US EPA's Renewable Fuel Standard (RFS) and the California Air Resources Board (ARB) for qualification to participate in low carbon fuel credit markets. These markets are necessary for biofuel producers to be competitive with conventional fossil fuel producers.

A consequential life cycle assessment is considered for this study, which addresses the impacts of the produced products and coproducts will have on other markets. The effect on other markets is the specific intent of programs such as California's Low Carbon Fuel Standard, which assumes a reduction of carbon emissions due to the reduction of demand for fossil fuels when biofuels are introduced to the market. Coproducts are treated similarly, but to avoid complicated allocation schemes, system expansion with product displacement is used. In this method, the GHG emissions of the given coproduct are subtracted from the GHG emissions due to production of the biodiesel product.

In addition to the GHG emissions impact, a net energy ration (NER) is presented. This is defined as the energy in the biofuel product divided by the energy consumed by the production. Similar to the system expansion with product displacement method, a credit is taken for the coproducts of the facility. Wastewater treatment is based on literature values for conventional wastewater treatment and the higher heating value is used for naphtha.

Scope Definition

This assessment is performed by modeling the presented biomass production and biofuels processing systems to identify all inputs and outputs of these systems. Modeling of inputs and outputs to this model, such as electricity and waste disposal, are outside of the scope of this document. Instead, the GHG emissions of these inputs are taken from comprehensive studies already performed by subject matter experts in their relative fields. The GHG emissions of the process is normalized to the functional unit of grams of CO_2 equivalent per megajoule of fuel consumed for transportation ($gCO_{2\text{-}eq}/MJ$). The emissions from the combustion of the fuel are included in this analysis, and therefore consider the efficiency of various engine types (i.e. spark plug versus compression ignition). This functional unit standard for the approval of RFS and LCFS biofuel pathways and is therefore used as opposed to km traveled or km-person transported. The system boundaries for the present LCA are shown in Figure 123.

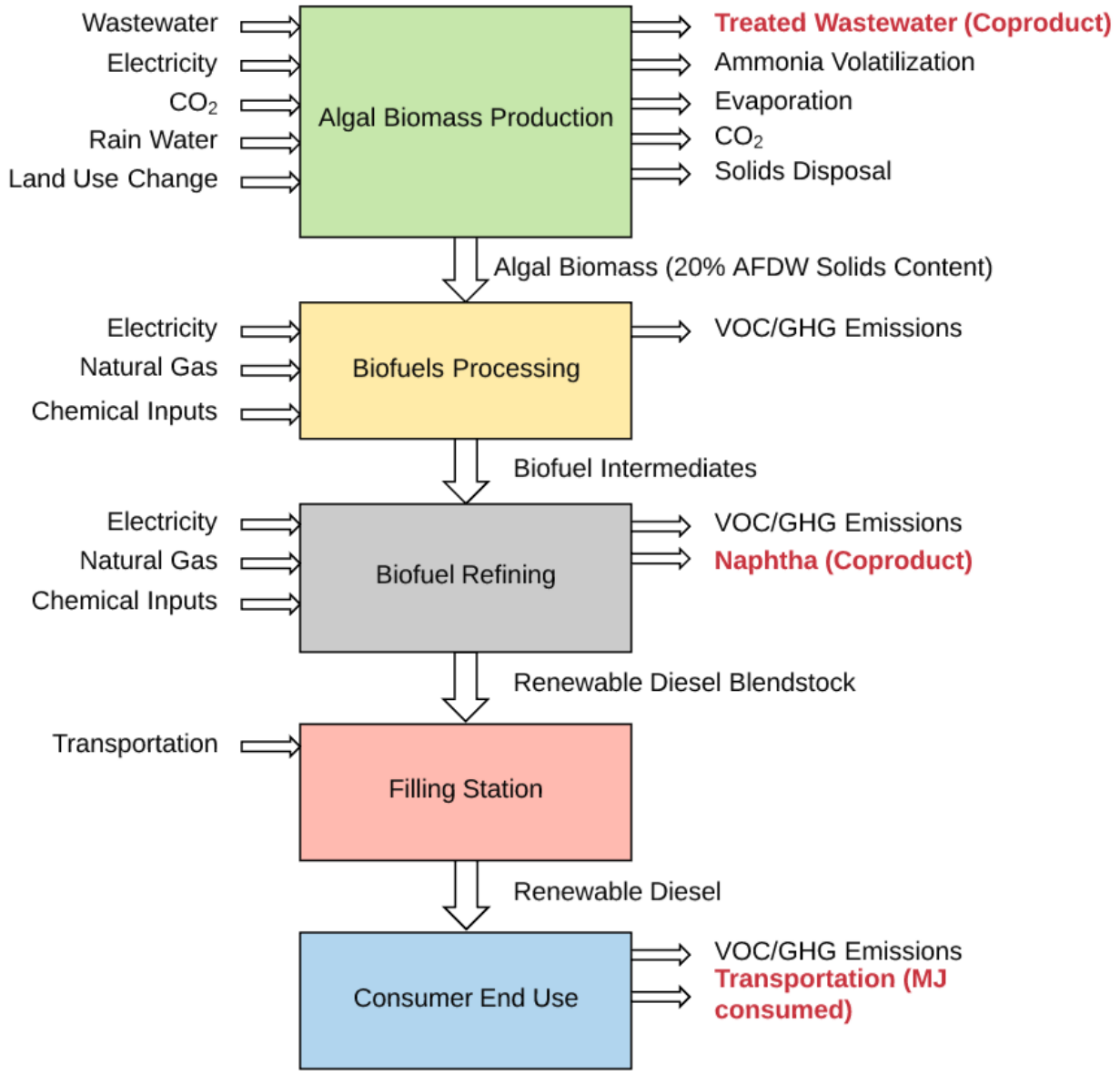

Figure 123: A system boundary diagram of the algal biofuels production facility analyzed in the life cycle assessment. Inputs enter at the right of the diagram while outputs and products exit the left side. Products and co-products are showed in bold, red text.

Life Cycle Inventory

As noted in the goal and definition section, literature values are used for most of the inputs and outputs of the system. GHG emissions and energy values of inputs and outputs are listed in Table 66.

Table 66: Data and assumptions used as inputs and outputs to the LCA calculation are listed.

Description	Value	Units	Comment Source
Calif. grid electricity (ELC002)	105.16	gCO_{2eq}/MJ_e	ARB ELC 2014
US Land Use Change	136	kg $CO_{2\text{-}eq}$/ha	ecoinvent 3.3, IPCC 2013 100 year

Natural Gas	0.355	kg $CO_{2\text{-eq}}/m^3$	ecoinvent 3.3, IPCC 2013 100 year
Natural Gas Heat Content	1020	Btu/ft^3	EIA
Wastewater volume treatment emission factor	0.14	kg CO_{2eq}/m^3	ecoinvent 3.3
Wastewater flow treatment energy use intensity	10,000	MMBTU/MGD	EPA Energy Star
Naphtha	0.589	$kgCO_{2\text{-eq}}/kg$	ecoinvent 3.3 model/IPCC 2013 100 year
Naphtha HHV	48.1	MJ/kg	Biomass Energy Data Book 2011
ULSD tank to wheels	74.86	$gCO_{2\text{-eq}}/MJ$	ARB ULSD 2014
ULSD Transport to Bulk/Filling Stations	0.35	$gCO_{2\text{-eq}}/MJ$	ARB ULSD 2014
ULSD Transport to Bulk/Filling Stations, Energy	4271	J/MJ	ARB ULSD 2014
ULSD GHG emissions	102.82	$gCO_{2\text{-eq}}/MJ$	ARB ULSD 2014

A system model for the CO_2 extraction and compression system was created separately because literature values for GHG emissions and energy intensity specifically were not found. The process was modeled using values as provided by the US National Energy Technology Laboratory in the comprehensive study *Carbon Dioxide Capture from Existing Coal-fired Power Plants* (Ramezan 2007). These values were used as inputs to model using openLCA software and the ecoinvent 3.3 LCI database. Inputs and outputs and results of the model are shown in Figure 124 with values presented in Table 67. Using the IPCC 2013 100-year life cycle impact assessment methods, this modeling resulted in GHG emissions of 0.319 kg $CO_{2\text{-eq}}/kg\ CO_2$ captured and compressed for transportation.

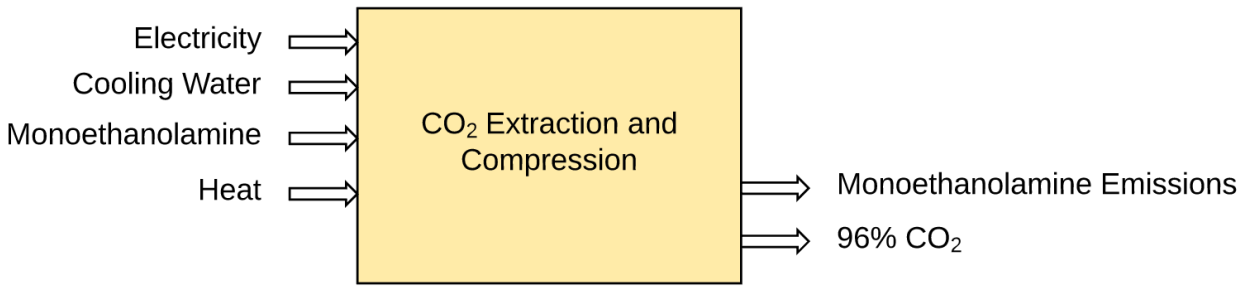

Figure 124: System boundary diagram for the modeled amine-based CO_2 concentration system.

Table 67: Summary of inputs and GHG conversion factors for the modeled amine CO_2 concentration system.

Description	Value	Units	Comment Source
Electricity (input)	0.15	kWh/kg CO_2	ecoinvent 3.3, market group for electricity, US
Cooling water (input)	0.046	$m^3/kg\ CO_2$	ecoinvent 3.3

Monoethanolamine (input)	0.0033	kg/kg CO_2	ecoinvent 3.3, global market group
Heat (input)	2.7	MJ/kg CO_2	ecoinvent 3.3, natural gas combined cycle power plant
Monoethanolamine emissions (output)	0.0033	kg/kgCO_2	ecoinvent 3.3
Capture CO_2 (reference flow)	1	kg CO_2	

Similarly, the GHG emissions impact due to solids disposal for material remaining in the blowdown evaporation beds was modeled using openLCA. Figure 125 shows the boundaries of this model, while Table 68 lists the input values. Using the IPCC 2013 100 yr. LCIA methods, the result is 0.00735 $kgCO_{2\text{-}eq}$/kg

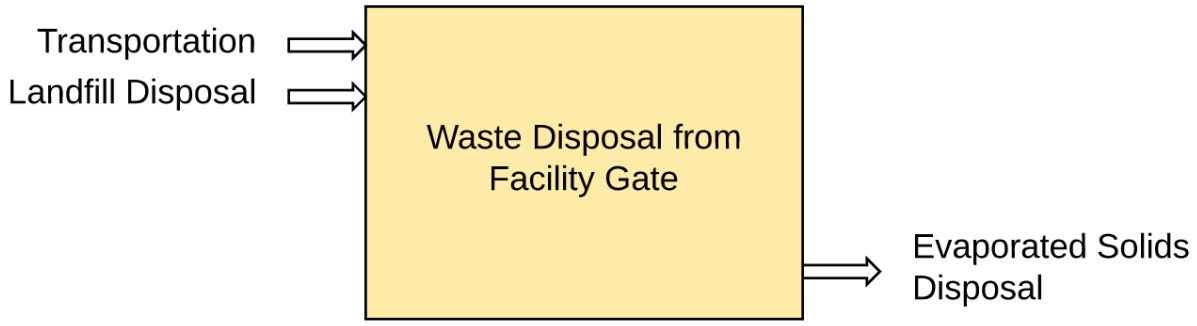

Figure 125: System boundary diagram for the modeled solids disposal process.

Table 68: Summary of inputs and GHG conversion factors for the modeled solids disposal process.

Description	Value	Units	Comment Source
Transport	0.032	mt-km	ecoinvent 3.3, freight, lorry, unspecified
Landfill disposal	1	kg	ecoinvent 3.3, process-specific burdens, residual material landfill
Disposed solids (reference flow)	1	kg solids	

Volatile organic compound (VOC) and greenhouse gas (GHG) fugitive emissions are assumed to be emitted from the biofuels processing and refining facilities. However, since a full-scale system does not exist and data for these emissions is limited, they are assumed to be below the typical cut-off point for LCA of 1%. Ammonia volatilization is present in the model; however, this does not contribute to GWP. Similarly, monoethanolamine emissions do not contribute to GHG emissions. These emissions are included in the boundary diagram to completeness. If a full LCA was conducted, these emissions could impact other environmental impact indicators such has toxicity or eutrophication.

Results

Engineering Model Refinement and Full-Scale Evaluation (ML5.3, 5.6; S5.0, 5.1, 5.2, 5.4, 5.5)

Harvesting and Dewatering Study

Harvesting and dewatering technologies were evaluated on an economic and environmental impact GHG emissions basis to decide the best unit processes to model for the full-scale biomass production facility. For harvesting and initial settling to ~2-3% AFDW, gravity settling processes were evaluated for a scenario with a bioflocculating algal culture with no chemical addition and a scenario with coagulant addition to a colloidal algal culture, similar to typical wastewater treatment sludge removal. Three unit processes were evaluated to concentrate the biomass to 20% AFDW; centrifugation, screw pressing, and solar drying.

Total capital investment (TCI) was calculated as previously described for each harvesting technology including indirect costs, financing, and working capital but excludes land costs. Operating expenses were calculated similar to above, but with a reduced labor cost as shown in Table 69.

Table 69: Labor rates and staff positions as used to calculate total annualized costs for the evaluation of dewatering technologies.

Description	Qty	Unit	Unit Rate	Total
Plant Engineers	0.5	ea.	$82,590	$41,295
Plant Supervisors	0.5	ea.	$55,500	$27,750
Plant Operators	4.0	ea.	$36,482	$36,482
Plant Technicians	1.0	ea.	$42,286	$84,572

Depreciation was calculated based on the TIC of the harvesting materials and equipment. The TCI and operating expenses were summed to calculate the total annualized expense of the system.

The GHG emissions contribution from the harvesting system was calculated based on the GHG emissions of the electricity consumed by the unit process as well as the GHG emissions of the coagulant. Life cycle inventory data of the algae specific coagulant used at Delhi is not available, so the GHG emissions of aluminum sulfate (a typical coagulant used in industrial and municipal wastewater treatment) was used as a surrogate. This was calculated using ecoinvent LCI data for the production of aluminum sulfate, and the US EPA TRACI 2.0 life cycle impact assessment methodology. Table 70 summarizes the results of the economic and environmental impact analysis, which indicate that the use of coagulants to concentrate biomass for biofuels production is not feasible. Therefore, a bioflocculating system is required for economic biomass production and used in the modeling of the proposed n^{th} plant facility.

Table 70: The results of the Harvesting study are summarized. The use of algae specific coagulant, as currently used at the Delhi WWTP, increase operating expenses of the unit operation by 7x. The GHG emissions contribution of the harvest and dewater step and increased 6x as well. This indicates that the use of chemical coagulants in biofuels production is not feasible.

Description	Total Capital Investment	Operating Expense	Total Annualized Expense	GHG emissions Contribution
	2011 USD	2011 USD/year	2011 USD/year	(gCO2e/MJ)
Gravity settling and thickening	$8,260,000	$1,760,000	$3,390,000	1.1
Gravity settling + thickening with coagulant	$8,260,000	$21,900,000	$23,500,000	6.6

Dewatering unit processes were evaluated using the same methodology as the harvesting technologies. Dewatering equipment installation costs for centrifuges and screw presses were scaled from literature values (Perinpanayagam, 2013). Solar drying bed costs were estimated using construction and material costs from RS MEANS 2015. Labor costs used above for harvesting were also included in the dewatering calculation, however the solar drying scenario reduced this labor to a half time supervisor, two operators, and one technician due to the simplicity of this drying method. The results of this analysis are summarized in Table 71.

Table 71: The results of the harvest dewatering study are shown below. The capital costs of each system are similar; however, the operating expense of the solar drying beds is significantly lower than screwpresses or centrifuges. The GHG emissions of the centrifuges are significantly higher than the other technologies, although the solar drying bed GHG emissions are not well understood due to the lack of information regarding potential N_2O emissions from decomposing biomass.

Description	Total Capital Investment	Operating Expense	Total Annualized Expense	GHG emissions Contribution
	2011 USD	2011 USD/year	2011 USD/year	(gCO2e/MJ)
Centrifuge	$4,950,000	$921,000	$2,340,000	0.44
Screw Press	$5,170,000	$883,000	$2,310,000	0.09
Solar Drying Bed	$4,800,000	$624,000	$2,030,000	NA

Although the results of this analysis show centrifugation has a slightly higher total annualized expense and GHG emissions impact, it was the chosen technology to be modeled for several reasons. Centrifugation of algal biomass has been demonstrated at lab scale without the use of chemical coagulants. Screw presses typically require higher doses of coagulants to have a similar solid capture rate as centrifuges in municipal wastewater treatment. Concentration of algal biomass by screw press has not been demonstrated using only bioflocculated algae. The solar drying beds used at the Delhi WWTP use an additional dewatering polymer, which adds significant operating expenses. Also, during the wets season the drying beds are not operable. This leads to decomposition of the biomass, which releases nitrogenous greenhouse gasses such as N_2O. Little if any LCI data is available to account for these emissions.

Techno-Economic Analysis

The expenses and revenue streams of the proposed facility are summarized in Table 72. These values allow the calculation of the minimum fuel selling price (MFSP) by dividing cash flow from biofuel sales required by the gasoline gallon energy equivalent of diesel blendstock produced.

Table 72: Summary of the calculation for the minimum fuel selling price of the produced diesel blendstock.

TEA Financial Summary	
Total Capital Investment	$219,399,299
Annual Bond Repayment	$14,084,134
Annual Operating Expense	$31,220,022
Annual Net Cash Inflow Required @ 20% IRR	$17,493,718
Annual WWT Coproduct Revenue	$12,416,242
Annual Naphtha Coproduct Revenue	$3,787,637
Potential Annual LCFS/RIN Credit Revenue	$10,880,005

Total Additional Revenues	$27,083,887
Cash Flow from Biofuel Sales Required	$35,713,987
Minimum Fuel Selling Price	$7.14

Several MFSP scenarios can be iterated from these values. Figure 126 shows various MFSP values depending on revenue streams.

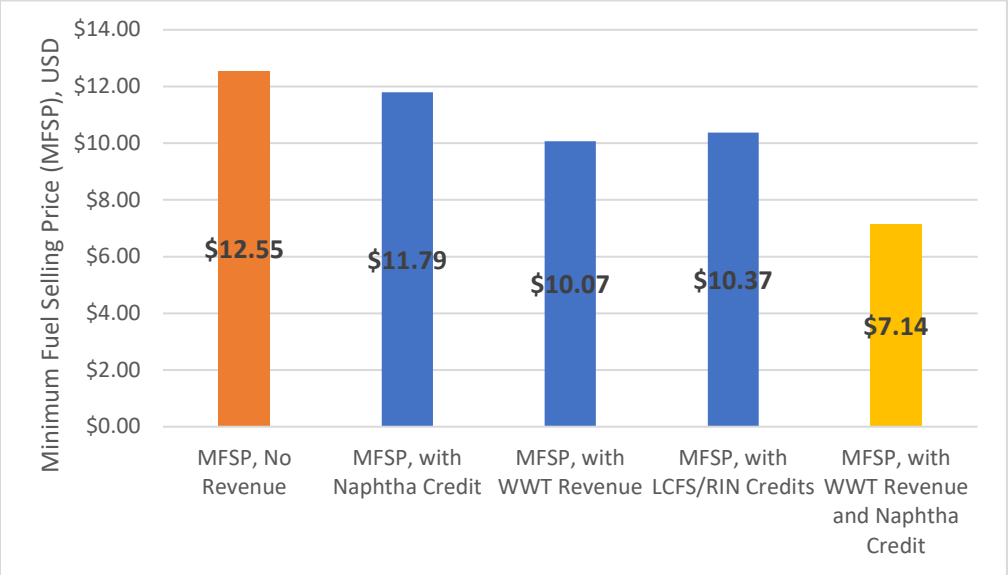

Figure 126: The MFSP of the produced diesel blendstock depends on the co-products and carbon credit revenue received. Both wastewater treatment and carbon fuel credits significantly reduce the selling price of the biofuel.

Life Cycle Impact Assessment

Since this LCA is streamlined to GHG emissions and energy only, a life cycle impact assessment (LCIA) method was not used for the entire system. The LCIA methods used for individual inputs and outputs are listed in the LCI section. Table 73 shows the summation of the individual GHG emissions and energy impacts to calculate the NER and the total GHG emissions impact.

Table 73: A summary table of the well-to-wheels calculation of the produced diesel blendstock. For comparison, the well-to-wheels emissions of CARBOB gasoline is 99.78 gCO_2e/MJ.

Source	Reference Flow Value	Reference Flow Units	Energy Required (J/MJ)	GHG Emissions (gCO2e/MJ)
Anthropogenic CO_2 Credit	71	g CO_2/MJ	-	(71.0)
Captured CO_2	71	g CO_2/MJ	447,446	35.4
Land Use Change	0.00000049	ha/MJ	-	0.00007
Biomass Production Electricity	0.02	kWh/MJ	73,914	7.77
Biofuel Processing Electricity	0.00071	kWh/MJ	2,554	0.269
Biofuel Processing NG	0.0039	m^3/MJ	150,744	1.43
Solid Waste Disposal	0.00030	kg/MJ	-	0.002
Diesel Transport and Distribution	4271	J/MJ	4,721	0.350
Wastewater Treatment Displacement Credit	0.0172	gpd/MJ	(181,957)	(3.34)
Naphtha Displacement Credit	0.0014	gallons/MJ	(172,050)	(2.11)
Total Well to Tank			**325371**	**-29.12**
Carbon in Fuel			1000000	74.10
Vehicle CH_4 and N_2O			0.00	0.76
Total Tank to Wheel			**1000000**	**74.86**
Total Well to Wheel			**1,325,371**	**45.7**

Sensitivity Analysis

The results of this analysis are highly sensitive to the assumptions made for inputs. A contribution analysis was performed to identify which variables had the highest impact on MFSP, GHG emissions, and NER. These values were then varied to see how the results of the modeling were affected. The analysis was divided into a TEA and LCA section.

Techno Economic Sensitivity Analysis

The total annualized costs of the facility are distributed across three categories as seen in Figure 127; Cash Flow, Bond Payment, Variable OPEX, and Fixed OPEX. Major contributors to these categories are identified and varied to observe the sensitivity of these assumptions to the MFSP. Results are shown in Figure 129 at the end of this section.

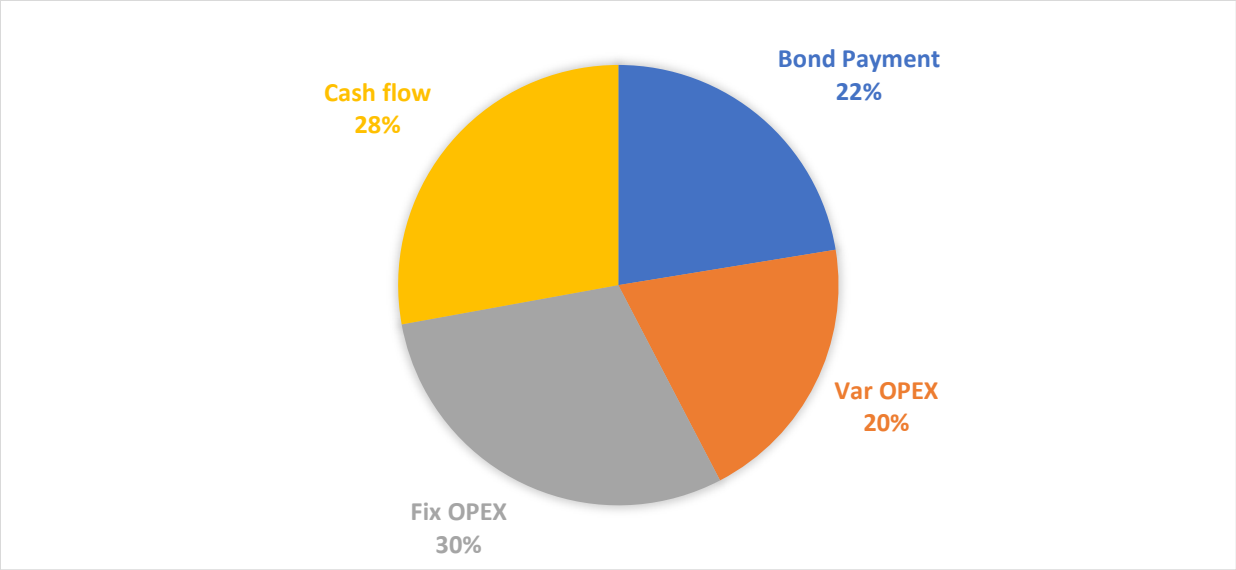

Figure 127: The pie chart above shows the distribution of total annualized cost across three categories; fixed operating expenses, cash flow, bond payment, and variable operating expenses.

Both the required cash flow and the bond payment are affected by major contributions to the total capital investment. The largest contributions are shown in Figure 128, with biofuels processing equipment and the production ponds having the highest value. These values were varied +/-50% in the sensitivity analysis. Another major assumption affecting the TCI is the use of unlined ponds. A scenario including fulling lined ponds is also evaluated.

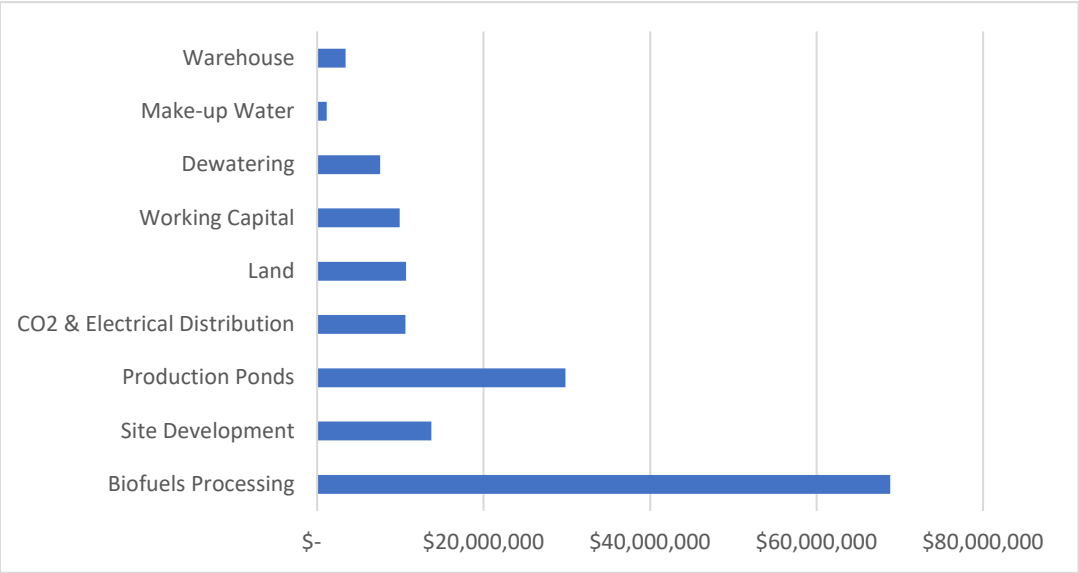

Figure 128 shows the most significant capital contributions to the bond payment category. Biofuels processing and production ponds have the largest contributions and were chosen as variables in the sensitivity analysis.

The required cash flow and bond payment categories are also affected by the assumed internal rate of return (IRR) and bond interest rate respectively. The IRR is varied from 15% to 20% while the bond interest rate is varied from 3% to 5%.

The fixed operating expense category is affected by the overall cost of labor, and the maintenance rate. The maintenance rate is varied from 1% to 5%. The overall cost of labor is varied from 75% to 125% of the calculated value.

The major contributions to the variable operating expenses are the cost of CO_2 and the cost of electricity the cost of CO_2 is varied from $40 to $120. The cost of electricity is varied from $0.08/kWh to $0.16/kWh.

Besides the economic assumptions made, the process variable having the largest impact on the MFSP is the biomass productivity. This value was varied +/-10 g/m^2-d from the experimentally demonstrated value of 33 g/m^2-d.

The selected variables were adjusted in the process model to generate the tornado chart shown in Figure 129.

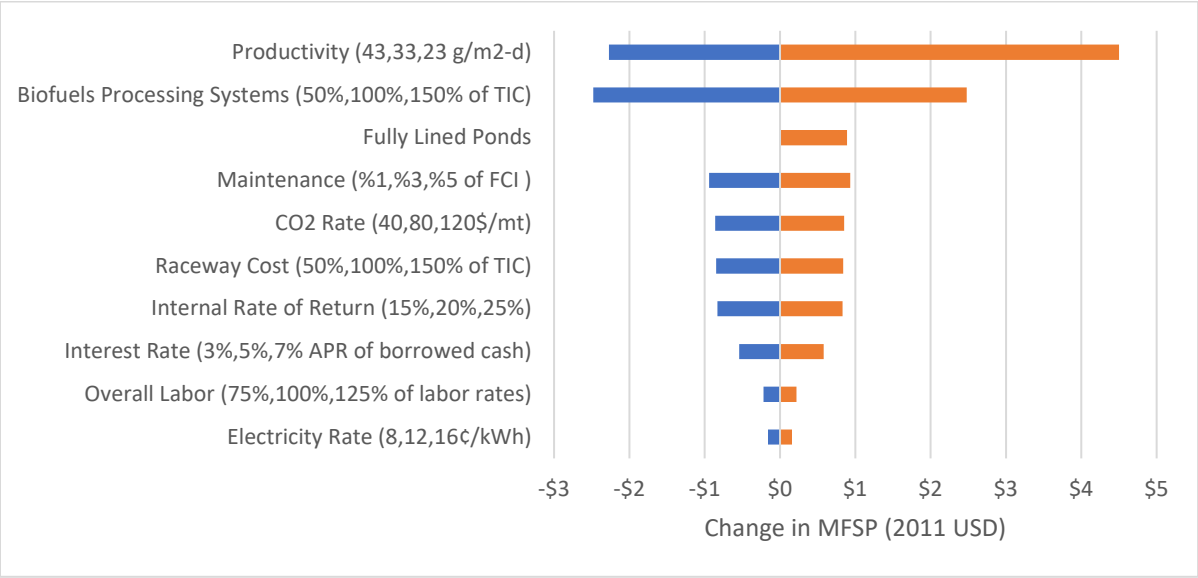

Figure 129: This tornado graph shows which variables are the most sensitive when calculating the minimum fuel selling price. Productivity values and the overall cost of the biofuels processing systems are the most sensitive.

Life Cycle Assessment Sensitivity Analysis

A contribution analysis was performed to determine the most sensitive variables affecting the GHG emissions of the diesel blendstock fuel product. The waterfall chart shown in Figure 130 indicates the major categories to be evaluated in the sensitivity analysis.

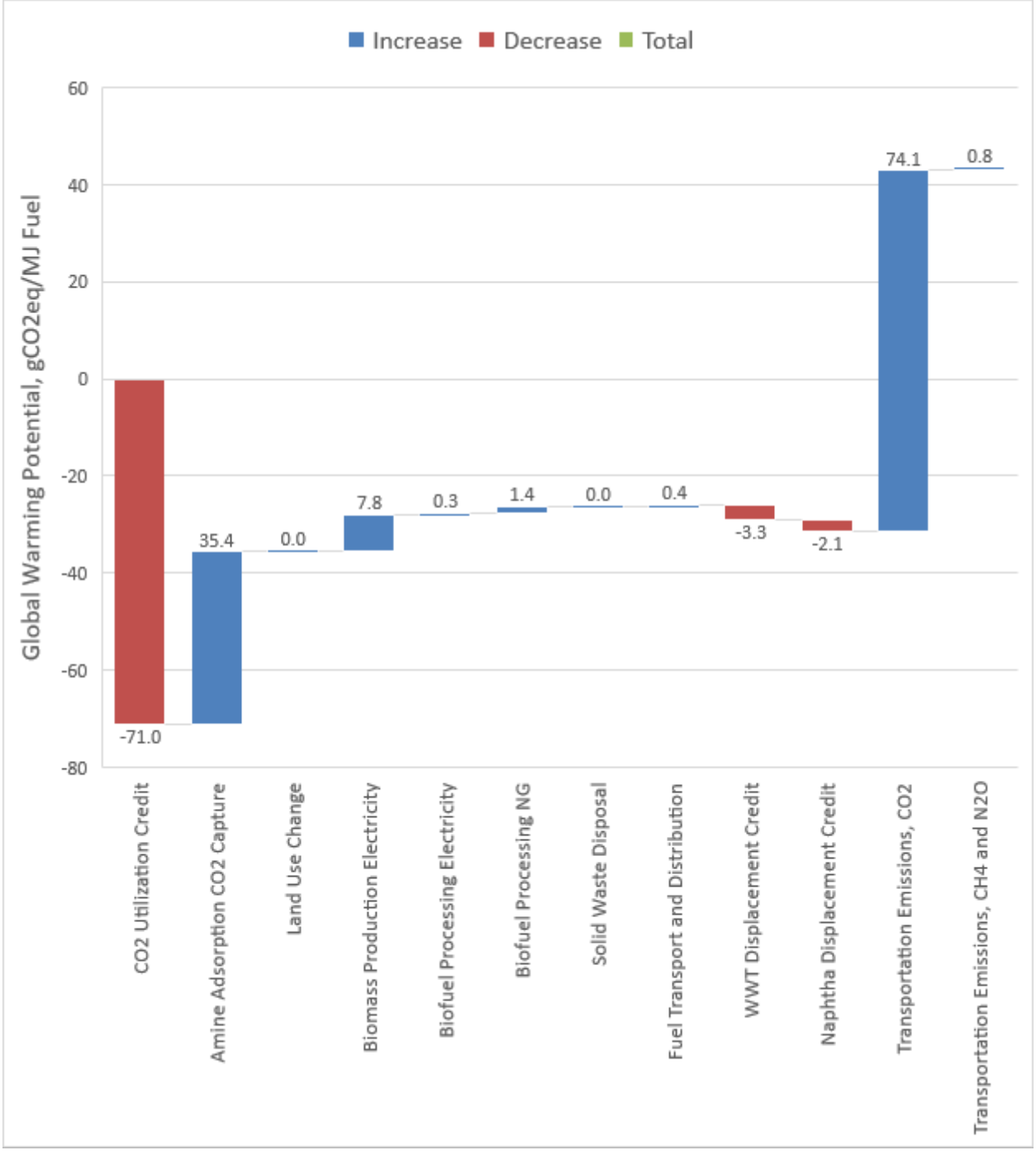

Figure 130 is a waterfall chart showing which processes have the largest contribution to the overall GHG emissions of the produced biofuel. The largest contributors were chosen to be varied in the sensitivity analysis.

Similar to the GHG emissions waterfall chart, major contributors to the NER were identified and are shown in Figure 131.

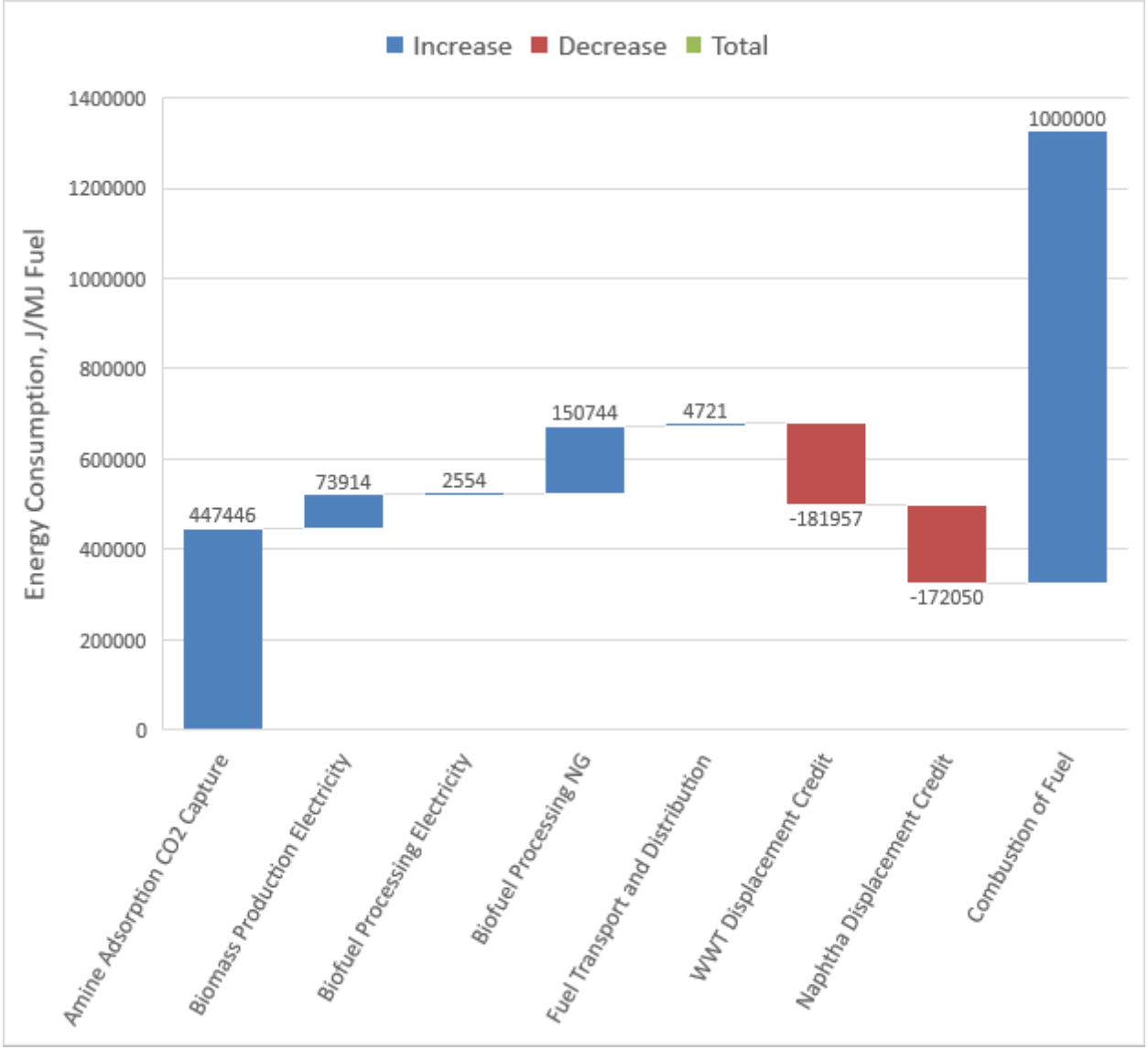

Figure 131 is a waterfall chart showing which processes have the largest contribution to the overall energy consumption of the produced biofuel. The largest contributors were chosen to be varied in the sensitivity analysis.

The variables affecting the GHG emissions typically have a similar effect on the NER. Therefore, the same variables were chosen for both GHG emissions and NER for the sensitivity analysis. The largest variable affecting both the GHG emissions and NER is the sorbent regeneration energy of the amine absorption CO_2 capture system. This value was varied +/-50% of the assumed value. The inclusion of co-product displacement credits (naphtha and wastewater treatment) also have a large affect or GHG emissions and NER, thus the removal of these credits was evaluated. The overall electrical consumption was varied +/-50%, and the removal of the electrical generation from waste steam in the biofuels processing system was evaluated as well. Lastly, similar to the MFSP, productivity is the major process variable affecting both the GHG emissions and NER. The results of the sensitivity analysis are shown in Figure 132 for GHG emissions and in Figure 133 for NER.

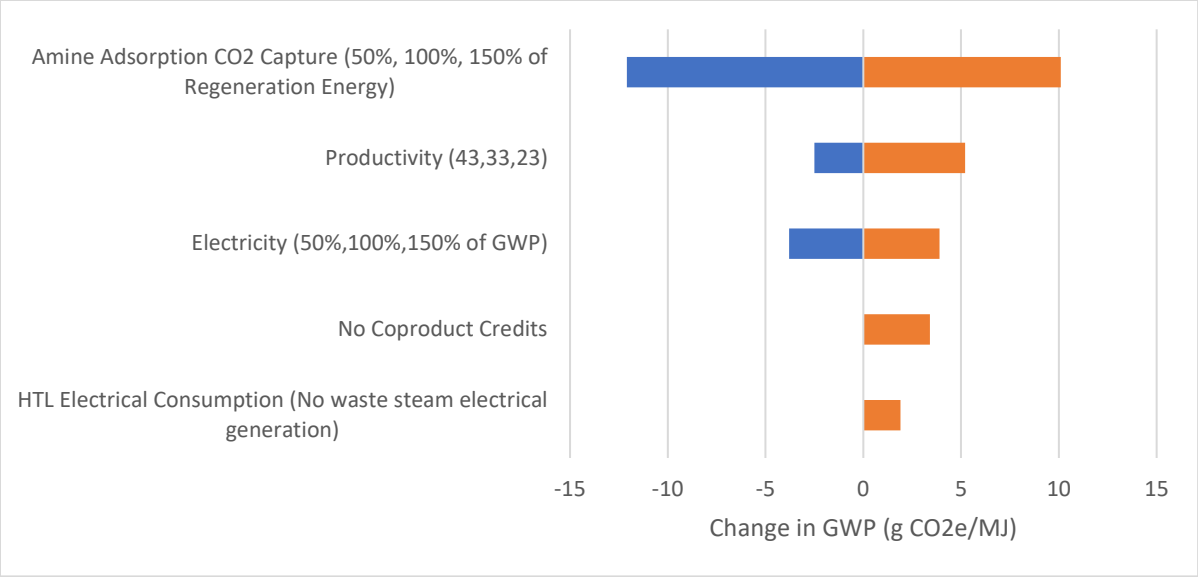

Figure 132: Tornado graph showing which variables are the most sensitive when calculating the well-to-wheels GHG emissions. The amine adsorption CO_2 capture system and biomass productivity have the greatest effect on the well-to-wheels GHG emissions.

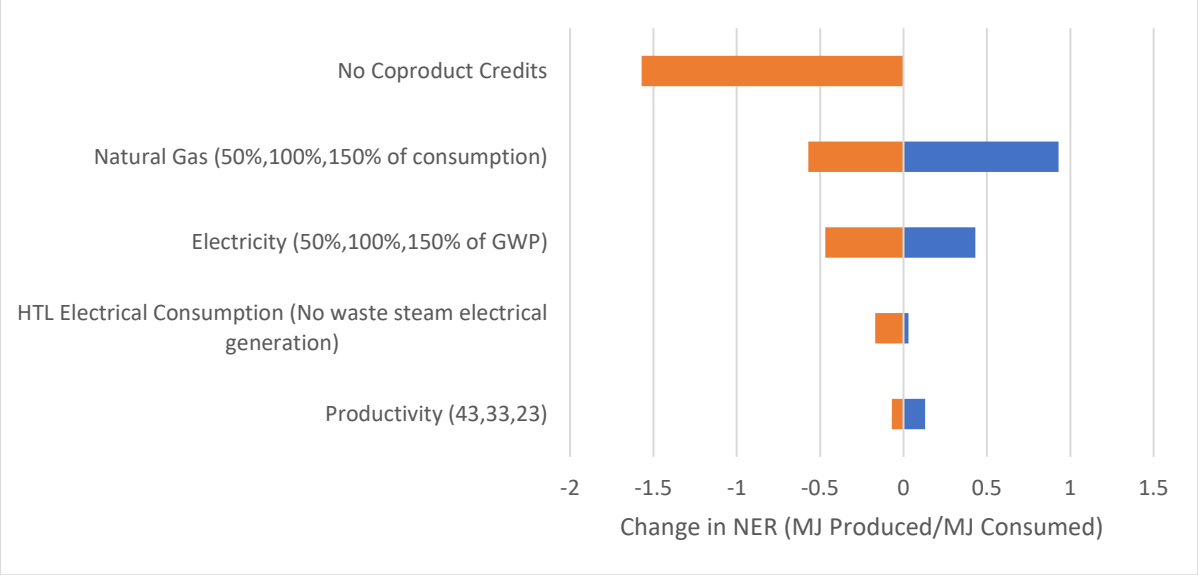

Figure 133: This tornado graph shows which variables are the most sensitive when calculating the NER. Co-product displacement credits and natural gas consumption rate have the greatest effect on the overall NER.

The sensitivity analysis shows that at the current technology readiness level, the calculated values of MFSP, GHG emissions, and NER are highly dependent on the chosen variables. Also, as expected, improvements in productivity and CO_2 capture can yield significant gains in economics and environmental impact. The results of this research are also highly dependent on the development of the HTL process.

Conclusions and Recommendations

Interpretation of Results

The results of the dewatering study indicated dewatering by centrifugation provides the best balance of economics and environmental impacts when concentrating the biomass to 20% AFDW (as required by the HTL fuel conversion process). This is primarily due to the adverse economic and environmental impacts from the addition of coagulant needed for screwpressing. Screwpressing of bioflocculated biomass without chemical addition has not yet been demonstrated and is unlikely. Drying bed technology is similar in cost but needs additional research to determine the biomass losses due to decomposition and the GHG emissions impact due to the potential release of N_2O and CH_4.

The diesel blendstock baseline MFSP of $12.55/GGE is well above the BETO goal of $3.00/GGE. However, by creating coproducts, coupling with wastewater treatment, and the addition of potential revenue from low carbon fuel credits from California and Federal programs, the MFSP is lowered to a more reasonable value of $7.14/GGE. Future work on the improvement of biomass productivity, HTL yield, and reducing the cost of CO_2 capture will bring the MFSP of this process closer to the $3.00/GGE goal.

The results of the LCA show that the renewable biodiesel product has a GHG emissions of 45.7 $gCO_{2\text{-}eq}$/MJ of fuel. This is substantially lower than the conventional ultra-low sulfur diesel GHG emissions of 102.82 $gCO_{2\text{-}eq}$/MJ (ARB 2014). In addition, the parasitic energy consumption of 325,371 J/MJ equates to a net energy ratio of 3.1, meaning slightly over 3 times the energy consumed is produced. These results suggest that this renewable diesel pathway would reduce net carbon emissions in the transportation market if it were widely utilized.

Sources

Andreadakis, A. D. (1993). Physical and chemical properties of activated sludge floc. *Water Research*, *27*(12), 1707-1714.

APHA. (2005). *Standard methods for the examination of water and wastewater.* Washington, D.C.: American Public Health Association, American Waterworks Association, and Water Pollution Control Federation.

Asadollahzadeh, M. J., Ardjmand, M., Seafkordi, A. A., & Heydarian, S. M. (2014). Efficient storage and utilization of CO 2 in open raceway ponds for cultivation of microalgae. *Korean Journal of Chemical Engineering*, *31*(8), 1425-1432.

Benemann, J. (2013). Microalgae for biofuels and animal feeds. *Energies*, *6*(11), 5869-5886.

Bowman, J. P., Nichols, C. M., & Gibson, J. A. (2003). Algoriphagus ratkowskyi gen. nov., sp. nov., Brumimicrobium glaciale gen. nov., sp. nov., Cryomorpha ignava gen. nov., sp. nov. and Crocinitomix catalasitica gen. nov., sp. nov., novel flavobacteria isolated from various polar habitats. *International journal of systematic and evolutionary microbiology*, *53*(5), 1343-1355.

Blackwell S., Crowe B., Hutton M., Poole K., Spierling R., Lundquist T. 2017. Development of Water and Nutrient Recycling Capabilities in Algae Biofuels Production Systems. WBS: 9.5.1.5, Award Number: DE-EE0005994. Final Report to the DOE.

California Air Resources Board (ARB ULSD) (2014). California-Modified GREET Pathways: Detailed California-Modified GREET Pathway for Ultra Low Sulfur Diesel (ULSD) from Average Crude Refined in California. LCFS Pathway ULSD001. Revised May 2014. California EPA.

California Air Resources Board (ARB ELC) (2014). Detailed California-Modified GREET Pathway for California Average and Marginal Electricity. LCFS Pathway ULSD001. Revised December 2014. California EPA.

Carney, L. T., Reinsch, S. S., Lane, P. D., Solberg, O. D., Jansen, L. S., Williams, K. P., ... & Lane, T. W. (2014). Microbiome analysis of a microalgal mass culture growing in municipal wastewater in a prototype OMEGA photobioreactor. *Algal Research*, *4*, 52-61.

Carney, L. T., Wilkenfeld, J. S., Lane, P. D., Solberg, O. D., Fuqua, Z. B., Cornelius, N. G., ... & Lane, T. W. (2016). Pond Crash Forensics: Presumptive identification of pond crash agents by next generation sequencing in replicate raceway mass cultures of Nannochloropsis salina. *Algal Research*, *17*, 341-347.

Chang, Michael. 2014. Water and Nutrient Recycling in Wastewater Fed High Rate Algae Ponds. Thesis. California Polytechnic State University.

Craggs, Rupert, Donna Sutherland, and Helena Campbell. "Hectare-scale demonstration of high rate algal ponds for enhanced wastewater treatment and biofuel production." *Journal of Applied Phycology* 24.3 (2012): 329-337.

Davis, R., Markham, J., Kinchin, C., Grundl, N., Tan, E. C., & Humbird, D. (2016). *Process design and economics for the production of algal biomass: algal biomass production in open pond systems and processing through dewatering for downstream conversion* (No. NREL/TP--5100-64772). NREL (National Renewable Energy Laboratory (NREL), Golden, CO (United States)).

District, S. J. (1992). *San Joaquin Valley APCD List of Current Rules.* Retrieved from RULE 2021 EXPERIMENTAL RESEARCH OPERATIONS: https://www.arb.ca.gov/drdb/sju/curhtml/R2021.HTM

District, S. J. (2005). *San Joaquin Valley APCD List of Current Rules.* Retrieved from RULE 4623 - STORAGE OF ORGANIC LIQUIDS: https://www.arb.ca.gov/drdb/sju/curhtml/R4623.PDF

Dunlap, Patrick J., and Andrew R. Shaw. *Recycling of Multiple Waste Streams for*

Transportation Fuel Production via Algae Cultivation at Wastewater Treatment Plants. Proc. of World Environmental and Water Resources Congress 2009: Great Rivers. American Society of Civil Engineers. 2145-152. May 2009.

Edgar, R. C. (2017). SEARCH_16S: A new algorithm for identifying 16S ribosomal RNA genes in contigs and chromosomes. *bioRxiv*, 124131

EPA Wastewater Technology Fact Sheet 2002 *https://www3.epa.gov/npdes/pubs/faclagon.pdf*

European Commission - Joint Research Centre - Institute for Environment and Sustainability: International Reference Life Cycle Data System (ILCD) Handbook - General guide for Life Cycle Assessment - Detailed guidance. First edition March 2010. EUR 24708 EN. Luxembourg. Publications Office of the European Union; 2010

Garcia, J., R. Mujeriego, and M. Hernandez-Marine. "High rate algal pond operating strategies for urban wastewater nitrogen removal." *Journal of Applied Phycology* 12.3-5 (2000): 331-339.

Green, Don W. Perry's Chemical Engineers' Handbook. McGraw-Hill, 2008.

Hannon, Michael, et al. "Biofuels from algae: challenges and potential." *Biofuels* 1.5 (2010): 763-784.

Hreiz, R., Sialve, B., Morchain, J., Escudié, R., Steyer, J. P., & Guiraud, P. (2014). Experimental and numerical investigation of hydrodynamics in raceway reactors used for algaculture. *Chemical Engineering Journal*, *250*, 230-239.

Huesemann, M., Crowe, B., Waller, P., Chavis, A., Hobbs, S., Edmundson, S., & Wigmosta, M. (2016). A validated model to predict microalgae growth in outdoor pond cultures subjected to fluctuating light intensities and water temperatures. *Algal Research*, *13*, 195-206.

Huesemann, M., Dale, T., Chavis, A., Crowe, B., Twary, S., Barry, A., ... & Cullinan, V. (2017a). Simulation of outdoor pond cultures using indoor LED-lighted and temperature-controlled raceway ponds and Phenometrics photobioreactors. *Algal Research*, *21*, 178-190.

Huesemann, M., Chavis, A., Edmundson, S., Rye, D., Hobbs, S., Sun, N., & Wigmosta, M. (2017b). Climate-simulated raceway pond culturing: quantifying the maximum achievable annual biomass productivity of Chlorella sorokiniana in the contiguous USA. *Journal of Applied Phycology*, 1-12.

Huesemann, M., Williams, P., Edmundson, S., Chen, P., Kruk, R., Cullinan, V., & Lundquist, T. (2017c). The laboratory environmental algae pond simulator (LEAPS) photobioreactor: Validation using outdoor pond cultures of Chlorella sorokiniana and Nannochloropsis salina. *Algal Research*, *26*, 39-46.

Huntley, M. E., Johnson, Z. I., Brown, S. L., Sills, D. L., Gerber, L., Archibald, I., ... & Greene, C. H. (2015). Demonstrated large-scale production of marine microalgae for fuels and feed. *Algal Research*, *10*, 249-265.

IEAGHG, "CO_2 Capture at Gas Fired Power Plants, 2012/8, July 2012.

Jenkins, D., Richard, M. G., & Daigger, G. T. (1993). Manual on the causes and control of activated sludge bulking and foaming. 2. In *Manual on the causes and control of activated sludge bulking and foaming. 2. ed*. Lewis.

Jones S, R Davis, Y Zhu, C Kinchin, D Anderson, R Hallen, D Elliott, A Schmidt, K Albrecht, T Hart, M Butcher, C Drennan, L Snowden-Swan. "Process Design and Economics for the Conversion of Algal Biomass to Hydrocarbons: Whole Algae Hydrothermal Liquefaction and Upgrading." PNNL-23227, Pacific Northwest National Laboratory, Richland, WA. 2014 https://www.pnnl.gov/main/publications/external/technical_reports/PNNL-23227.pdf

Jones, S., Zhu, Y., Snowden-Swan, L., Anderson, D., Hallen, R., Schmidt, A., . . . Elliott, D. (2014). *Whole Algae Hydrothermal Liquefaction: 2014 State of Technology.* Richland, Wa.: Pacific Northwest National Laboratory.

Ju, F., & Zhang, T. (2015). Bacterial assembly and temporal dynamics in activated sludge of a full-scale municipal wastewater treatment plant. *The ISME journal*, *9*(3), 683-695.

Kraetsch, Justin. 2015. Nutrient Removal from Clarified Municipal Wastewater Using Microalgae Raceway Ponds. Thesis. California Polytechnic State University.

Laurens, L. (2018). *National Renewable Energy Laboratory*. Retrieved from Microalgae Compositional Analysis Laboratory Procedures: https://www.nrel.gov/bioenergy/microalgae-analysis.html

Lee, N., la Cour Jansen, J., Aspegren, H., Henze, M. N. P. H., Nielsen, P. H., & Wagner, M. (2002). Population dynamics in wastewater treatment plants with enhanced biological phosphorus removal operated with and without nitrogen removal. *Water science and technology*, *46*(1-2), 163-170.

Lee, J., Cho, D. H., Ramanan, R., Kim, B. H., Oh, H. M., & Kim, H. S. (2013). Microalgae-associated bacteria play a key role in the flocculation of Chlorella vulgaris. *Bioresource technology*, *131*, 195-201.

Letcher, P. M., Lopez, S., Schmieder, R., Lee, P. A., Behnke, C., Powell, M. J., & McBride, R. C. (2013). Characterization of Amoeboaphelidium protococcarum, an algal parasite new to the cryptomycota isolated from an outdoor algal pond used for the production of biofuel. *PloS one*, *8*(2), e56232

Loh H. P. et al., "Process Equipment Cost Estimation Final Report." U.S. Department of Energy – National Energy Technology Laboratory, DOE/NETL-2002/1169, November 2007.

Lucker, B. F., Hall, C. C., Zegarac, R., & Kramer, D. M. (2014). The environmental photobioreactor (ePBR): An algal culturing platform for simulating dynamic natural environments. *Algal Research*, *6*, 242-249.

Lundquist, Tryg J., et al. "A realistic technology and engineering assessment of algae biofuel production." *Energy Biosciences Institute* (2010): 1-178

Ma, M., Yuan, D., He, Y., Park, M., Gong, Y., & Hu, Q. (2017). Effective control of Poterioochromonas malhamensis in pilot-scale culture of Chlorella sorokiniana GT-1 by maintaining CO2-mediated low culture pH. *Algal Research*, *26*, 436-444.

McLellan, S. L., Huse, S. M., Mueller-Spitz, S. R., Andreishcheva, E. N., & Sogin, M. L. (2010). Diversity and population structure of sewage-derived microorganisms in wastewater treatment plant influent. *Environmental microbiology*, *12*(2), 378-392.

Metcalf & Eddy, Inc. (2003). Wastewater engineering: treatment and reuse. Boston: McGraw-Hill.

Montemezzani, V. (2017). *Zooplankton Dynamics in Wastewater Treatment High Rate Algal Ponds and development of effective control methods* (Doctoral dissertation, The University of Waikato).

Mostertz, M., J. Naumovitz, H. Kistenmacher, B. Saydah, D. Venardos "Carbon Dioxide Management for Enhanced Plant growth, Learning from Terrestrial Plants to Full Solutions for Algae Biofuels." Presented at the Algae Biomass Summit 2014, San Diego, CA, USA, 29 September to 02 October 2014. https://www.researchgate.net/profile/Mathias_Mostertz/publication/272439289_Carbon_Dioxide_Management_for_Enhanced_Plant_Growth_Learning_from_Terrestrial_Plants_to_Full_Solutions_for_Algae_Biofuels/links/54e464ce0cf282dbed6f626a/Carbon-Dioxide-Management-for-Enhanced-Plant-Growth-Learning-from-Terrestrial-Plants-to-Full-Solutions-for-Algae-Biofuels.pdf

MWH, J. (2005). "Water treatment: Principles and design." New Jersey, John Wiley & Sons, Inc. ISBN 0-471-11018-3.

NACWA (National Association of Clean Water Agencies). Opportunities & Challenges in Clean Water Utility Financing and Management, Financial Survey Highlights, February 2015.

Neenan, B. (1986). *Fuels from microalgae: Technology status, potential and research requirements*. Solar Energy Research Institute.

Oswald, W. J., et al. "Algae in waste treatment [with discussion]." *Sewage and Industrial Wastes* 29.4 (1957): 437-457.

Painter, H. A., & Loveless, J. E. (1983). Effect of temperature and pH value on the growth-rate constants of nitrifying bacteria in the activated-sludge process. *Water research*, *17*(3), 237-248.

Park, J. B. K., Craggs, R. J., & Shilton, A. N. (2011). Recycling algae to improve species control and harvest efficiency from a high rate algal pond. *Water research*, *45*(20), 6637-6649.

Park, J. B. K., R. J. Craggs, and A. N. Shilton. "Wastewater treatment high rate algal ponds for biofuel production." *Bioresource technology* 102.1 (2011): 35-42.

Park, J. B. K., & Craggs, R. J. (2010). Wastewater treatment and algal production in high rate algal ponds with carbon dioxide addition. *Water Science and Technology*, *61*(3), 633-639.

Pienkos, Philip T., and A. L. Darzins. "The promise and challenges of microalgal-derived biofuels." *Biofuels, Bioproducts and Biorefining: Innovation for a sustainable economy* 3.4 (2009): 431-440.

Perinpanayagam, M. et al., "Mechanical Dewatering Alternatives Evaluation," HDR for City of Folsom – Utilities Department, 14 August 2013.

Pittner C. 2018. Increasing Algal Productivity and Treatment Potential in Raceways Fed Clarified Municipal Wastewater. Thesis. California Polytechnic State University.

Ramanan, R., Kang, Z., Kim, B. H., Cho, D. H., Jin, L., Oh, H. M., & Kim, H. S. (2015). Phycosphere bacterial diversity in green algae reveals an apparent similarity across habitats. *Algal Research*, *8*, 140-144.

Ramezan M. et al., "Carbon Dioxide Capture from Existing Coal-fired Power Plants." U.S. Department of Energy – National Energy Technology Laboratory, DOE/NETL-401/110907, November 2007.

Reiff, Carter. 2015. Nutrient Transformations in Algae Raceway Ponds Fed Municipal Wastewater. Thesis. California Polytechnic State University.

Ripley, Elliot. 2013. Settling Performance in Wastewater Fed High Rate Algae Ponds. Thesis. California Polytechnic State University.

Roberts, Alec. 2015. Production and Harvest of Microalgae in Wastewater Raceways with Resource Recycling. Thesis. California Polytechnic State University.

Sadalgekar, V. V., Mahajan, B. A., & Shaligram, A. M. (1988). Evaluation of sludge settleability by floc characteristics.

Sanapareddy N, Hamp TJ, Gonzalez LC, Hilger HA, Fodor AA, Clinton SM. (2009). *Molecular diversity of a North Carolina wastewater treatment plant as revealed by pyrosequencing*. *Appl Environ Microbiol* **75**: 1688–1696.

Schmid, M., Thill, A., Purkhold, U., Walcher, M., Bottero, J. Y., Ginestet, P., ... & Wagner, M. (2003). Characterization of activated sludge flocs by confocal laser scanning microscopy and image analysis. *Water research*, *37*(9), 2043-2052.

SEW Eurodrive. (2010, December). Power Factors and Efficiencies - DR/DT/DV Motors. Retrieved October 13, 2015, from http://v5.ptpilot.com/PTPilot/documents/M-011-03.pdf

Suvorov Y., Pittner C., Adler N., Spierling R., Lundquist T. (2015). Optimization of Algae Biomass Productivity and Harvesting at Existing High-Rate Pond Municipal Wastewater Treatment Plant. Algae Biomass, Biofuels and Bioproducts Conference Jun 7-10, San Diego CA. Poster presentation.

Te Chow, Ven. (1959). "Open channel hydraulics." Retrieved October 2015. http://www.fsl.orst.edu/geowater/FX3/help/8_Hydraulic_Reference/Mannings_n_Tables.htm

Urbain, V., Block, J. C., & Manem, J. (1993). Bioflocculation in activated sludge: an analytic approach. *Water Research*, *27*(5), 829-838.

USBR. (2001). Water Measurement Manual. Revised Reprint. Retrieved February 2017. <https://www.usbr.gov/tsc/techreferences/mands/wmm/chap06_07.html>

US Department of Energy, B. T. (2014). *Bioenergy Technologies Office Multi-Year Program Plan.* Washington, D.C.: US Department of Energy.

US Department of Energy, Office of Energy Efficiency and Renewable Energy. (2016). *Funding Opportunity Announcement (FOA) Number: DE-FOA-0001471, ADVANCEMENTS IN ALGAL BIOMASS YIELD, PHASE 2 (ABY2).* Washington, D.C.: US Department of Energy.

Valigore, J. M., Gostomski, P. A., Wareham, D. G., & O'Sullivan, A. D. (2012). Effects of hydraulic and solids retention times on productivity and settleability of microbial (microalgal-bacterial) biomass grown on primary treated wastewater as a biofuel feedstock. *Water research*, *46*(9), 2957-2964.

Van Wychen, S., & Laurens, L. (2013). *Determination of Total Carbohydrates in Algal Biomass.* 2013: National Renewable Energy Laboratory. Retrieved from https://www.nrel.gov/docs/fy16osti/60957.pdf

Van Wychen, S., & Laurens, L. (2013). *Determination of Total Solids and Ash in Algal Biomass.* Golden, CO: National Renewable Energy Laboratory. Retrieved from https://www.nrel.gov/docs/fy16osti/60956.pdf

Van Wychen, S., Ramirez, K., & Laurens, L. (2013). *Determination of Total Lipids as Fatty Acid Methyl Esters (FAME) by in situ Transesterification Laboratory Analytical Procedure (LAP).* Golden, CO: National Renewable Energy Laboratory. Retrieved from https://www.nrel.gov/docs/fy16osti/60958.pdf

Verlaan, P., Van Eijs, A. M. M., Tramper, J., Van't Riet, K., & Luyben, K. C. A. (1989). Estimation of axial dispersion in individual sections of an airlift-loop reactor. *Chemical Engineering Science*, *44*(5), 1139-1146.

Voncken, R. M., Holmes, D. B., & Den Hartog, H. W. (1964). Fluid flow in turbine-stirred, baffled tanks—III: Dispersion during circulation. *Chemical Engineering Science*, *19*(3), 209-213.

Wanner, J. (1994). *Activated sludge: bulking and foaming control*. CRC Press.

Weissman, J. C., Goebel, R. P., & Benemann, J. R. (1988). Photobioreactor design: mixing, carbon utilization, and oxygen accumulation. *Biotechnology and bioengineering*, *31*(4), 336-344.

White, R. L., & Ryan, R. A. (2015). Long-term cultivation of algae in open-raceway ponds: lessons from the field. *Industrial Biotechnology*, *11*(4), 213-220.

Wigmosta, M. S., Coleman, A. M., Skaggs, R. J., Huesemann, M. H., & Lane, L. J. (2011). National microalgae biofuel production potential and resource demand. *Water Resources Research*, *47*(3).

Woertz, I.C., L. Fulton, and T.J. Lundquist, “Nutrient removal & greenhouse gas abatement with CO_2-supplemented algal high rate ponds.” Paper written for the WEFTEC annual conference, Water Environment Federation, October 12-14, 2009, Orlando, Florida, pp. 13.